

Epigenetic remodeling through a mitochondrial redox signal in
an experimental model of Parkinson's disease

Epigenetische Restrukturierungen durch ein Redox-Signal
mitochondriellen Ursprungs in einem experimentellen Modell
der Parkinson'schen Krankheit

Dissertation

Zur Erlangung des Grades Doktor der Naturwissenschaften

Vorgelegt am Fachbereich Biologie der Johannes Gutenberg-Universität Mainz von

Marius Wilhelm Baeken

geboren am 04.12.1990 in Jülich

Mainz, 2019

Dekan: [REDACTED]

1. Berichterstatter: [REDACTED]

2. Berichterstatter: [REDACTED]

Tag der Promotion:

Ich Marius Wilhelm Baeken erkläre hiermit, dass die vorgelegte Dissertation von mir selbstständig, ohne unzulässige Hilfe Dritter und ohne Benutzung anderer als der angegebenen Hilfsmittel, angefertigt wurde. Alle von mir benutzten Veröffentlichungen, ungedruckten Materialien, sonstige Hilfsmittel sowie Textstellen, die ich wörtlich oder inhaltlich aus gedruckten oder ungedruckten Arbeiten übernommen habe, habe ich als solche gekennzeichnet und mit den erforderlichen bibliographischen Angaben nachgewiesen. Unterstützungsleistungen, die ich von anderen Personen erhalten habe, wurden in der Dissertationsschrift als solche benannt.

Mainz, Juli 2019

Marius Wilhelm Baeken

*„Natürlicher Verstand kann fast jeden Grad von Bildung ersetzen, aber keine Bildung
den natürlichen Verstand.“*

~Arthur Schopenhauer



| | |
|--|-------------|
| I. Table of content | |
| Table of content | I |
| Table of abbreviations | V |
| Table of figures | XI |
| List of tables | XIII |
| Danksagung | XIV |
| 1.1 Abstract | 1 |
| 1.2 Deutsche Zusammenfassung | 2 |
| 2 Introduction | 3 |
| 2.1 Parkinson's disease | 3 |
| 2.1.1 The nigrostriatal system | 3 |
| 2.1.2 Pathophysiology of Parkinson's disease | 4 |
| 2.1.3 The genesis of Parkinson's disease | 5 |
| 2.2 Three major theories of the onset of Parkinson's disease | 7 |
| 2.2.1 Dopaminergic neurons in Parkinson's disease suffer disruption of their protein homoeostasis | 7 |
| 2.2.2 Microglia activation eradicates dopaminergic neurons | 7 |
| 2.2.3 Oxidative phosphorylation and Parkinson's disease | 8 |
| 2.3 Oxidative stress | 11 |
| 2.3.1 Endogenous ROS sources | 11 |
| 2.3.2 ROS classification and mechanism of oxidation | 11 |
| 2.3.3 Endogenous removal of ROS | 13 |
| 2.3.4 Increased ROS vulnerability of SN <i>pars compacta</i> neurons | 14 |
| 2.3.5 Exogenous ROS sources | 15 |
| 2.4 Models of PD | 15 |
| 2.4.1 Oxidopamine | 15 |
| 2.4.2 1-Methyl-4-phenylpyridinium | 16 |
| 2.4.3 Rotenone | 16 |
| 2.4.4 Paraquat | 17 |
| 2.4.5 Other models | 17 |

| | |
|--|----|
| 2.5 Antioxidants as possible therapeutics | 18 |
| 2.5.1 Vitamin E, C and CoQ10 | 18 |
| 2.5.2 MitoQ and MitoVitE | 19 |
| 2.5.3 Phenothiazine | 20 |
| 2.6 Epigenetics and Parkinson’s disease | 21 |
| 2.6.1 Epigenetics | 21 |
| 2.6.2 DNA methylation | 22 |
| 2.6.3 Histone modifications | 24 |
| 2.6.4 Epigenetic changes in Parkinson’s disease | 25 |
| 2.7 Aim of this thesis | 26 |
| 3 Materials and methods | 28 |
| 3.1 Materials | 28 |
| 3.1.1 Antibodies | 28 |
| 3.1.1.1 Primary antibodies | 28 |
| 3.1.1.2 Secondary antibodies | 28 |
| 3.1.2 Chemicals | 29 |
| 3.1.3 Solutions | 31 |
| 3.1.3.1 Crafted solutions | 31 |
| 3.1.3.2 Purchased solutions | 36 |
| 3.1.4 Kits | 36 |
| 3.1.5 Cell lines | 37 |
| 3.1.6 Animals | 37 |
| 3.1.7 Equipment | 37 |
| 3.2 Methods | 39 |
| 3.2.1 Cell culture | 39 |
| 3.2.1.1 Coating | 39 |
| 3.2.1.2 LUHMES cells | 39 |
| 3.2.1.2.1 Stem cells | 39 |
| 3.2.1.2.2 Differentiation | 40 |
| 3.2.2 Biochemical protocols | 41 |
| 3.2.2.1 Western blot | 41 |
| 3.2.2.1.1 Protein isolation | 41 |
| 3.2.2.1.2 Protein concentration determination | 41 |

| | | |
|-----------|---|----|
| 3.2.2.1.3 | SDS Laemmli gel manufacture..... | 42 |
| 3.2.2.1.4 | SDS PAGE..... | 42 |
| 3.2.2.1.5 | Protein transfer..... | 43 |
| 3.2.2.1.6 | Blocking and primary antibody..... | 43 |
| 3.2.2.1.7 | Secondary antibody and development..... | 43 |
| 3.2.2.2 | DNA dot blot..... | 44 |
| 3.2.2.2.1 | DNA isolation..... | 44 |
| 3.2.2.2.2 | DNA dot blot..... | 44 |
| 3.2.2.2.3 | Antibodies and development..... | 44 |
| 3.2.2.3 | Transcriptomics..... | 45 |
| 3.2.2.3.1 | RNA isolation..... | 45 |
| 3.2.2.3.2 | RNASeq..... | 45 |
| 3.2.2.4 | Immunocytochemistry (ICC)..... | 46 |
| 3.2.2.5 | SIRT1 activity assay..... | 46 |
| 3.2.3 | <i>In vivo</i> mouse system..... | 47 |
| 3.2.3.1 | Establishing the model..... | 47 |
| 3.2.3.2 | Rota Rod..... | 48 |
| 3.2.3.3 | Tissue sampling..... | 49 |
| 3.2.3.4 | Western blot..... | 49 |
| 3.2.3.5 | Cryosections..... | 49 |
| 3.2.3.6 | Immunohistochemistry (IHC)..... | 49 |
| 3.2.4 | Evaluation..... | 50 |
| 3.2.4.1 | Microscopy..... | 50 |
| 3.2.4.2 | Densitometry..... | 51 |
| 3.2.4.3 | Statistics..... | 51 |
| 4 | Results..... | 52 |
| 4.1 | Adjusting the optimal working concentrations of MPP ⁺ and PHT..... | 52 |
| 4.2 | MPP ⁺ causes protein hyperacetylation in differentiated LUHMES cells..... | 54 |
| 4.3 | MPP ⁺ induced hyperacetylation can be augmented by the HDAC inhibitor TSA, but not EX-527..... | 56 |
| 4.4 | SIRT1 activity and protein level decrease in a PHT responsive manner under MPP ⁺ | 59 |
| 4.5 | SIRT3 protein levels and localization change in MPP ⁺ treated LUHMES cells..... | 61 |

| | |
|---|-----|
| 4.6 Antioxidants protect dopaminergic neurons from MPTP induced cell death <i>in vivo</i> | 63 |
| 4.7 MPTP causes protein hyperacetylation <i>in vivo</i> | 65 |
| 4.8 MPP⁺ treatment causes DNA hypometyhlation and disturbances in DNMT level and localization | 68 |
| 4.9 MPP⁺ induces gene expression of nuclear encoded mitochondrial respiratory chain subunits and causes mitochondria to favour replication over transcription | 75 |
| 4.10 MPP⁺ promotes exploration of alternative energy sources | 79 |
| 4.11 MPP⁺ influences the transcription of genes involved in epigenetic regulation | 82 |
| 4.12 Graphical abstract | 88 |
| 5 Discussion | 91 |
| 5.1 Epigenetic changes are part of PD's pathology | 91 |
| 5.2 ROS dependant loss of SIRT1 activity ultimately causes lysine hyperacetylation and histone H1 hypertranscription | 94 |
| 5.3 MPP⁺ disrupts the SIRT homoeostasis | 97 |
| 5.4 MPP⁺ disrupts the HDAC/HAT homoeostasis | 99 |
| 5.5 ROS dependant loss of DNMT3B causes DNA hypomethylation | 101 |
| 5.6 Increased supply of energy generators in the MPP⁺ model of PD | 104 |
| 5.7 Mitochondria in MPP⁺ treated cells favour replication over transcription | 108 |
| 5.8 PHT the future PD drug? | 109 |
| 6 Literature | 111 |

II. Table of abbreviations

| | |
|-----------------------|---|
| PD | Parkinson's disease |
| ROS | Reactive oxygen species |
| MPP ⁺ | 1-Methyl-4-phenylpyridinium |
| MPTP | 1-Methyl-4-phenyl-1,2,3,6-tetrahydropyridin |
| LUHMES | Lund human mesencephalic |
| ATP | Adenosine triphosphate |
| NADH/NAD ⁺ | Nicotinamide adenine dinucleotide |
| PHT | Phenothiazine |
| DNA | Deoxyribonucleic acid |
| SIRT | Sirtuin |
| DNMT | DNA-methyltransferase |
| SN | Substantia nigra |
| GABA | Gamma-aminobutyric acid |
| REM | Rapid eye movement |
| Fig | Figure |
| SNCA | Alpha-synuclein |
| UBQ | Ubiquitin |
| CRYAB | Alpha B crystalline |
| NF | Neurofilament |
| ATP13A2 | Cation-transporting ATPase 13A2 |
| LRRK2 | Leucine-rich repeat serine-threonine protein kinase-2 |
| ATG9 | Autophagy related 9 |
| VEGF | Vascular endothelial growth factor |
| CoQ10 | Ubiquinone |
| FMN | Flavin mononucleotide |
| Fe-S | Iron sulfur |
| TCA | Tricarboxylic acid |
| FAD | Flavin adenine dinucleotide |
| CoQ10H• | Ubisemiquinone |

Table of abbreviations

| | |
|-------------------------------|--|
| ADP | Adenosine diphosphate |
| P _i | Inorganic phosphate |
| BBB | Blood brain barrier |
| NADPH | Nicotinamide adenine dinucleotide phosphate |
| NGB | Neuroglobin |
| •O ₂ ⁻ | Superoxide anion |
| HO ₂ • | Hydroperoxyl radical |
| H ₂ O ₂ | Hydrogen peroxide |
| •OH | Hydroxyl radical |
| HOCl | Hypochlorous acid |
| ONOO ⁻ | Peroxynitrite |
| NO ₂ ⁻ | Nitrite |
| SOD | Superoxide dismutase |
| GSH | Glutathione |
| GSSG | Glutathione disulfide |
| PAH | Polycyclic aromatic hydrocarbon |
| TiO ₂ | Titan oxide |
| 6-ODHA | Oxidopamine |
| DAT | Dopamine transporter |
| MPPP | Desmethylprodine |
| MAO-B | Monoaminoxigenase B |
| PINK1 | Phosphatase and tensin homolog induced putative kinase 1 |
| PRKN | Parkin |
| PARK7 | Parkinson disease protein 7 |
| TPP | Triphenylphosphonium |
| MitoQ | Mitoquinone |
| MBD | Methyl binding domain |
| TET | Ten-eleven translocase |
| TDG | Thymine DNA glycolyase |
| HMT | Histone methyltransferase |

Table of abbreviations

| | |
|--------|--|
| JDCD | Jumonji domain-containing demethylase |
| LSD | Lysine-specific histone demethylase |
| PRMT | Protein arginine N-methyltransferase |
| HAT | Histone acetyl transferase |
| HDAC | Histone deacetylase |
| DMR | Differentially methylated region |
| iPSC | Induced pluripotent stem cell |
| mtDNA | mitochondrial DNA |
| D-loop | Displacement loop |
| CYP2E1 | Cytochrome P450 enzyme 2E1 |
| cAMP | Cyclic adenosine monophosphate |
| CREBBP | cAMP response element-binding protein |
| TH | Tyrosine hydroxylase |
| H3 | Histone 3 |
| H3K14 | Lysine 14 of H3 |
| ac | Acetylation |
| SLC6A3 | Solute carrier family 6 member 3 |
| TUBB | Tubulin beta |
| TUB | Tubulin alpha |
| TEFM | Transcription elongation factor, mitochondrial |
| GLUT3 | Glucose transporter type 3 |
| HRP | Horse radish peroxidase |
| MPHT | N-Methylphenothiazine |
| APHT | 2-Acetylphenothiazine |
| 6-TG | 6-Thioguanine |
| BafA1 | Bafilomycin A1 |
| TSA | Trichostatin A |
| PLO | Poly-L-ornithine |
| FGF | Fibroblast growth factor |
| GDNF | Glial cell-derived neurotrophic factor |

Table of abbreviations

| | |
|----------------------------------|--|
| SDS | Sodium dodecyl sulfate |
| EDTA | Ethylenediaminetetraacetic acid |
| EGTA | Ethylene glycol-bis(β -aminoethyl ether)-N,N,N',N'-tetraacetic acid |
| HCl | Hydrochloric acid |
| NaOH | Sodium hydroxide |
| NaCl | Sodium chloride |
| KCl | Potassium chloride |
| Na ₂ HPO ₄ | Disodium phosphate |
| KH ₂ PO ₄ | Monopotassium phosphate |
| BSA | Bovine serum albumin |
| TRIS | Tris(hydroxymethyl)aminoethane |
| NFDMP | Non fat dried milk powder |
| PFA | Paraformaldehyde |
| DMSO | Dimethyl sulfoxide |
| TEMED | Tetramethylethylenediamine |
| APS | Ammonium persulfate |
| NaN ₃ | Sodium azide |
| PBS | Phosphate buffered saline |
| TBS | TRIS buffered saline |
| FCS | Fetal calf serum |
| AB-AM | Antibiotic antimycotic |
| DMEM | Dulbecco's modified eagle's medium |
| BCA | Bicinchoninic acid |
| ICC | Immunocytochemistry |
| bw | bodyweight |
| ip | Intraperitoneal |
| ICH | Immunohistochemistry |
| LSM | Laser scanning microscope |
| BH | Benjamini-Hochberg |
| ANOVA | Analysis of variance |

Table of abbreviations

| | |
|----------|--|
| PTM | Posttranslational modification |
| TP53 | Tumor protein 53 |
| MAP1LC3B | Microtubule-associated proteins 1A/1B light chain 3B |
| MPP | Mitochondrial processing peptidase |
| L-DOPA | L-dihydroxyphenylalanine |
| VTA | Ventral tegmental area |
| SSBP | Single strand binding protein |
| POLRMT | Mitochondrial RNA polymerase |
| POLG | Polymerase gamma |
| TOP1MT | Mitochondrial topoisomerase 1 |
| TWINK | Twinkle helicase |
| DNA2 | DNA replication helicase/nuclease 2 |
| SUPV3L1 | Suppressor of Var1, 3-like 1 |
| PIF1 | Petite integration frequency 1 |
| KAT | Lysine acetyltransferase |
| ATF2 | Activating transcription factor 2 |
| TAF1 | TATA box binding protein associated factor 1 |
| CLOCK | Circadian locomotor output cycles kaput protein |
| EP300 | E1A binding protein p300 |
| CREB | cAMP responsive element binding |
| NCOA | Nuclear receptor coactivator |
| SLC7A5 | Solute carrier family 7 member 5 |
| AADC | Aromatic L-amino acid decarboxylase |
| COMT | Catechol-O-methyltransferase |
| TF | Transcription factor |
| sir2 | Silent mating type information regulation 2 |
| PPARGC1A | Peroxisome proliferator-activated receptor gamma coactivator 1-alpha |
| AMPK | 5' Adenosine monophosphate-activated protein kinase |
| RELA | V-rel avian reticuloendotheliosis viral oncogene homolog A |
| mTORC1 | Mammalian target of rapamycin complex 1 |

Table of abbreviations

| | |
|--------|--|
| CPS1 | Carbamoyl phosphate synthase 1 |
| NFE2L2 | Nuclear factor, erythroid 2 like 2 |
| HSPA1 | Heat-shock 70 kDa protein 1 |
| SAM | S-adenosyl methionine |
| BER | Base excision repair |
| ATP5S | ATP synthase subunit S |
| HK | Hexokinase |
| PFK | Phosphofructokinase |
| SUCL | Succinate-CoA ligase |
| NDPK | Nucleoside-diphosphate kinase |
| LDH | Lactate dehydrogenase |
| DLD | Dihydrolipoamide dehydrogenase |
| DLAT | Dihydrolipoamide S-acetyltransferase |
| PDHX | Pyruvate dehydrogenase complex component X |
| PDH | Pyruvate dehydrogenase E1 |
| ME | Malic enzyme |
| GLUD1 | Glutamate dehydrogenase |

III. Table of figures

| | |
|--|----|
| Figure 2.1: The nigrostriatal pathway..... | 4 |
| Figure 2.2: The respiratory chain..... | 10 |
| Figure 2.3: PD linked toxins..... | 18 |
| Figure 2.4: Antioxidants..... | 21 |
| Figure 2.5: DNA methylation and demethylation..... | 23 |
| Figure 2.6: Posttranslational modifications of core histones (H2A, H2B, H3 and H4)..... | 24 |
| Figure 3.1: MPTP Mouse model..... | 48 |
| Figure 4.1: Morphological analysis of LUHMES cells treated with different concentrations of MPP ⁺ | 53 |
| Figure 4.2: Quantitative ROS analysis of LUHMES cells treated with MPP ⁺ and PHT..... | 54 |
| Figure 4.3: Changes in acetylation levels in differentiated LUHMES cells..... | 55 |
| Figure 4.4: Lysine acetylation status in LUHMES cells treated with MPP ⁺ , TSA, EX-527 and PHT..... | 58 |
| Figure 4.5: SIRT1 activity, expression and degradation in LUHMES cells treated with MPP ⁺ | 60 |
| Figure 4.6: Reallocation of SIRT3 in LUHMES cells treated with MPP ⁺ and PHT..... | 62 |
| Figure 4.7: Effects of MPTP and PHT on cell survival and motoric capabilities <i>in vivo</i> | 64 |
| Figure 4.8: Histone acetylation status of the SN after MPTP and PHT treatments..... | 65 |
| Figure 4.9: Biochemical analysis of protein acetylation and SIRT protein levels after MPTP and PHT treatments..... | 67 |
| Figure 4.10: DNA hypomethylation in LUHMES cells after MPP ⁺ and PHT treatments..... | 69 |
| Figure 4.11: DNMT1 reallocation in LUHMES cells treated with MPP ⁺ and PHT..... | 70 |
| Figure 4.12: Status of DNMT3A in LUHMES cells treated with MPP ⁺ and PHT..... | 71 |
| Figure 4.13: Status of DNMT3B in LUHMES cells treated with MPP ⁺ and PHT..... | 72 |
| Figure 4.14: <i>In vivo</i> and <i>in vitro</i> biochemical analysis of DNMT3B after treatments with MPTP/MPP ⁺ and PHT..... | 74 |
| Figure 4.15: Transcriptional regulation of nuclear encoded mitochondrial subunits in MPP ⁺ and PHT treated cells..... | 76 |
| Figure 4.16: Transcriptional regulation of mitochondrial encoded mitochondrial subunits in MPP ⁺ and PHT treated cells..... | 77 |
| Figure 4.17: MPP ⁺ and PHT alter replication of mitochondrial DNA..... | 78 |

Figure 4.18: Transcriptional regulation of energy suppliers in MPP⁺ and PHT treated cells.. 81

Figure 4.19: GLUT3 protein levels in MPP⁺ and PHT treated LUHMES cells..... 82

Figure 4.20: Transcriptional regulation of SIRT6 in MPP⁺ and PHT treated cells..... 83

Figure 4.21: Transcriptional regulation of HDACs in MPP⁺ and PHT treated cells..... 83

Figure 4.22: Transcriptional regulation of HATs in MPP⁺ and PHT treated cells..... 84

Figure 4.23: Transcriptional regulation of DNMTs and TETs in MPP⁺ and PHT treated cells.85

Figure 4.24: Transcriptional regulation of histones in MPP⁺ and PHT treated cells.....86

Figure 5.1: ROS dependent loss of heterochromatin.....104

Figure 5.2: Restoration of energy dysbalance.....107

Figure 5.3: G4-quadruplex..... 109

IV. List of tables

| | | |
|--------------------|--------------------------------|----|
| Table 2.1: | Reactive oxygen species..... | 12 |
| Table 3.1: | Primary antibodies..... | 28 |
| Table 3.2: | Secondary antibodies..... | 28 |
| Table 3.3: | Chemicals..... | 29 |
| Table 3.4: | Purchased solutions..... | 36 |
| Table 3.5: | Kits..... | 36 |
| Table 3.6: | Cells..... | 37 |
| Table 3.7: | Animals..... | 37 |
| Table 3.8: | Equipment..... | 37 |
| Table 3.9: | Media volumes..... | 39 |
| Table 3.10: | LUHMES cell treatments..... | 40 |
| Table 3.11: | Separation gel..... | 42 |
| Table 3.12: | Collection gel..... | 42 |
| Table 5.1: | Histone acetylation sites..... | 90 |

V. Danksagung

[REDACTED]

[REDACTED]

[REDACTED]

[REDACTED]

[REDACTED]

[REDACTED]

1.1 Abstract

Together with the prospect of an ever-older growing society, so will the prevalence of age-associated neurodegenerative disorders like Parkinson's disease (PD) rise. Thus, it becomes ever more important to possess adequate means to treat and manage such malignancies. Unlike its onset, the pathophysiology of motoric deficits in PD is quite well understood these days. A precise and profound loss of dopaminergic neurons in the *substantia nigra pars compacta*, a mesencephalic structure, develops the well known and described symptoms of PD.

One major hypothesis for the onset of PD revolves around oxidative stress created by a dysbalance in the generation and/or deetoxification of reactive oxygen species (ROS). These are usually conceived through a leakage of electrons from the respiratory complexes to molecular oxygen, which is turned into superoxide, yet rapidly transformed into non-hazardous forms by the cellular antioxidant defence system. Many models of PD, which do not follow a genetic paradigm, rely on an excessive production of ROS.

One of these models, if not the most popular one, the 1-methyl-4-phenylpyridinium (MPTP/MPP⁺) model, was used in this work to establish the nature of epigenetic changes in dopaminergically differentiated LUHMES cells and mice. The MPTP/MPP⁺ model relies on electron transfer disruption in the complex I of the respiratory chain, thus causing increased amounts of ROS, as well as ATP and NAD⁺ depletion. The strong antioxidant phenothiazine (PHT) was administered as well to survey protective effects and sever ROS mediated from metabolic stress effects. Metabolic changes this profound require the cells to adapt, which is often accompanied by epigenetic changes. This work aims to further solidify and expand the understanding of energetic, epigenetic, biochemical and molecular pathologies of PD, while also offering new treatment possibilities through the antioxidant PHT. In the PD models system, the cell's epigenome changes and is entirely turned around, while heterochromatin in form of DNA methylation appears to disappear and euchromatin markers in form of histone acetylation accumulate. Through this work all of these effects can be traced back to a loss of function of the ROS sensitive sirtuin 1 (SIRT1) and the *de novo* DNA methyltransferase 3B (DNMT3B). If protected by PHT, these enzymes could possibly allow the cell's chromatin to rearrange and stabilize.

The epigenetic changes are accompanied by their consequential changes of transcription, especially in regard to energy acquisition by turning on the transcription of nuclear encoded mitochondrial genes. Restored chromatin may be beneficial to the process of adaptation and the cells may be able to adjust more properly to their new environment with a disabled complex I.

1.2 Deutsche Zusammenfassung

Einhergehend mit einer alternden Gesellschaft wird auch die Frequenz altersbedingter neurodegenerativer Erkrankung, wie dem Morbus Parkinson (Parkinson's disease, PD), steigen. Somit wird es immer wichtiger geeignete Mittel zur Behandlung solcher Krankheiten zu finden. Obwohl die Pathophysiologie der motorischen Defizite der PD heutzutage sehr wohl verstanden ist, bleibt seine Genese doch unbekannt. PD rührt von einem präzisen und schweren Verlust dopaminerger Neurone in der *Substantia nigra pars compacta*, einer Struktur des Mesencephalons, her.

Eine der Haupttheorien über die Entstehung von PD fußt auf oxidativem Stress verursacht durch ein Ungleichgewicht in der Erzeugung und/oder Entsorgung von reaktiven Sauerstoffspezies (reactive oxygen species, ROS). Diese entstehen i.d.R. durch einen ungeordneten Ausfluss der Elektronen in der Atmungskette zu molekularem Sauerstoff, welcher in Superoxid umgewandelt, doch rasch vom antioxidativem Verteidigungssystem der Zelle zu ungefährlichen Sauerstoff Spezies transformiert wird. Viele Modelle des PD, welche keinem genetischen Paradigma folgen, fußen auf einer exzessiven Produktion von ROS.

Das wahrscheinlich populärste dieser Modelle ist das 1-Methyl-4-phenylpyridinium (MPTP/MPP⁺) Modell, welches in dieser Arbeit verwendet wurde, um die Art der metabolischen und epigenetischen Veränderungen dopaminerg differenzierter LUHMES Zellen und Mäusen zu ergründen. Das MPTP/MPP⁺ Modell verursacht eine Störung der Elektronenleitung im Komplex I der Atmungskette und führt somit zu erhöhter ROS Produktion, wie auch zu ATP und NAD⁺ Mangel. Parallel wurde das überaus starke Antioxidans Phenothiazin (PHT) verwendet, um protektive Effekte zu bewerten und RSS abhängige von Metabolismus abhängigen Effekten zu trennen. Metabolische Veränderungen dieses Ausmaßes verlangen von der Zelle sich anzupassen, was oft von epigenetischen Veränderungen begleitet wird.

Diese Arbeit setzt sich zum Ziel das Verständnis für energetische, epigenetische, biochemische und molekulare Pathologien des PD zu festigen und zu erweitern und bietet neue Behandlungsmöglichkeiten durch das Antioxidans PHT. Das Epigenom der Zelle wird geprägt durch das Verschwinden von Heterochromatin Markern wie Methylierung der DNA, während Marker des Euchromatin, wie Acetylierung von Histonen, akkumulieren. Durch diese Arbeit können jene Effekte auf das ROS sensitive Sirtuin 1 und die *de novo* DNA Methyltransferase 3B zurückverfolgt werden.

Die epigenetischen Veränderungen werden begleitet von Veränderungen auf der Ebene der Transkription, insbesondere in Bezug auf die Energieproduktion durch das Antreiben der Transkription nuklear kodierter mitochondrialer Gene. Wiederhergestelltes Chromatin könnte dem Prozess der Adaptation begünstigen und die Zellen könnten somit in der Lage sein sich besser an ihre neue Umwelt und einem dysfunktionalen Komplex I anpassen.

2 Introduction

2.1 Parkinson's disease

2.1.1 The nigrostriatal system

The nigrostriatal dopaminergic system describes the facilitation of information between the *substantia nigra pars compacta* and the *striatum* through dopaminergic synapses originating in the *substantia nigra* (SN) and projecting to the *striatum* (Fig. 2.1). The SN is a mesencephalic basal ganglia structure that appears in darker colouring than the surrounding brain tissue. Thus, it was named *substantia nigra* or „black substance“, when it was first described in 1784 by the French physician Félix Vicq-d'Azyr (Tubbs et al., 2011). The dark colour emanates from the pigment neuromelanin, which accumulates as the organism ages (Rabey et al., 1990; Herrero et al., 1993). Interestingly, human nigral neurons harbor a lot more neuromelanin than those of other primates (Fedorow et al., 2005). Neuromelanin is biosynthesized from dopamine, but its biological properties are still subjected to disparate discussion (Zecca et al., 2001). Some believe it protects neurons from iron-induced oxidative stress, while others claim it to be the origin of that stress (Zucca et al., 2017). The *substantia nigra* can be divided into two functionally and sterically different parts, the *pars compacta* and the *pars reticulata* (Fig. 2.1). The former is involved in motor control, temporal processing and learning. The influence on motor control, albeit the most prominent one, is rather indirect since electrical stimulation of the *pars compacta* does not immediately result in movement *per se*. Through excitatory stimulation of the *striatum* by dopamine, the *striatum* releases gamma-aminobutyric acid (GABA) onto the *globus pallidus*, which in turn inhibits the *thalamic nucleus*. This causes excitation of thalamocortical pathways and thus initiation of movement through the *prefrontal cortex* (Fig. 2.1) (Haber, 2016). Additionally, the *pars compacta* also plays a role in temporal processing through time reproduction (Jahanshahi et al., 2006). Deficits have been linked to insomnia and rapid eye movement (REM) sleep disturbances (Gerashchenko et al., 2006).

In contrast to the neurons of the *pars compacta*, the neurons of the *pars reticulata* are GABAergic and inhibitoric, not dopaminergic and excitatoric (Fig. 2.1). Their synapses extend to the basal ganglia of the *thalamus* and the *superior colliculus* (Zhou et al., 2011). Through so-called axon collaterals – smaller side branches of the main axon – the *pars reticulata* may also partly inhibit the *pars compacta* (Mailly et al., 2003). The neurons of the *pars reticulata* generate spontaneous action potentials whose frequency can be increased by excitation from the *subthalamic nucleus* and decreased by active movement of the organism (Sato et al., 2002). The generation of the action potentials, however, is considered to be of autonomous nature (Atherton et al., 2005).

Neurons of the *pars compacta* have been in the focus of research for centuries, especially since their disappearance is directly connected to the pathology of a neurodegenerative disorder called Parkinson's disease (PD). It is noteworthy, however, that also the *pars reticulata* is not unaffected in this disease. Neuronal hypertrophy for example has been shown to occur in the *pars reticulata* of PD patients (Neal et al., 1991).

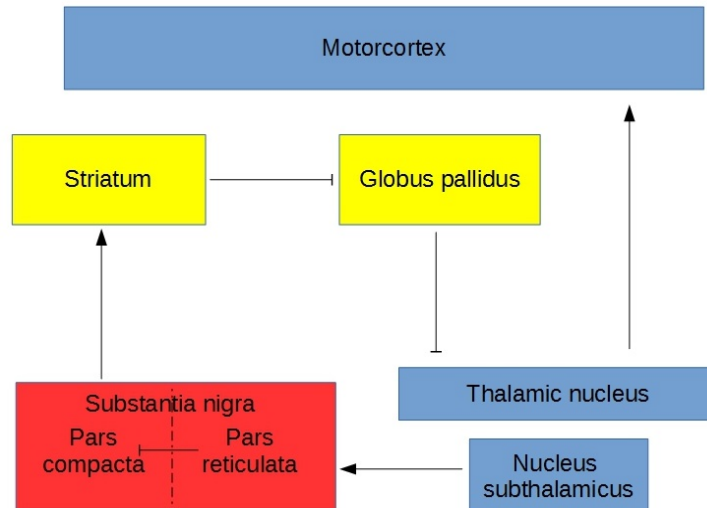


Figure 2.1: The nigrostriatal pathway. The *substantia nigra pars compacta* excites the *striatum* through dopamine, which then inhibits the *globus pallidus* via GABA, which in turn inhibits the *thalamic nucleus* through GABA, which finally excites the motorcortex through glutamate. The *pars compacta* is inhibited through GABA of the *pars reticulata*, which is excited by the *nucleus subthalamicus* through glutamate.

2.1.2 Pathophysiology of Parkinson's disease

The most prominent derangement of the nigrostriatal pathway is the neurodegenerative disorder Parkinson's disease, named after its avant-garde James Parkinson, who winnowed the disease he referred to as „the shaking palsy“ from other neurodegenerative disorders in 1817 (Parkinson, 2002). In fact, PD has already been observed and described in ancient times, yet rise of modern technology allowed more precise and thorough cataloguing of pathologies. Hoary Ayurvedic or Egyptian texts describe symptoms strongly resembling those of PD and Galenus of Pergamon recorded cases of PD in Roman times (García Ruiz 2004; Galenus et al., 1976). It is worth to note that the recommended remedies in those days derived from the *mucuna* family, a group of plants rich in L-DOPA, a still common drug to treat the symptoms of PD (Birkmayer et al., 1962; Chattopadhyay et al., 1994). Nowadays the pathology and devolution of PD have become clearer, yet the origin remains elusive, except for special cases, where the afflicted person was exposed to a specific toxin, e.g. the pesticides paraquat and rotenone, for a certain amount of time (Tanner et al., 2011). Indeed, PD caused in farmers after chronic exposure to these substances, which they used as pesticides, has been recognized as a work-related disease (Semchuk et al., 1992).

However well the pathology is understood, every case of PD presents itself in a different manner

due to factors yet not perceived. A number of four disparate, so called cardinal symptoms exist of which two have to be present to warrant a PD diagnosis. The first and most important symptom is bradykinesia, which needs to be displayed by the afflicted for a positive PD diagnosis and causes movements to be executed at a much slower pace leading the afflicted to scuffle (Parkinson 2002; Brumlik et al., 1966). The three remaining cardinal symptoms include rigor, resting tremor and postural instability. Rigor develops through the simultaneous excitation of muscle agonists and antagonists, which is caused by dopamine deprivation in the extrapyramidal system, a motor system network governing involuntary actions and – among others – including the nigrostriatal pathway (Jellinger 2012; Charcot et al., 1886). Resting tremor describes a rhythmic, repetitive twitching of the body extremities through contraction of antagonistic groups of muscles. These tremors also occur in healthy organisms, but their intensity and frequency is increased in afflicted organisms (McLeod 1971; Charcot et al., 1886). Postural instability portrays as observable posture correction while sitting and standing of the afflicted, since their subconscious and subtle means to correct their posture have been lost. Through the loss of nigrostriatal neurons, the information supply for the muscles to uphold the righting reflex ceases and the afflicted have to correct their posture consciously and visibly (Parkinson 2002; Traub et al., 1980).

The cardinal symptoms are often times accompanied by a number of facultative symptoms, which may not be present or develop during the progression of the disease. They can be divided into vegetative, sensory and psychological disturbances. Affliction of the vegetative system usually occurs in later stages of the disease. They involve increased tallow production (Burton et al., 1973), especially in facial areas, orthostatic hypotension (Vanderhaeghen et al., 1970), bladder (Murnaghan, 1961) and sexual dysfunction (Bowers et al., 1971), digestive disturbances (Edwards et al., 1992) and deranged thermoregulation (De Marinis et al., 1991). Sensory symptoms include hyposmia (Murofushi et al., 1991) as well as joint and muscle pain and can manifest in earlier stages of the disease (Roos et al., 1989). Psychological changes contain depression (Kearney, 1964) and bradyphrenia, a deceleration of thought processes (Rogers, 1988). All these symptoms can in some way be traced back to the loss of dopaminergic neurons in the SN *pars compacta*.

2.1.3 The genesis of Parkinson's disease

While the above-mentioned symptoms and their origin are well studied and clarified, the root of the actual disease, the question why the dopaminergic neurons die remains unanswered. To treat and fight the disease it is imperative to find the answer to that question. Especially since the first symptoms start to appear after already 31% of the dopaminergic nigral cells – age adjusted – are gone (Fearnley et al., 1991). A method to diagnose the disease in much earlier stages is important as

well and can also be addressed if the cause of the neuronal cell death is discovered. Around 75% of all PD cases are considered idiopathic; meaning the actual cause of the onset is unknown. The remaining 25% are hereditary and passed down on specific genes (Klein et al., 2012).

The past years, many scientists have channelled their resources to create different hypotheses and accumulated data that may confirm these. The first observation at the cellular level in human dopaminergic neurons of the SN was made by Lewy in 1912. He noticed some odd aggregated proteins, which he described as “serpentine or elongated eosinophilic intracytoplasmic balls”, found in the brains of patients had made them act and think differently (Lewy et al., 1912). These aggregated proteins came to be known as Lewy-bodies named after their discoverer.

Lewy did not have the means of more modern times to further study the nature and composition of these protein bodies. Now it is known fairly well that Lewy-bodies mostly comprise of the protein alpha-synuclein (SNCA), as well as ubiquitin (UBQ) (Engelender, 2008), alpha B crysalline (CRYAB) (Rekas et al., 2004), neurofilaments (NFs) (Goldman et al., 1983) and, occasionally, Tau proteins (Ishizawa et al., 2003). SNCA is expressed mostly in neurons and localizes to presynaptic terminals, that release neurotransmitters into the synaptic cleft between the SN *pars compacta* and the *striatum*. There, SNCA interacts with other proteins and phospholipids in SNARE complexes and is believed to cluster synaptic vesicles to maximize release of the neurotransmitter (Burré et al., 2010). Thus, its over-representation in PD patients might point to a compensatory effect to increase dopamine levels in the synaptic cleft.

The other three common components of Lewy-bodies (UBQ, CRYAB, NFs) normally work as partners to ensure SNCA degradation. Damaged SNCA is marked with UBQ to prepare it for degradation (Engelender, 2008), while CRYAB, as a heat-shock protein, prevents aggregation of the damaged proteins (Cox et al., 2017) and NF plays a part in the transport between cell body and synapse (Hoffman et al., 1975). It is interesting to note, that Lewy-bodies first occur in the *medulla oblongata*, the *bulbus olfactorius* and the *pontine tegmentum* without causing any symptoms (Braak et al., 2006).

The *medulla oblongata* is part of the brain stem and responsible for autonomic functions like breathing (Breckenridge et al., 1950), heart rate (Rosen, 1961) and blood pressure (Gutman et al., 1962), while the *bulbus olfactorius* is a prosencephalic structure linking to the nasal cavity that transmits olfactory information to the *hippocampus* (Cragg, 1960) or the *amygdala* (Fujita et al., 1964). Further, it is linked to the cortex via the *rhinencephalon* and the *thalamus* or to the *hypothalamus* through the *septum pellucidum* and the *tuberculum olfactorium* (Courtiol et al., 2017). The *pontine tegmentum* is also part of the brain stem close to the *medulla oblongata* and also governs autonomic functions like sleep (Zolovick et al., 1973), arousal (Chu et al., 1974) and vigilance (Sato et al., 1979). Non-pathological Lewy-bodies at these sites may point to a higher

vulnerability to stress in the neurons of the SN *pars compacta*.

2.2 Three major theories of the onset of Parkinson's disease

2.2.1 Dopaminergic neurons in Parkinson's disease suffer disruption of their protein homoeostasis

Lewy bodies are a central point in the first hypothesis that aims to explain the cause of the dopaminergic cell death. For the protein to aggregate to an amount that the cellular prevention system cannot process anymore, the SNCA production, its degradation or both have to be gravely altered. In cells, two waste disposal systems exist to get rid of bad proteins. One of them is called autophagy, a process during which the bad proteins are wrapped inside a membrane called phagophore to build autophagosomes and later degraded in acidic conditions after fusion of the autophagosome with a lysosome to efficiently recycle the resources that were used to build the proteins (Mizushima et al., 2011). The other one is the proteasome, a big protein complex build from two subunits that destroys the peptide bond of threonines through a nucleophilic attack of the hydroxyl group of the amino acid (Bochtler et al., 1999).

The theory of autophagic system breakdown as a cause for PD is supported by different studies, describing genes that are implicated in familial PD and related to autophagy. Loss of function mutations of the cation-transporting ATPase 13A2 (ATP13A2) have been shown to cause hereditary PD. The protein encoded by the gene ATP13A2 is important for lysosomal acidification through ATP dependent pumping of protons into the lysosome (Ramirez et al., 2006). Leucine-rich repeat serine-threonine protein kinase-2 (LRRK2) mutations can also cause familial PD. The protein itself is not immediately involved with autophagy, but its loss causes SNCA to be hyperphosphorylated at S129, thus preventing autophagic degradation of SNCA (Qing et al., 2009). In turn, SNCA itself inhibits autophagy by displacing the protein autophagy related 9 (ATG9), a key member for phagophore formation (Winslow et al., 2010).

2.2.2 Microglia activation eradicates dopaminergic neurons

The second theory of PD's onset revolves around microglia and the blood-brain-barrier. Brain tissue does not only feature neurons. There are also astroglia, oligodendrocytes and microglia. The former supply neurons with nutrients from the blood, clear neurotransmitters from synaptic clefts, regulate ion concentrations of the cerebral fluids and dispose of the neuronal waste (Bélanger et al., 2009). Oligodendrocytes support neurons by isolating the axons with myelin, thus increasing the speed the

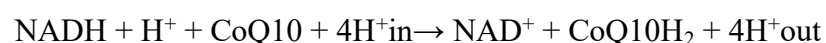
electrical signal can travel across the axon (Simons et al., 2015). Microglia take care of pathogens and aberrant cells. They always survey their surroundings for possible hazards and, once found, they change into an active state, phagocytose the pathogens and send out a complex set of extracellular signaling molecules that promotes inflammation in infected or damaged tissue. Should the microglia phagocytose a certain amount of hazardous substances, they lose their ability to phagocytose and become so-called inactive glitter cells (Fu et al., 2014).

In PD *post mortem* brains it was shown, that the SN features a lot of activated microglia in response to Lewy-bodies. Chronic tissue inflammation like this has proven to be toxic to the surrounding neurons, due to the cytotoxic nature of the extracellular signaling molecules of the microglia (Vila et al., 2001). The simultaneous release of cytokines – a set of small extracellular signaling proteins that cause inflammatory responses – and the presence of protein aggregates damage the blood-brain-barrier by interacting with receptors of the endothelial cells (Zlokovic, 2008). To supply the brain capillaries with fresh endothelial cells the vascular endothelial growth factor (VEGF) together with its receptor keep the cell in a proliferative state. Over time, without replenishing the old capillaries break down, causing the overall tissue structure to weaken and a shortage of nutrients. On top of that, gap junctions, that normally allow only a certain set of molecules to enter the cerebral environment, also break down causing vascular leakiness allowing potentially harmful molecules to enter the brain (Sweeney et al., 2018).

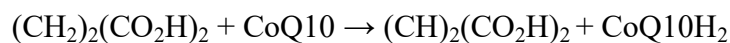
2.2.3 Oxidative phosphorylation and Parkinson's disease

Finally, the third major hypothesis for the origins of PD revolves around the mitochondria. These are semi autonomous cell organelles that supply the cell with high amounts of adenosine triphosphate (ATP) via the respiratory chain, a set of five large complexes located inside the inner membrane of mitochondria (Fig. 2.2). The respiratory chain is an electron transport system with connected redox molecules that gradually reduces the energy level of the electrons (Sousa et al., 2018).

The first and largest enzyme of this system is the NADH:ubiquinone oxidoreductase, also referred to as complex I, that catalyzes the transfer of electrons from the reduced form of nicotinamide adenine dinucleotide (NADH) to ubiquinone (CoQ10) and also transfers four protons per NADH oxidation from the matrix across the inner mitochondrial membrane into the intermembrane space. The equation of the reaction is as follows:

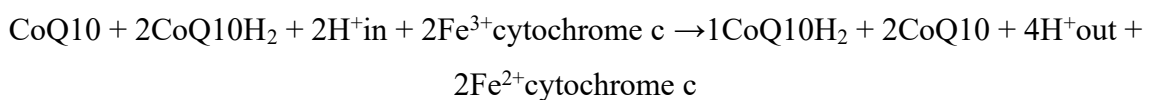


The complex I can be divided into two distinct parts. A hydrophobic intermembrane arm that catalyzes the proton transport and a hydrophilic arm inside the mitochondrial matrix. All redox reactions occur in the latter. In the first step, bound NADH transfers two electrons to the complex I integrated flavin mononucleotide (FMN) to produce FMNH₂. Through seven different iron sulfur (Fe-S) clusters the electrons are then transferred to CoQ10. This transfer also causes conformational changes in the enzyme allowing four protons to traverse the inner membrane (Sousa et al., 2018). The succinate dehydrogenase – or complex II – is the smallest subunit of the respiratory chain and also a source of CoQ10H₂ independent of complex I. The equation of the reaction is as follows:



This reaction is also part of the tricarboxylic acid (TCA) cycle, a separate source of energy, and the only interface between the respiratory chain and the TCA cycle. Succinate, derived from the TCA cycle, may bind to the complex II and become oxidized to fumarate through an elimination reaction with flavin adenine dinucleotide (FAD) as electron acceptor, thus producing FADH₂. The electrons are then again transferred to three different Fe-S clusters that finally deliver them onto the CoQ10 to yield CoQ10H₂ (Sousa et al., 2018).

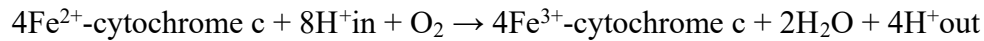
Third in row is the coenzyme Q – cytochrome c reductase, or complex III, that receives the CoQ10H₂ from the complexes I and II for further processing, facilitating the reaction of the so called “Q cycle”. The equation of the reaction is as follows:



One molecule of CoQ10H₂ and CoQ10 simultaneously bind the complex III, two electrons of the CoQ10H₂ are taken up by a Fe-S cluster and a B_L heme, thus causing two protons to be released into the intermembrane space. The electron bound to the B_L heme is transferred to a B_H heme and subsequently moved to the CoQ10 finally yielding an ubisemiquinone (CoQ10H•). The electron bound to the Fe-S cluster is first moved to cytochrome c₁, a subunit of the complex III, and finally to a cytochrome c molecule, reducing the bound Fe³⁺ to Fe²⁺. The newly oxidized CoQ10 is released and replaced by another molecule of CoQ10H₂ while the CoQ10H• remains bound. The new bound CoQ10H₂ repeats the previously described process, causing the CoQ10H• to be reduced to CoQ10H₂ and released (Sousa et al., 2018).

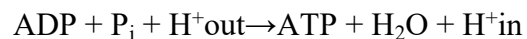
The freshly reduced cytochrome c is transferred to the cytochrome c oxidase, or complex IV. Here the reduced cytochrome c is, through a complex series of reactions, used to reduce oxygen to water.

The equation of the reaction is as follows:



The electrons delivered by the cytochrome c are transferred to one of the two copper centers, Cu_A , inside the enzyme and subsequently delivered to a cytochrome a, which then moves an electron into the binuclear cytochrome a_3 - Cu_B center. Here O_2 and four protons from the mitochondrial matrix together react to H_2O . This reaction allows four additional protons to be moved from the matrix towards the intermembrane space (Sousa et al., 2018).

The last unit of the respiratory chain, the ATP synthase, or complex V, uses the electrochemical proton gradient established by the combined activity of the other four complexes to synthesize ATP from adenosine diphosphate (ADP) and inorganic phosphate (P_i). The equation of the reaction is as follows:



The complex V can be divided into two parts, a hydrophobic part (F_O) anchored in the membrane that constitutes a tunnel for proton movement along the electrochemical gradient and a hydrophilic part (F_1) in the mitochondrial matrix that hydrolyzes the ADP to ATP through a rotational motor mechanism. Passing protons cause a subunit of F_1 through conformational changes of the F_O to rotate and force the P_i and the ADP to unify (Sousa et al., 2018).

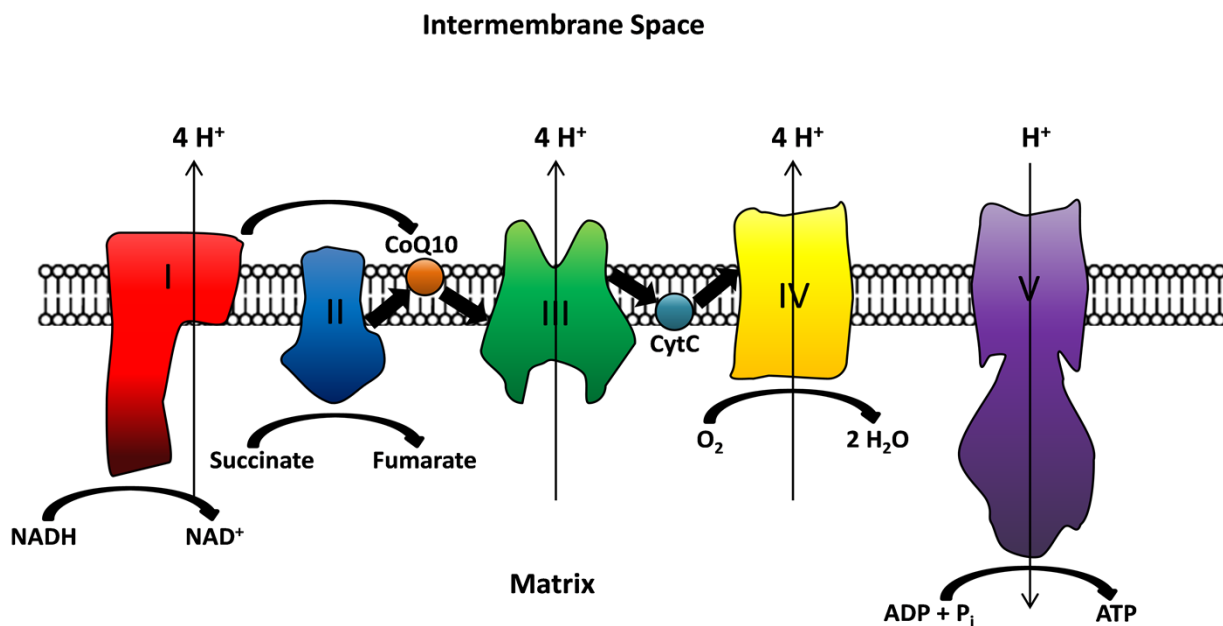


Figure 2.2: The respiratory chain. Complexes I and II shuttle electrons through CoQ10 to the complex III, while regenerating NAD^+ or participating in the TCA. The complex I translocates four H^+ to the intermembrane space.

Complex III transfers the electrons from CoQ10 to cytochrome C and also translocates four H⁺. Complex IV transfers the electrons from cytochrome C to O₂, generating water, and transferring two protons per cytochrome C. The complex V uses the established H⁺ gradient to generate ATP.

Cases of PD have reportedly shown disturbances in their mitochondrial metabolism and homeostasis. The electron transport system across the mitochondrial complexes is prone to the production of reactive oxygen species (ROS), especially when CoQ10H•, an unstable radical, is produced as an intermediate (Turrens et al., 1985). Electrons from these radicals or from the Fe-S clusters may leak to oxygen molecules to yield ROS, which may damage other parts of the mitochondria or the cell. Usually mitophagic processes get rid of dysfunctional mitochondria. However, disturbances in either of these two processes surrounding mitochondria may lead an accumulation of ROS and thus cell death (Radogna et al., 2016).

Excessive ROS production might also account for the formerly explained two theories of PD's onset. SNCA oligomers have been shown to induce ROS (Deas et al., 2016). Active microglia also produce a lot of ROS and use them to signal to peripheral immune cells, which might cause damage to the blood brain barrier (BBB) (da Fonseca et al., 2014). On the other hand, excessive cellular ROS production leads to increased amounts of damaged cell compartments that need to be repaired or replaced, thus pushing the cellular waste disposal systems to their limits (Liu et al., 2007). Postmortem brain tissue from sporadic PD patients consistently show high levels of oxidation in the SN (Jenner et al., 1996).

2.3 Oxidative stress

2.3.1 Endogenous ROS sources

Upheaval of the balance between ROS production and detoxification, be it an increase of the former or a decrease of the latter, results in oxidative stress. ROS are mostly, but not exclusively, formed at the mitochondria during the course of oxidative phosphorylation. Cells that lack mitochondrial activity through genetic manipulation still show basal levels of ROS, indicating that mitochondria are not the sole source of these damaging agents (Seaver et al., 2004). Indeed, certain sets of enzymes that include xanthine oxidases, nicotinamide adenine dinucleotide phosphate (NADPH) oxidases and cytochrome P450 enzymes also produce ROS. The former is part of the catabolism of purines (Aitken et al., 1993), while NADPH oxidases cause ROS to be imported into the cell (Miesel et al., 1995). Cytochrome P450 enzymes belong to a super-family of proteins that usually detoxify possible pathogens, which often generate ROS as a side product (Bondy et al., 1994).

2.3.2 ROS classification and mechanism of oxidation

Not every ROS is the same. They differ in their chemical properties, their composition and their reactivity, but carry at least one atom of oxygen (Table 2.1).

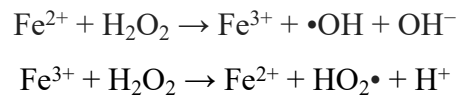
| ROS | Formula | Half life |
|-----------------------|------------------------|--------------------------------------|
| Superoxide anion | $\bullet\text{O}_2^-$ | 10^{-5} s (Reth, 2002) |
| Hydrogen peroxide | H_2O_2 | 1 ms (Reth, 2002) |
| Hydroperoxyl radical | $\text{HO}_2\bullet$ | 10 s (Cutler et al., 2003) |
| Hydroxyl ion | OH^- | Stable |
| Hydroxyl radical | $\bullet\text{OH}$ | 10^{-9} s (Halliwell et al., 1999) |
| Organic hydroperoxide | ROOH | Stable |
| Alkoxy radical | $\bullet\text{RO}$ | 10^{-5} s (Fuchs, 1992) |
| Peroxy radical | $\bullet\text{ROO}$ | 10 s (Cutler et al., 2003) |
| Hypochlorous acid | HOCl | <1 min (Mütze et al., 2003) |
| Peroxynitrite | ONOO^- | 10^{-3} s (Pacher et al., 2007) |

Table 2.1: Reactive oxygen species. Overview of ROS species with full name, chemical formula and half time.

Due to its high reaction potential, is O_2 not allowed to freely float through the cell. In neurons, O_2 is bound to neuroglobin (NGB), a globin protein, to directly deliver it to the mitochondria, where it is used in the complex IV (Burmester et al., 2000, 2009). Other cellular processes might also require O_2 , but about 95% of the oxygen is consumed in the mitochondria (Wilson et al., 2012). High concentrations of O_2 in the mitochondria, however, can give rise to ROS through electron leakage (Turrens et al., 1980).

The most common result of electron leakage is a superoxide anion ($\bullet\text{O}_2^-$) (Turrens et al., 1980). By itself, $\bullet\text{O}_2^-$ is not very reactive, but it can remove Fe^{2+} from the Fe-S clusters inside the complexes, thus interrupting the electron chain, possibly producing more $\bullet\text{O}_2^-$ (Popović-Bijelić et al., 2016; Halliwell et al., 1976). In aqueous solution, $\bullet\text{O}_2^-$ reacts with water to hydroperoxyl radicals ($\text{HO}_2\bullet$) in an equilibrium (Halliwell et al., 1999). Unlike $\bullet\text{O}_2^-$, $\text{HO}_2\bullet$ is more reactive and can remove hydrogen atoms from polyunsaturated fatty acids possibly initiating lipid peroxidation by forming lipid radicals that propagate throughout and destabilize the membrane from one carbon to the next (Bieri, 1959). Lipid radicals can react with molecular oxygen leading to lipid peroxy radicals that in turn can react with another lipid to form lipid hydroperoxide and another lipid radical (Wolfson et al., 1956). Especially unsaturated fatty acids are prone for peroxidation (Bunyan et al., 1968), which increases membrane rigidity (Dobretsov et al., 1977) and alters their permeability (Smolen et al., 1974).

Hydrogen peroxide (H₂O₂) is a thermodynamically unstable metabolite of •O₂⁻ and may decompose to O₂ and H₂O (Davey, 1925). However, if Fe²⁺ is present, it undergoes a different reaction, called Fenton reaction that auto-catalytically produces highly reactive radicals (Fenton, 1894).



The two radicals produced by the Fenton reaction, •OH and HO₂•, are both capable of initiating lipid peroxidation (Gutteridge, 1984). The hydroxyl radical (•OH), however, is far more dangerous than the HO₂•, since it is even less stable, with a half-life of 10⁻⁹ s *in vivo*, and will react with any macromolecule in its path, be it carbohydrates, nucleic acids, lipids or proteins (Cutler et al., 2003). On the other hand, ROS do not only damage compartments of the cells. They are also utilized by macrophages and micorglia to get rid of infectious organisms like bacteria (Ano et al., 2010) or in signaling pathways (Rhee, 2006).

Hypochlorous acid (HOCl), for example, is produced through a myeloperoxidase that combines a molecule of H₂O₂ with a chloride ion and also belongs to the group of ROS (Harrison et al., 1976). It can easily oxidize thiol groups and amino groups of proteins (Pereira et al., 1973). Usually, protein oxidation leads to a swift degradation of the damaged protein, but sometimes this damage is intentional. Through the oxidation of methionine – a process the cell can reverse (Sharov et al., 2000) – subsequent phosphorylation of nearby serine, threonine or tyrosine sites is inhibited and thus the protein's function is heavily influenced (Veredas et al., 2017). Due to these features HOCl is also used to defend the cell against intruders (Thomas, 1979) similar to •O₂⁻ (Ano et al., 2010) as well as peroxynitrite (ONOO⁻) (Augusto et al., 1996), which is produced from a reaction of H₂O₂ and nitrite (NO₂⁻) (Saha et al., 1998).

2.3.3 Endogenous removal of ROS

Superoxide dismutase (SOD) enzymes detoxify the •O₂⁻, generating O₂ and H₂O₂ (McCord et al., 1969). Two different kinds of SODs exist. The cytosolic CuZn-SOD, SOD1 and the mitochondrial Mn-SOD, SOD2. The catalyzed reaction, however, is very similar. In a first step the Cu²⁺ or the Mn³⁺ is reduced to oxidize the •O₂⁻ to O₂. Cu and Mn are regenerated through reduction of another •O₂⁻ with 2H⁺ to H₂O₂. (Tainer et al., 1983; Borgstahl et al., 1992) This, however, leaves mitochondrial produced H₂O₂ in close proximity to iron, which may initiate Fenton chemistry and severely damage mitochondrial compartments.

Damage to the mitochondrial genome through ROS, for example, can lead to critical mutations that

will slowly dysfunctionalize the mitochondria (Tanaka et al., 1996). Since repair systems are not as efficient as inside the nucleus (Larsen et al., 2005), H_2O_2 must be taken care of before it can react with the iron ions. Cells use the enzyme catalase to remove H_2O_2 molecules and turn them into H_2O and O_2 (Loew, 1900).

Vitamin E and C as well as glutathione (GSH) can intercept the lipid peroxidation cycle at different points. The vitamins can substitute for a lipid in the reaction with the lipid peroxy radical, resulting in stable vitamin radicals and lipid hydroperoxide. However, since lipid hydroperoxide itself is still quite unstable, GSH can detoxify it to stable lipid alcohols. GSH is dimerised to glutathione disulfide (GSSG) that is reconstituted by a GSH reductase. On top of that, GSH might also intercept lipid radicals to return them to their previous state (Ayala et al., 2014; Benzie, 1996).

2.3.4 Increased ROS vulnerability of SN *pars compacta* neurons

Dopaminergic neurons of the SN *pars compacta* have been shown to be highly susceptible to oxidative stress that was often traced back to strained mitochondria (Henchcliffe et al., 2008). Those neurons have an intrinsic pacemaker driven by Ca^{2+} channels that works without afference to maintain basal dopamine levels in *striatum* (Sanghera et al., 1984). Constant use of this channel leads to high intracellular Ca^{2+} levels that need to be removed through ATP dependent carrier proteins (Ivannikov et al., 2010). Yet, mitochondrial mass in dopaminergic neurons of the SN *pars compacta* is low compared to other dopaminergic neurons (Liang et al., 2007). Increased ATP demand paired with lower amounts of mitochondria likely overburdens the organelles making them more prone for ROS production.

Dopamine itself also makes the cells more vulnerable to oxidative stress. Usually the neurotransmitter is mostly stored in vesicles (Mosharov et al., 2003), but should it accumulate in the cytosol, it is rapidly degraded either by a monoamine oxidase (Rosengren, 1960) bound to the outer mitochondrial membrane (Greenwalt et al., 1970) or through autoxidation. Enzymatic degradation of dopamine yields 3,4-dihydroxyphenylacetaldehyde and 3,4-dihydroxyphenylacetic acid and H_2O_2 (Hornykiewicz et al., 1987), which may react according to Fenton chemistry, due to high levels of iron in these neurons (Francois et al., 1986). Autoxidative dopamine degradation, on the other hand, leads to leucoaminochrome that in a cyclic reaction may reduce O_2 to $\bullet O_2^-$ and become aminochrome-*o*-semiquinone which again reduces another molecule of O_2 to $\bullet O_2^-$ and become aminochrome. Through a DT-diaphorase, the aminochrome reacts to leukaminochrome. Another $\bullet O_2^-$ may also demerge from aminochrome yielding indolequinone which is transformed into neuromelanin (Graham, 1986). Thus, high levels of cytosolic dopamine leads to high levels of ROS and cell death.

2.3.5 Exogenous ROS sources

Air and water pollutants have high potential to damage nigral neurons through ROS. Prior to the appearance of clinical symptoms, classical PD pathology reportedly occurs in the *bulbus olfactorius*, which suggests a possible role of inhaled toxins (Braak et al., 2006). Deceased residents of highly polluted areas like Mexico City show high levels of neuroinflammation and accumulation of encapsulated SNCA (Calderón-Garcidueñas et al., 2008). High exposure to particulate matter (PM) has been linked to an increased risk of PD (Liu, et al. 2016), but this is currently still under discussion. In animal models, however, PMs were shown to reach the brain and act as neurotoxins (Calderón-Garcidueñas et al., 2002; Zanchi et al., 2008).

The composition of these PMs can vary depending on the surrounding environment and is important in regard to their ability to produce ROS (Perrino et al., 2015; Mateus et al., 2013). PMs in rural areas consist of pollen and crustal materials, in urban areas of exhaust and combustion, side products of anthropogenic origin (Kundu et al., 2014). Generally, in urban areas PMs have high amounts of metals (Cr, Co, Ni, Mn, Zn, V, Cu and mostly Fe) and polycyclic aromatic hydrocarbons (PAHs) (Harrison et al., 1995). Especially Fe and Cu can accelerate ROS generation through Fenton chemistry (Gutteridge, 1983). In human endothelial lung cells, ultrafine (20-80 nm diameter) titan oxide (TiO₂) particles have been shown to elicit release of free radicals (Singh et al., 2007). Another study found increased lipid peroxidation as well as SOD and catalase levels after PM exposure *in vivo* (Gurgueira et al., 2002). Through the *bulbus olfactorius* possible pathogens like TiO₂ may bypass the BBB (Hanson et al., 2008).

2.4 Models of PD

2.4.1 Oxidopamine

Over the course of time, a few chemical models of PD have been established deriving from different herbicides, most of which have become banned from using. The first model, oxidopamine (6-ODHA) (Fig. 2.3), established in the 1960s, however, was never used as a pesticide. 6-ODHA is structural analogous to dopamine, that has one additional hydroxyl-group and demonstrates similar autoxidative properties to dopamine (Soto-Otero et al., 2000). Since it has been shown to appear in brain (Curtius et al., 1974) and urine (Andrew et al., 1993) of PD patients, 6-ODHA is considered an endogenous neurotoxic factor in the pathogenesis of PD.

It is used as an *in vivo* model to generate lesions in the dopaminergic neurons of the SN. The specificity of the chemical is given through its dependance on dopamine transporters (DATs) to

enter the cell (Ungerstedt, 1968). A big downside of this model is its technical limitations. Since the 6-OHDA cannot transverse the BBB, it has to be injected directly into the SN to take its effect (Blandini et al., 2008). Over a short period of time (12 hours to 2-3 days), the cells of the *pars compacta* die (Ungerstedt, 1968). Often the VTA, which is dopaminergic, yet only implicated in late stage PD, is used as a control to judge the toxicity of the model (Przedborski et al., 1995). Unlike the disease, this model does not feature an accumulation of Lewy-bodies (Ungerstedt, 1968).

2.4.2 1-Methyl-4-phenylpyridinium

In the 1970s, the chloride salt of 1-methyl-4-phenylpyridinium (MPP^+) (Fig. 2.3) was used as a herbicide under the term cyperquat, until in 1976 a young man named Barry Kidston showed up with PD like symptoms (Vinken et al., 1994; Langston et al., 2014). He had ingested home-brewed desmethylprodine (MPPP), that was polluted with 1-methyl-4-phenyl-1,2,3,6-tetrahydropyridine (MPTP) (Langston et al., 1983). He died 18 months later from an overdose of cocaine. During his autopsy, forensics discovered a loss of dopaminergic neurons in the SN and an accumulation of Lewy-bodies (Davis et al., 1979). In subsequent studies in rodents and non-human primates, MPTP was verified as the origin of Kidston's Parkinsonism (Langston et al., 1984). However, scientists were unable to reliably reproduce the Lewy-body pathology in the MPTP model, except for some primate studies (Kowall et al., 2000). Regardless, ever since its discovery, MPTP has been the most common *in vivo* model system for PD, since it is much more easy to incorporate than 6-OHDA.

The mechanism behind the MPTP mediated pathology has, of course, also been studied extensively. Once MPTP enters the brain area, it is metabolized in astrocytes by the monoaminoxigenase B (MAO-B) to MPP^+ (Ransom et al., 1987). Due to its structural similarity to dopamine, MPP^+ can specifically enter dopaminergic neurons through DATs (Kitayama et al., 1993). There, it interferes with the complex I of the mitochondria and uncouples the electron chain, causing massive amounts of ROS to be released and thus cell death of dopaminergic neurons in the SN (Nicklas et al., 1985). Where exactly the MPP^+ interferes with the complex I remains in the open. MPP^+ itself cannot cross the BBB, thus MPTP has to be administered if the model is to be used *in vivo* (Riachi et al., 1989).

2.4.3 Rotenone

Another common chronic model of PD, called rotenone (Fig. 2.3), follows a similar mechanism. Rotenone is an isoflavone that, like MPP^+ , was also used as a pesticide (Ebeling, 1945) and reportedly causes cell death of the dopaminergic neurons in the SN (Betarbet et al., 2000). Unlike

the previous models, the rotenone model features Lewy-body pathology (Sherer et al., 2003) and the toxic mechanism is similar to that of MPP⁺ (Oberg, 1961). Rotenone inserts itself into the complex I and disrupts the electron transfer at the CoQ10 binding site (Horgan et al., 1967). Overflowing electrons are then transferred to O₂ and thus produce ROS (Li et al., 2003). Rotenone is lipophilic and can cross the BBB like MPTP (Caboni et al., 2004). However, rotenone lacks the specificity of 6-OHDA or MPTP. It can enter any cerebral cell and is not limited to dopaminergic neurons. Thus, concentrations have to be adjusted very carefully. Due to this, the model often encounters problems with high mortality rates (Zhang et al., 2017). While rotenone and MPTP strongly increase ROS output, they also cause ATP depletion in affected cells, since the complex I can no longer help to sustain the proton gradient used by the complex V (Giordano et al., 2012). Especially, rotenone and MPP⁺ are nowadays very often used as model systems, because complex I inhibition has also been shown to be a possible pathology of PD (Schapira et al., 1990).

2.4.4 Paraquat

The most recent model, paraquat (Fig. 2.3), was also used as a herbicide, but got banned in the EU in 2007 when it became evident that paraquat exposure associated with a higher risk of PD affliction (Court of first instance of the european union, 2007). Paraquat has a similar structure to MPP⁺ and also uses DATs to enter specifically dopaminergic neurons, but does not interfere with the complex I (Rappold et al., 2011). It rather works as a redox cyler by taking electrons from donors like NADPH and transferring it to O₂ yielding •O₂⁻ (Bus et al., 1984). Paraquat treatment in mice has shown impairment of motor activity and a loss of dopaminergic cell mass in the SN (Brooks et al., 1999) with the presence of Lewy-bodies (Manning-Bog et al., 2002). At the moment, there is still a discussion whether or not paraquat is a sufficient model system (Berry et al., 2010).

2.4.5 Other models

Of course, not only these described chemicals can induce PD like symptoms. Chronic exposure to the highly controversial glyphosate (Fig. 2.3), for example, has been reported to induce mitochondrial dysfunction and increased ROS generation *in vitro* (Kašuba et al., 2017), in *C. elegans* (Bailey et al., 2018) and in rats (Astiz et al., 2012). The mechanism behind this, however, remains elusive. So far, glyphosate may not be used as a model of PD, but in the future, it might become one. These environmental toxins have been shown to cause PD like symptoms, but these are not the only models used to study PD. Molecular structures of some molecu

Hereditary models of mutations, that actually account for ~25% of PD cases worldwide, exist.

These genes include SNCA, LRRK2, phosphatase and tensin homolog induced putative kinase 1 (PINK1), Parkin (PRKN) and Parkinson disease protein 7 (PARK7). It is interesting to note that all of these corresponding proteins have been implicated in clearance of ROS or removal of damaged mitochondria, also supporting the ROS theory (Deng et al., 2018).

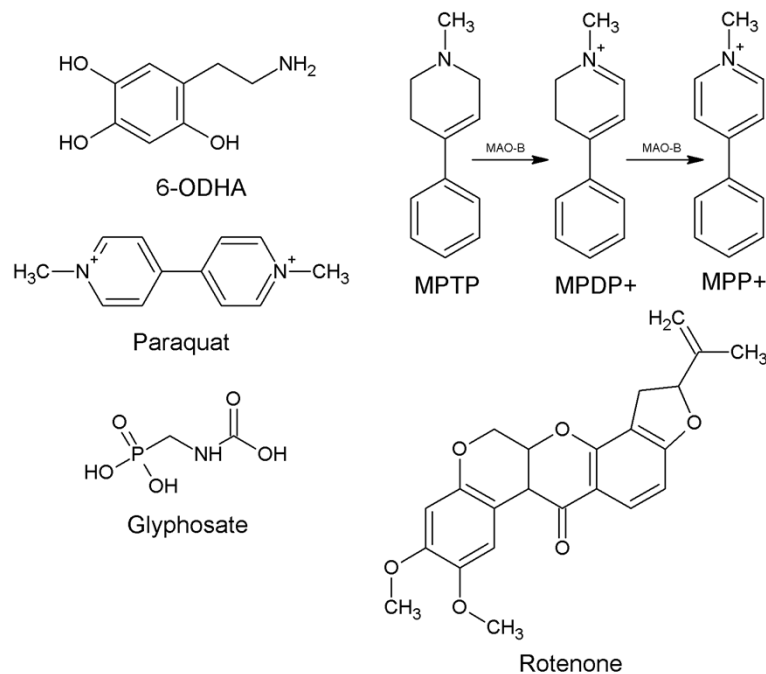


Figure 2.3: PD linked toxins. Formula of small molecules causing PD like pathologies. MPTP is a protoxin that is metabolized by MAO-B to yield the toxin MPP⁺. Structures were created using ChemSketch V5, Advanced Chemistry Development, Inc., Toronto, On, Canada, www.acdlabs.com, 2019.

2.5 Antioxidants as possible therapeutics

2.5.1 Vitamin E, C and CoQ10

As already mentioned, cells have many ways to deal with ROS. However, a lot of different compounds can be used by the cell to dispose of ROS independent of enzymes. Vitamin E (α -tocopherol) (Fig. 2.4) is highly lipophilic and distributed abundantly throughout a cell's membrane (Wang et al., 1999). It is a scavenger for ROS and breaks the lipid peroxidation chain (Traber et al., 2007). Vitamin C (Fig. 2.4), on the other hand, is water soluble and reacts with ROS in the cytosol, while also regenerating vitamin E from its radical (Guaiquil et al., 2001). CoQ10 (Fig. 2.4), the final electron acceptor in complexes I and II, can protect lipids, proteins and DNA by directly quenching ROS and taking two electrons to form CoQ10H₂ (Frei et al., 1990).

Since vitamin E and C are used by the cell itself to fight ROS, many studies have investigated whether additional vitamins might prove beneficial for PD patients. Unfortunately, a lot of those studies contradict each other. An investigation whether vitamin E administration was able to protect

from 6-OHDA induced cell death proved successful *in vivo* (Roghani et al., 2001). While a combined treatment with vitamin E and C in humans at first showed promising results (Fahn, 1992), double blind follow up trials completely belie those data, showing no benefits in PD (Parkinson Study Group, 1993). On the other hand, a study more recently suggested that high dietary uptake of vitamin E reduced the risk of PD (Zhang et al., 2004). For vitamin C, the results are even more disappointing. Some studies report a positive (Zhang et al., 2004), some none (Etminan et al., 2005) and some even a negative response (Heikkila et al., 1987).

Other postmortem studies have shown an accumulation of CoQ10H₂ in the blood plasma and platelets of PD patients (Buhmann et al., 2004). This might point to an overload of the CoQ10 dependent redox system and administration of additional CoQ10 might prove beneficial. Indeed, CoQ10 was able to avert rotenone and paraquat induced mitochondrial dysfunction and neurodegeneration in mesencephalic primary neurons. This extended even to a protection of the mitochondrial membrane potential and caused the organelles to produce less ROS (Moon et al., 2005). This was verified *in vivo* in mice exposed to MPTP (Beal, 1998). Oral treatment in primates also showed protective effects of CoQ10 (Horvath et al., 2003). However, in clinical trials only high amounts of oral administration of CoQ10 showed a protective trend, but no significances (NINDS NET-PD Investigators, 2007).

2.5.2 MitoQ and MitoVitE

Since usually a lot of these antioxidants have to be administered in clinical studies to observe beneficial effects, antioxidants have been developed that are immediately localized to the mitochondria. This is achieved by merging the antioxidant to a lipophilic cation such as triphenylphosphonium (TPP). Through its hydrophobic surface TPP has the ability to swiftly cross membranes (Ross et al., 2005). The positively charged phosphorous atom ensures accumulation inside the mitochondria driven by the membrane potential generated by the proton gradient (Lieberman et al., 1969).

Mitoquinone (MitoQ) is such a merged antioxidant. It predominantly locates to the matrix-facing surface of the inner mitochondrial membrane with the quinone part of the compound integrating into the interior of the membrane. There, the MitoQ confidentially scavenges ROS and protects the membrane from lipid peroxidation (Kelso et al., 2001). After detoxification complex II recycles the MitoQ. Complex I, on the other hand, only reduces oxidized MitoQ poorly (James et al., 2005). However, MitoQ redox cycling can also, under certain circumstances, generate ROS like its parent CoQ10 (Doughan et al., 2007). In PD model studies *in vitro* as well as *in vivo*, MitoQ has shown very promising effects. It was able to be neuroprotective against MPP⁺ and MPTP, protecting the

dopaminergic neurons of the SN (Ghosh et al., 2010). Clinical trials of MitoQ so far, however, have been unsuccessful (Snow et al., 2010).

Vitamin E was chronologically the first antioxidant conjugated to TPP. The result of this reaction was referred to as MitoVitE, which accumulated in high amounts inside the mitochondria and efficiently scavenged ROS (Smith et al., 1999). When given to mice, MitoVitE is rapidly distributed to tissue that shows the highest oxidative stress, suggesting that the organism's vitamin E transportation is readily used for MitoVitE as well (Smith et al., 2003). High levels of MitoVitE, however, proved to be cytotoxic (Covey et al., 2006). As of now, clinical data regarding the potential of MitoVitE are still lacking.

2.5.3 Phenothiazine

So far, however, all of the other antioxidants have been lackluster in clinical trials (Fahn, 1992; Parkinson Study Group, 1993; Etminan et al., 2005; NINDS NET-PD Investigators, 2007; Snow et al., 2010). They are either not strong enough in their antioxidative properties, unable to pass the BBB or can cause secondary negative effects in the patient. A few years ago, a promising antioxidant taking the name of phenothiazine (PHT) (Fig. 2.4) has emerged (Moosmann et al., 2001). It has shown very strong neuroprotective effects in primary neuronal cell cultures in the MPP⁺ model (Hajieva et al., 2009), as well as in *C. elegans* even in very low doses (Mocko et al., 2010). How it fares in *in vivo* studies in mammals or humans still remains to be seen.

PHT is likely to travel through the BBB since many of its derivatives are commonly used antipsychotics. Before it was superseded by better drugs, PHT was used as antihelmintic in humans. Thus, possible side effects are known and shown to be quite scarce (Ohlow et al., 2011). PHT might have what it takes to become a possible treatment option for PD, but more studies have to be done at first. Since the available PD treatment so far only revolves around symptom management through L-DOPA and acetylcholinesterase inhibitors in late stage PD, a dependable drug that could halt the progression of the disease would be very welcome indeed.

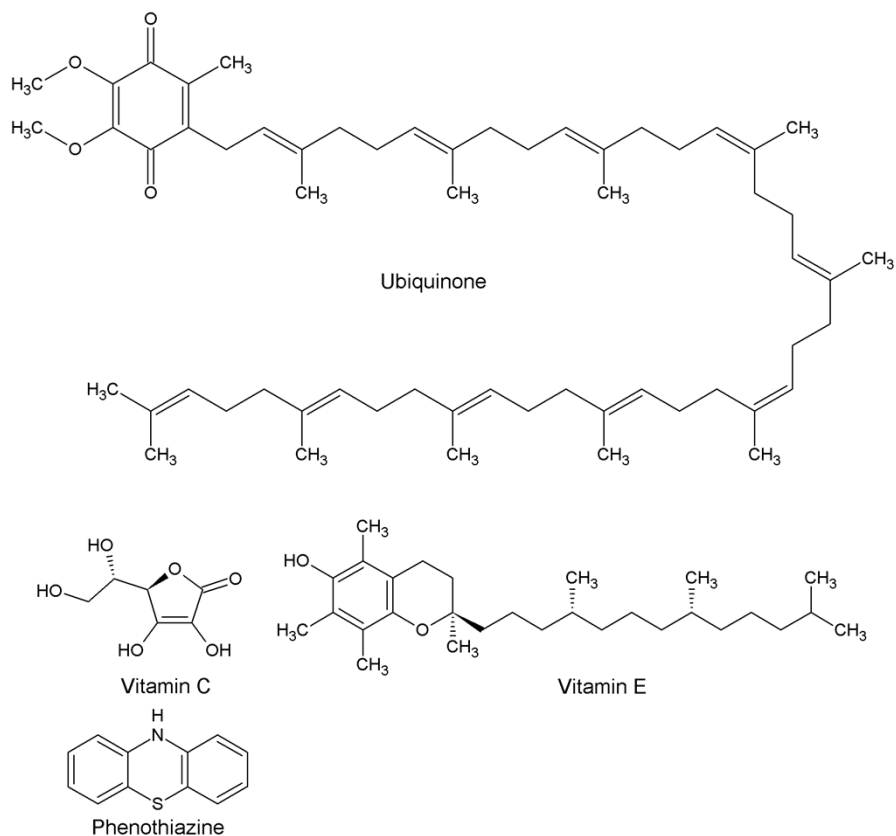


Figure 2.4: Antioxidants. Formula of antioxidants, which have shown protective properties in models of PD. Structures were created using ChemSketch V5, Advanced Chemistry Development, Inc., Toronto, On, Canada, www.acdlabs.com, 2019.

2.6 Epigenetics and Parkinson's disease

2.6.1 Epigenetics

Genetic information is known to be stored on the DNA, the information is then processed and delivered via RNA and finally turned into a functional protein. How and when the information from the DNA is transcribed into RNA without changing the genetic code itself, is regulated by epigenetics which may alter phenotype without altering genotype.

Adrian Bird, a pioneer in the field of epigenetics, once defined epigenetics as the structural adaptation chromosomal regions to code, signal and conserve changed states of activation. These changes in state of activation extends from the development of a cell from a totipotent stemcell to a differentiated somatic cell towards adaptational processes in response to environmental stimuli (Bird, 2007). Nutrient availability in the parent generation has reportedly affected the epigenetic status of their offspring (Geraghty et al., 2016). In turn, oxidative conditions would require the cells to adapt, to either increase assembly of the defense system or shut down the ROS generation sources. Whether epigenetic factors are relevant for neurodegenerative disorders like PD remains to

be seen, but epigenetic adaptations to excessive amounts of ROS have been shown (Franco et al., 2008).

Epigenetic modifications stretch from direct DNA modifications to post translational modifications of DNA adjacent proteins as well as silencing RNA effects (Bird, 2007). Through changes to the nucleosome the DNA is packaged more tightly or opened up resulting in higher or lower transcription levels. These two states are referred to as euchromatin (open) and heterochromatin (closed) (Hsu, 1962). The latter can further be classified as facultative or constitutive heterochromatin. Constitutive heterochromatin is almost always present and required for chromosomal stability for example at the centromere (Saksouk et al., 2015), while facultative heterochromatin is more dynamic and depends on tissue and cell type (Gilbert et al., 2003).

2.6.2 DNA-methylation

Immediate DNA modification in eukaryotes is mostly restricted to methylation of the 5th carbon (C) atom of cytosine in the carbon ring (Hotchkiss, 1948). Cytosine methylation represses transcription of the associated gene most of the times, either through sterical effects or by recruiting with a methyl binding domain (MBD) that blocks the RNA polymerase and causes dissociation of the transcription complex (Rösl et al., 1993).

In mammals, most cytosine methylation is found adjacent to another guanine, termed CpG-methylation (Sinsheimer, 1955). Especially in neurons, however, many non CpG-methylation sites can be observed (Lister et al., 2013). In somatic cells of vertebrates, about 80% of the existing CpG sites are methylated (Ehrlich et al., 1982). The remaining 20%, which are not methylated, are called CpG-islands of which about 50% are located in gene promoter regions (Saxonov et al., 2006). In somatic cells 10% of the CpG islands are indeed methylated, silencing the associated gene's transcription (Jeziorska et al., 2017). Interestingly, CpG islands do not occur as often as expected in the human genome (Lander et al., 2001). This is testimony to a high susceptibility of 5-methylcytosine to mutate. Desamination turns 5-methylcytosine into a thymine, causing a guanine thymine mismatch. Sometimes the DNA repair system is unable to return the base pair to its former state, instead removing the guanine and replacing it with an adenine (Duncan et al., 1980).

Cytosine methylation in humans is established through a family of three enzymes called DNA methyltransferases (DNMTs). This family can be divided into two different kinds of DNMTs, DNMT1 on one side and DNMT3A and DNMT3B on the other side. DNMT1 is a maintenance methyltransferase that is active during replication and requires a hemi-methylated DNA strand as a blueprint (Pradhan et al., 1999; Leonhardt et al., 1992). DNMT3A and DNMT3B on the other hand can establish DNA methylation patterns *de novo* (Okano et al., 1999). DNMT3A and DNMT3B

both can to some degree compensate for a loss of DNMT1 (Rhee et al., 2000), but DNMT1 cannot compensate for a loss of either DNMT3A or DNMT3B (Chen et al., 2003). The *de novo* DNMTs are required for genomic imprinting (Hata et al., 2002), X chromosome inactivation (Nesterova et al., 2008), development (Okano et al., 1999) and epigenetic adaptation (Watson et al., 2014). The former is an epigenetic regulation by which in a parent-of-origin kind of matter one allele is silenced through cytosine methylation (Monk, 1987). For humans about 75 imprinted genes are described (Peters, 2014). X chromosome inactivation, on the other hand, is an example of facultative heterochromatin that almost completely silences randomly one of the two X chromosomes of a female, known as Barr body (Ohno et al., 1959; Lyon, 1961).

Removal of cytosine methylation is catalyzed by enzymes of the ten-eleven translocase (TET) family through stepwise oxidation of the methyl group (Tahiliani et al., 2009). The first intermediate is 5-hydroxymethylcytosine (Tahiliani et al., 2009), which was found to be quite abundant in neuronal cells (Szwagierczak et al., 2010). The second intermediate is 5-formylcytosine and the last 5-carboxycytosine (Ito et al., 2011). These two last intermediates can be targeted by thymine DNA glycolyase (TDG) to excise the base (Maiti et al., 2010; He et al., 2011). The thusly-produced abasic site is then replaced by a cytosine by a DNA polymerase (Weber et al., 2016).

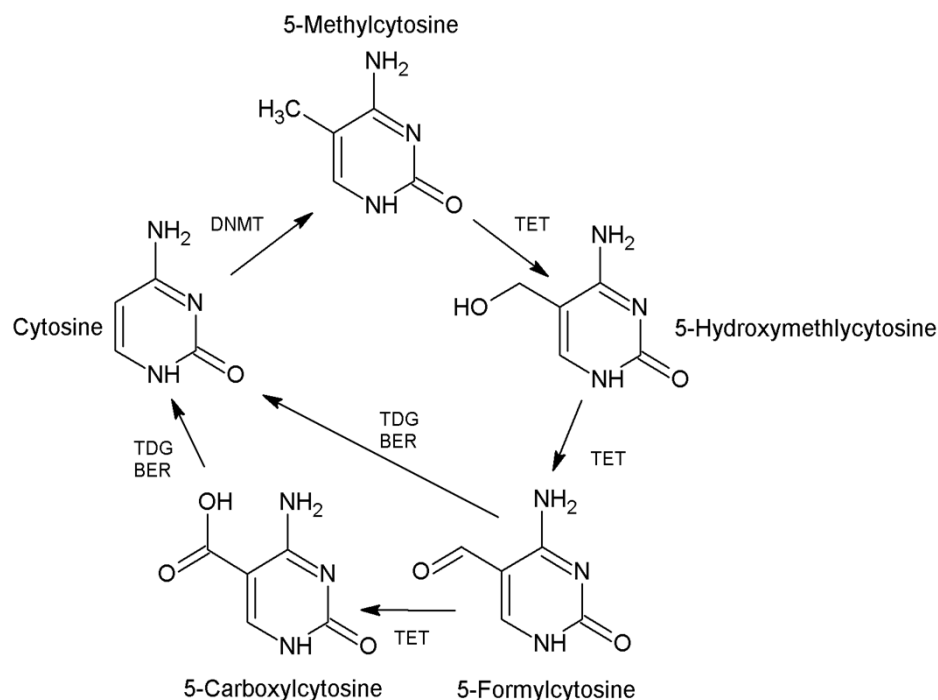


Figure 2.5: DNA methylation and demethylation. Methylation is established by DNMTs and removed through stepwise oxidation by TETs. 5-fC and 5-caC can be removed via TDG BER. Structures were created using ChemSketch V5, Advanced Chemistry Development, Inc., Toronto, On, Canada, www.acdlabs.com, 2019.

2.6.3 Histone modifications

Histones enable another layer of epigenetic regulation through post translational modification that either change the histones chemistry or allow a certain set of interaction partners (Allfrey et al., 1964; Bannister et al., 2004). Dimers of four different of these small proteins (H2A, H2B, H3 and H4) build an octamer the DNA is wrapped around. This octamer together with the DNA is called a nucleosome (Kornberg, 1974). A fifth histone, H1, also sometimes called histone 5, officiates as a linker between the histone cores (Zhou et al., 1998). Organized packaging of the DNA greatly stabilizes the stored information and may protect it from hazards like oxidative stress (Ljungman et al., 1992).

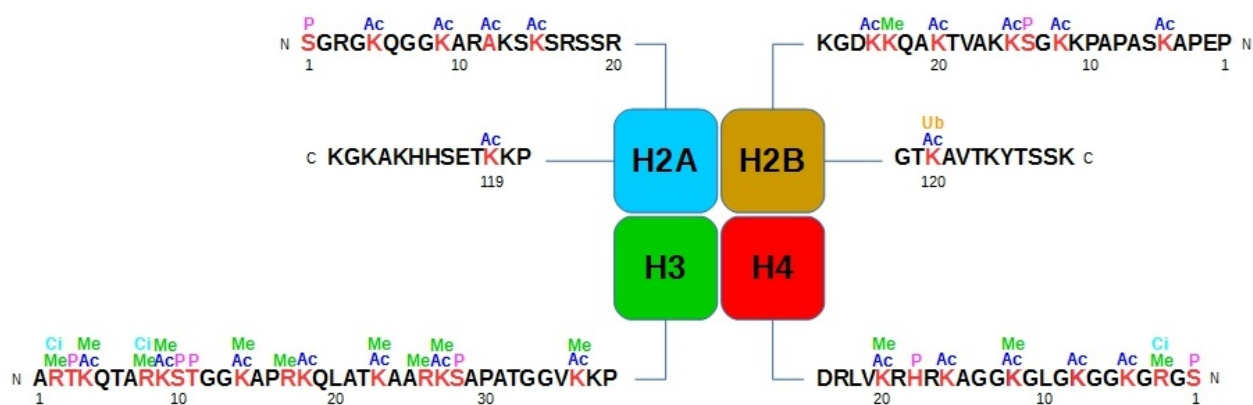


Figure 2.6: Posttranslational modifications of core histones (H2A, H2B, H3 and H4). Modified amino acids are highlighted in red, methylation in green, acetylation in blue, phosphorylation in magenta and citrullination in teal.

Lysines of histones may become mono-, di- or even trimethylated by different sets of enzymes called histone methyltransferases (HMTs) (Rice et al., 2003). These side groups leave the charge of the amino acid intact and only contribute little sterical effect. They rather regulate gene expression by interacting with different secondary enzymes that allow or repress transcription, depending on which lysine is methylated and how (Trojer et al., 2007; Nielsen et al., 2001). The methylation can be removed again by jumonji domain-containing demethylases (JDCDs) (Tsukada et al., 2006) or lysine-specific histone demethylases (LSDs) (Shi et al., 2004).

Arginines can also become methylated in a similar way to lysines. They can be mono- or dimethylated (Allfrey et al., 1964) and interact with proteins harboring a Tudor domain that may affect transcription in either way (Gayatri et al., 2014). This modification is established by protein arginine N-methyltransferases (PRMTs) (Chen et al., 1999). Arginines can also be citrullinated (Hagiwara et al., 2002). This modification removes a positive charge from the amino acid causing the binding between the histone and the DNA backbone to weaken to increase accessibility of the

transcription machinery to the DNA (Christophorou et al., 2014).

As for many other proteins, the serines, tyrosines and threonines of histones can be phosphorylated. Histone phosphorylation can have many different effects. It can regulate transcription factors (Lau et al., 2011), but it can also loosen the bound DNA, especially allowing the DNA repair system to easily access the DNA (Downs et al., 2000). Links between histone phosphorylation and lysine acetylation have been reported (Lo et al., 2000).

Much like arginine citrullination, lysine acetylation removes a positive charge from the amino acid and weakens the binding between histone and DNA. Thus, high amounts of lysine acetylation correlate with high transcriptional activity (Allfrey et al., 1964; Marushige, 1976). Furthermore, acetylated lysines may recruit transcription factors with bromodomains that further activate transcription (Dhalluin et al., 1999). Lysine acetylation is established by histone acetyl transferases (HATs) (Racey et al., 1971) and removed by histone deacetylases (HDACs) (Kaneta et al., 1974).

2.6.4 Epigenetic changes in Parkinson's disease

Based on the accumulation of SNCA in PD, initial studies focused on epigenetic changes at this gene's site. Indeed, when intron 1 of the gene's body was hypomethylated, expression of SNCA increased (Matsumoto et al., 2010). This methylation status was confirmed in the SN of PD patients (Jowaed et al., 2010). Interestingly, methylation levels of the SNCA promoter positively correlated with the amount of administered L-DOPA (Schmitt et al., 2015). Nevertheless, the reduction in 5-methylcytosine levels is not restricted to the SNCA gene's body. A genome wide analysis of the frontal cortex of PD patients found 80% of the differentially methylated regions (DMRs) to be hypomethylated (Masliah et al., 2013).

When high levels of SNCA are present, DNMT1 appears to be sequestered into the cytosol and blocked from entering the nucleus (Desplats et al., 2011). This could explain the lowered levels of 5-methylcytosine in dopaminergic SN neurons. Dynamic changes to the DNA methylation levels might also account for the high vulnerability of those specific neurons, since dopaminergic cells derived from induced pluripotent stem cells (iPSCs) of PD patients showed different methylation patterns compared to parent cells or fibroblast derived from them (Fernández-Santiago et al., 2015). On top of that, demethylation processes are not restricted to the nucleus. The mitochondrial DNA (mtDNA) displacement loop (D-loop) showed also lesser levels of 5-methylcytosine in SN neurons of PD patients (Blanch et al., 2015). Additionally, the transcription of cytochrome P450 enzyme 2E1 (CYP2E1) is increased in the SN of PD patients, while the gene locus becomes demethylated (Kaut et al., 2012). CYP2E1 metabolizes xenobiotics and benzene – a side product of incomplete combustion (Rothman et al., 1997) – among others, and produces ROS in the process (Nieto et al.,

2002).

At the SNCA gene locus an H3K27ac dependent enhancer sequence has been identified (Vermunt et al., 2014). Another study specified the general histone acetylation status looking at specific lysine sites *in vitro* and *in vivo* using the MPTP model and postmortem PD patient brains. Some, but not all, of them were hyperacetylated, but never hypoacetylated in MPTP treated mice and cells (Park et al., 2016). The same study found HDAC1 and HDAC2 levels decreased and accumulated in autophagosomes. The observed hyperacetylation, combined with the decreased HDAC activity was confirmed in the paraquat model as well (Song et al., 2010). Mice treated with the proteasome inhibitor dieldrin showed increased histone acetylation in the SN, that was dependent on cyclic adenosine monophosphate (cAMP) response element-binding protein (CREBBP) and could be averted through treatment with anacardic acid, a HAT inhibitor (Song et al., 2010).

Since epigenetics have not been in the focus of PD, literature and studies are still quite scarce. However, the data that is already established, points to relevant processes of PD's pathology to be constituted through more or less a breakdown of epigenetic systems. Considering that epigenetics are heavily influenced by ageing and environmental toxins, two of the main risk factors of PD, this seems very likely.

2.7. Aim of this thesis

At this point, it can be summarized that PD's pathology is quite well known, while knowledge surrounding its pathogenesal origin remains far from being complete. Since PD onset can sometimes be related to exposure of environmental toxins, an involvement of environmental factors in general seems likely, which in turn would point towards epigenetics that is heavily influenced by the former. So far, some epigenetic factors have been investigated in the context of PD, but insight in the underlying mechanisms or the consequences of these epigenetic alterations remains lackluster at the best.

This thesis now aims to shed a more focused light on the nature of the epigenetic changes by addressing different factors and their behavior in the MPP⁺ model of PD. Differentiated human dopaminergic neurons (Lund human mesencephalic, LUHMES) cells, and an *in vivo* study using mice will help understanding the nature of these alterations as closely to the actual disease as possible. Since MPP⁺ causes energetic instability and excessive ROS generation, the additional treatment with the strong antioxidant PHT, will allow linking the observed changes either to energy deprivation or increased ROS levels.

Once the nature of the changes is established, a thorough investigation of the writers and erasers of epigenetic modifications is in order. It is required to understand whether alterations to the DNA

methylome, for example, are dependent on DNMT or TET disturbances. This will hopefully generate new possible treatment targets.

Finally, an adequate analysis of the implications and consequences of the alterations, most likely in the form of transcriptomics, will allow to put the observations into a bigger picture, especially in the context of mitochondrial involvement, as they are the primary target of most PD models.

Together these data will provide possible opportunities to further understand the pathogenesis of PD in regard of epigenetics, mitochondrial constitution and general energetic mechanisms, while also allowing a thorough analysis of PHT as a possible drug to prevent PD outbreak.

3 Materials and methods

3.1 Materials

3.1.1 Antibodies

3.1.1.1 Primary antibodies

| Target | Host species | Dilution WB/ SB | Dilution ICC/ IHC | Supplier | Catalogue |
|--------------------|--------------|--------------------|----------------------|-----------------|------------|
| TH | Rabbit | - | 1:1000 | Abcam | ab112 |
| H3K14ac | Rabbit | 1:1000 | 1:250 | Cell Signalling | 7627 |
| Total acetyllysine | Rabbit | 1:1000 | 1:200 | Cell Signalling | 9441 |
| 5-methylcytosine | Rabbit | 1:1000 | 1:500 | Cell Signalling | 28692 |
| SLC6A3 | Mouse | - | 1:100 | Abcam | ab128848 |
| DNMT1 | Mouse | 1:1000 | 1:200 | Abcam | ab13537 |
| DNMT3A | Rabbit | 1:1000 | 1:200 | Cell Signalling | 2160 |
| DNMT3B | Rabbit | 1:100 | 1:100 | Cell Signalling | 67259 |
| TUBB | Mouse | - | 1:500 | Millipore | MAB1637 |
| SIRT1 | Mouse | 1:1000 | 1:200 | Cell Signalling | 8469 |
| SIRT3 | Rabbit | 1:1000 | 1:200 | Cell Signalling | 2627 |
| SIRT4 | Rabbit | 1:1000 | - | Abcam | ab90485 |
| H3 | Mouse | 1:1000 | - | Cell Signalling | 14269 |
| TUB | Mouse | 1:5000 | - | Sigma | T9026 |
| TEFM | Rabbit | 1:1000 | - | Novus | NBP1-82109 |
| GLUT3 | Rabbit | 1:1000 | - | Abcam | ab191071 |

Table 3.1: Primary antibodies. Overview of used primary antibodies, their supplier and host and used dilutions.

3.1.1.2 Secondary antibodies

| Fluorophore/ Target | Host species | Dilution WB/ SB | Dilution ICC/ IHC | Supplier | Catalogue |
|-----------------------------|--------------|--------------------|----------------------|----------|-------------|
| Cy3-Anti-rabbit | Donkey | - | 1:500 | Dianova | 711-165-152 |
| Cy2-Anti-mouse | Donkey | - | 1:400 | Dianova | 715-225-151 |
| Alexa Fluor 647-anti-rabbit | Donkey | - | 1:500 | Dianova | 711-605-152 |
| Horse radish peroxidase | Donkey | 1:10000 | - | Dianova | 715-035-151 |

| | | | | | |
|------------------|--------|---------|---|---------|-------------|
| (HRP)-Anti-mouse | | | | | |
| HRP-Anti-rabbit | Donkey | 1:10000 | - | Dianova | 711-035-152 |

Table 3.2: Secondary antibodies. Overview of used secondary antibodies, their supplier and host and used dilutions.

3.1.2 Chemicals

| Chemical | Supplier | Catalogue |
|---|----------------------------|-------------|
| 1-Methyl-4-phenylpyridinium (MPP ⁺) | Sigma Aldrich | D048 |
| Phenothiazine (PHT) | Sigma Aldrich | 88580 |
| N-Methylphenothiazine (MPHT) | Sigma Aldrich | 425346 |
| 2-Acetylphenothiazine (APHT) | Sigma Aldrich | 175226 |
| 6-Thioguanine (6-TG) | Tocris | 4061 |
| Bafilomycin A1 (BafA1) | Toronto research chemicald | B110000 |
| EX-527 | Sigma Aldrich | E7034 |
| Trichostatin A (TSA) | Sigma Aldrich | T8552 |
| CellROX deep red | Thermo Fisher | C10422 |
| Fibronectin | Sigma Aldrich | F1141 |
| Poly-L-ornithine (PLO) hydrobromide | Sigma Aldrich | P3655 |
| Fibroblast growth factor (FGF) | Sigma Aldrich | F0291 |
| Glial cell-derived neurotrophic factor (GDNF) | R&D biosystems | 212-GD |
| Tetracycline | Fluka | 87128 |
| cAMP | Sigma Aldrich | A165 |
| Chloroform | Carl Roth | Y015.1 |
| Isopropanol | Carl Roth | 6752.2 |
| Ethanol | Carl Roth | 9065.2 |
| Trypan blue | Sigma Aldrich | T8154 |
| Sucrose | Carl Roth | 4661.2 |
| Sodium dodecyl sulfate (SDS) | BioRad | 161-0302 |
| Ethylenediaminetetraacetic acid (EDTA) | AppliChem | A2937 |
| Ethylene glycol-bis(β -aminoethyl ether)-N,N,N',N'-tetraacetic acid (EGTA) | Carl Roth | 3054 |
| Protease inhibitor cocktail | Sigma Aldrich | 11836145001 |
| Phosphatase inhibitor cocktail 3 | Sigma Aldrich | P0044 |
| Hydrochloric acid (HCl) 37% | Carl Roth | 4625.1 |
| Sodium hydroxide (NaOH) | Carl Roth | 6771.1 |
| Sodium chloride (NaCl) | Carl Roth | 3957.5 |

Materials and methods

| | | |
|--|-------------------|--------------|
| Potassium chloride (KCl) | Carl Roth | 6781.3 |
| Disodium phosphate (Na ₂ HPO ₄) | Carl Roth | 4984.1 |
| Monopotassium phosphate (KH ₂ PO ₄) | Carl Roth | 3904.1 |
| Tween 20 | Carl Roth | 9127 |
| Triton X-100 | Sigma Aldrich | T8787 |
| Bovine serum albumin (BSA) | Sigma Aldrich | A7906 |
| Tris(hydroxymethyl)aminoethane (TRIS) HCl | Carl Roth | 9090.3 |
| TRIS | Carl Roth | 4855.2 |
| 2-Mercaptoethanol | Carl Roth | 4227.3 |
| Glycerol | VWR | 1.04092.1000 |
| Bromophenol blue | BioRad | 161-0404 |
| Non fat dried milk powder (NFDMP) | AppliChem | A0830 |
| Sodium citrate | Sigma Aldrich | S4641 |
| Paraformaldehyde (PFA) | Merck | 818715 |
| Dimethyl sulfoxide (DMSO) | Carl Roth | A994.1 |
| Tetramethylethylenediamine (TEMED) | BioRad | 1610801 |
| Methanol | Carl Roth | 8388,1 |
| Bisbenzimidazole H 33258 Fluorochrome, Trihydrochloride | Calbiochem | 382061 |
| Ammonium persulfate (APS) | Sigma | A3678 |
| PageRuler Prestained Protein Ladder | Thermo Scientific | 26617 |
| Sodium azide (NaN ₃) | Sigma Aldrich | S8032 |
| Polyvinyl alcohol | Sigma Aldrich | P8136 |
| Luminol | Sigma Aldrich | 123072 |
| p-Hydroxycoumaric acid | Sigma Aldrich | C9008 |
| 30% H ₂ O ₂ | Sigma Aldrich | H1009 |
| Glycine | Carl Roth | 3908.3 |

Table 3.3: Chemicals. Tabular overview of used chemicals and their supplier.

3.1.3 Solutions

3.1.3.1 Crafted solutions

10x Phosphate buffered saline (PBS)

| | |
|----------------------------------|--------------------------------|
| NaCl | 80 g |
| KCl | 2 g |
| Na ₂ HPO ₄ | 14.2 g |
| KH ₂ PO ₄ | 2.4 g |
| H ₂ O | 1 l |
| pH | 7.4 adjusted with HCl and NaOH |

1x PBS

| | |
|------------------|--------------------------------|
| 10x PBS | 100 ml |
| H ₂ O | 900 ml |
| pH | 7.4 adjusted with HCl and NaOH |

1x PBS-T

| | |
|------------------|--------------------------------|
| 10x PBS | 100 ml |
| H ₂ O | 900 ml |
| Tween 20 | 0.5% |
| pH | 7.4 adjusted with HCl and NaOH |

3x Lysis buffer

| | |
|----------|--------------------------------|
| Sucrose | 30% |
| TRIS HCl | 150 mM |
| EDTA | 1.5 mM |
| EGTA | 1.5 mM |
| pH | 6.8 adjusted with HCl and NaOH |

20% SDS solution

| | |
|------------------|-------|
| SDS | 10 g |
| H ₂ O | 50 ml |

10x PhosphoStop

| | |
|----------------------------------|----------|
| Phosphatase inhibitor cocktail 3 | 1 tablet |
| H ₂ O | 1 ml |

50x PIC

| | |
|-----------------------------|----------|
| Protease inhibitor cocktail | 1 tablet |
| H ₂ O | 1 ml |

1x Lysis buffer

| | |
|------------------|--------------------------------|
| 3x Lysis buffer | 333 µl |
| 20% SDS | 100 µl |
| 10x PhosphoStop | 100 µl |
| 50x PIC | 20 µl |
| H ₂ O | 447 µl |
| pH | 7.4 adjusted with HCl and NaOH |

10x TRIS buffered saline (TBS)

| | |
|------------------|--------------------------------|
| NaCl | 1.5 M |
| TRIS HCl | 500 mM |
| H ₂ O | 1 l |
| pH | 7.6 adjusted with HCl and NaOH |

1x TBS-T

| | |
|------------------|--------------------------------|
| 10x TBS | 100 ml |
| H ₂ O | 900 ml |
| Tween 20 | 0.5% |
| pH | 7.6 adjusted with HCl and NaOH |

20x SSC

| | |
|------------------|------------------------------|
| NaCl | 3 M |
| Sodium citrate | 300 mM |
| H ₂ O | 1 l |
| pH | 7 adjusted with HCl and NaOH |

10x SSC

| | |
|------------------|-------|
| 20x SSC | 50 ml |
| H ₂ O | 50 ml |

5x Loading buffer

| | |
|-------------------|--------------------------------|
| TRIS HCl | 750 mM |
| SDS | 15% |
| Bromophenol blue | 0.1% |
| H ₂ O | 3.85 ml |
| Glycerol | 3.85 ml |
| 2-Mercaptoethanol | 2.5 ml |
| pH | 6.8 adjusted with HCl and NaOH |

10x Running buffer

| | |
|------------------|--------------------------------|
| Glycine | 1.92 M |
| TRIS | 152.7 mM |
| TRIS HCl | 97.3 mM |
| SDS | 1% |
| H ₂ O | 4 l |
| pH | 8.3 adjusted with HCl and NaOH |

1x Running buffer

| | |
|--------------------|--------|
| 10x Running buffer | 100 ml |
| H ₂ O | 900 ml |

Transfer buffer

| | |
|--------------------|--------|
| 5x Transfer buffer | 200 ml |
| Ethanol | 200 ml |
| H ₂ O | 600 ml |

4x Collection gel buffer

| | |
|------------------|--------------------------------|
| TRIS HCl | 0.6 M |
| SDS | 0.4% |
| H ₂ O | 1 l |
| pH | 6.8 adjusted with HCl and NaOH |

Separation gel buffer

| | |
|------------------|--------------------------------|
| TRIS | 1.5 M |
| SDS | 0.4% |
| H ₂ O | 1 l |
| pH | 8.8 adjusted with HCl and NaOH |

10% APS

| | |
|------------------|-------|
| APS | 1 g |
| H ₂ O | 10 ml |

10% BSA

| | |
|------------------|-------|
| BSA | 1 g |
| H ₂ O | 10 ml |

Blocking solution

| | |
|-------|--------|
| NFDMP | 4 g |
| PBS-T | 100 ml |

10% NaN₃

| | |
|------------------|-------|
| NaN ₃ | 1 g |
| H ₂ O | 10 ml |

Primary antibody solution

| | |
|----------------------|--------------------------------|
| PBS-T | 10 ml |
| 10% NaN ₃ | 100 µl |
| Primary antibody | See table 3.1 (Dilution WB/SB) |

Secondary antibody solution

| | |
|--------------------|--------------------------------|
| PBS-T | 10 ml |
| Secondary antibody | See table 3.2 (Dilution WB/SB) |

2x DNA denaturation buffer

| | |
|------|--------|
| NaOH | 200 mM |
| EDTA | 20 mM |

4% PFA

| | |
|------------------|-------|
| PFA | 2 g |
| H ₂ O | 50 ml |

Immuno blocking solution

| | |
|--------------|--------|
| 10% BSA | 300 µl |
| Triton X-100 | 1 µl |
| 1x PBS | 699 µl |

Primary antibody immuno solution

| | |
|------------------|--------------------------------|
| 10% BSA | 100 µl |
| 1x PBS | 900 µl |
| Primary antibody | See table 2 (Dilution ICC/IHC) |

Secondary antibody immuno solution

| | |
|--------------------|--------------------------------|
| 10% BSA | 100 µl |
| 1x PBS | 900 µl |
| Secondary antibody | See table 3 (Dilution ICC/IHC) |

DAPI stock

| | |
|-------------------------|--------|
| Bisbenzimidazole H33258 | 5 mg |
| Methanol | 100 ml |

DAPI solution

| | |
|------------|--------|
| DAPI stock | 1 µl |
| PBS | 999 µl |

Mounting media

| | |
|-----------------|------------------------------------|
| 1x PBS | 7 ml |
| Elvanol | 1 g ---> solved at 60 °C in 1x PBS |
| Glycerol | 3 ml |
| p-Phenyldiamine | 10 mg |
| pH | 8 adjusted with HCl and NaOH |

Solution was transferred to 1ml syringes and stored at -80 °C.

ECL solution A

| | |
|---------------|------------------------------|
| 0.1M TRIS-HCl | 100 ml |
| Luminol | 25 mg |
| pH | 7 adjusted with HCl and NaOH |

ECL solution B

| | |
|-----------------|-------|
| DMSO | 10 ml |
| p-Coumaric acid | 11 mg |

Blot developer solution

| | |
|-----------------------------------|--------|
| ECL solution A | 1 ml |
| ECL solution B | 100 µl |
| 30% H ₂ O ₂ | 1 µl |

3.1.3.2 Purchased solutions

| Solution | Supplier | Catalogue |
|--|-------------------|------------------|
| DEPC treated H ₂ O | Ambion | AM9916 |
| TissueTek O.C.T. Compound | Science Services | 4583 |
| OmniPur Acrylamide: Bis Solution 29:1 (Acrylamide) | Merck | 1690-OP |
| Trypsin-EDTA | Gibco | 15400054 |
| Fetal calf serum (FCS) inactive | Life technologies | 10270106 |
| Antibiotic antimycotic (AB-AM) solution | Gibco | 15240062 |
| TRI-Reagent | Sigma | T9424 |
| Dulbecco's modified eagle's medium (DMEM)/ F12 | Lonza | BE 12-719F/12M |
| N-2 Supplement | Gibco | 17502048 |
| 5x Transfer buffer | BioRad | 10026938 |

Table 3.4: Purchased solutions. Tabular overview of purchased solutions and their supplier.**3.1.4 Kits**

| Kit | Supplier | Catalogue |
|------------------------------|-----------------|------------------|
| Pierce BCA protein assay kit | Thermo Fisher | 23225 |
| DNeasy blood & tissue kit | Qiagen | 69504 |

| | | |
|--|-------------------|----------------|
| FLUOR DE LYS SIRT1 fluorometric drug discovery assay kit | Enzo Lifesciences | BML-AK555-0001 |
| TruSeq stranded mRNA LT Sample Prep Kit | Illumina | RS-122-2101 |
| Qubit dsDNA HS Assay Kit | Thermo Fisher | Q32854 |

Table 3.5: Kits. Tabular overview of used kits and their supplier.

3.1.5 Cell lines

| Cell line | Source | Type | Supplier |
|---|--------|------------------|------------------------------|
| Lund human mesencephalic (LUHMES) cells | Human | Neural stemcells | Laboratory of Jochen Klucken |

Table 3.6: Cells. Tabular overview of used cell lines and their supplier.

3.1.6 Animals

| Mouse line | Provider | Age at start | Sex |
|------------|----------------------------|----------------|------|
| C57Bl/6J | Charles River Laboratories | 10 +/- 2 weeks | Male |

Table 3.7: Animals. Tabular overview of used mouse lines, their provider, age and sex.

3.1.7 Equipment

| Item | Supplier |
|----------------------------------|-------------------|
| Trans-Blot Turbo Transfer System | BioRad |
| BIO-LINK BLX-254 | Peqlab |
| CKX31 | Olympus |
| Heraeus Multifuge 3 S-R | Thermo Scientific |
| BL 6100 | Sartorius |
| Neubauer counting chamber | OptikLabor |
| NanoDrop 1000 | Peqlab |
| AF 80 | Scotsman |
| 1000µl Blue, Graduated Tip | TipOne |
| 100µl Yellow, Graduated Tip | TipOne |
| 10µl White, Graduated Tip | TipOne |
| E 26 | Heidolph |
| Water bath 18L 462-0558 | VWR |
| Duomax 1030 | Heidolph |
| Axiovert 200 | Zeiss |

| | |
|--|-----------------------------|
| CELLSTAR serological pipette (10 ml) | Greiner bio-one |
| Cell spatula | TPP |
| CELLSTAR TUBES (15 ml) | Greiner bio-one |
| CELLSTAR TUBES (50 ml) | Greiner bio-one |
| Reaction tube 0.5 ml | A.Hartenstein |
| Reaction tube 1.5 ml | A.Hartenstein |
| Reaction tube 2 ml | A.Hartenstein |
| Multiskan SC | Thermo Labsystems |
| UP50H | Hielscher |
| Amersham imager 600 | GE-Healthcare Life Sciences |
| Milli-Q reference A+ | Millipore |
| Thermomixer comfort | Eppendorf |
| ROCKER 2D basic | IKA |
| Research plus 0.5-10 µl | Eppendorf |
| Gilson PIPETMAN Classic 20-200 µl | Fisher Scientific |
| Gilson PIPETMAN Classic 100-1000 µl | Fisher Scientific |
| Heraeus Fresco 17 centrifuge | Thermo Scientific |
| PowerPac Basic | BioRad |
| Tissue Culture Dish (22.1 cm ²) | TPP |
| Tissue Culture Dish (60.1 cm ²) | TPP |
| Tissue Culture Test Plate (96-well) | TPP |
| Tissue Culture Test Plate (24-well) | TPP |
| Microscope Coer Glasses 12 mm | VWR |
| 100 Deckgläser 24x50 mm | Carl Roth |
| SuperFrost Plus Objektträger | Hartenstein |
| Mini-PROTEAN Tetra Cell Casting clamp | BioRad |
| Mini-PROTEAN Tetra Cell Casting stand | BioRad |
| Short plate | BioRad |
| Spacer plate (1.0 mm) | BioRad |
| Gel comb (10 lanes) | BioRad |
| Gel comb (15 lanes) | BioRad |
| Nitrocellulose | BioRad |
| Blotting paper | BioRad |
| Mini-PROTEAN Tetra Vertical Electrophoresis Cell | BioRad |
| HERAcell 240i | Thermo Fisher |
| 1420 Multilabel Counter VICTOR ³ V | Perkin Elmer |

| | |
|---|--------------------------|
| BD Microlance 3 | BD |
| RCT basic | IKA Labortechnik |
| Nylonmembrane | Boehringer Mannheim |
| CM 1900 | Leica |
| MAS20 | MAS Medical & Scientific |
| Multiskan | Thermo Laboratories |
| Minifold Vakuumfiltrationssystem SRC 96-D | Schleicher&Schuell |
| Bioanalyzer 2100 | Agilent Technologies |
| Qubit 2.0 Fluorometer | Life Technologies |
| TCS SP5 Confocal microscope | Leica |
| NextSeq 500 High Output Flowcell | Illumina |

Table 3.8: Equipment. Tabular overview of used equipment and their supplier.

3.2 Methods

3.2.1 Cell culture

3.2.1.1 Coating

TPP plastics and glass cover slips were coated with PLO and fibronectin in H₂O (Table 3.9) over night at 37 °C with 20% O₂ and 5% CO₂. Coating media was removed the next day and coated surfaces washed three times with H₂O with the same volume as administered coating media.

| Surface | Coating media | Culture media | Trypsin |
|-----------------------------|---------------|---------------|---------|
| Cover slip in 24 well plate | 500 µl | 500 µl | 100 µl |
| 6cm dish | 1 ml | 3 ml | 1 ml |
| 10cm dish | 4 ml | 7 ml | 2 ml |

Table 3.9: Media volumes. Overview media volumes used in cell culture.

3.2.1.2 LUHMES cells

3.2.1.2.1 Stem cells

Lund human mesencephalic (LUHMES) stem cells were incubated in 37 °C pre-warmed F12/DMEM media supplemented with 1x N-2 supplement, 40 ng/ml FGF, 0.5% FCS and 1x AB-

AM on PLO and fibronectin coated TPP plastics at 37 °C with 20% O₂ and 5% CO₂. Medium was changed every other day and cells were moved once they had reached a confluency of 80%. Cells were dissociated with 1x trypsin-EDTA (Table 3.9) over 3min at 37°C with 20% O₂ and 5% CO₂ and removed from the plastic with supplement free media and transferred to a 15 ml tube. The suspended cells were centrifuged at 500 g for 4 min at room temperature. The old media was removed and the cells were reconstituted in supplemented media (Table 3.9) and transferred at ratio 1:5 to newly coated plastics.

3.2.1.2.2 Differentiation

LUHMES stem cells were dissociated from the plastic with 1x trypsin-EDTA (Table 3.9) over 3 min at 37 °C with 20% O₂ and 5% CO₂, removed from the plastic with supplement free, 37 °C pre-warmed media and transferred to a 15 ml tube. 50 µl of the cell suspension was moved to a 96-well plate and mixed with 50 µl 1x trypan blue. While the suspension cells were centrifuged at 500 g for 4min at room temperature, the cells in the trypan blue mix were counted using a Neubauer counting chamber under the CKX31 microscope from Olympus. The result was divided by two and multiplied by the volume of the cell suspension media.

After centrifugation the old media was removed and replaced by 1 ml 37 °C pre-warmed media without supplements. 7×10^4 cells/cm² were seeded on 22.1 cm² dishes or glass cover slips in a 24-well Tissue Culture Test Plate in 37 °C pre-warmed F12/DMEM media supplemented with 1x N2, tetracycline, 1 mM cAMP, 2 ng/ml GDNF and 1x AB-AM (Table 3.9). Cells were incubated at 37 °C with 20% O₂ and 5% CO₂. Media was changed after two days and again after five days. After five days, cells were treated with different compounds (Table 3.10) in fresh media.

| Compound | Final concentration | Duration |
|-----------------------------|---------------------|----------|
| 1-Methyl-4-phenylpyridinium | 10 µM | 48 h |
| Phenothiazine | 20 nM | 48 h |
| N-Methylphenothiazine | 20 nM | 48 h |
| 2-Acetylphenothiazine | 20 nM | 48 h |
| 6-Thioguanine | 1 µM | 48 h |
| Bafilomycin A | 500 nM | 4 h |
| EX-527 | 100 nM | 48 h |
| Trichostatin A | 50 nM | 48 h |
| CellROX deep red | 5 µM | 30 min |
| Vehicle | 0.001% | - |

Table 3.10: LUHMES cell treatments. Overview of treatments with final concentration and duration. Duration of vehicle treatment depended on duration of the treatment.

3.2.2 Biochemical protocols

3.2.2.1 Western Blot

3.2.2.1.1 Protein isolation

After treatment, media was removed and 200 µl 1x lysis buffer were added. Cells were dissociated with a cell spatula and collected in a 1.5 ml reaction tube. To disrupt cellular membranes and compartments, the suspension was sonicated at cycle 1, amplitude 70, two times for 10 s with the UP50H.

3.2.2.1.2 Protein concentration determination

Protein concentration were measured using the bicinchoninic acid (BCA) approach that is based on the concept of two reactions. First, present Cu^{2+} ions are reduced by the peptide bonds of proteins to Cu^+ ions which is chelated by two BCA molecules in the second reaction building a purple complex whose density can be measured at the wavelength of 562 nm (Smith, et al. 1985).

BSA standard was prepared according to protocol (2, 1, 0.5, 0.25, 0.125, 0.0625, 0.03125 mg/ml). Samples were measured in duplicates. 2 µl of standard or samples were put into a well of a 96 well plate. BCA developer solution was prepared according to manufacturer's instructions from the Pierce BCA protein assay kit. To each used well, 200 µl of BCA developer solution were added and the plate was incubated for 30 min at 60 °C to increase complex formation. Afterwards, protein concentration was measured using the Multiskan SC with a 562 nm filter. Using the standard the software would calculate a curve that correlates signal intensity with protein amount, which would allow to cross-read the protein amount in the samples from the signal intensity.

3.2.2.1.3 SDS Laemmli gel manufacture

SDS Laemmli gels were prepared according to the following tables:

Separation gel:

| Percentage | Acrylamide | Separation gel buffer | H ₂ O | 10% APS | TEMED | Total volume |
|------------|------------|-----------------------|------------------|---------|-------|--------------|
| 6% | 1.5 ml | 2.5 ml | 6 ml | 100 µl | 10 µl | 10 ml |
| 10% | 2.5 ml | 2.5 ml | 5 ml | 100 µl | 10 µl | 10 ml |
| 15% | 3.75 ml | 2.5 ml | 3.75 ml | 100 µl | 10 µl | 10 ml |

Table 3.11: Separation gel. Components, that were used to produce a gel at indicated percentage

Collection gel:

| Percentage | Acrylamide | Collection gel buffer | H ₂ O | 10% APS | TEMED | Total volume |
|------------|------------|-----------------------|------------------|---------|-------|--------------|
| 3% | 0.75 ml | 2.5 ml | 6.5 ml | 100 µl | 10 µl | 10 ml |

Table 3.12: Collection gel. Components, that were used to produce a collection gel.

A gel cassette was assembled from a short plate and with a spacer plate featuring 1.0mm integrated spacers. The glassware was then put into a Mini-PROTEAN Tetra Cell Casting clamp that was moved to a Mini-PROTEAN Tetra Cell Casting stand with the included thick rubber band at the bottom of the glass to seal the system.

The separation gel was the first to be prepared with 10% APS being the last component to be added because it initiates the polymerisation reaction (Brewer, 1967). The still fluid separation gel was cast inside the glass cassette and a layer of isopropanol was immediately added to guarantee a smooth and straight border at the gel's head. After polymerisation the isopropanol was washed out with H₂O and residual fluids were discarded.

Finally, the collection gel was prepared also with 10% APS being the last component to be added and put on top of the separation gel. A comb with 10 or 15 lanes was put inside the collection gel at the top of the glassware. After polymerisation the comb was removed and the gels were used immediately or stored at 4 °C.

3.2.2.1.4 SDS PAGE

Sufficient amounts of sample and 1x lysis buffer were put together to obtain 10 µg of protein in 20 µl of buffer. Samples were always kept on ice. Subsequently, 4 µl of 5x loading buffer were added and the proteins were denatured at 95 °C for 5 min on the Thermomixer comfort with 400 rpm.* Samples were centrifuged for 1 min at 7000 g and left on ice for 1min. Gels were installed into the Mini-PROTEAN Tetra Vertical Electrophoresis Cell and the chamber was flooded with 1 l 1x

running buffer. Each sample was transferred to one lane, with at least one lane being reserved for the PageRuler Prestained Protein Ladder. Electrophoresis was conducted at 80 V until the running front reached the threshold between collection and separation gel. From that point the voltage was increased to 120 V. Shortly before the running front would leak out of the gel, the electrophoresis was terminated and the gels put into protein transfer through semi-dry Western blotting.

3.2.2.1.5 Protein transfer

Proteins were transferred to a nitrocellulose membrane using the Trans-Blot Turbo system from BioRad. Blotting paper and membranes were also supplied by BioRad. Paper and membrane were briefly bathed in 1x blotting buffer. One layer of paper was placed on the bottom of the drawer, followed by the membrane. The gel from the SDS PAGE was freed from glass and put on top of the membrane. Air bubbles were removed and the second layer of paper was added on top of the gel. Gentle pressure was applied to the sandwich to remove excessive buffer. Free fluids were removed from the drawer and the lid was closed. The drawer was put into the machine and the gels were blotted for 30 min at 1.5 A and 25 V.

3.2.2.1.6 Blocking and primary antibody

After blotting, unspecific epitopes on the membrane were blocked with 25 ml blocking solution for 45 min at room temperature shaking gently on the ROCKER 2D basic from IKA at 40 rpm. The blocking solution was removed and the membrane washed three times with 15 ml PBS-T for 10 min each at room temperature shaking gently on the ROCKER 2D basic from IKA at 40 rpm. After washing the membrane was incubated with 10ml primary antibody solution over night at 4 °C shaking gently at 20 rpm on the DUOMAX 1030 from Heidolph.

3.2.2.1.7 Secondary antibody and development

Primary antibody solution was removed and the membrane washed three times with 15 ml PBS-T for 10 min each at room temperature shaking gently on the ROCKER 2D basic from IKA at 40 rpm. After washing, the membrane was incubated with secondary antibody solution for 2h at room temperature shaking gently on the ROCKER 2D basic from IKA at 40 rpm. The secondary antibody solution was removed and the membrane washed again three times for 10min each with 15 ml PBS-T shaking gently on the ROCKER 2D basic from IKA at 40 rpm. Finally, the membrane was placed inside the Amersham imager 600 developer with 1 ml blot developer solution. After development,

the membrane was washed again three times with 15 ml PBS-T for 10 min each at room temperature shaking gently on the ROCKER 2D basic from IKA at 40 rpm. From this point, the development could be repeated using different primary antibodies, if they would not cross-react with previous antibodies and the background noise remained low enough.

3.2.2.2 DNA dot blot

3.2.2.2.1 DNA isolation

Media was removed and LUHMES cells were harvested in 200 μ l 1x PBS with a cell spatula and collected in a 1.5 ml reaction tube. DNA was extracted using the DNeasy blood and tissue kit from Qiagen according to the manufacturer's protocol. Extracted DNA was fragmented by sonification at cycle 1, amplitude 50, two times for 10 s with the UP50H. DNA concentration was measured by NanoDrop 1000 blanked to the kit's elution buffer.

3.2.2.2.2 DNA dot-blot

DNA was diluted to 10 ng/ μ l in 10 μ l H₂O and denatured by adding 10 μ l 2x DNA denaturation buffer and incubation at 95 °C for 10 min on the Thermomixer comfort with 200 rpm. After denaturation, 20 μ l 20x SSC buffer were added and the samples left on ice for 5 min. The wells of the dot blot apparatus were rinsed three times with 100 μ l 10x SSC. A nylon membrane was soaked in 20 ml 10x SSC. The membrane was placed inside the dot blot apparatus and dried through application of vacuum. Finally, 10 μ l H₂O were added to the samples to a final volume of 50 μ l per sample. Samples were then transferred to the membrane inside the dot blot apparatus and applied vacuum sucked the fluid through the membrane. Afterwards, the DNA was UV cross-linked to the nylon membrane at 1200 J/m² using the BIO-LINK BLX-254 from Peqplab.

3.2.2.2.3 Antibodies and development

The membrane was blocked using 25 ml DNA blocking solution for 1 h at room temperature shaking gently. From this point onwards, the same protocol as described in 3.2.2.1.6 and 3.2.2.1.7 was applied with the exception of TBS-T replacing PBS-T as washing agent.

3.2.2.3 Transcriptomics

3.2.2.3.1 RNA isolation

Media was removed and LUHMES cells were harvested in 500 μ l TRI-Reagent with a cell spatula and collected in a 1.5 ml reaction tube. Samples were vortexed vigorously and centrifuged at 12000 g for 10 min at 4 °C in the Heraeus Fresco 17 centrifuge, which was used for all subsequent centrifugation steps as well. Samples were transferred to fresh 1.5 ml microcentrifuge vials without the insoluble pellet. Afterwards, 100 μ l chloroform were added to the samples and vortexed. Samples were left at room temperature for 10 min and centrifuged for 15 min at 12000 g and 4 °C. Centrifugation separated the sample into three phases, a lower phase containing proteins, an intermediate phase containing DNA and an upper phase containing RNA.

The upper, aqueous phase was transferred into a fresh 1.5 ml microcentrifuge vial and 250 μ l isopropanol were added to rinse the RNA. Samples were mixed gently and remained at room temperature for 7 min. RNA was precipitated under centrifugation at 12000 g for 10 min at 4 °C. The supernatant was discarded and replaced by 500 μ l 75% ethanol. Samples were centrifuged again at 7500 g for 5 min at 4 °C. The supernatant was discarded and the RNA pellet reconstituted in 20 μ l DEPC treated H₂O.

Residual DNA was removed by addition of 2 μ l Dnase and incubation at 37 °C for 1 h. Afterwards, 500 μ l 75% ethanol were added and the samples washed again through centrifugation at 7500 g for 5 min at 4 °C. The supernatant was discarded and the RNA pellet reconstituted in 50 μ l DEPC treated H₂O. RNA concentration was measured by NanoDrop 1000 blanked on DEPC treated H₂O.

3.2.2.3.2 RNA-Seq

RNA-seq library prep was performed with Illumina's TruSeq stranded mRNA LT Sample Prep Kit following Illumina's standard protocol (Part # 15031047 Rev. E). Libraries were prepared with a starting amount of 1000ng and amplified in 10 PCR cycles. Libraries were profiled in a High Sensitivity DNA on a 2100 Bioanalyzer and quantified using the Qubit dsDNA HS Assay Kit, in a Qubit 2.0 Fluorometer. All samples were pooled in equimolar ratio and sequenced on 1 NextSeq 500 High Output Flowcell, SR for 1x 84 cycles plus 7 cycles for the index read. These steps were commissioned to the genomics core facility of the IMB Mainz. The assembly and mapping of the libraries were performed by the bioinformatics core facility of the IMB Mainz.

3.2.2.4 Immunocytochemistry (ICC)

Old media was removed from LUHMES cells grown on cover slips inside a 24-well plate and replaced by 500 μ l 4% PFA to cross-link cellular compartments over 20 min at room temperature. PFA was removed and the well washed three times with 500 μ l 1x PBS for 5 min each.* After washing, 200 μ l immuno blocking solution were added to block and permeabilize the samples for 5 min at 4 °C. Samples were washed again three times with 200 μ l 1x PBS at room temperature for 5 min each. 150 μ l Primary antibody immuno solution were added and incubated over night at 4 °C. On the next day, antibody solution was removed and samples were washed three times with 200 μ l 1x PBS at room temperature for 5 min each. After washing, 150 μ l secondary antibody immuno solution were added and samples incubated for 2 h at room temperature. From this step onward, the samples were protected from light. Afterwards, samples were washed once with 200 μ l 1x PBS at room temperature for 5 min and treated with 200 μ l DAPI solution for 20 min at room temperature. Samples were washed two times with 200 μ l 1xPBS for 5 min. One drop of mounting media was applied to a SuperFrost Plus Objektträger microscope slide. Coverslips were removed from the 24-well plate, residual fluids removed and cell side down transferred onto the mounting media drop. Residual mounting media was carefully removed and the coverslips fixated to the slide with nail polish.

*For 5-methylcytosine immunocytochemistry the samples were treated with 1.5 M HCl for 30 min at room temperature to denature DNA after PFA fixation. Samples were washed two times 1x PBS for 5 min at room temperature before blocking and permeabilization.

3.2.2.5 SIRT1 activity assay

Materials required for the performed SIRT1 activity assay were obtained from the FLUOR DE LYS SIRT1 fluorometric drug discovery assay kit from Enzo Lifesciences. Media was removed and LUHMES cells were harvested in 200 μ l SIRT1 assay buffer with a cell spatula and collected in a 1.5 ml microcentrifuge vial. Samples were sonicated at cycle 1, amplitude 70, two times for 10 s. Protein concentration was measured by NanoDrop 1000 blanked on SIRT1 assay buffer.

The assay was prepared in a white 96-well plate included in the kit. The highest possible amount of protein, 181 μ g, was diluted in SIRT1 assay buffer to a final volume of 35 μ l. Four wells per sample were loaded with protein lysate and kept on ice for the remaining procedure. 64 μ M of the SIRT1 substrate, FLUOR DE LYS SIRT1, and 500 μ M of NAD⁺ were diluted in 15 μ l SIRT1 assay buffer and added to three of the four sample wells. The fourth sample received only 15 μ l SIRT1 assay buffer to allow quantification of lysate background, while one well only received 50 μ l SIRT1 assay

buffer and one well received sample buffer with NAD⁺ and FLUOR DE LYS SIRT1 to allow quantification of component's background. The plate was incubated at 37 °C for 1 h.

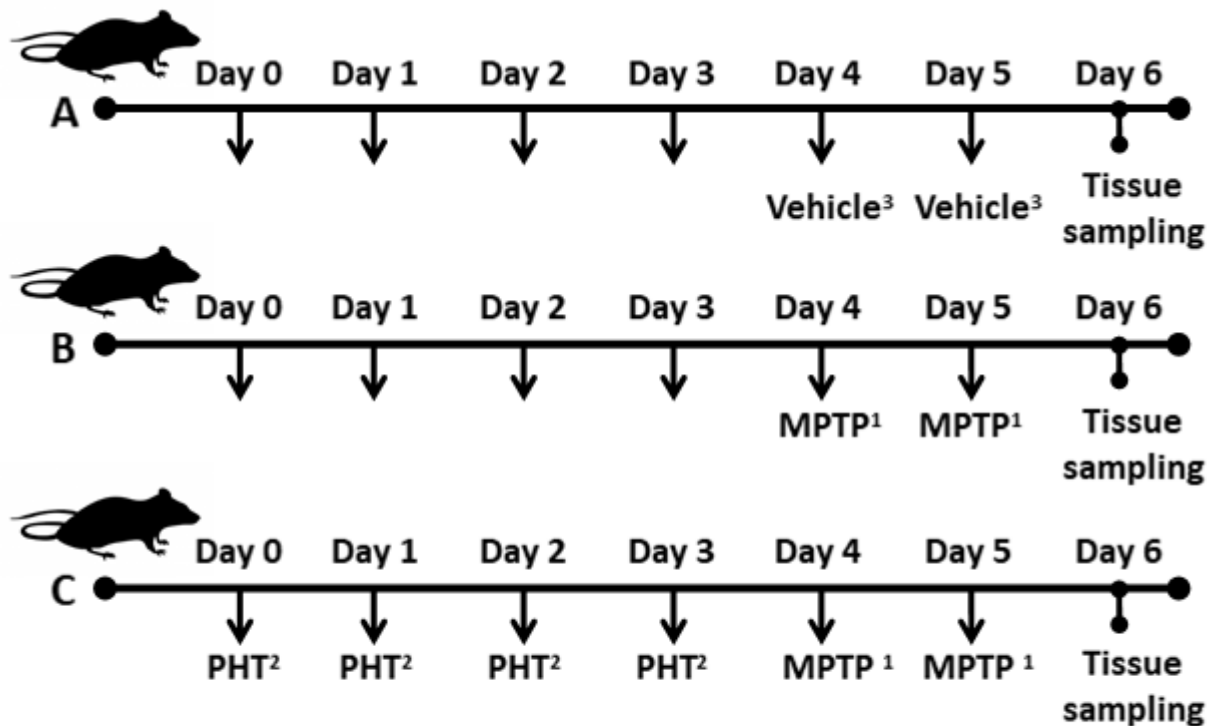
The developer solution was prepared with SIRT1 assay buffer, 2 mM nicotinamide to stop additional reactions, and 1x FLUOR DE LYS Developer II. 50 µl of the developer solution were added to each well, except the background control for the NAD⁺ and FLUOR DE LYS SIRT1 and the SIRT1 assay buffer wells. Instead, those wells received only 50 µl SIRT1 assay buffer. Two additional wells were prepared, one that only received 50 µl SIRT1 assay buffer and 50 µl developer solution and one received 64 µM FLUOR DE LYS Deacetylated Standard in 50 µl SIRT1 assay buffer and 50 µl developer solution, to allow quantification of developer solution's background as well as a potential signal maximum. The plate was then incubated at 37 °C for 45 min. Afterwards, fluorescent signal was quantified using the Multilabel Counter VICTOR ³V.

3.2.3 *In vivo* mouse system

3.2.3.1 Establishing the model

Thirty male mice were allocated to three different treatment groups (A to C). The animal handling was done by QPS, Parkring 12, 8074 Grambach, Austria. MPTP (20 mg/kg bodyweight (bw) four times, 2 h inter-treatment interval) was injected intraperitoneal (ip) on day 4 (groups B and C). One group of animals (group A) was sham lesioned by ip administration of the MPTP vehicle (0.9% saline). The application volume was 10 µl/g bw.

PHT (10 mg/kg bw per application) was administered per oral (po) twice a day (4 h inter-treatment interval) for five days (group C). Groups A and B received the vehicle (DMSO in Corn oil (1:50 dilution)). The applied volume was 2.5 μ l/g bw.



¹ 4 injections MPTP 2 hours interval

² 2 oral administrations PHT 4 hours interval

³ 4 injections vehicle 2 hours interval

Figure 3.1: MPTP Mouse model. Schematic overview of the different treatment groups. Group A only received vehicles, while group B received MPTP with the PHT vehicle. Group C received MPTP and PHT. PHT treatment began day 0, MPTP treatment day 4. Animals were sacrificed on day 6.

3.2.3.2 Rota Rod

The Rota Rod test was used to assess motor coordination of the animals by placing them on a rotating rod that runs at an accelerating speed. If a mouse lost its balance and fell onto an underlying platform, the rod did automatically stop and record a measure of the latency to fall.

Prior to the first test session, the mice were habituated to the testing system, until they were able to stay on the rod at a constant speed of 2 rpm for approximately one minute. During testing, a single animal was exposed to the apparatus three times for a 180 s trial. The initial speed increased from 2 rpm to 20 rpm over an accelerating time of 180 s. If the mice fell, the session was over.

3.2.3.3 Tissue sampling

On day 6, after finishing Rota Rod testing, the mice were sacrificed and their brains were collected. Therefore, mice were deeply anaesthetized by pentobarbital injection (600 mg/kg bw). Then, the animals were transcardially perfused with 0.9% saline and brains were removed and hemisected. The left hemispheres were subdivided into striatal tissue, midbrain (including SN) as well as residual brain, immediately frozen and stored at -80 °C.

Right brain hemispheres were fixed by immersion in freshly prepared 4%PFA in 1x PBS (pH=7.4) for one hour at room temperature. Thereafter, right hemispheres were transferred to a 15% sucrose 1x PBS solution until sunk to ensure cryo-protection. On the next day, fixed hemispheres were frozen embedded in O.C.T media within cryo-molds in dry-ice cooled liquid isopentane and stored at -80 °C.

3.2.3.4 Western blot

Midbrains of the left hemispheres were transferred into 1x lysis buffer in a 1.5 ml reaction tube and mashed through mechanical force. The formed debris was further minced by sonification at cycle 1, amplitude 100, three times for 10 s with the UP50H.

The Western Blot protocol described under 3.2.2.1.2 – 3.2.2.1.7 was also applied for the blotting of the *in vivo* material with the exception of 20 µg protein loading mass instead of 10 µg.

3.2.3.5 Cryosections

Perfused and PFA fixated, frozen right hemispheres were cut into 10µm small slices in the CM 1900 at -20 °C. The slice was transferred to a SuperFrost Plus Objektträger microscope slide. A drop of H₂O was applied to the slice to remove remaining TissueTek O.C.T. Compound. The slides were kept warm at 28 °C to accelerate H₂O evaporation. The slides were kept at -80 °C until further use.

3.2.3.6 Immunohistochemistry (IHC)

Brain slices were defrosted and small rectangles were cut into the glass surrounding the tissue with a diamond pen to prevent fluids from diffusing. The tissue was rinsed once in 50 µl 1x PBS for 5 min at room temperature. Excessive fluids were carefully removed through adhesion with a piece of paper. Tissue was blocked and permeabilized with 50 µl immuno blocking solution and incubated

for 1 h at room temperature. Tissue was washed three times with 50 μ l 1x PBS at room temperature for 5 min each. 50 μ l Primary antibody immuno solution were added and incubated over night at 4 °C.

On the next day, antibody solution was removed and samples were washed three times with 50 μ l 1x PBS at room temperature for 5min each. After washing, 50 μ l secondary antibody immuno solution were added and samples incubated for 2 h at room temperature. From this step onward, the samples were protected from light. Afterwards, samples were washed once with 50 μ l 1x PBS at room temperature for 5min and treated with 50 μ l DAPI solution for 20 min at room temperature. Samples were washed two times with 50 μ l 1xPBS for 5 min. One drop of mounting media was added on top of the tissue and a coverslip was sealed to the microscope slide by nail polish.

3.2.4 Evaluation

3.2.4.1 Microscopy

Slides generated through immunohistochemistry were recorded with the Axiovert 200 fluorescent microscope from Zeiss using blue, green and red filters and objectives for 4x and 10x magnifications. Pictures were evaluated using the ImageJ software. Tyrosine hydroxylase (TH) staining was measured after the signal was „watershed“. This used algorithm calculates signal maxima and can thus confidently locate cell cell borders. Cells were quantified using the “analyse particles” function from ImageJ that counts each continuous signal as one particle. Through this approach cells can be evaluated regardless of the size of their on the slide represented body.

For H3K14ac staining, total nuclei on the slide were quantified with DAPI using again the “analyse particle” function of the ImageJ software. The same process was repeated for the H3K14ac staining and the quotient H4K14ac/DAPI was calculated.

Slides generated through immunocytochemistry were recorded with the Axiovert 200 fluorescent microscope from Zeiss using blue and green and an objective with 20x magnifications and the laser scanning microscope (LSM) TCS SP5 from Leica.

Total acetyllysine, DNMT3A, DNMT3B, and 5-methylcytosine were quantified by dividing the total grey value measured by ImageJ with the amount of cells present indicated by DAPI. Staining of DNMT1 was rather evaluated for its nuclear presence by counting the amount of DNMT1 positive nuclei and dividing it with the total amount of cells present indicated by DAPI.

3.2.4.2 Densitometry

Western blots were evaluated by densitometry. Blot development ideally gave one specific band whose signal intensity was quantified by ImageJ and normalized on the signal intensity of the loading control developed on the same membrane. *In vitro* Western blots were normalized on histone H3, while *in vivo* Western blots were normalized on alpha tubulin (TUB). H3K14ac signal *in vivo* was first normalized on H3 and then on TUB. TUB was not eligible as a loading control *in vitro* due to protein levels changing upon MPP⁺ treatment.

Autophagic accumulation was calculated by calculating the ratio between BafA1 untreated and treated samples after normalization on H3.

Southern blots were also evaluated by densitometry. The signal intensity was quantified by ImageJ and normalized on the total DNA input amount.

3.2.4.3 Statistics

Total lysine immunocytochemistry results were statistically evaluated by Benjamini-Hochberg (BH) adjusted two-way analysis of variance (ANOVA) using the GraphPad Prism version 7.00 for Windows, GraphPad Software, La Jolla California USA, www.graphpad.com. All remaining results were evaluated by BH adjusted one-way ANOVA. Significant changes compared to the control group are indicated by *, while significant changes from the MPTP/MPP⁺ treated group are indicated by #. The number of * or # correlates with the p-value: * = p<0.05, ** = p<0.01, *** = p<0.001.

Evaluations of the transcriptomics data do not indicate p-value strength and significant differences between the control and the PHT/MPP⁺ treated group are indicated by !.

4 Results

4.1 Adjusting the optimal working concentrations of MPP⁺ and PHT

Before any experiments to gather new data were carried out, the optimal working concentration of MPP⁺ in differentiated LUHMES cells had to be established. Optimal conditions for the subsequent experiments would represent the tipping point of cellular decline and feature minimal amount of cell death and little to none effect on cellular constitution. Toxic effects of MPP⁺ were measured through qualitative examination of neuronal morphology.

Previous studies regarding the neurotoxicity of MPP⁺ in cultures of primary neurons have shown that treatment over a course of 48 h causes the most reliable manifestation of toxic effects. Cells treated over longer periods would already go into remission (Hajieva et al., 2009). Reference values from this study regarding the concentration of MPP⁺, however, could not be taken into accord, since primary cultures, unlike LUHMES cultures, are rarely 100% neuronal, but rather a mix of neurons and glial cells, which likely support the neurons and make the culture less vulnerable to toxic effects.

Thus, differentiated LUHMES cells were subjected to different concentrations (100 μ M, 75 μ M, 50 μ M, 25 μ M and 10 μ M) of MPP⁺ over 48 h (Fig. 4.1). Cells treated with 100 μ M and 75 μ M showed high levels of cell death with almost no surviving cells. Treatment with 50 μ M still caused a moderate amount of cell death, while axons of most surviving cells disappeared. Lower amounts of cell death could be observed at 25 μ M MPP⁺. However, the cells were void of axons and appeared to have moved closer together, thus constituting small spherical structures. Only cells treated with 10 μ M showed very low to no levels of cell death, while the cells retained their regular habitus. Thus, 10 μ M was chosen as the working concentration, since treated cells showed no major morphological impairment. Earlier studies in LUHMES cells also confirm these observations (Smirnova et al., 2016).

The optimal working concentration for PHT would be as little as possible and as much as necessary to protect from MPP⁺ mediated toxic effects. This was already determined in previous *in vitro* studies with primary neurons from *rattus norvegicus* (Hajieva et al., 2009). There, 20 nM of PHT have been shown to protect neurons from MPP⁺ mediated toxicity. Thus, 20 nM were chosen as the working concentration.

Finally, to visualize MPP⁺ induced ROS production and protective effects of PHT the CellROX dye from Thermo Fisher was used. The dye reacts with ROS and forms a deep red fluorescent signal that is PFA fixation compatible. Exposure to MPP⁺ caused ROS levels to increase by roughly 100%, while PHT successfully protected the cells (Fig. 4.2) and reduced ROS signal to control levels.

Interestingly, the distribution of ROS changed throughout the cellular body. Under control conditions ROS were focussed in a cloud in perinuclear regions. MPP⁺ treatment disintegrated the cloud and caused the ROS to spread throughout the entire cell with perinuclear foci. Co-treatment with PHT caused the signal to be concentrated in perinuclearly distributed centres again. This experiment was performed in triplicate.

This confirms the viability of the chosen concentrations of MPP⁺ and PHT and time frame as a suitable setup for further experiments.

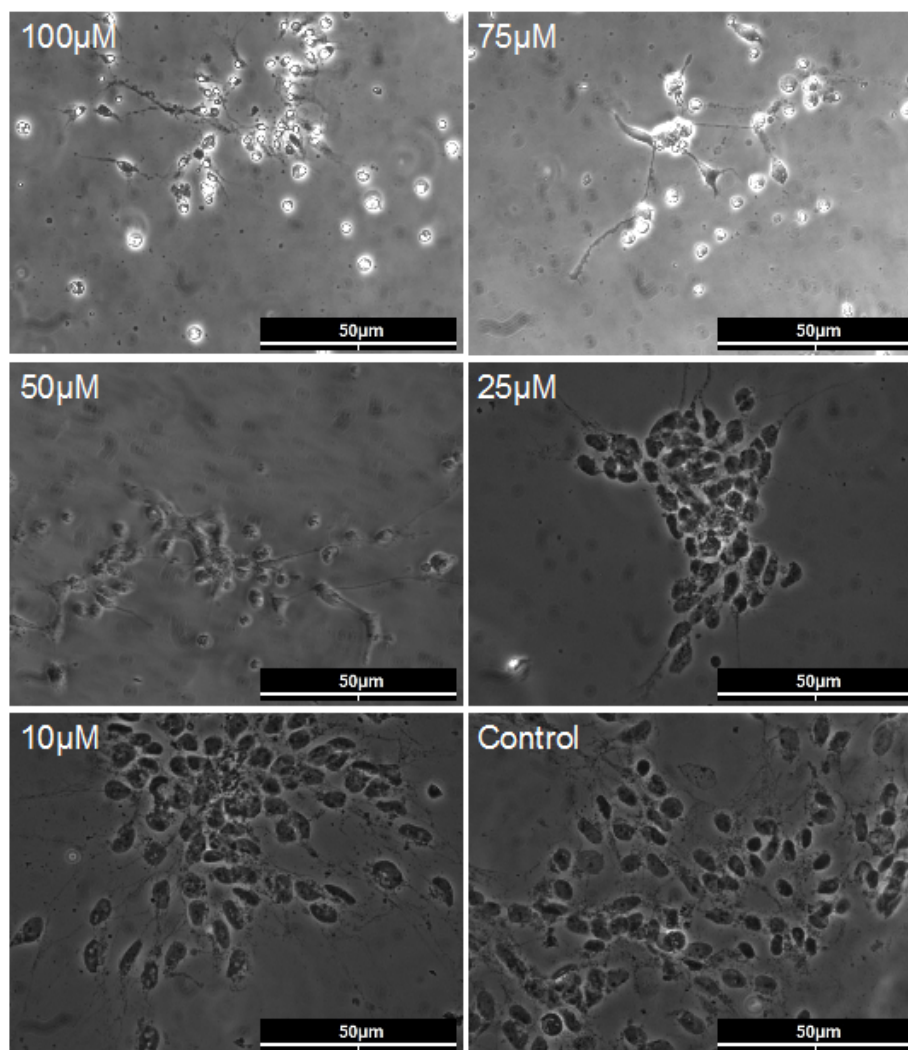


Figure 4.1: Morphological analysis of LUHMES cells treated with different concentrations of MPP⁺. Shown are representative transmission light microscope pictures of differentiated LUHMES cells at 40x magnification treated with different the indicated amounts of MPP⁺ for 48 h. From top left to bottom right: 100 μM, 75 μM, 50 μM, 25 μM, 10 μM and the untreated control. High levels of MPP⁺ caused severe amount of cell death and habitual changes.

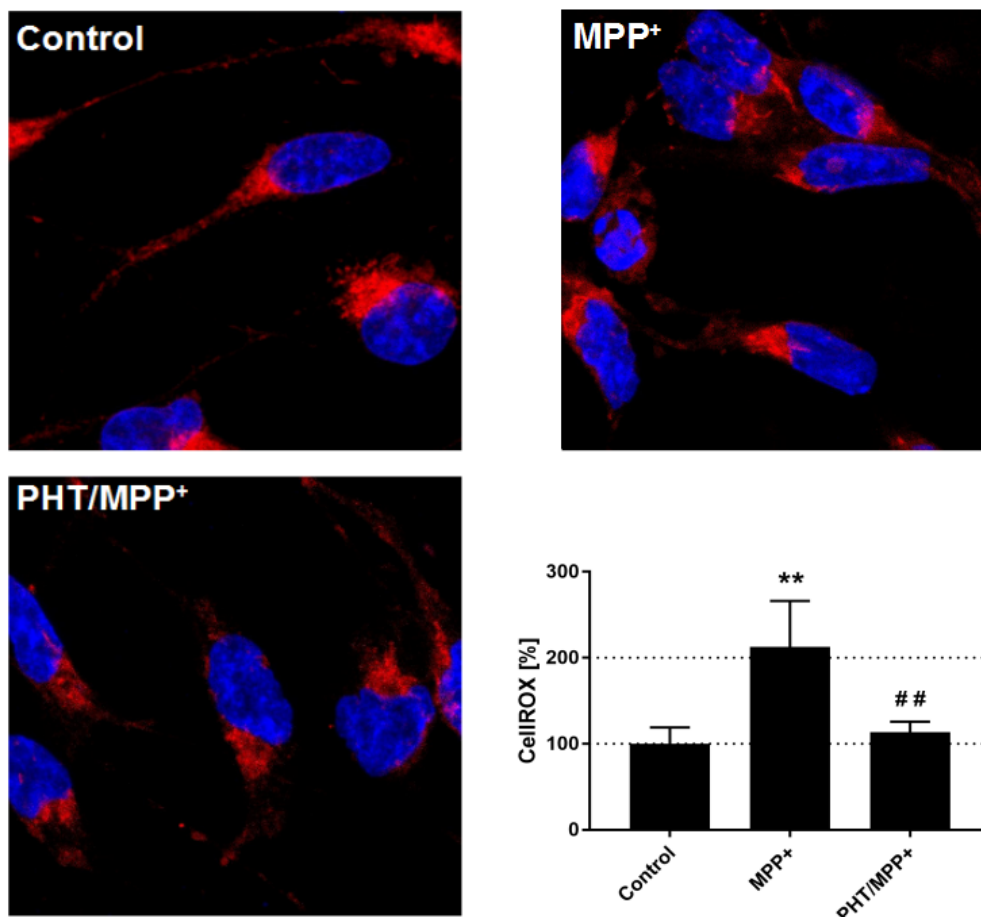


Figure 4.2: Quantitative ROS analysis of LUHMES cells treated with MPP⁺ and PHT. Shown are representative LSM pictures of differentiated LUHMES cells treated with 10 μ M MPP⁺ and 20 nM PHT for 48 h with 63x magnification, zoom factor 3 and the CellROX quantification illustrated in a bar graph diagram. CellROX signal is shown in red, DAPI in blue. Signal intensity increases under MPP⁺ and decreases again if PHT is present. '*' indicates significant differences compared to the control group, while '#' indicate significant differences compared to the MPP⁺ treated group. Symbol number indicates the grade of significance with * = $p < 0.05$, ** = $p < 0.01$, and *** = $p < 0.001$. Data represented as mean and standard deviation. n=3.

4.2 MPP⁺ causes protein hyperacetylation in differentiated LUHMES cells

Previous studies have shown that many, but not all, lysine acetylation sites of histone proteins are hyperacetylated *in vitro* and *in vivo* in the MPTP/MPP⁺ model of PD. There, H3K9ac has shown a non-significant tendency to be hyperacetylated in cells and animals treated with MPP⁺ (Park et al., 2016). However, the implications of H3K14ac, a posttranslational modification (PTM), that may act upstream of H3K9ac and thus be a possible treatment candidate, remain unknown (Karmodiya et al., 2012).

Indeed, densitometric analysis of Western blots of differentiated LUHMES cells showed a highly significant increase in H3K14ac levels normalized on total histone H3 protein upon MPP⁺ treatment to over 750% (Fig. 4.3). In general, MPP⁺, through its complex I inhibitory properties, causes

increased ROS production as well as ATP depletion (Singer et al., 1988). To judge which of these two conditions may be responsible for the observed hyperacetylation at H3K14 and whether antioxidants may have protective effects on epigenetic regulations, the established antioxidant PHT, as well as its less potent derivative APHT and the inactive MPHT, have been applied in combination with MPP⁺. PHT and APHT, although to a much smaller degree, were significantly able to reduce MPP⁺ mediated H3K14 hyperacetylation to control levels or 200%, while MPHT showed no significant improvements whatsoever. To screen for possible artefacts, PHT was also applied to LUHMES cells by itself, where it showed no significant impact on H3K14ac levels. To compare protective effects of PHT with those of APHT and MPHT, the same concentrations of the derivatives were applied. This experiment was performed in triplicate.

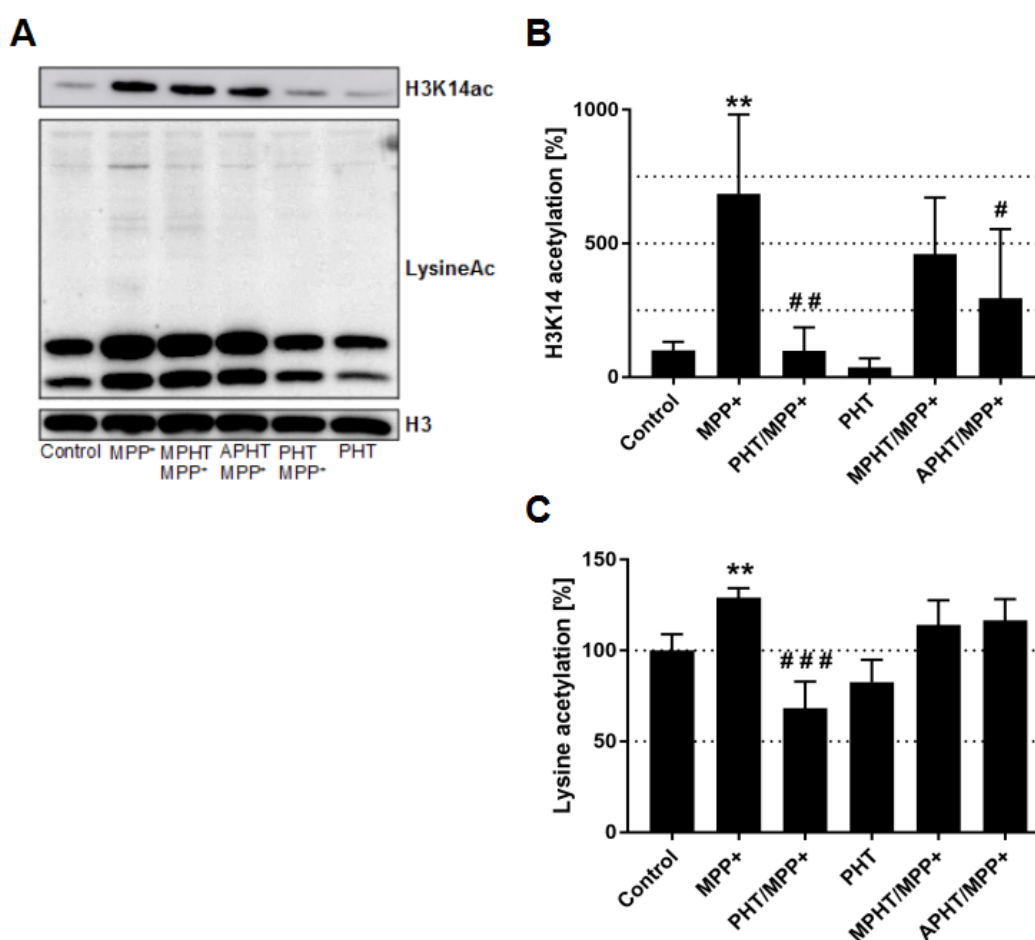


Figure 4.3: Changes in acetylation levels in differentiated LUHMES cells. A: Representative Western Blots of lysates obtained from differentiated LUHMES cells with indicated treatments (MPP⁺ 10 μ M, PHT 20 nM, MPHT 20 nM, APHT 20 nM) over 48 h showing H3K14ac, total lysine acetylation and H3. B: Densitometric quantification of H3K14ac illustrated in a bar graph diagram. C: Densitometric quantification of total lysine acetylation illustrated in a bar graph diagram. Acetylation levels increased upon MPP⁺ treatment, and responded to PHT treatment. '*' indicates significant differences compared to the control group, while '#' indicate significant differences compared to the MPP⁺ treated group. Symbol number indicates the grade of significance with * = $p < 0.05$, ** = $p < 0.01$, and *** = $p < 0.001$. Data represented as mean and standard deviation. $n=3$.

Protein acetylation in general is regulated by two protein families. Histone acetyltransferases (HATs) establish acetylation (Racey et al., 1971), while HDACs remove them (Kaneta et al., 1974). Since many histone PTMs are reportedly affected by MPP⁺ at the same time, a screening of the acetylation status of all lysines might show whether the effects are restricted to histones. Densitometric analysis of Western blots of total acetylated lysines, coined “LysineAc”, normalized on total histone H3 protein showed a significant increase by about 30% upon MPP⁺ treatment, that was significantly decreased to control levels by PHT, but not by APHT or MPHT (Fig. 4.3). Sole PHT treatment had no significant effects on general lysine acetylation status. This experiment was performed in triplicate.

Taken together these and the published data might rather point to a general disturbance of the protein acetylation system than to a specific regulatory process.

4.3 MPP⁺ induced hyperacetylation can be augmented by the HDAC inhibitor TSA, but not EX-527

Protein acetylation is governed by two kinds of enzymes. HATs write acetylations on proteins and HDACs erase them. Different HDAC inhibitors that can target a specific HDAC or a broad spectrum of HDACs allow for a more thorough investigation of their involvement in the so far observed hyperacetylation events. HAT inhibitors, on the other hand, are fewer in number and have smaller spectra than available HDAC inhibitors. Thus, two HDAC inhibitors, TSA and EX-527, were chosen to further narrow down the root of the observed hyperacetylation. TSA is a pan HDAC inhibitor that targets all class I, II and IV HDACs, but not class III HDACs, which are called sirtuins (SIRT) (Yoshida et al., 1990). EX-527, on the other hand, mainly targets sirtuin 1 (SIRT1), but can also inhibit sirtuin 2 (SIRT2) and sirtuin 3 (SIRT3) in higher concentrations (Napper et al., 2005). The remaining four sirtuins have not been reported to be affected by EX-527.

Inhibitory effects were examined through immunocytochemistry, because it would also allow assessment of cellular distribution of lysine acetylation. Differentiated LUHMES cells were treated with MPP⁺, PHT or both with and without TSA, EX-527 or both (Fig. 4.4). Under control conditions, lysine acetylation was mostly restricted to the nucleus, while MPP⁺ treated cells also showed cytosolic signal. This signal disappeared again, when PHT was also administered. When quantified, MPP⁺ treated cells compared to the control show a significant increase in lysine acetylation by almost 70% that is significantly decreased again by PHT by 50%. Exclusive PHT treatment had no significant effect on lysine acetylation levels (Fig. 4.4).

TSA treatment induced protein acetylation by roughly 50% compared to the control in a similar manner to MPP⁺, while the combination of both toxins caused even higher acetylation levels. This

increase amounted over 100% in total, was significant and demonstrated a ratio between MPP⁺ treated and non-treated cells similar to the TSA free samples. PHT, again, was able to significantly suppress the MPP⁺ effect by about 50%, but not the induction caused by TSA (Fig. 4.4).

EX-527 also caused significant lysine hyperacetylation by over 50% comparable to that of TSA. In this case, however, MPP⁺ was unable to further significantly induce lysine acetylation, while PHT also showed no significant effect on lysine acetylation (Fig. 4.4).

Combined treatment of TSA and EX-527 showed significantly increased acetylation levels by over 100%. Treatment with MPP⁺ significantly induced the system even further by an additional 150%, while PHT was again only able to significantly revert the hyperacetylation induced by MPP⁺ by more than 100% (Fig. 4.4). This experiment was performed in triplicate.

The unresponsiveness of EX-527 treated cells to MPP⁺ point towards a dysfunction of SIRT rather than other HDACs. Thus, further investigations focussed on SIRT.

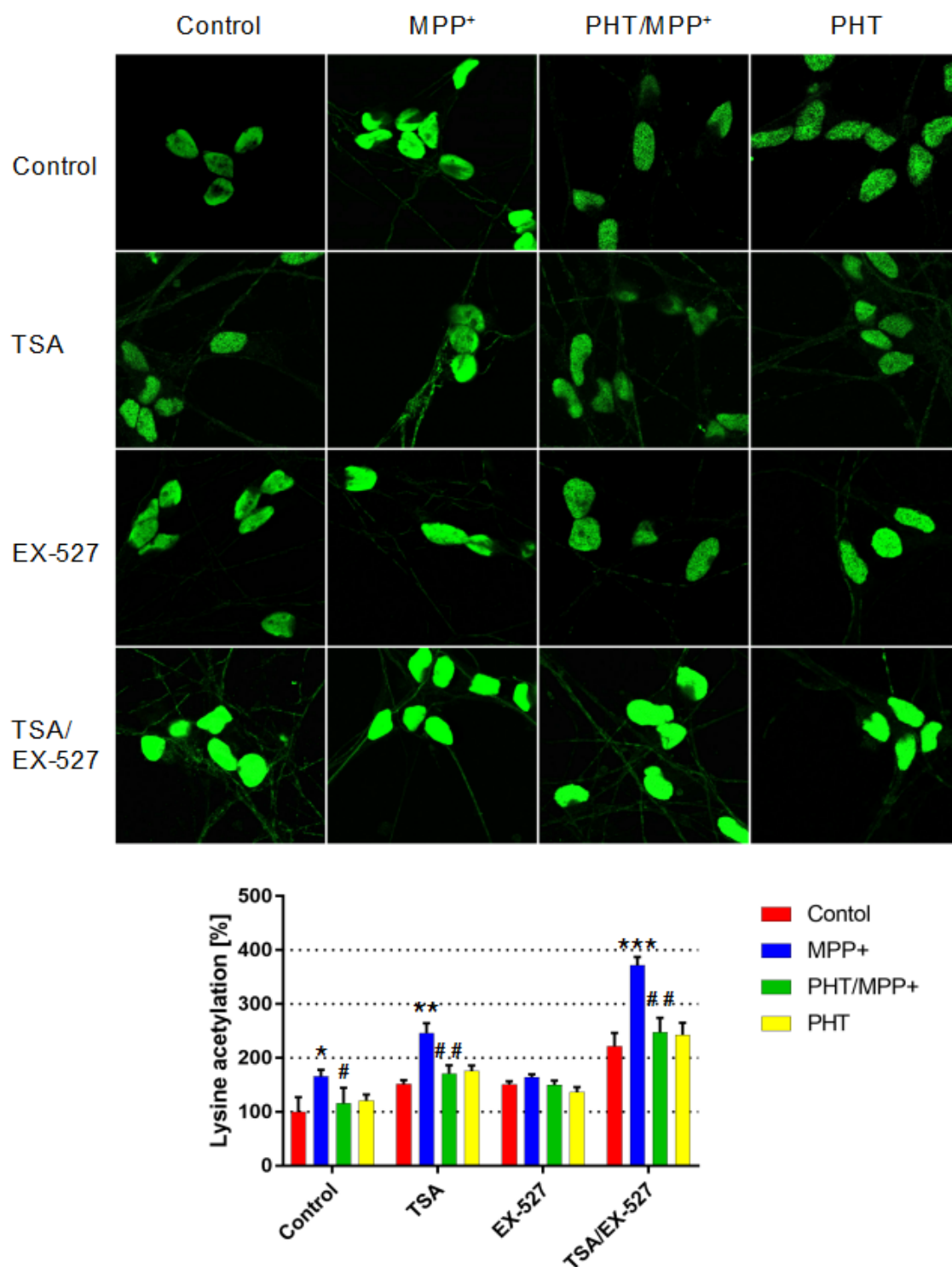


Figure 4.4: Lysine acetylation status in LUHMES cells treated with MPP⁺, TSA, EX-527 and PHT. Shown are representative LSM pictures at 63x magnification of differentiated LUHMES cells treated with the indicated compounds for 48 h (10 μ M MPP⁺, 20 nM PHT, 50 nM TSA and 100 nM Ex-527). Lysine acetylation is visualized with green colour. Quantification is illustrated in a bar graph diagram, showing increased acetylation levels upon MPP⁺, TSA and EX-527 treatment. PHT was only able to avert MPP⁺ induced hyperacetylation, while MPP⁺ was incapable of increasing the acetylation status of EX-527 treated cells. '*' indicates significant differences compared to the control group, while '#' indicate significant differences compared to the MPP⁺ treated group. Symbol number indicates the grade of significance with * = $p < 0.05$, ** = $p < 0.01$, and *** = $p < 0.001$. Data represented as mean and standard deviation. n=3.

4.4 SIRT1 activity and protein level decrease in a PHT responsive manner under MPP⁺

Since EX-527 mainly antagonizes SIRT1 (Napper et al., 2005), activity and availability of said protein were assessed. SIRT1 is a HDAC not only governing histones, but also other proteins like tumor protein (TP53) (Vaziri et al., 2001) or microtubule-associated proteins 1A/1B light chain 3B (MAP1LC3B) (Huang et al., 2015), and involved in many different cellular processes ranging from metabolic regulation (Lan et al., 2008) to genetic regulation (Pruitt et al., 2006). Its cellular availability runs anti-proportional to ageing (Longo et al., 2006), a strong risk factor for PD (Koller et al., 1987).

The activity of SIRT1 was measured using the SIRT1 activity assay from Enzo. The kit contains a small peptide that was manufactured from well-understood SIRT1 targets and can only be deacetylated by SIRT1. In a second reaction the deacetylated peptide reacts with the developer, which produces a fluorescent signal. Thus, the measured signal is proportional to the amount of active SIRT1 protein available. Activity measurements revealed a significant decrease in SIRT1 activity by roughly 25% in lysates from MPP⁺ treated cells, which can be significantly reverted by co-treatment with PHT by almost 15%, but not with MPHT. However, the cells treated with MPP⁺ and PHT still showed a significant decrease in SIRT1 activity by 10%. Exclusive treatment with PHT caused no significant changes (Fig. 4.5). This experiment was performed in triplicate.

Western Blot analysis deriving from the exact same lysates also showed a significant decrease in SIRT1 protein levels by over 30% after MPP⁺ application that persisted through MPHT co-treatment. PHT, on the other hand, significantly reduced the MPP⁺ effect by almost 20%, while exclusive PHT treatment again showed no significant effects on SIRT1 protein levels (Fig. 4.5). This experiment was performed in triplicate.

To further elucidate the mechanism behind the decreased SIRT1 protein levels, differentiated LUHMES cells were treated with MPP⁺ and PHT/MPP⁺ as well as Bafilomycin A1 (BafA1). BafA1 is a V-ATPase inhibitor that suppresses lysosomal acidification (Yoshimori et al., 1991). Usually, lysosomes may fuse with autophagosomes, vesicular structures that envelope cellular substances that are to be degraded in the autophagolysosome, the fused structure of autophagosome and lysosome (Kimura et al., 2007). Through inhibition of lysosomal acidification, the autophagosomal cargo can no longer be degraded and thus accumulates (Yoshimori et al., 1991). Recently, mass spectrometry analysis of autophagosomal content revealed the possibility to also analyse accumulation of autophagosomal cargo through BafA1 (Le Guerroué F et al., 2017).

SIRT1 accumulation through BafA1 treatment alone was only minor over the course of 4 h. In the MPP⁺ treated cells, the accumulated autophagosomes, visualized through BafA1 treatment, showed increased amounts of SIRT1 than the BafA1 untreated MPP⁺. The ratio of accumulation increased

significantly by over 60%. The ratio of accumulation was reduced to control levels in cells treated with PHT/MPP⁺ compared to the MPP⁺ treated group (Fig. 4.5). This experiment was performed in triplicate.

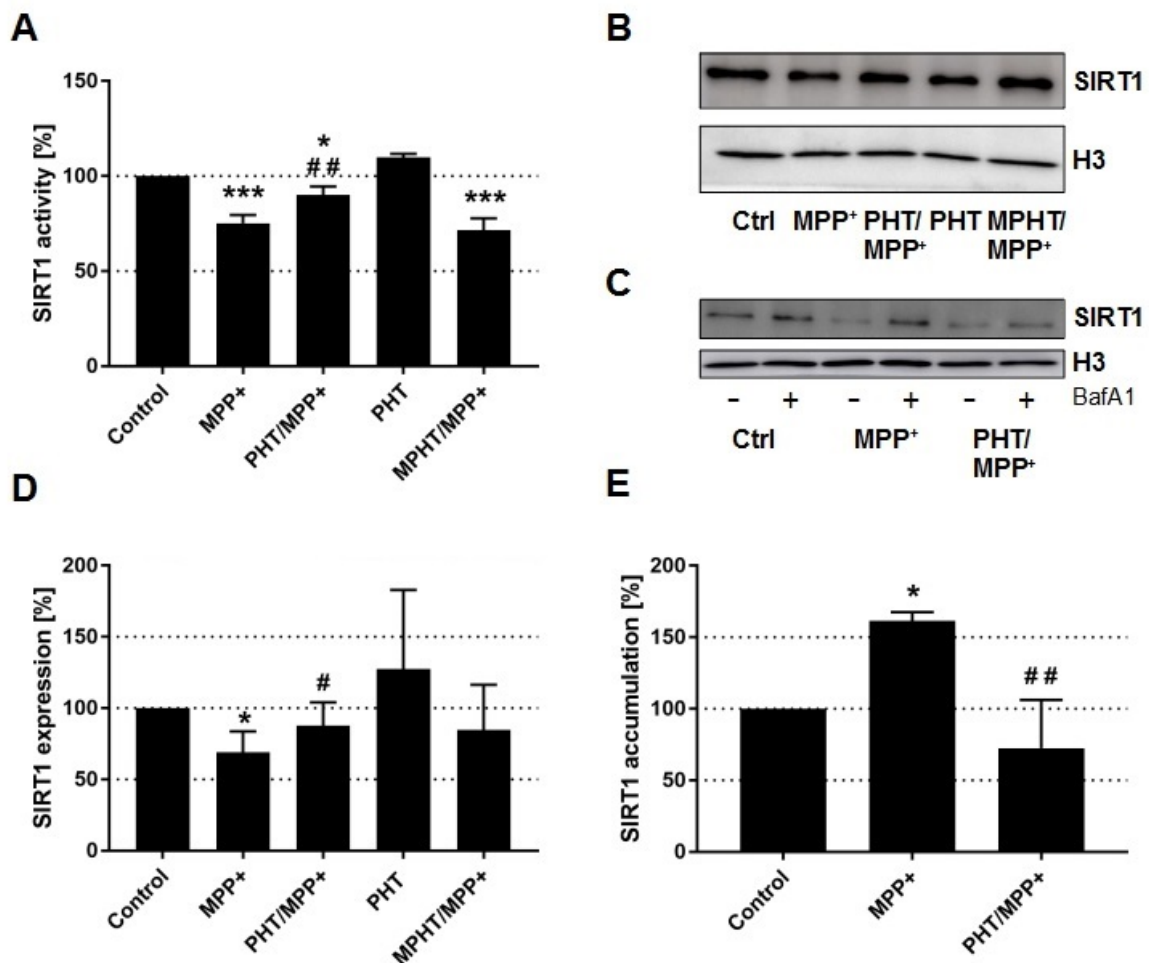


Figure 4.5: SIRT1 activity, expression and degradation in LUHMES cells treated with MPP⁺. Shown are the results regarding SIRT1. A: Evaluation of the SIRT1 activity assay results from lysates of differentiated LUHMES cells treated with the indicated compounds (MPP⁺ 10 μ M, PHT 20 nM, MPHT 20 nM) for 48 h. The immediate signal intensity was compared between the indicated treatment groups. MPP⁺ treatment showed decreased SIRT1 activity, while PHT, but not MPHT, showed significant protective effects. B: Representative Western blots from lysates of LUHMES cells of SIRT1 and H3 for total protein comparison from lysates used in the activity assay. C: Representative Western blots from lysates of LUHMES cells treated with 10 μ M MPP⁺ with and without 20 nM PHT of SIRT1 and H3 after 4 hs of BafA1 treatment. D: Densitometric analysis of the Western blots shown in B illustrated in a bar graph diagram. E: Densitometric analysis of the Western blots shown in C illustrated in a bar graph diagram. SIRT1 protein level decreased under MPP⁺, while the protein accumulated, if cells were also treated with BafA1. PHT reverted both of these effects. '*' indicates significant differences compared to the control group, while '#' indicate significant differences compared to the MPP⁺ treated group. Symbol number indicates the grade of significance with * = $p < 0.05$, ** = $p < 0.01$, and *** = $p < 0.001$. Data represented as mean and standard deviation. n=3.

These experiments demonstrate that ROS originating from MPP⁺ inhibited mitochondria severely obstructs SIRT1s activity. Previous studies already revealed SIRT1's structure to be intendedly

vulnerable to ROS (Shao et al., 2014), which then apparently leads to degradation of SIRT1 through autophagic means.

4.5 SIRT3 protein levels and localization change in MPP⁺ treated LUHMES cells

The inactivation of SIRT1 may cause other SIRTs to be up-regulated in an effort to compensate for the loss of SIRT1. A likely candidate for this is SIRT3, which is mostly found in mitochondria, the primary target of MPP⁺ (Schwer et al., 2002), while it can occasionally be encountered in the nucleus as well (Scher et al., 2007). These previous observations make SIRT3 a possible agent to establish communication between mitochondria and the nucleus.

SIRT3 is the main mitochondrial HDAC, that governs many different processes inside the mitochondria, e.g. OXPHOS activity (Ahn et al., 2008), TCA cycle (Ozden et al., 2014) or mitochondrial transcription (Liu et al., 2014). SIRT3 may present itself in two different peptides. A smaller peptide of ~28 kDa and a larger one of ~40 kDa. The former is a product of the latter one's cleavage by the mitochondrial processing peptidase (MPP) (Schwer et al., 2002), a protein located on the mitochondrial outer membrane, that governs the passage of proteins into the mitochondria (Koutnikova et al., 1998). The larger, full-length peptide is located to the nucleus (Scher et al., 2007), where it may regulate histone acetylation (Vaquero et al., 2007), as well as nuclear transcription factors (Sundaresan et al., 2009). Especially the MPP dependant distribution of SIRT3 may constitute a valid reason to investigate it in experimental models of PD.

Interestingly, differentiated LUHMES cells usually only present the smaller mitochondrial peptide and are void of the longer one (Fig. 4.6). This changes upon MPP⁺ treatment. Here the smaller peptide levels were significantly reduced by over 30%, while levels of the longer peptide were significantly induced by over 100%. Co-treatment with MPHT showed no difference, while co-treatment with PHT only increased the protein level of the smaller isoform significantly to control levels. Protein levels of the longer peptide, however, remained elevated.

The overall SIRT3 protein amount did not change significantly in MPP⁺ treated cells (Fig. 4.6). Co-treatment with PHT, however, caused a significant increase of the total amount of SIRT3 protein by almost 40%. When looking at BafA1 treated cells, the smaller peptide would accumulate under MPP⁺ in a significant manner by over 50%, while the longer one would not. This increase was significantly quenched by PHT to control levels (Fig. 4.6). Both experiments were performed in triplicates.

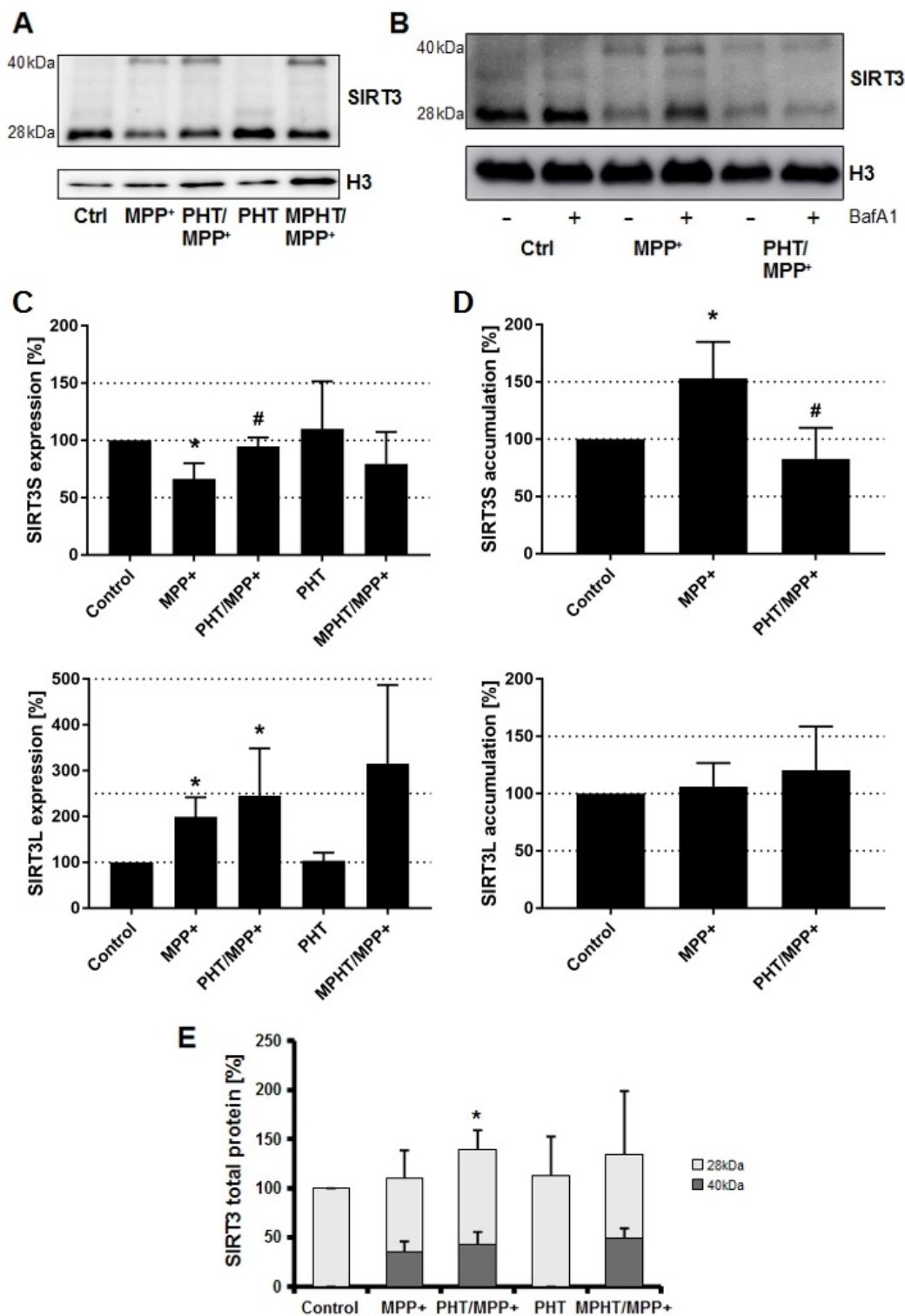


Figure 4.6: Reallocation of SIRT3 in LUHMES cells treated with MPP⁺ and PHT. Shown are the results regarding SIRT3. A: Representative Western blots of lysates from differentiated LUHMES cells treated with the indicated compounds (MPP⁺ 10 μ M, PHT 20 nM, MPHT 20 nM) for 48 h with SIRT3 and H3. B: Representative Western blots from lysates of LUHMES cells treated with 10 μ M MPP⁺ with and without 20 nM PHT of SIRT3 and H3 after 4 hs of BafA1 treatment. C: Densitometric analysis of the Western blots shown in A illustrated in a bar graph diagram. D: Densitometric analysis of the Western blots shown in B illustrated in a bar graph diagram. Under control conditions, SIRT3 only shows one isoform at ~28 kDa. When MPP⁺ is present, a second band at ~40 kDa appeared, which does not disappear upon PHT co-treatment. E: Densitometric analysis of the Western blots shown in B for total protein levels of

SIRT3, which increased in the MPP⁺/PHT treated group, illustrated in a bar graph diagram. '*' indicates significant differences compared to the control group, while '#' indicate significant differences compared to the MPP⁺ treated group. Symbol number indicates the grade of significance with * = $p < 0.05$, ** = $p < 0.01$, and *** = $p < 0.001$. Data represented as mean and standard deviation. n=3.

These data demonstrate a sudden shift of SIRT3s cellular distribution upon MPP⁺ mediated stress, which is irreversible by PHT. This may thus likely be a respond to the energetic impairments caused by OXPHOS malfunction. The nuclear translocation of SIRT3 may also compensate for the reduced activity of SIRT1, since they do have some overlapping targets (Scher et al., 2007, Imai et al., 2000).

4.6 Antioxidants protect dopaminergic neurons from MPTP induced cell death *in vivo*

To validate the relevance of the hitherto observed data an *in vivo* mouse model was established. Three groups of ten mice each were treated with either MPTP (20 mg/kg bodyweight), PHT (10 mg/kg bodyweight)/MPTP or the vehicles the chemicals (saline or corn oil) were administered in. MPTP was applied four times a day within 2 h intervals intraperitoneally, two days prior to sampling. PHT was administered orally starting four days prior to MPTP treatment until tissue sampling twice a day within 4 h interval (Fig. 3.1). Because MPP⁺ is unable to pass the blood brain barrier, the animals received treatment of the pro-toxin MPTP, which is metabolised in astrocytes to MPP⁺ (Ransom, et al. 1987). Two animals total, one from the MPTP and one from the PHT/MPTP group, died during the course of the experiment and were excluded from all subsequent evaluations. Prior to any possible epigenetic involvements it was required to inspect the status of the substantia nigra (SN) to confirm toxic effects of MPTP and the estimated protective properties of PHT (Moosmann et al., 2001).

The left hemispheres of the mice were cut into 10 μ m thin slices that were subjected to immunohistochemical assessment of the protein tyrosine hydroxylase (TH) to examine the integrity of dopaminergic SN neurons. TH is the bottleneck protein of dopamine production, that catalyses the first and rate limiting step that converts L-tyrosine to L-dihydroxyphenylalanine (L-DOPA) (Nagatsu et al., 1964) and is commonly used as a marker for dopaminergic cell loss in PD (Haavik et al., 1998). To bypass the increasing loss of TH in PD, L-DOPA is administered as treatment (Cotzias, 1968), which would allow the following steps of dopamine production to be performed.

The amount of surviving cells were thus quantified using TH immunohistochemistry. MPTP treatment caused severe and significant loss of dopaminergic neurons in the SN by 55.97%, leaving

the ventral tegmental area (VTA), another set of dopaminergic neurons, intact. Co-treatment with PHT significantly protected almost all of the present cells with 97.26% of the cells remaining (Fig. 4.7).

Furthermore, the animals were examined on the Rotarod prior to sacrifice. During the Rotarod performance test the animals are placed on a horizontal, rotating cylinder above a cage floor, high enough to induce avoidance of fall, but low enough to not injure the animals upon falling. Thus, the animals try to stay on top of the cylinder. This test is commonly used to investigate the motoric capabilities of mice in PD model systems (Rozas et al., 1997). MPTP treated animals were unable to remain on the Rotarod apparatus for as long as the vehicle treated group. The mean of the PHT/MPTP treated animals, on the other hand, were able to stay longer on the device compared to the MPTP group (Fig. 4.7).

These data confirm the viability of the established *in vitro* model when it is extended towards an *in vivo* paradigm at least on a cellular level. These effects also impact the motoric capabilities of the mice to some degree.

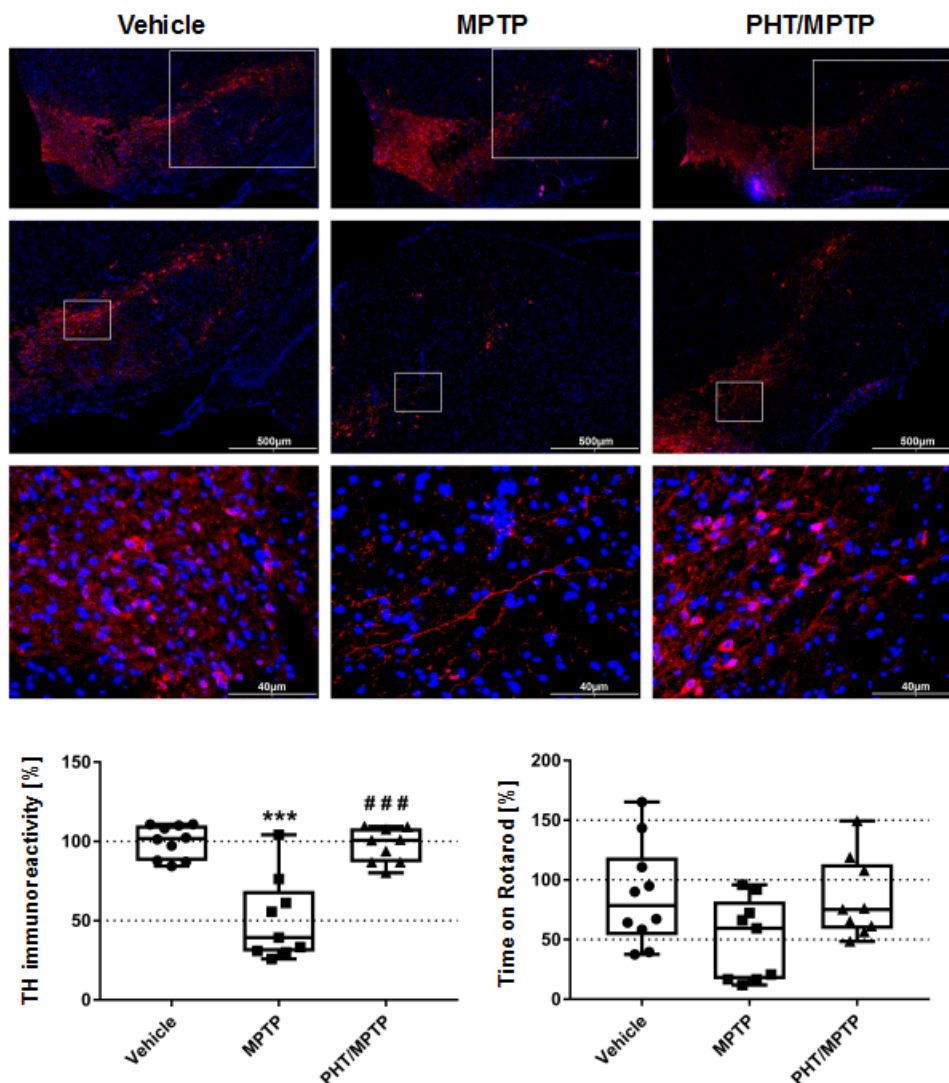


Figure 4.7: Effects of MPTP and PHT on cell survival and motoric capabilities *in vivo*. Shown are representative pictures from immunohistochemistry of mice brains that were captured using a fluorescence microscope. Three groups of ten mice each were treated with either MPTP (20 mg/kg bodyweight), PHT (10 mg/kg bodyweight)/MPTP or the vehicles the chemicals (saline or corn oil) were administered in. MPTP was applied four times a day within 2 h intervals intraperitoneally, two days prior to sampling. PHT was administered orally starting four days prior to MPTP treatment until tissue sampling twice a day within 4 h interval. The upper row shows an overview of the SN, the middle row a picture with 4x magnification and the lower row a picture with 20x magnification. TH is visualized in red, DAPI in blue. Quantification of TH signal and Rotarod performance are shown in two box-plot diagrams. In both cases, the MPTP group performed worse than the other two. '*' indicates significant differences compared to the vehicle treated group, while '#' indicate significant differences compared to the MPTP treated group. Symbol number indicates the grade of significance with * = $p < 0.05$, ** = $p < 0.01$, and *** = $p < 0.001$. Error bars in 5%/95%. n=10 (vehicle), 9 (MPTP, PHT/MPTP).

4.7 MPTP causes protein hyperacetylation *in vivo*

The H3K14 acetylation status in the murine brains was used to assess possible hyperacetylation events *in vivo* that were previously observed *in vitro*. Immunohistochemistry revealed that the H3K14 locus was indeed significantly hyperacetylated by roughly 50% in the SN of the mice when they were treated with MPTP. Orally administered PHT, however, was still able to reduce the effects to control levels in a significant manner (Fig. 4.8). The dopamine transporter (DAT) was used to locate the SN.

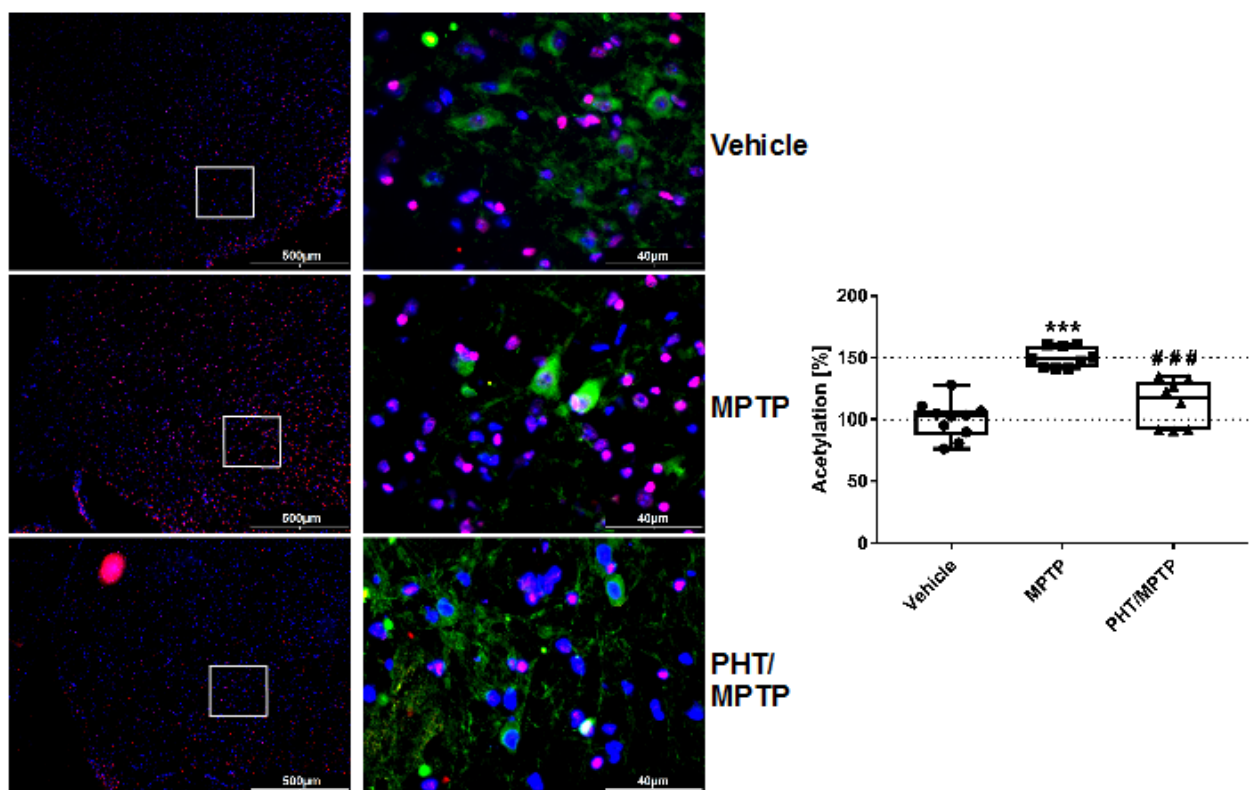


Figure 4.8: Histone acetylation status of the SN after MPTP and PHT treatments. Shown are representative pictures from immunohistochemistry of mice brains that were captured using a fluorescence microscope. Three groups

Results

of ten mice each were treated with either MPTP (20 mg/kg bodyweight), PHT (10 mg/kg bodyweight)/MPTP or the vehicles the chemicals (saline or corn oil) were administered in. MPTP was applied four times a day within 2 h intervals intraperitoneally, two days prior to sampling. PHT was administered orally starting four days prior to MPTP treatment until tissue sampling twice a day within 4 h interval. Left column shows pictures at 4x magnification, the right one at 20x magnification. H3K14ac is visualized in red, DAT in green and DAPI in blue. Signal intensity increases in the MPTP group and decreases again in the PHT/MPTP group. '*' indicates significant differences compared to the vehicle treated group, while '#' indicate significant differences compared to the MPTP treated group. Symbol number indicates the grade of significance with * = $p < 0.05$, ** = $p < 0.01$, and *** = $p < 0.001$. Error bars in 5%/95%. n=10 (vehicle), 9 (MPTP, PHT/MPTP).

Western blot analysis of the midbrain of the right hemispheres confirmed these observations. MPTP significantly induced H3K14ac by over 150%, while PHT significantly reduced the acetylation to control levels. The same was true for general lysine acetylation. On Western blot level, MPTP, again, caused a significant hyperacetylation of total lysines by more than 50%, that was also significantly reduced to control levels by PHT (Fig. 4.9).

When looking at the so far investigated different SIRTs, SIRT1 was significantly up-regulated in both the MPTP and the PHT/MPTP group by almost 30% each, while SIRT3 was significantly down-regulated in the MPTP group by roughly 30%. The effect on SIRT3 was significantly blocked by PHT. Here, SIRT3 only showed one band at ~38 kDa.

Since SIRT3 here only showed one band, its localization cannot be properly investigated. Thus, SIRT4, another mitochondrial sirtuin, was also examined. Unlike SIRT1 and SIRT3, who have a very broad set of targets, SIRT4's set is quite narrow. SIRT4 regulates the acetyl-CoA supply of the cells by deactivating the producing enzymes through PTM (Mathias et al., 2014; Haigis et al., 2006). SIRT4 is also significantly down-regulated in the MPTP group by almost 25%. As was the case for SIRT3, PHT significantly blocked the MPTP effect on SIRT4 (Fig. 4.9).

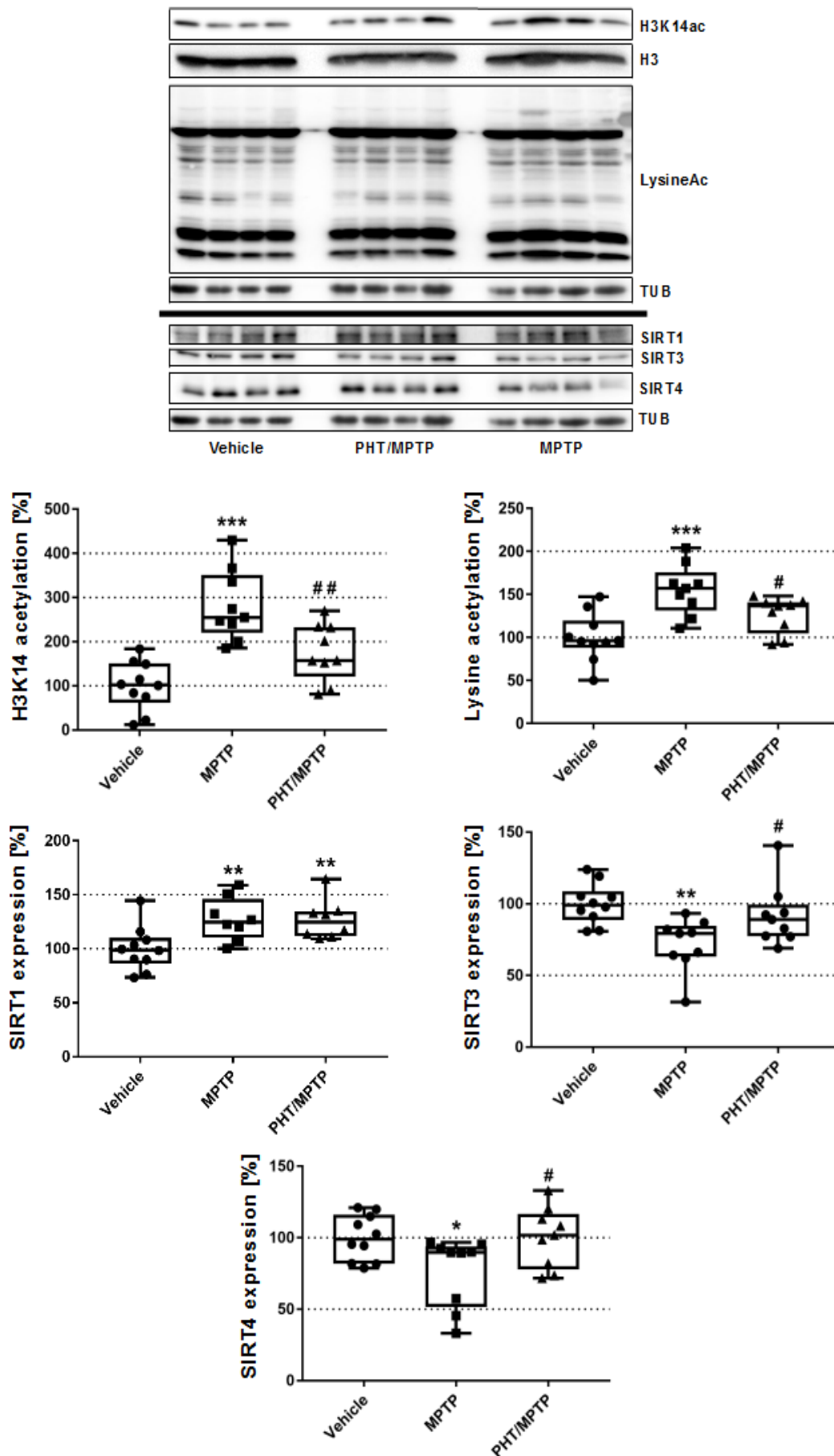


Figure 4.9: Biochemical analysis of protein acetylation and SIRT protein levels after MPTP and PHT treatments.

Three groups of ten mice each were treated with either MPTP (20 mg/kg bodyweight), PHT (10 mg/kg bodyweight)/MPTP or the vehicles the chemicals (saline or corn oil) were administered in. MPTP was applied four times a day within 2 h intervals intraperitoneally, two days prior to sampling. PHT was administered orally starting four days prior to MPTP treatment until tissue sampling twice a day within 4 h interval. Shown are representative Western blots of H3K14ac, H3, LysineAc, TUB, SIRT1, SIRT3 and SIRT4 from mid-brain lysates of the mice. Densitometric quantification of the blots is shown in box-plot diagrams normalized on TUB. Acetylation levels were increased under MPTP, but were protected by PHT. SIRT3 and SIRT4 were both down-regulated under MPTP which was averted by PHT. SIRT1 was up-regulated in both groups. '*' indicates significant differences compared to the vehicle treated group, while '#' indicate significant differences compared to the MPTP treated group. Symbol number indicates the grade of significance with * = $p < 0.05$, ** = $p < 0.01$, and *** = $p < 0.001$. Error bars in 5%/95%. n=10 (vehicle), 9 (MPTP, PHT/MPTP).

4.8 MPP⁺ treatment causes DNA hypomethylation and disturbances in DNMT level and localization

Epigenetic regulatory functions of SIRT, especially of SIRT1, are not restricted to histone acetylation. SIRT1 has been shown to be an important partner of DNMTs by coordinating the deacetylation of histones and the methylation of DNA, thus forming silent heterochromatin (Peng et al., 2011; Wakeling et al., 2015). Previous studies have shown that the DNA of dopaminergic neurons in the SN from PD patients is hypomethylated (Desplats et al., 2011) and a generally hypomethylated DNA may constitute histone hyperacetylation (Jackson et al., 2004) and vice versa (Pikaart et al., 1998). Thus, the DNA methylation status in LUHMES cells was investigated next.

DNA methylation levels were measured via immunocytochemistry and Southern blot using an antibody against 5-methyl-cytosine. Immunocytochemistry showed that the amount of 5-methyl-cytosine was significantly decreased in cells treated with MPP⁺ by more than 50%, which was significantly prevented by PHT. As a positive control, 6-thioguanine (6-TG) was used to validate the assay- 6-TG is a guanine analogous, that is integrated into the DNA and then prevents the methylation establishing enzymes of the DNA-methyltransferase (DNMT) family from methylating the corresponding cytosine (Hogarth et al., 2008). In this case, DNA was also significantly hypomethylated by over 60%, which would validate the viability of this analysis. This experiment was performed in triplicate.

These data were confirmed by DNA dot blot. Here, MPP⁺ treated cells also showed a decrease in 5-methyl-cytosine level that was precluded by PHT (Fig. 4.10). This experiment was performed once to support the immunocytochemical data. Both experiments reveal severe hypomethylation of the DNA in cells treated with MPP⁺, which can be traced back to increased ROS production due to PHT being able to protect the DNA methylation status.

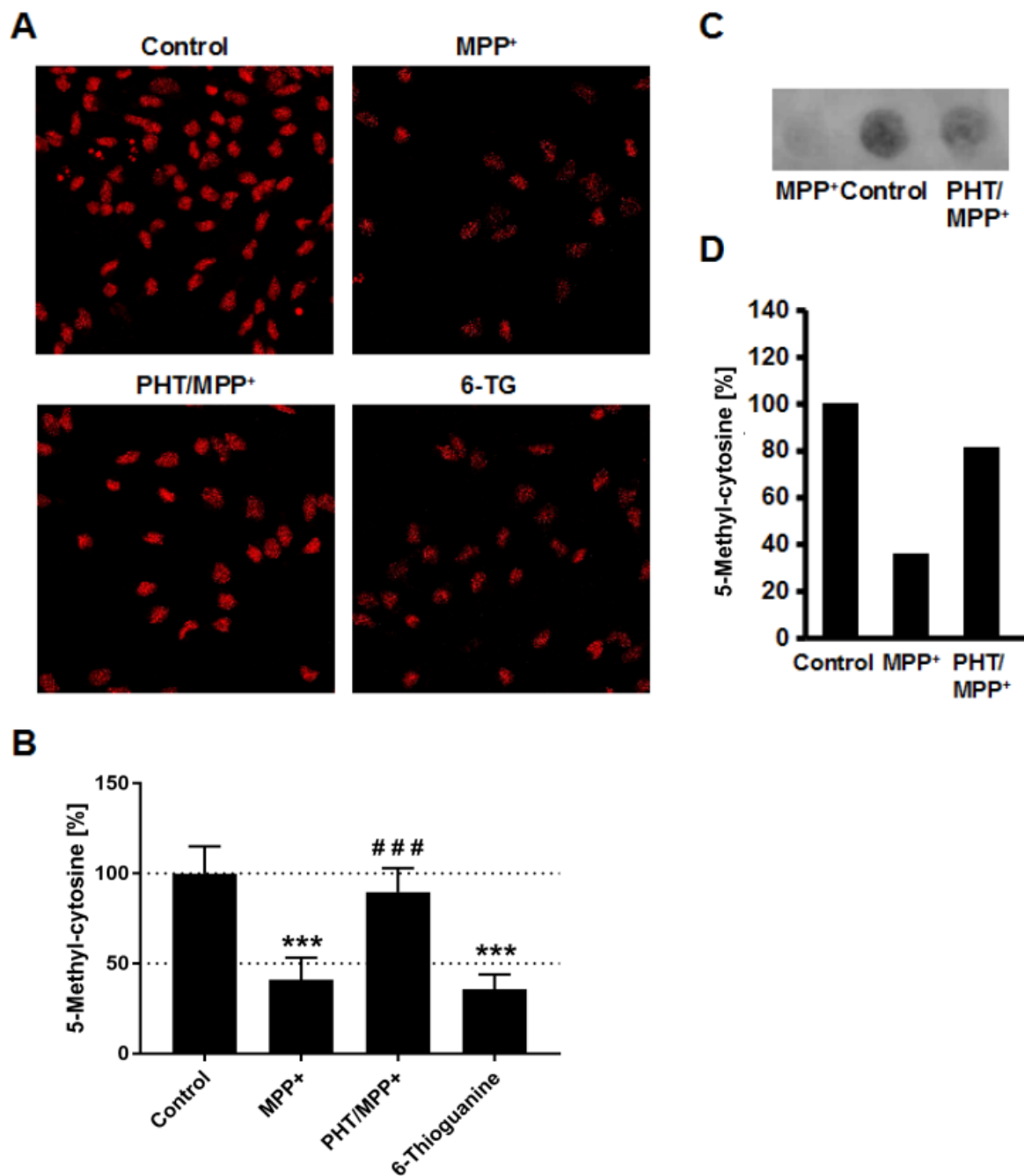


Figure 4.10: DNA hypomethylation in LUHMES cells after MPP⁺ and PHT treatments. Shown are results concerning DNA hypomethylation. A: Shown are representative LSM pictures of differentiated LUHMES cells treated with 10 μ M MPP⁺, 20 nM PHT or 1 μ M 6-TG for 48 h with 63x magnification. 5-methylcytosine is visualized in red. Observed signals are restricted to the nucleus. B: Quantification of A illustrated in a bar graph diagram. MPP⁺ and 6-TG treated cells showed a reduced 5-methylcytosine signal. Symbol number indicates the grade of significance with * = $p < 0.05$, ** = $p < 0.01$, and *** = $p < 0.001$. Data represented as mean and standard deviation. $n=3$. C: DNA dot blot of differentiated LUHMES cells treated with 10 μ M MPP⁺ and 20 nM PHT over 48 h. D: Densitometric analysis of C illustrated in a column graph diagram. '*' indicates significant differences compared to the vehicle treated group, while '#' indicate significant differences compared to the MPP⁺ treated group. $n=1$.

To gain a better understanding of the underlying mechanism, the cellular distribution of DNMTs was investigated through immunocytochemistry. The maintenance DNMT, DNMT1 is usually

located to the nucleus, where most DNA is stored, but can also in a lesser extent be found inside the cytosol (Ratnam et al., 2002). Treatment with MPP⁺, however, caused the DNMT1 to rather be localized to the cytosol rendering the nucleus completely void of the protein. This was not amendable through PHT treatment. Interestingly, 6-TG also caused a minor, but significant dislocalization of DNMT1. Counting of DNMT1 negative nuclei normalized on the total amount of nuclei revealed a significant decline of DNMT1 positive nuclei under MPP⁺, PHT/MPP⁺ and 6-TG by roughly 50% each in each group (Fig. 4.11). This experiment was performed in triplicate.

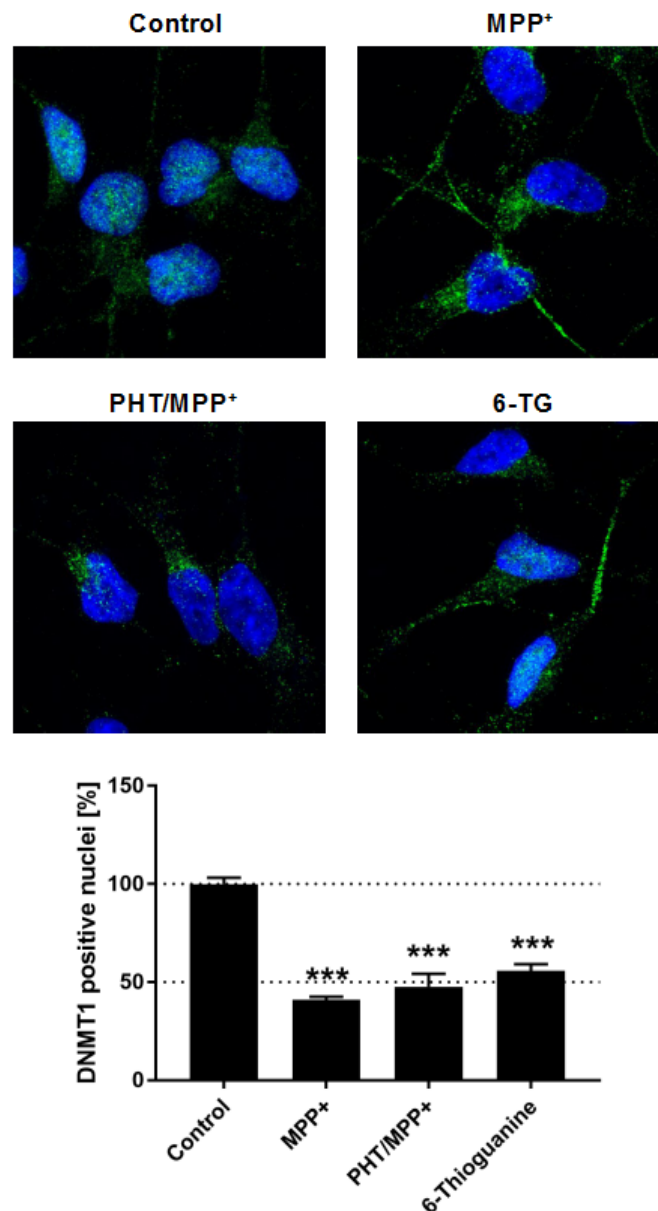


Figure 4.11: DNMT1 reallocation in LUHMES cells treated with MPP⁺ and PHT. Shown are representative LSM pictures of differentiated LUHMES cells treated with 10 μ M MPP⁺, 20nM PHT or 1 μ M 6-TG for 48h with 63x magnification, zoom factor 3 and a bar graph diagram of their quantification. DNMT1 is visualized in green and DAPI in blue. Under control conditions DNMT1 was mostly located to the nucleus, while MPP⁺ and PHT/MPP⁺ treated cells showed DNMT1 void nuclei. 6-TG treated cells also showed empty nuclei, but to a lesser extent. '*' indicates significant differences compared to the vehicle treated group, while '#' indicate significant differences compared to the MPP⁺

Results

treated group. Symbol number indicates the grade of significance with * = $p < 0.05$, ** = $p < 0.01$, and *** = $p < 0.001$. Data represented as mean and standard deviation. $n=3$.

The DNMTs capable of establishing DNA methylation patterns *de novo*, DNMT3A and DNMT3B (Okano et al., 1999), gave a different picture. Control conditions showed DNMT3A to be distributed throughout the cell, organized in cytosolic and nuclear foci. The signal intensity significantly decreased upon MPP⁺ treatment by almost 50% that was not responsive to PHT. In both cases, nuclear and cytosolic signal were decreased, except for one big perinuclear focus. 6-TG also caused a smaller but still significant decline of DNMT3A signal by more than 30% (Fig. 4.12). This experiment was performed in triplicate.

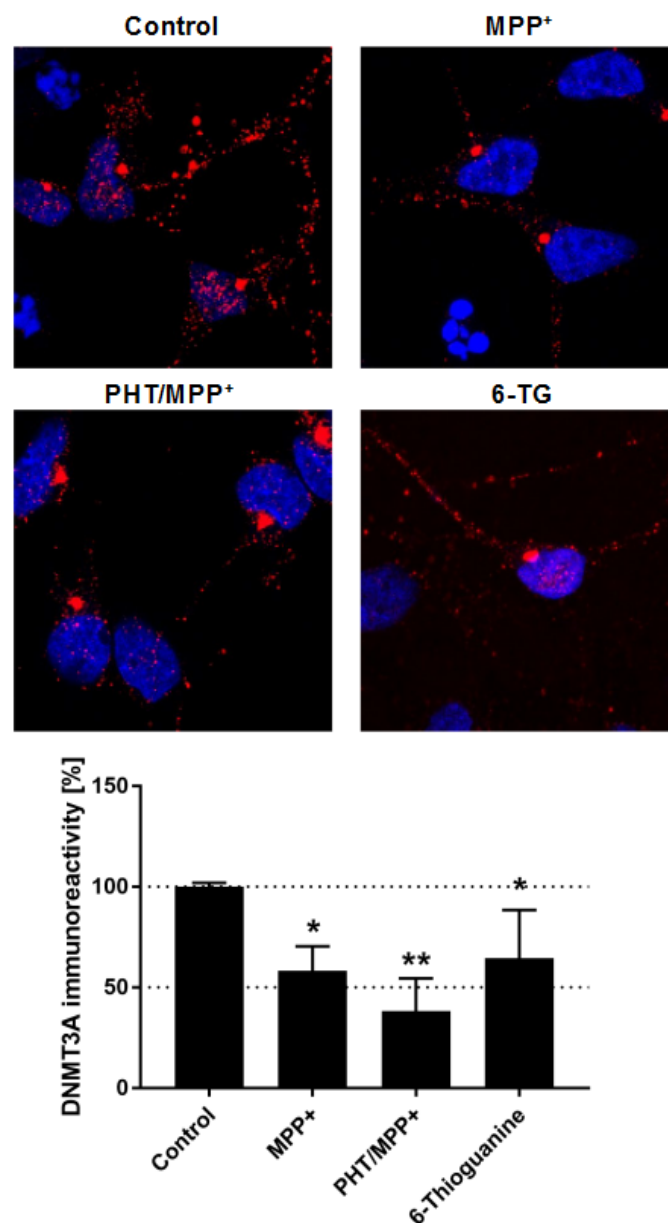


Figure 4.12: Status of DNMT3A in LUHMES cells treated with MPP⁺ and PHT. Shown are representative LSM pictures of differentiated LUHMES cells treated with 10 μM MPP⁺, 20 nM PHT or 1 μM 6-TG for 48 h with 63x magnification, zoom factor 3 and a bar graph diagram of their quantification. DNMT3A is visualized in red and DAPI

Results

in blue. DNMT3A signal was organized in foci and distributed throughout the entire cell with a slight bias for nuclear localization. The signal decreased when MPP⁺ was present, regardless of PHT. '*' indicates significant differences compared to the vehicle treated group, while '#' indicate significant differences compared to the MPP⁺ treated group. Symbol number indicates the grade of significance with * = $p < 0.05$, ** = $p < 0.01$, and *** = $p < 0.001$. Data represented as mean and standard deviation. n=3.

DNMT3B, on the other hand, could mainly be found inside the nucleus with almost no signal inside the cytosol. Signal intensity significantly diminished in MPP⁺ treated cells by more than 50%. Here, however, a significant protective effect by PHT could be observed. The signal was even stronger and significantly intense than in the untreated control group by over 50%. 6-TG showed no significant effect on DNMT3B signal intensity (Fig 4.13). This experiment was performed in triplicate.

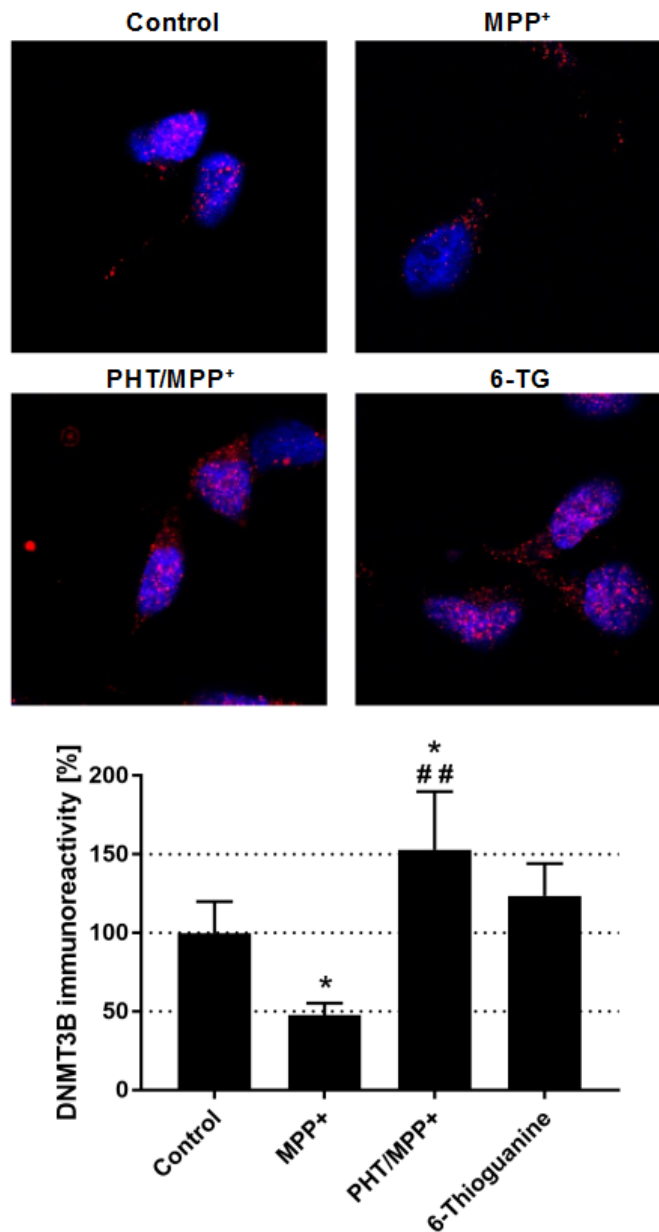


Figure 4.13: Status of DNMT3B in LUHMES cells treated with MPP⁺ and PHT. Shown are representative LSM

Results

pictures of differentiated LUHMES cells treated with 10 μM MPP⁺, 20 nM PHT or 1 μM 6-TG for 48 h with 63x magnification, zoom factor 3 and a bar graph diagram of their quantification. DNMT3B is visualized in red and DAPI in blue. DNMT3B signal was almost exclusive to the nucleus and decreased under MPP⁺, but not under PHT/MPP⁺ or 6-TG. PHT/MPP⁺ treatment caused an increase in signal also compared to control. '*' indicates significant differences compared to the vehicle treated group, while '#' indicate significant differences compared to the MPP⁺ treated group. Symbol number indicates the grade of significance with * = $p < 0.05$, ** = $p < 0.01$, and *** = $p < 0.001$. Data represented as mean and standard deviation. n=3.

Western blot analysis of DNMT3B revealed two major bands, one at ~72 kDa and one at ~100 kDa. Both bands showed a significant decrease in protein level under MPP⁺, by almost 30% (72 kDa) and more than 20% (100 kDa). PHT treatment always yielded significantly increased protein levels by roughly 50%, but only for the smaller band. PHT demonstrated no significant effects on protein levels of the long isoform. MPHT showed no significant protective effect on either form (Fig. 4.14). When looking at Western blots of the murine midbrain lysates from the established and previously described *in vivo* model treated with MPTP, PHT/MPTP or just the vehicle, changes in protein levels of DNMT3B could be observed as well. MPTP caused a significant decrease in protein levels by almost 25% that was significantly attenuated by PHT. Here the blot only showed one band at ~100 kDa (Fig. 4.14).

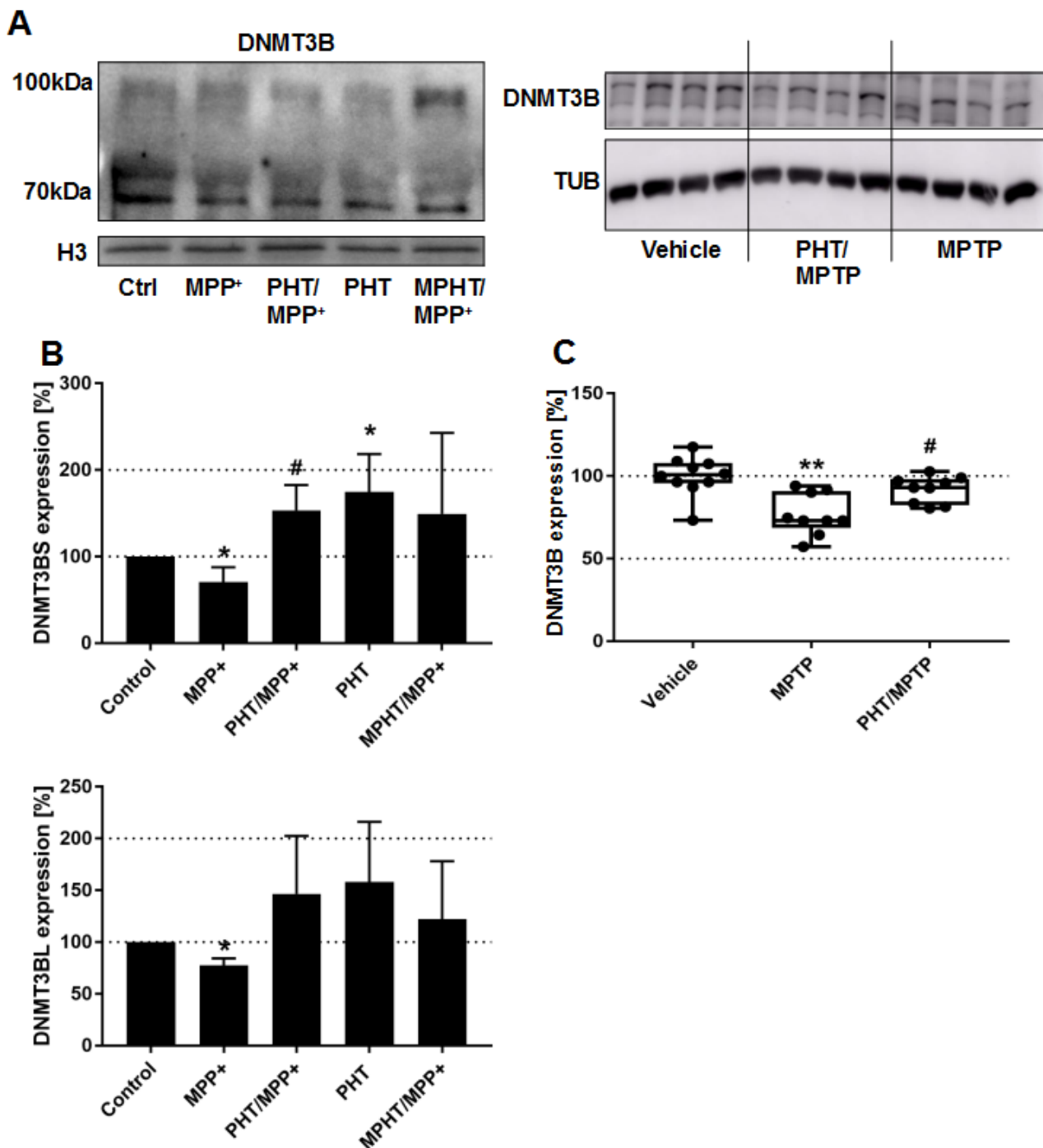


Figure 4.14: *In vivo* and *in vitro* biochemical analysis of DNMT3B after treatments with MPTP/MPP⁺ and PHT. Shown are Western blot data regarding DNMT3B. A: Representative Western blots of differentiated LUHMES cells treated with indicated compounds (MPP⁺ 10 μ M, PHT 20 nM, MPHT 20 nM) for 48 h for DNMT3B and H3. The DNMT3B blot shows two bands at \sim 100 kDa and \sim 70 kDa. Three groups of ten mice each were treated with either MPTP (20 mg/kg bodyweight), PHT (10 mg/kg bodyweight)/MPTP or the vehicles the chemicals (saline or corn oil) were administered in. MPTP was applied four times a day within 2 h intervals intraperitoneally, two days prior to sampling. PHT was administered orally starting four days prior to MPTP treatment until tissue sampling twice a day within 4 h interval. Representative Western blots of murine midbrain lysates for DNMT3B and TUB. Here only one band appears at \sim 100 kDa. B: Bar graph diagrams of the densitometric quantifications of A normalized on H3. Both isoforms respond to MPP⁺ with a reduction in protein level. C: Box-plot diagrams of the densitometric quantifications of E normalized on TUB. *In vivo* data complement the *in vitro* results. '*' indicates significant differences compared to

the vehicle treated group, while '#' indicate significant differences compared to the MPP⁺ treated group. Symbol number indicates the grade of significance with * = $p < 0.05$, ** = $p < 0.01$, and *** = $p < 0.001$. Data represented as mean and standard deviation. n=3.

Taken together, these data indicate that a loss of DNMT3B protein is responsible for the DNA hypomethylation and neither DNMT1, nor DNMT3A, since only the DNA methylation and DNMT3B effects are responsive to PHT treatment.

4.9 MPP⁺ induces gene expression of nuclear encoded mitochondrial respiratory chain subunits and causes mitochondria to favour replication over transcription

So far, a loss of heterochromatin through DNA hypomethylation and histone hyperacetylation could be described. To assess the repercussions of this loss through evaluation of its immediate consequences in transcription, RNASeq of enriched mRNA from differentiated LUHMES cells treated with MPP⁺ or PHT/MPP⁺ or the vehicle was performed.

Yielded reads were mapped to the human genome and in depth analysis of the data was conducted by looking at the regulation of gathered transcripts that are associated with specific pathways to evaluate whether changes occur randomly or whether an enrichment of certain pathways or supercomplexes can be observed. Because MPP⁺ is first and foremost a mitochondrial respiratory poison (Nicklas et al., 1985), transcripts of nuclear encoded mitochondrial respiratory complexes were examined first.

Indeed, enrichment analysis revealed transcription of the complexes I, III, IV and V, but not the complex II, to be significantly up-regulated in MPP⁺ treated cells. Compared to that, the PHT/MPP⁺ group showed significant down-regulation of the complexes III, IV and V, but not of the complexes I and II (Fig. 4.15).

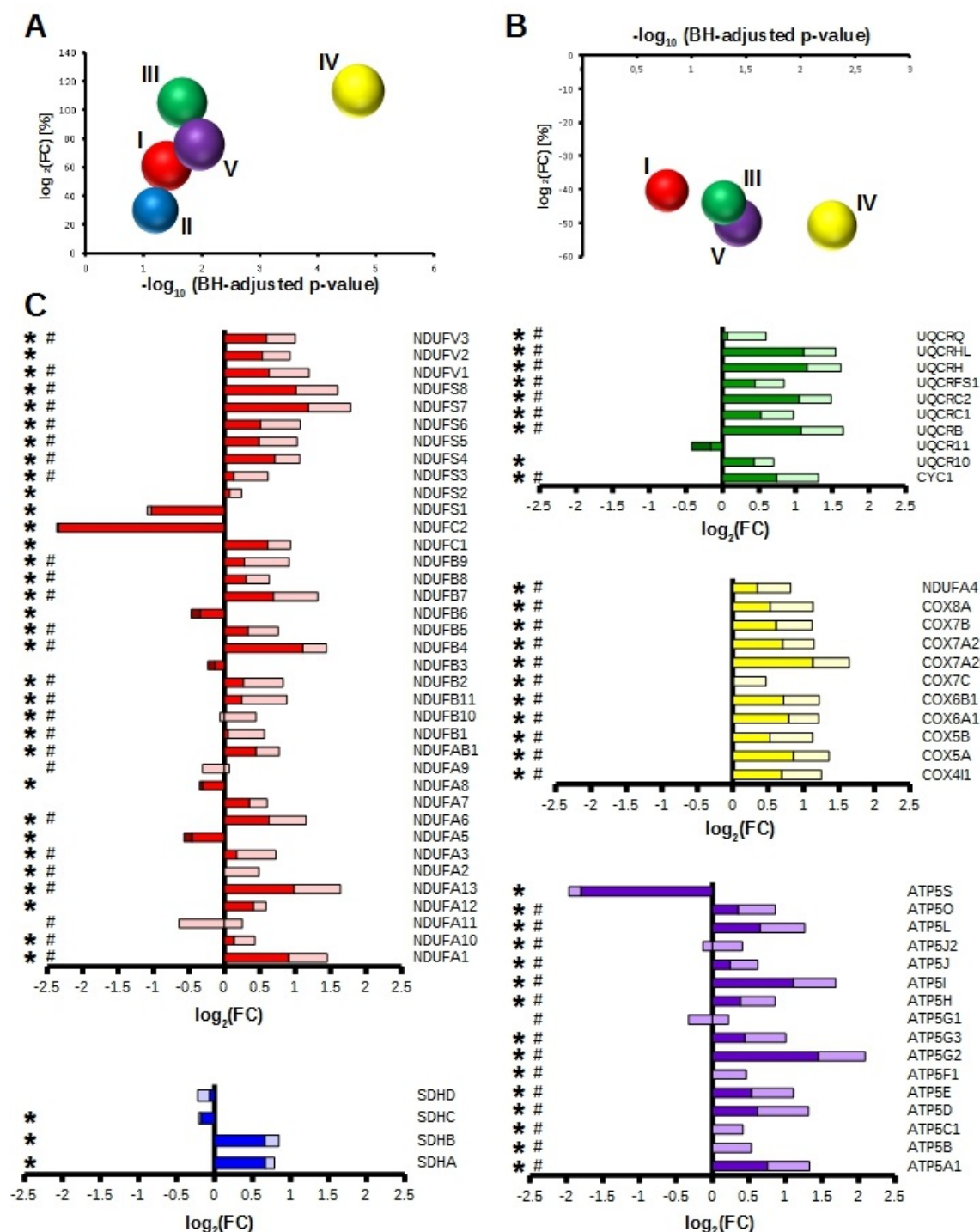


Figure 4.15: Transcriptional regulation of nuclear encoded mitochondrial subunits in MPP⁺ and PHT treated cells. Transcriptional changes of nuclear encoded respiratory complex subunits in differentiated LUHMES cells treated with 10 μM MPP⁺ and 20 nM PHT over 48 h. A: Bubble diagram visualizing the overall regulation of respiratory subunits transcripts under MPP⁺. Red represents complex I, blue II, green III, yellow IV and purple V. Bubble size indicates the fraction of significantly regulated transcripts divided by the total number of complex related transcripts. Bubble position on the Y-axis relates to log₂ mean regulation, position on the X-axis relates to -log₁₀ mean of the p-value. B: Bubble diagram comparing PHT/MPP⁺ to MPP⁺. C: Graphs showing regulation of nuclear encoded subunits. Regulation under MPP⁺ is indicated by graph size, regulation under PHT/MPP⁺ indicated by a lighter colour, if the MPP⁺ effect is reduced, or by a darker colour, if the MPP⁺ effect is amplified. '*' indicates if the MPP⁺ treatment is significantly different compared to the control, while '#' indicates if the MPP⁺/PHT treated group is significantly different compared to the MPP⁺ treated group. Data represented as mean. n=3.

Interestingly, these regulations did not extend to the mitochondrial encoded subunits of the respiratory complexes. They are, indeed, all significantly down-regulated under MPP⁺ when compared to the control. PHT/MPP⁺ revealed no regulation in one way or the other when compared to MPP⁺ (Fig. 4.16).

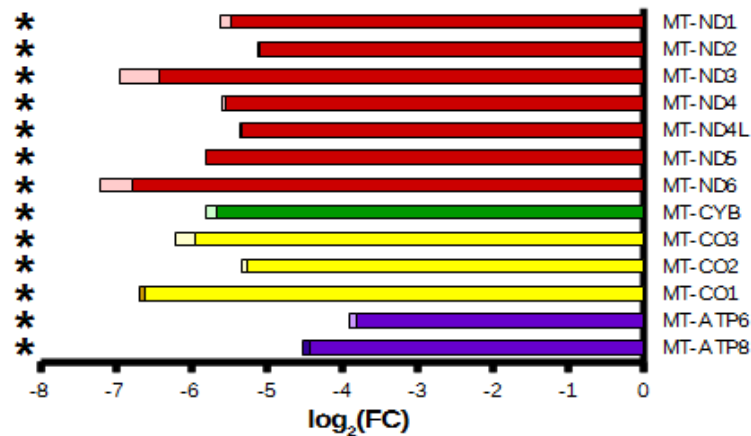


Figure 4.16: Transcriptional regulation of mitochondrial encoded mitochondrial subunits in MPP⁺ and PHT treated cells. Bar graphs showing regulation of all mitochondrial encoded complex subunits in differentiated LUHMES cells treated with 10 μ M MPP⁺ and 20 nM PHT over 48 h.. Red represents complex I, blue complex II, green complex III, yellow complex IV and purple complex V. Regulation under MPP⁺ is indicated by graph size, regulation under PHT/MPP⁺ indicated by a lighter colour, if the MPP⁺ effect is reduced, or by a darker colour, if the MPP⁺ effect is amplified. '*' indicates if the MPP⁺ treatment is significantly different compared to the control. Data represented as mean. n=3.

Increased transcription of nuclear encoded OXPHOS components might be part of an increased mitochondrial turnover. Old or damaged mitochondria are usually removed by mitophagy and need to be replaced with fresh ones. To produce new mitochondria, the mitochondrial DNA needs to be replicated. Like the nuclear replication process, the mitochondrial one requires a DNA polymerase, a primase, a DNA topoisomerase, a single strand binding protein (SSBP) and a helicase.

Interestingly, mitochondrial replication and transcription are mutually exclusive, due to the transcription elongation factor mitochondrial (TEFM) protein. If present, TEFM clamps the mitochondrial RNA polymerase (POLRMT) to the mitochondrial DNA, thus enforcing transcription. When TEFM is missing, the RNA polymerase dissociates from the DNA after it has generated the primer necessary for replication. The primer is then elongated by the mitochondrial DNA polymerase consisting of two subunits, polymerase gamma (POLG) and POLG2 (Agaronyan et al., 2015). Also part of the canonical mitochondrial replication complex are the mitochondrial topoisomerase 1 (TOP1MT), SSBP1 and the twinkle helicase (TWNK). However, apart from SSBP1, SSBP2 has also been shown to be present in mitochondria (Kato et al., 2009). Likewise, other helicases have also been reported to be located to the mitochondria. Next to TWNK, there are

Results

DNA replication helicase/nuclease 2 (DNA2) (Zheng et al., 2008), suppressor of Var1, 3-like 1 (SUPV3L1) (Minczuk et al., 2002) and petite integration frequency 1 (PIF1) (Futami et al., 2007). Interestingly, of all helicases only DNA2 was up-regulated in MPP⁺ treated cells, albeit it in a non-significant way. Transcription of the other three helicases was significantly down-regulated. PHT was able to quench the down-regulation of TWNK and PIF1 in a significant way, but the transcription remained significantly down-regulated compared to the control group, while transcription of DNA2 was even further increased in a significant manner compared to the control (Fig. 4.17).

SSBP1 was also significantly down-regulated in cells treated with MPP⁺, as well as cells treated with PHT/MPP⁺. On the other hand, SSBP2 was significantly up-regulated in both cases. In MPP⁺ treated cells, TOP1MT was also significantly up-regulated and remained significantly up-regulated in PHT/MPP⁺ treated cells, albeit significantly down-regulated compared to the MPP⁺ treated group. Transcription of POLRMT showed no significant regulation under MPP⁺, but a significant up-regulation in PHT/MPP⁺ treated cells. POLG2, but not POLG, was significantly up-regulated in MPP⁺ treated cells, while both were significantly up-regulated under PHT/MPP⁺ compared to the control group. The transcriptional clamp, TEFM, was significantly down-regulated in both treatment groups. Western blots revealed a similar picture with TEFM protein levels decreasing in a significant manner in both treatment groups by about 35% or more than 40% (Fig. 4.17).

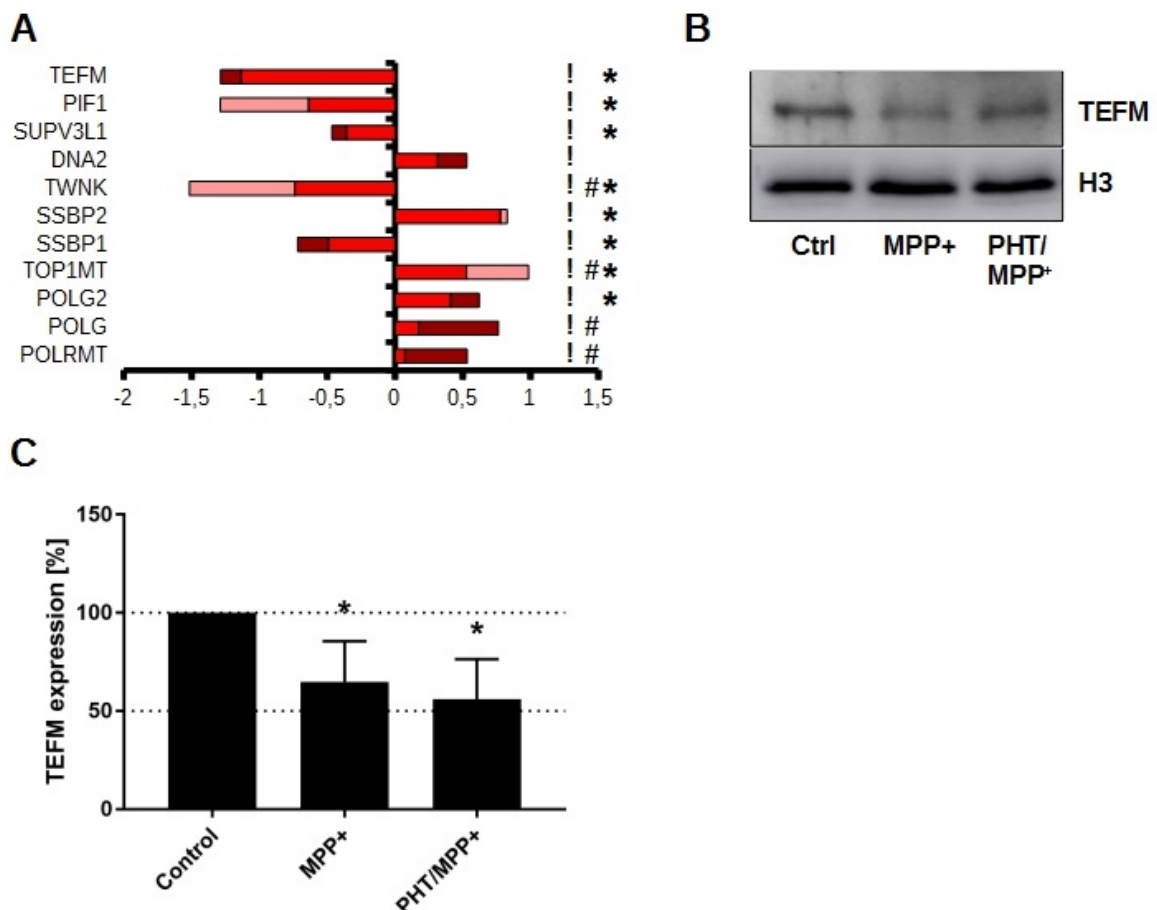


Figure 4.17: MPP⁺ and PHT alter replication of mitochondrial DNA. Results regarding mitochondrial DNA replication A: Bar graphs showing transcriptional regulation of mitochondrial DNA replication components in differentiated LUHMES cells treated with 10 μ M MPP⁺ and 20 nM PHT over 48 h. Regulation under MPP⁺ is indicated by graph size, regulation under PHT/MPP⁺ indicated by a lighter colour, if the MPP⁺ effect is reduced, or by a darker colour, if the MPP⁺ effect is amplified. '*' indicates if the MPP⁺ treatment is significantly different compared to the control, while '#' indicates if the MPP⁺/PHT treated group is significantly different compared to the MPP⁺ treated group. '!' indicates if the MPP⁺/PHT treatment is significantly different compared to the control group. Data represented as mean. n=3. B: Representative Western blots of differentiated LUHMES cells with TEFM and H3 treated with 10 μ M MPP⁺ and 20 nM PHT over 48 h. C: Bar graph diagram visualizing the densitometric analysis of B normalized on H3. TEFM protein levels decrease in the MPP⁺ and MPP⁺/PHT groups. '*' indicates significant differences compared to the vehicle treated group, while '#' indicate significant differences compared to the MPP⁺ treated group. Symbol number indicates the grade of significance with * = $p < 0.05$, ** = $p < 0.01$, and *** = $p < 0.001$. Data represented as mean and standard deviation. n=3.

This points to an overall process of mitochondrial replenishment in MPP⁺ treated cells that is reliant on an epigenetic mechanism. The possibly increased replication of mitochondrial DNA in cells treated with MPP⁺, which not only persists, but increases even further through PHT treatment may be a relevant factor to enable the discrepancy between transcription of complex subunits encoded in the nucleus or the mitochondria.

4.10 MPP⁺ promotes exploration of alternative energy sources

Of course, the cell does not only require complexes of the oxidative phosphorylation to perpetuate their energy supply. There are also other pathways, like glycolysis. Through degradation of glucose, energy is directly produced in the form of ATP and indirectly in form of NADH, which is the substrate of the complex I (Sousa, et al. 2018). Glycolysis may thus produce energy autonomously, albeit not as effective as mitochondrial respiration. Through a couple of reactions that are catalysed by many different enzymes, glucose is degraded to pyruvate. It generates four ATP per glucose, but also consumes two molecules of ATP and two molecules of NAD⁺ (Meyerhof et al., 1947). Should glycolysis occur independent of the OXPHOS it is referred to as anaerobic glycolysis, which has been shown to be protective in the MPP⁺ model (Williams et al., 2007).

Pyruvate is then mostly turned into acetyl-CoA through pyruvate dehydrogenases to feed the TCA cycle (Coxon et al., 1949). It can, however, also be transformed into lactate by lactate dehydrogenases. This would regenerate one NAD⁺ per pyruvate (Baumberger et al., 1933), which would also be lacking in complex I inhibited cells, since NAD⁺ is mostly regenerated through said complex.

Another way intertwined with OXPHOS through complex II is the TCA cycle. Unlike glycolysis,

the TCA machinery is also located in the mitochondria. The TCA cycle relies on a supply with acetyl-CoA and oxaloacetate originating from other pathways like glycolysis and beta-oxidation. In the cycle acetyl-CoA and oxaloacetate are combined to citrate, which is then stepwise degraded to oxaloacetate. The formulation of acetyl-CoA from pyruvate requires one molecule of NAD^+ . The cycle produces one molecule of GTP and one molecule of FADH_2 through consumption of three molecules of NAD^+ (Krebs et al., 1937).

Through stepwise degradation of fatty acids to acetyl-CoA, the beta-oxidation delivers more possible substrates for the TCA cycle. Four steps are repeated in a cycle and break off one molecule of acetyl-CoA until only a molecule of acetyl-CoA remains. Per repetition of those steps one molecule of FADH_2 is generated, one molecule of NAD^+ consumed (Knoop, 1904).

All three of those pathways are significantly up-regulated under MPP^+ and they remain so under PHT/ MPP^+ (Fig. 4.18).

Taken together these data indicate a transcriptional activation upon MPP^+ treatment, which is not restricted to the nuclear encoded subunits of mitochondrial complexes, but also extends to other pathways required for energetic supply. Unlike the transcriptional effects of PHT on the transcription of the nuclear encoded subunits of mitochondrial complexes, the overall regulation of neither glycolysis, nor TCA cycle, nor pyruvate metabolism, nor beta-oxidation is significantly altered.

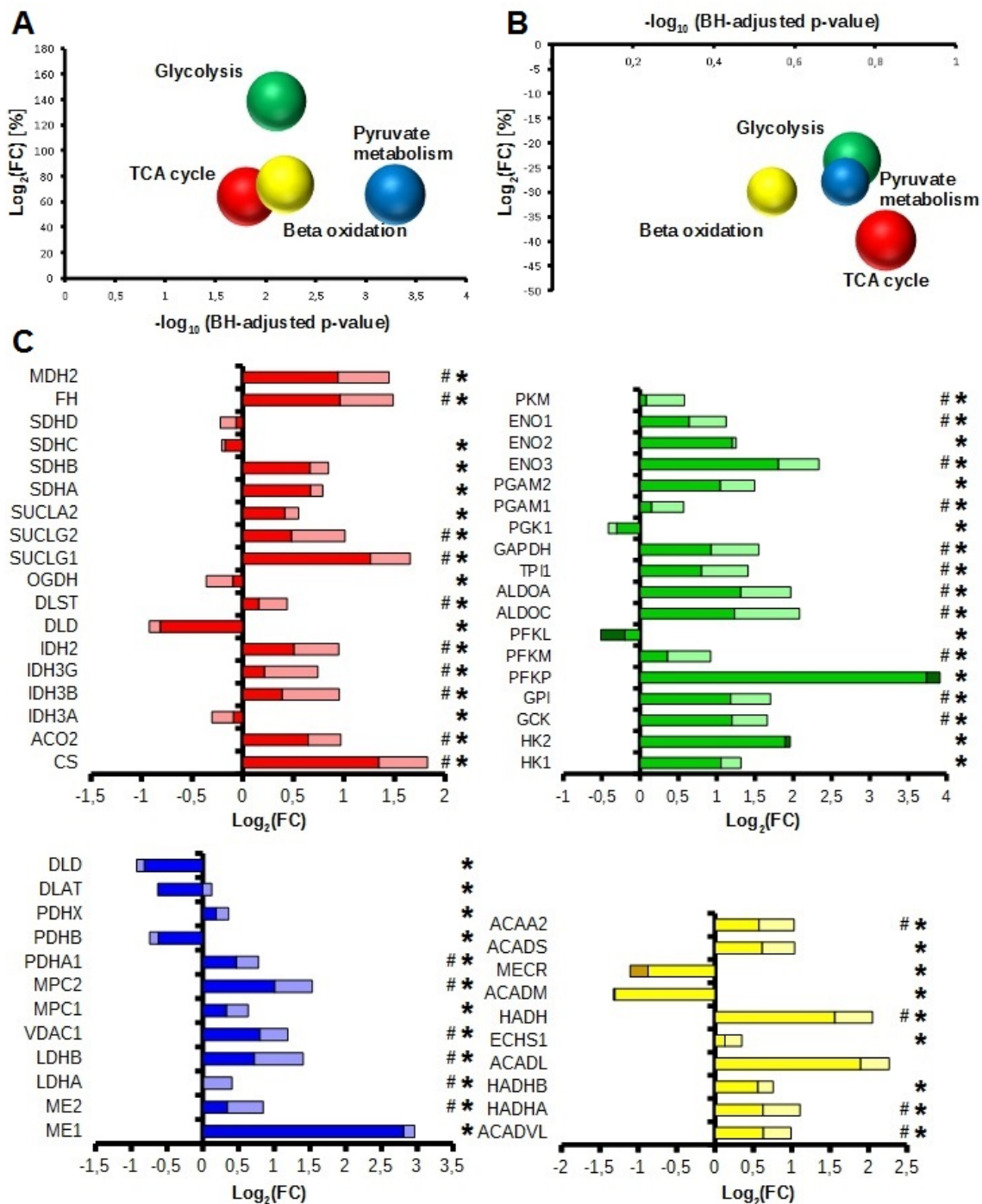


Figure 4.18: Transcriptional regulation of energy suppliers in MPP⁺ and PHT treated cells. Graphs illustrating the changes in transcription of enzymes related to glycolysis, TCA cycle, pyruvate metabolism and beta oxidation in differentiated LUHMES cells treated with 10 μM MPP⁺ and 20 nM PHT over 48 h. A: Bubble diagram visualizing the overall regulation under MPP⁺. Red represents glycolysis, blue TCA cycle and green beta-oxidation. Bubble size indicates the fraction of significantly regulated transcripts divided by the total number of complex related transcripts. Bubble position on the Y-axis relates to log_2 mean regulation, position on the X-axis relates to $-\text{log}_{10}$ mean of the p-value. B: Bubble diagram comparing PHT/MPP⁺ to MPP⁺. C: Bar graphs showing regulation of all four pathways. Regulation under MPP⁺ is indicated by graph size, regulation under PHT/MPP⁺ indicated by a lighter colour, if the MPP⁺ effect is reduced, or by a darker colour, if the MPP⁺ effect is amplified. '*' indicates if the MPP⁺ treatment is significantly different compared to the control, while '#' indicates if the MPP⁺/PHT treated group is significantly different compared to the MPP⁺ treated group. Data represented as mean. n=3.

Glucose is a fundamental source of energy in neuronal cells. It fuels the cellular energy supply through glycolysis and OXPHOS. To supply the glycolytic pathway with fresh substrate, a transporter named glucose transporter type 3 (GLUT3) is incorporated into the neuronal membrane (Maher et al., 1991).

LUHMES cells treated with MPP⁺, PHT/MPP⁺ and MPHT/MPP⁺ demonstrated a significant increase in protein level by about 150%, 160% and over 200%. Exclusive PHT treatment showed no significant effect on GLUT3 protein levels (Fig. 4.19). Higher levels of GLUT3 would indicate the cell's increased requirement of glucose to sustain its energy supply.

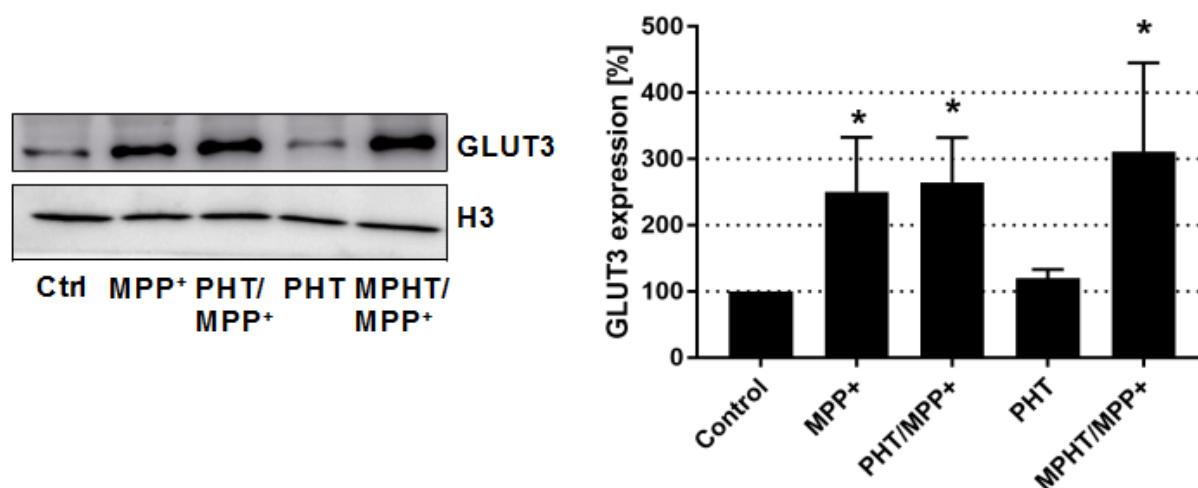


Figure 4.19: GLUT3 protein levels in MPP⁺ and PHT treated LUHMES cells. Shown are representative Western blots of GLUT3 and H3 of LUHMES cells treated with indicated compounds (MPP⁺ 10 μ M, PHT 20 nM, MPHT 20 nM) for 48 h and the densitometric quantification of GLUT3 protein levels normalized on H3 illustrated in a bar graph diagram. Presence of MPP⁺ dictates increased protein levels of GLUT3. '*' indicates significant differences compared to the vehicle treated group, while '#' indicate significant differences compared to the MPP⁺ treated group. Symbol number indicates the grade of significance with * = $p < 0.05$, ** = $p < 0.01$, and *** = $p < 0.001$. Data represented as mean and standard deviation. $n=3$.

4.11 MPP⁺ influences the transcription of genes involved in epigenetic regulation

When looking at the transcription levels of lysine acetylation modulators, a very complex picture is painted since regulations do not extend to a group of enzymes, but rather affect each gene in a unique way. SIRT1, for example, showed no significant regulation under neither MPP⁺ nor PHT/MPP⁺. On the other hand, SIRT2 was significantly up-regulated under MPP⁺, a circumstance not significantly averted by PHT. SIRT5 and SIRT3 were both significantly down-regulated in MPP⁺ treated cells, of which only SIRT3's transcription is protected by PHT. SIRT4, SIRT6 and SIRT7 showed no significant regulation by MPP⁺, but SIRT4 was significantly up-regulated under PHT/MPP⁺. Expression of SIRT6 and SIRT7 was also not affected by PHT/MPP⁺ (Fig. 4.20).

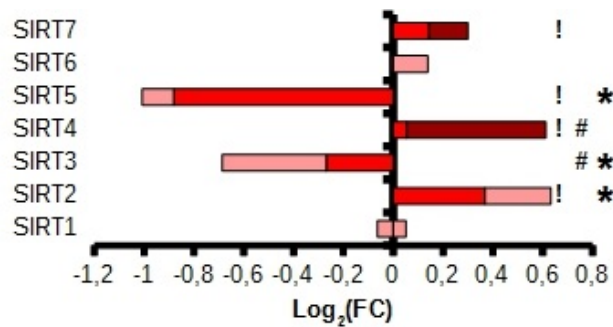


Figure 4.20: Transcriptional regulation of SIRT in MPP⁺ and PHT treated cells. Bar graphs showing transcriptional regulation of all SIRTs in differentiated LUHMES cells treated with 10 μM MPP⁺ and 20 nM PHT over 48 h. Regulation under MPP⁺ is indicated by graph size, regulation under PHT/MPP⁺ indicated by a lighter colour, if the MPP⁺ effect is reduced, or by a darker colour, if the MPP⁺ effect is amplified. '*' indicates if the MPP⁺ treatment is significantly different compared to the control, while '#' indicates if the MPP⁺/PHT treated group is significantly different compared to the MPP⁺ treated group. '!' indicates if the MPP⁺/PHT treatment is significantly different compared to the control group. Data represented as mean. n=3.

Of the remaining HDACs in class I, II and IV, HDAC6, HDAC1, HDAC5, HDAC11, HDAC3, HDAC10 and HDAC2 were significantly up-regulated in MPP⁺ treated cells, while HDAC7, HDAC8 and HDAC9 were not regulated and HDAC4 was significantly down-regulated. Significant protective effects by PHT could be observed for HDAC4, HDAC6, HDAC3 and HDAC2, but not for HDAC1, HDAC5, HDAC8, HDAC9, HDAC10 and HDAC11. Transcription of HDAC7 was significantly up-regulated in cells treated with PHT/MPP⁺ (Fig. 4.21).

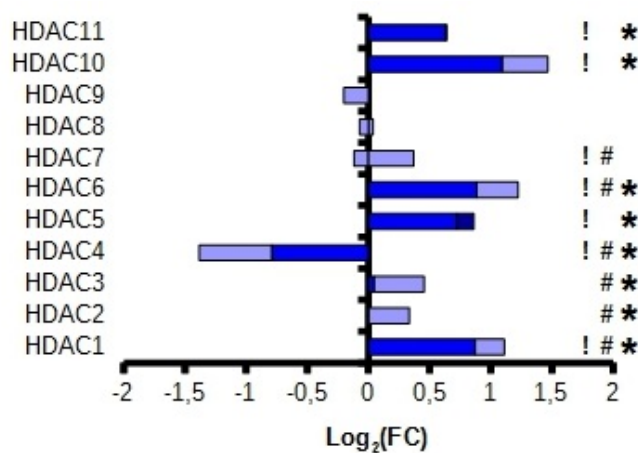


Figure 4.21: Transcriptional regulation of HDACs in MPP⁺ and PHT treated cells. Bar graphs showing transcriptional regulation of all class I, II and IV HDACs in differentiated LUHMES cells treated with 10 μM MPP⁺ and 20 nM PHT over 48 h. Regulation under MPP⁺ is indicated by graph size, regulation under PHT/MPP⁺ indicated by a lighter colour, if the MPP⁺ effect is reduced, or by a darker colour, if the MPP⁺ effect is amplified. '*' indicates if the MPP⁺ treatment is significantly different compared to the control, while '#' indicates if the MPP⁺/PHT treated group is significantly different compared to the MPP⁺ treated group. '!' indicates if the MPP⁺/PHT treatment is significantly different compared to the control group. Data represented as mean. n=3.

On the other side of the lysine acetylation machinery, the HATs, lysine acetyltransferase 2A (KAT2A), activating transcription factor 2 (ATF2), KAT5 and KAT7 were significantly up-regulated in MPP⁺ treated cells, while TATA box binding protein associated factor 1 (TAF1) and circadian locomotor output cycles kaput protein (CLOCK) showed no regulation and KAT2B, KAT6A, KAT6B, E1A binding protein p300 (EP300), cAMP responsive element binding (CREB) binding protein (CREBBP), nuclear receptor coactivator 1 (NCOA1), NCOA3 and NCOA2 were all down-regulated in MPP⁺ treated cells. Significant protective effects by PHT could be observed for expression of KAT5, KAT6A, EP300, CREBBP and NCOA3, but nor for KAT2A, KAT2B, ATF2, KAT7, KAT6B, NCOA1 and NCOA2. TAF1 and CLOCK, on the other hand, were both significantly up-regulated in cells treated with PHT/MPP⁺ (Fig. 4.22).

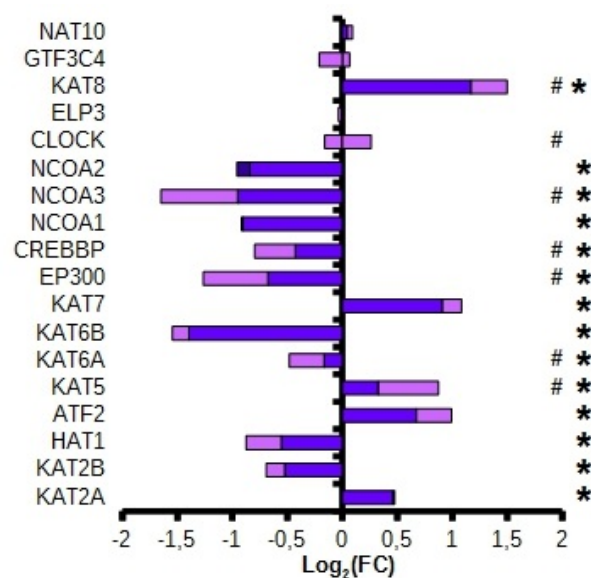


Figure 4.22: Transcriptional regulation of HATs in MPP⁺ and PHT treated cells. Bar graphs showing transcriptional regulation of all HATs in differentiated LUHMES cells treated with 10 μ M MPP⁺ and 20 nM PHT over 48 h. Regulation under MPP⁺ is indicated by graph size, regulation under PHT/MPP⁺ indicated by a lighter colour, if the MPP⁺ effect is reduced, or by a darker colour, if the MPP⁺ effect is amplified. '*' indicates if the MPP⁺ treatment is significantly different compared to the control, while '#' indicates if the MPP⁺/PHT treated group is significantly different compared to the MPP⁺ treated group. Data represented as mean. n=3.

The enzymes governing DNA methylation, DNMTs and TETs, were also regulated in a rather diverse manner. DNMTs establish DNA methylation (Leonhardt et al., 1992), while TETs remove it again through oxidation (Tahiliani et al., 2009). DNMT1 and DNMT3B, but not DNMT3A, were significantly down-regulated in cells treated with MPP⁺. Significant protective effects by PHT on transcription level could not be observed. TET1 was significantly up-regulated in MPP⁺ treated cell, while TET3 was significantly down-regulated. TET2 showed no regulation at all. PHT showed significant protective effects on TET3, but not on TET1 expression levels. Cells treated with PHT/MPP⁺ showed a significant increase in TET2 transcription (Fig. 4.23).

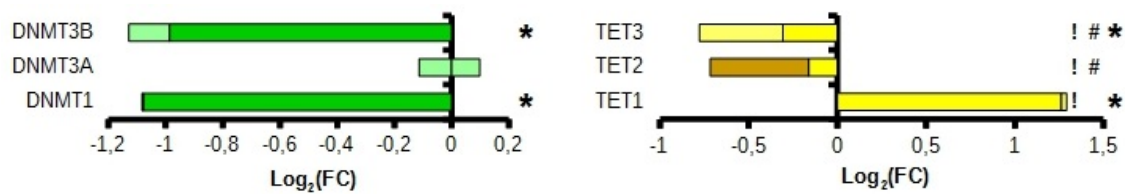


Figure 4.23: Transcriptional regulation of DNMTs and TETs in MPP⁺ and PHT treated cells. Bar graphs showing transcriptional regulation of all DNMTs and TETs in differentiated LUHMES cells treated with 10 μ M MPP⁺ and 20 nM PHT over 48 h. Regulation under MPP⁺ is indicated by graph size, regulation under PHT/MPP⁺ indicated by a lighter colour, if the MPP⁺ effect is reduced, or by a darker colour, if the MPP⁺ effect is amplified. '*' indicates if the MPP⁺ treatment is significantly different compared to the control, while '#' indicates if the MPP⁺/PHT treated group is significantly different compared to the MPP⁺ treated group. '!' indicates if the MPP⁺/PHT treatment is significantly different compared to the control group. Data represented as mean. n=3.

Regulation of this many epigenetic active enzymes is very likely related to the changes in DNA methylation and histone acetylation thus far. It is, however, of major interest, that gene expression of SIRT1 remains unaffected by either treatment, while SIRT3's shows a similar behaviour as the Western blot data presented earlier. SIRT1's reduced activity and protein levels are thus not a result of an epigenetic silencing of its transcription.

Interestingly, transcriptional regulation of epigenetic modulators was not restricted to catalytically active enzymes. In addition, transcription of histones was affected by MPP⁺ treatment. Enrichment analysis revealed expression of H1, but not of the others, to be significantly up-regulated. PHT/MPP⁺ treatment caused a significant protective effect regarding H1 expression levels (Fig. 4.24).

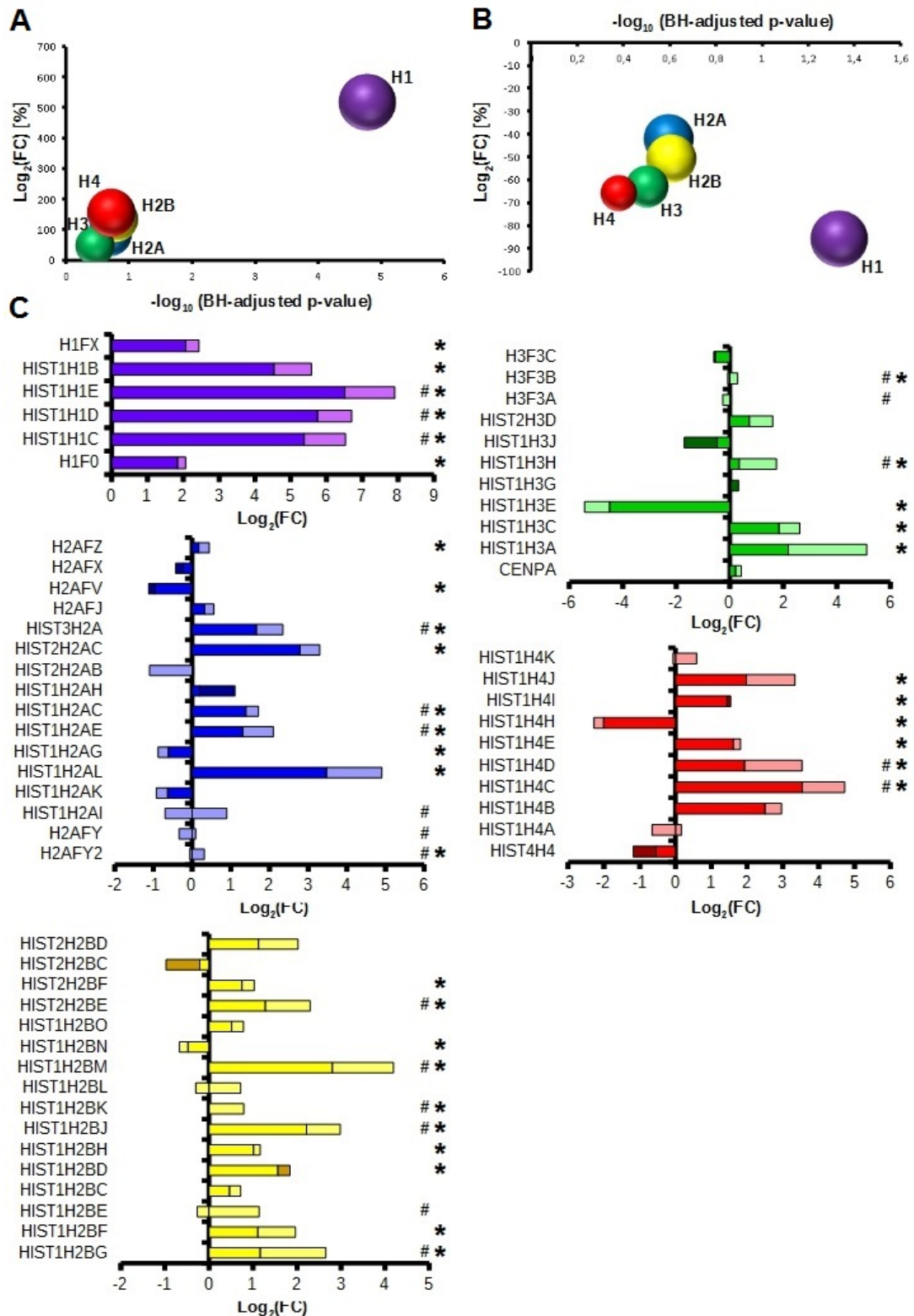


Figure 4.24: Transcriptional regulation of histones in MPP⁺ and PHT treated cells. Graphs illustrating the changes in transcription of histones in differentiated LUHMES cells treated with 10 μ M MPP⁺ and 20 nM PHT over 48 h. A: Bubble diagram visualizing the overall regulation under MPP⁺. Purple represents H1, blue H2A, yellow H2B, green H3 and red H4. Bubble size indicates the fraction of significantly regulated transcripts divided by the total number of complex related transcripts. Bubble position on the Y-axis relates to log₂ mean regulation, position on the X-axis relates to -log₁₀ mean of the p-value. B: Bubble diagram comparing PHT/MPP⁺ to MPP⁺. C: Graphs showing transcriptional regulation of all histones. Regulation under MPP⁺ is indicated by graph size, regulation under PHT/MPP⁺ indicated by a

Results

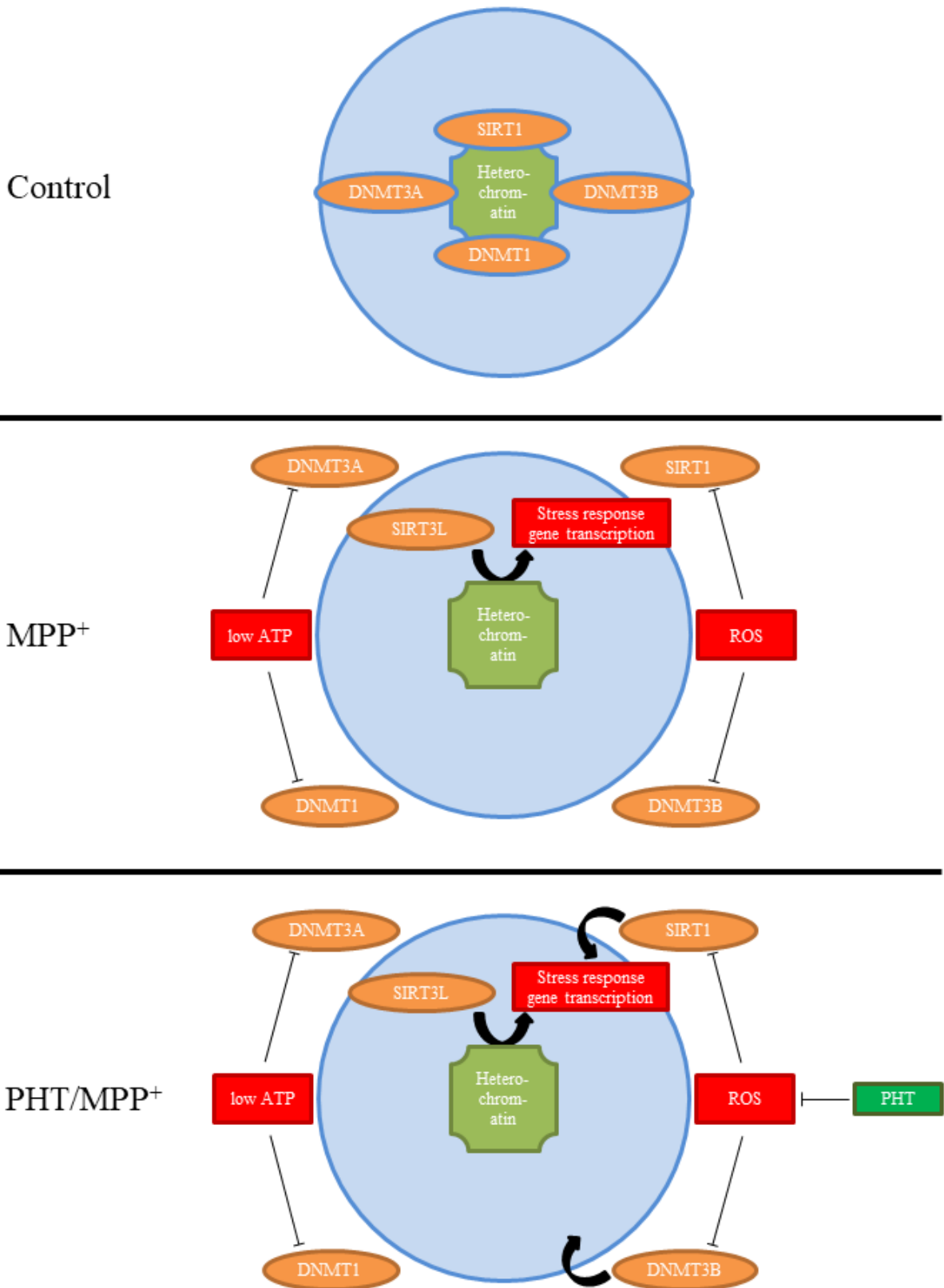
lighter colour, if the MPP⁺ effect is reduced, or by a darker colour, if the MPP⁺ effect is amplified. '*' indicates if the MPP⁺ treatment is significantly different compared to the control, while '#' indicates if the MPP⁺/PHT treated group is significantly different compared to the MPP⁺ treated group. Data represented as mean. n=3.

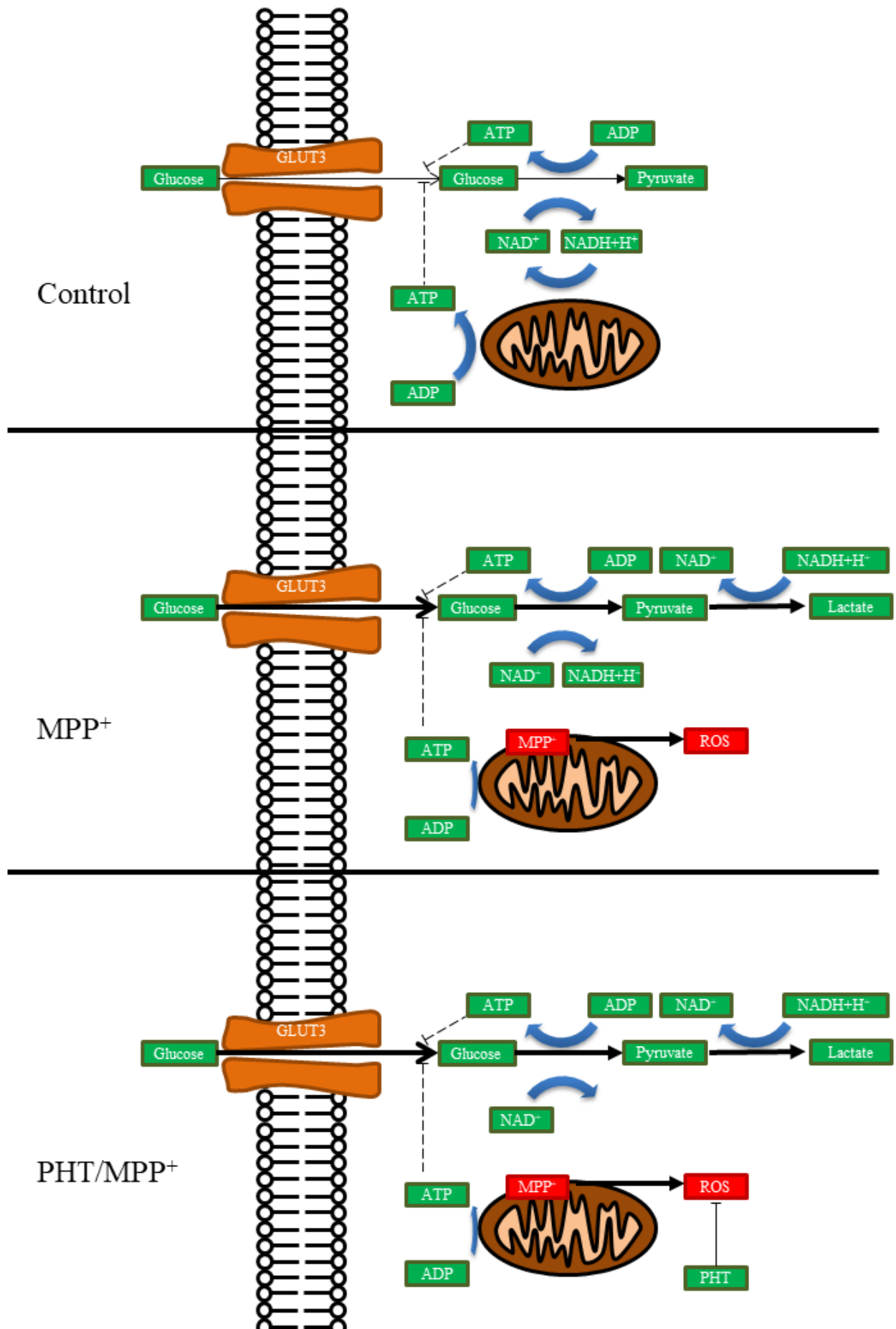
At this point it has become evident, that the cells alter their epigenetic status to supply the mitochondria not only with complex subunits, but also with enzymes, which supply the OXPHOS with substrates, as well as the means to amplify themselves. It is thus necessary to investigate whether these actions also result in altered mitochondrial constitution, respiration or health in future studies.

Overall, this work is able to provide ample data that are finally able to link the epigenetic phenomena observed in different models of PD, as well as in afflicted humans to ROS dependent mitochondrial distress. First, the nature and mechanism underlying the epigenetic changes could be traced back in *in vitro* studies to SIRT1 and DNMT3B malfunctions as their root, which could also be observed *in vivo*. These epigenetic changes seem to appear to rearrange the chromatin to increase transcription of nuclear encoded subunits of the mitochondrial complexes as well as adjacent pathways like glycolysis and TCA cycle. Also, mitochondrial replication through TEFM regulation and enhanced gene transcription of its machinery, appears induced, even more so, when PHT is present, thus also providing a fundamental tool in challenging these epigenetic disturbances in cells and tissue through its antioxidative properties.

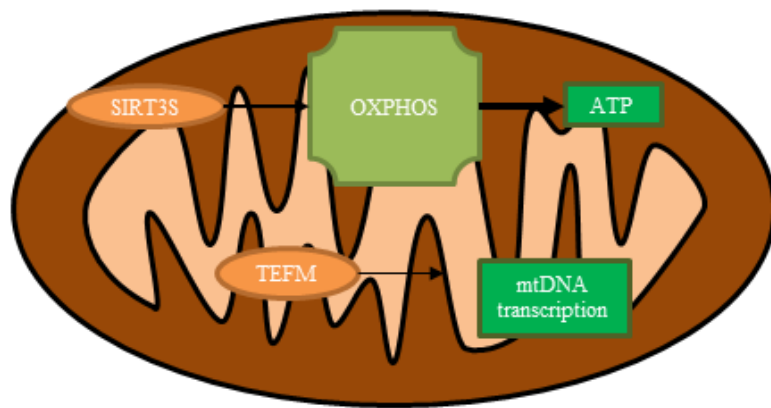
To finally understand the impact and importance of these findings, a thorough discussion of these by comparing them with results from other studies and looking at the grander picture of PD and the implications of epigenetics on mitochondrial health.

4.12 Graphical abstract

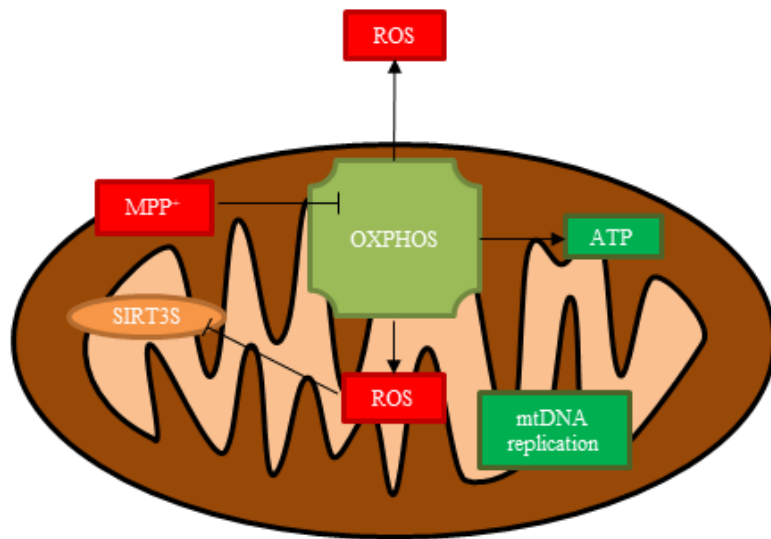




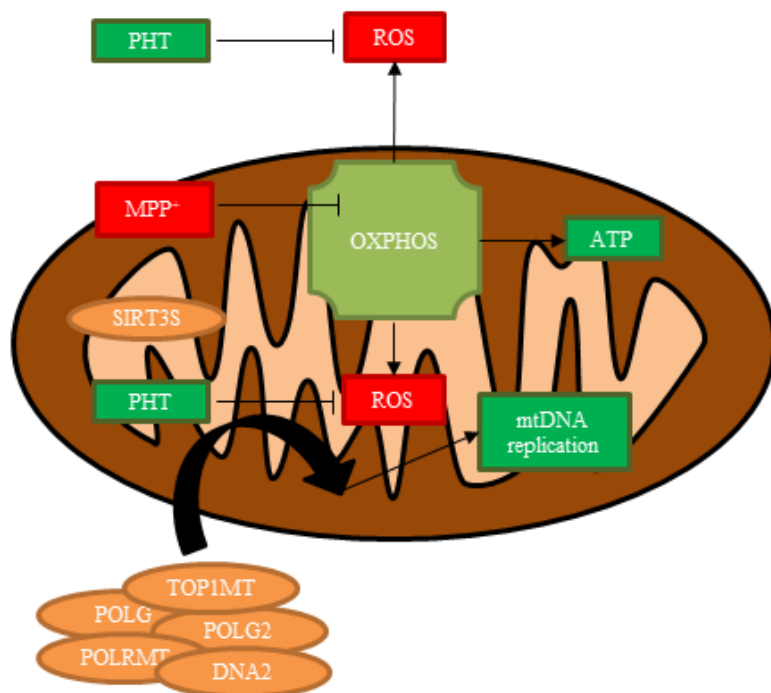
Control



MPP⁺



PHT/MPP⁺



5 Discussion

5.1 Epigenetic changes are part of PD's pathology

PD is not only the second most common neurodegenerative disorder among humans, but has also been proposedly linked to environmental factors (Dick et al., 2007). The pathology of the disease has been studied extensively, but the origin, the cellular alpha remains unbeknownst. Yet the omega, the destiny of the afflicted dopaminergic cell in the SN is explicitly precise. Over time, it withers, it wanes, it dies, leaving its work and duties to the remaining cells, who at one point will also succumb to the disease (Fearnley et al., 1991). Just as a worker who has to cover for a sick colleague exhausts faster, it seems plausible that the degeneration of those, that remain, would be accelerated. And just as a factory will cease to produce if enough workers are absent, so does the organism deteriorate from the cellular loss.

PD takes a very specific toll on the human body. Motoric capabilities of afflicted individuals are heavily impaired, while their mind remains conscious, aware and rational (Parkinson, 2002). These specific sets of deficits lead quondam scientists to the SN, a brain area that demonstrated morphological changes in PD afflicted individuals (Fearnley et al., 1991). The cell mass is reduced (Rudow et al., 2008), the cellular defence systems are engaged (Hunot et al., 2003) and protein aggregates amassed (Gundersen, 2010). These things have been described over a hundred years ago and progress has been made in spite of many setbacks. Nowadays the disease is manageable, granting afflicted individuals a more or less asymptomatic lifestyle through intake of different chemical compounds (Birkmayer et al., 1962; Gerstenbrand et al., 1965). A cure, however, has still not been found.

Modern PD treatments try to cover the loss of dopaminergic neurons by increasing the amount of available dopamine. This is achieved, for example, through administration of L-DOPA (Birkmayer et al., 1962), the metabolic precursor of dopamine (Blascko, 1939). Unlike its metabolic product, L-DOPA can pass the blood brain barrier through a solute carrier family 7 member 5 (SLC7A5) transporter (Kageyama et al., 2000) to supply the dopaminergic system. Dopamine, and thus L-DOPA, is, however, also a metabolic precursor of adrenaline (van der Schoot et al., 1965; Pendleton et al., 1976) an important hormone. Rash administration of L-DOPA thus would also cause accelerated adrenaline production possibly provoking cardiac arrest. To prevent this, the aromatic L-amino acid decarboxylase (AADC) inhibitors carbidopa (Marsden et al., 1973) or benserazide (van Wieringen, 1974), which may not pass the blood brain barrier, are administered together with L-DOPA. This causes the increased dopamine production to be restricted to the brain.

Other treatment options include catechol-O-methyltransferase (COMT) (Reches et al., 1984) and

MAO-B inhibitors (Ruggieri et al., 1986). The former enzyme would otherwise inactivate dopamine (Axelrod, 1957), the latter would even degrade it (Rosengren, 1960). These inhibitors are always combined with L-DOPA administration (Reches et al., 1984), since they themselves cannot compensate the loss of the dopaminergic neurons.

But to go further, to possibly find a cure or at least stop the disease's progress, it is important to find the root of PD's pathology. Imaginable theories are abound (see section 2.2), yet true proof for any of them is still lacking. Since this work, in its experimental design, mostly depended on the MPP⁺ model of PD as the main model system, discussion will be largely limited to the ROS theory. Lately, scientists have started looking towards epigenetics in the context of PD; a comprehensible development when looking at the major risk factors of PD, aside from its hereditary forms. The two major risk factors of PD are environmental factors and time in form of ageing (Dick et al., 2007; Koller et al., 1987). These two aspects can also influence the epigenome of the cell in many different ways (Bandyopadhyay et al., 2003; Cohet, 1975) and, intriguingly, are in turn influenced by ROS (Harman, 2009).

Two studies which can almost be called the foundation of epigenetic research in the context of PD revolve around changes to the acetylome of histones (Park et al., 2016) and methylome of the DNA (Desplats et al., 2011). The former showed, that many different histone loci are changed in *in vitro* and *in vivo* model systems of PD. To put this data in line with the results of this work, the actually enriched and not enriched acetylation sites have to be looked at in detail. Of course, both data cannot cover all possible known acetylation sites of all histones, so an absolute verdict at this point in time is not achievable. Thus, the histone lysines known to be hyperacetylated *in vivo* in the MPP⁺ model include H2AK5, H2AK15, H3K14 (Fig. 4.3, 4.8 and 4.9) and H4K5, while H3K9 and H4K12 can only exhibit a trending hyperacetylation and H3K18 seems not to be affected at all (Park et al., 2016).

The consequences of those seem to be quite apparent. Through the increased acetylation, the band between histone and DNA is weakened, heterochromatin disassembled and transcription activated (Allfrey et al., 1964; Marushige, 1976). The last point, however, may be challenged by the transcriptomics data of this work (Fig. 4.15, 4.17, 4.18, 4.20, 4.21, 4.22, 4.23 and 4.24), since no bias for transcriptional up-regulation could be observed. The general statement histone acetylation would lead to increased transcription can thus not be considered true. While it is true that, in theory, the DNA becomes more accessible for the transcription machinery, some genes heavily rely on transcription factors (TFs), which require histone methylation to successfully enhance or repress transcription (Sen et al., 2017). In this case, the acetylation would, theoretically, block the methylation, thus the TF and thus transcription. Because the consequences of increased lysine acetylation are very dynamic and can hardly be generalized, the only admissible conclusion from

this data may be that transcriptional changes are occurring, but may assess neither quality nor quantity of those changes.

Since acetylation does not come to pass spontaneously, but is regulated by HAT and HDAC enzymes, that write (Racey et al., 1971) or erase (Kaneta et al., 1974) this specific PTM, the affected lysines may serve as clues to point to the HAT and/or HDAC responsible. See the table below for further information.

| Locus | Writer | Eraser |
|--------------|--|---|
| H2AK5 | EP300 (Ogryzko et al., 1996), CREBBP (Ogryzko et al., 1996), HAT1 (Verreault et al., 1998) | HDAC3 (Johnson et al., 2002), HDAC1 (Johnson et al., 2002) |
| H2AK15 | KAT5 (Jacquet et al., 2016) | ? |
| H3K9 | CLOCK (Doi et al., 2006), KAT2A (Grant et al., 1999), KAT6A (Voss et al., 2009) | HDAC11 (Byun et al., 2017), SIRT1 (Imai et al., 2000), SIRT6 (Michishita et al., 2008), HDAC1 (Vermeulen, et al., 2004), HDAC2 (Vermeulen et al., 2004), SIRT3 (Scher et al., 2007) |
| H3K14 | EP300 (Ogryzko et al., 1996), CREBBP (Ogryzko et al., 1996), ELP3 (Winkler et al., 2002), KAT2A (Grant et al., 1999), KAT2B (Vicent et al., 2009) KAT7 (Kueh et al., 2011), CLOCK (Doi et al., 2006), KAT6A (Qiu et al., 2012), KAT6B (Klein et al., 2017) | SIRT1 (Imai et al., 2000), HDAC1 (Vermeulen et al., 2004), HDAC2 (Vermeulen et al., 2004) |
| H3K18 | EP300 (Ogryzko et al., 1996), CREBBP (Ogryzko et al., 1996), KAT2A (Grant et al., 1999) | SIRT7 (Barber et al., 2002), SIRT2 (Eskandarian et al., 2013), HDAC1 (Kelly et al., 2018), HDAC2 (Kelly et al., 2018) |
| H4K5 | EP300 (Ogryzko et al., 1996), CREBBP (Ogryzko et al., 1996), HAT1 (Verreault et al., 1998) | HDAC3 (Johnson et al., 2002), HDAC1 (Vermeulen et al., 2004), HDAC2 (Vermeulen et al., 2004) |
| H4K12 | HAT1 (Verreault et al., 1998), ATF2 (Kawasaki et al., 2000) | HDAC3 (Johnson et al., 2002), HDAC1 (Vermeulen et al., 2004), HDAC2 (Vermeulen et al., 2004), SIRT1 (Imai et al., 2000) |

Table 5.1: Histone acetylation sites. Overview of histone acetylation loci investigated in PD and their governing enzymes.

Some of the existing HATs and HDACs are not listed in the table. Of course, this short list only references those loci relevant to this or the previously mentioned work and not all enzymes are as well understood, as it would be necessary to correlate their activity to one specific locus. However, the table does yield a representative picture as to how dynamic the system is and how many

enzymes play a part.

Another very important antecedent work described that DNA showed reduced levels of methylation and a dislocalization of DNMT1 from the nucleus to the cytosol in humans afflicted with PD (Desplats et al., 2011). Both these described effects could not only be verified during the course of this work, but it also became evident that the dynamics behind these pathologies are more dynamic than thought at first (Fig. 4.10, 4.11, 4.12, 4.13 and 4.14). The reduced levels of DNA methylation could also be related to the observed transcriptional changes. DNA methylation mainly affects transcription in two different ways. First, the methylation itself may hamper the transcription machinery (Tippin et al., 1997), but more importantly the methyl group allows proteins with a MBD to bind to the DNA and recruit other proteins that condense the chromatin (Chandler et al., 1999). This may lead to the simplified conclusion reduced DNA methylation levels could only lead to increased transcription, yet similar to the data regarding histone acetylation the transcriptomics data expose this idea as sophism. Indeed, DNA methylation may, depending on its position, also increase transcription.

Taken together the epigenetic changes can maybe not yet be considered pathologies of PD, but at least of the MPP⁺ model of PD. Studies with human specimen are necessary to further validate and solidify these results, but they might already be considered to become tools for earlier diagnoses that would allow treatment before motoric symptoms would occur. However, changes to the transcription that are too strong and massiv may have detrimental effects on cellular health and might be a key process in cellular demise.

5.2 ROS dependant loss of SIRT1 activity ultimately causes lysine hyperacetylation and histone H1 hypertranscription

Finding the enzyme responsible for the observed hyperacetylation may yield a fitting target for future treatment options. To find that enzyme more experiments were conducted during the course of this work. A first clue could be found in the general acetylation status of lysines of the entire proteome. Lysine as an amino acid is, of course, found in more proteins than just histones and it can also be acetylated in that position. This can affect the thusly-acetylated protein in many different ways. It can activate the enzymatic function, it can decrease the function, it can increase or reduce the binding to cofactors and it can target or protect the protein from degradation. In this work, a general increase of lysine acetylation could be observed (Fig. 4.3, 4.3, 4.8 and 4.9).

This proved helpful to discern the HDAC involved in the hyperacetylation events, since the HDAC has to be present in the nucleus and the cytosol, which is not true for every HDAC. SIRT6 (Liszt et al., 2005) and SIRT7 (Kiran et al., 2013) could thus be excluded since they are exclusively nuclear,

while SIRT4 (Ahuja et al., 2007) and SIRT5 (Nakagawa et al., 2009) are exclusively mitochondrial and cannot affect histones. SIRT1 (Sun et al., 2016), SIRT2 (North et al., 2003) and SIRT3 (Onyango et al., 2002; Iwahara et al., 2012), on the other hand, are present in both, the nucleus and the cytoplasm or the mitochondria in SIRT3's case. Of the HDACs, HDAC11 (Gao et al., 2002) is more or less restricted to the nucleus, while HDAC1-10 (Viatour et al., 2003; Gu et al., 2005; Miska et al., 2001; Chawla et al., 2003; Verdell et al., 2000; Fischle et al., 2001; van den Wyngaert et al., 2000; Sugo et al., 2010; Kao et al., 2002) can occur in and outside of it.

Comparison of cells treated with the Zn²⁺ dependant HDAC inhibitor TSA (Yoshida et al., 1990) and the SIRT1 specific inhibitor EX-527 (Napper et al., 2005), can only lead to one conclusion. MPP⁺ could only induce hyperacetylation in neurons treated with TSA, but not with EX-527. This means, that the enzyme responsive to the MPP⁺ is not affected by TSA, but by EX-527, which would only leave SIRT1 as the responsible agent. Intriguingly, in table 5.1 SIRT1 only appears as eraser of H3K14 and H3K9 acetylation, but not of the other loci.

SIRT1 is a protein well studied and well romanticised. It first occurred in yeast in form of its homologue silent mating type information regulation 2 (*sir2*) (Rine et al., 1987) as a major player of epigenetic programming (Pillus et al., 1989) and became popular when it was shown that increased *sir2* activity correlated with decelerated ageing in yeast (Kaeberlein et al., 1999). Through these high levels of attention many studies have delivered vital insights in different pathways and regulations affected and mediated by SIRT1 including mitochondrial biogenesis through peroxisome proliferator-activated receptor gamma coactivator 1-alpha (PPARGC1A) (Rodgers et al., 2005), energy homeostasis through 5' adenosine monophosphate-activated protein kinase (AMPK) (Hou et al., 2008) and cell survival through TP53 (Vaziri et al., 2001) to name three examples. Many compounds to modulate SIRT1 activity, like resveratrol have thus also been described (Howitz et al., 2003). SIRT1 protein levels indeed do decrease in cells of aged organisms rendering SIRT1 a hallmark protein of ageing (Longo et al., 2006). In context of PD, SIRT1 has been shown to protect SY5Y neuroblastoma cells from ROS mediated cell death. Furthermore, the same study revealed SIRT1 to be down-regulated in post mortem brain tissue of PD patients (Singh et al., 2017).

As already mentioned, MPP⁺ treated LUHMES cells and MPTP treated mice showed high levels of acetylation at the H3K14 locus, a known target site of SIRT1 (Imai et al., 2000). Other SIRT1 target histone constituting lysines include H3K9 (Imai et al., 2000), H4K16 and H1K26 (Vaquero et al., 2004). Especially the last one deserves higher levels of attention. So far, no other HDAC has been described to deacetylate it. H1 is not only deacetylated by SIRT1 at H1K26, but also recruited to the nucleosome to constitute facultative heterochromatin (Vaquero et al., 2004). A lack of SIRT1 activity would thus cause great portions of the H1 protein pool to be kept outside of the chromatin

and left for degradation through proteolysis, which is acetylation dependent (Qian et al., 2016). Interestingly, H4K16 acetylation has also been linked to histone displacement and subsequent degradation (Lu et al., 2010), yet SIRT2 (Vaquero et al., 2006) and SIRT3 (Scher et al., 2007) may compensate a loss of SIRT1 in this case. This likely explains the very specific and highly significant induction of all in LUHMES cells expressed H1 genes (Fig. 4.24), because the degraded proteins need to be replenished. H1 may affect transcription in a very filigree yet simple way. Through its presence or its PTMs the position of nucleosomal beads changes, moving them closer together or further apart or changing their angles (Bednar et al., 2017; Öztürk et al., 2018). This likely causes rearrangement of silencer or enhancer motifs as well as affect transcription factor accessibility and thus may be a key factor for the observed transcriptional changes. Interestingly, disturbances of H1 homeostasis have also been reported in PD through accumulation of displaced H1 in Lewy-bodies (Duce, et al. 2006).

The activity assay from cell lysates showed a decline in SIRT1 activity, that is caused by MPP⁺ (Fig. 4.5). Dependant on the mechanism behind the toxin, four explanations are possible. When MPP⁺ decouples the electron chain in complex I, three disturbances that might affect SIRT1, may occur. First, the ROS created by electron leakage in the complex may damage SIRT1. Second, due to breakdown of the mitochondrial membrane potential, the ATP levels are decreased and the lack of energy may affect SIRT1 activity directly or indirectly. Third, SIRT1 requires NAD⁺ as a cofactor, but the damaged complex I may no longer be able to sustain the required levels of NAD⁺. A fourth possibility would be independent of MPP⁺'s main toxic effect and it could directly inhibit SIRT1. At least the third possible explanation can be discarded due to the paradigm of the activity assay. Since NAD⁺ is supplied in sufficient amounts in the assay reaction, a depletive effect on activity can be excluded.

Thus, the data gathered from the assay were supported by Western blots of SIRT1, which showed that SIRT1 protein levels were decreased in MPP⁺ treated cells (Fig. 4.5). Of course, a reduced amount of protein could account for the observed decreased activity, but transcriptomics revealed no regulation by MPP⁺ on SIRT1 transcription (Fig. 4.20), which in turn means the reduced protein levels cannot be explained through transcriptional effects. In another study fellow scientists revealed that cysteine residues in the SIRT1 protein are prone for oxidation through ROS. They created mutant forms of the protein that would replace the oxidation prone cysteines with serines. These mutant forms showed no functional impairment, while also no vulnerability towards ROS mediated damage (Shao et al., 2014). Since damaged proteins need to be degraded (Mizushima et al., 2011), the autophagic system was challenged in a set of cells through BafA1. Using this approach, damaged proteins would not be able to be degraded via autophagy, which would cause them to accumulate in the cells. Indeed, the SIRT1 ratio between BafA1 treated and untreated cells

– further called flux – increased in MPP⁺ treated cells, which translates to accelerated SIRT1 degradation (Fig. 4.5).

However, this data so far only reveal SIRT1 to be degraded at a faster pace, which results in decreased activity levels. When the cells treated with MPP⁺ were also treated with PHT, a potent antioxidant, the SIRT1 activity was similar to that of the control group (Fig. 4.5). The same is true for the H3K14 and lysine acetylation levels (Fig. 4.3, 4.8 and 4.9), the protein levels (Fig. 4.5) and the flux (Fig. 4.5). PHT treatment always killed the MPP⁺ effects, but never the hyperacetylations caused by other agents like TSA or EX-527 (Fig. 4.4). Since transcription levels of SIRT1 were also unaffected by PHT treatment (Fig. 4.20), the only permissible explanation must lead to a regulation of SIRT1 activity through ROS. This is further validated, by the inability of MPHT, an inactive form of PHT, to mimic PHT's influence, while APHT, a weaker antioxidant, still protects at least the H3K14 acetylation levels, albeit not as strong as PHT (Fig. 4.3).

The implemented *in vivo* mouse model complements most of these points. Acetylation levels of H3K14 and total lysine were increased in the MPTP treated group and similar to control levels in the PHT/MPTP treated group (Fig. 4.8 and 4.9). However, SIRT1 levels in MPTP and PHT/MPTP treated mice were increased, not decreased (Fig. 4.9). This can be caused by a lot of different factors. First, SIRT1 may be regulated differently in mice than it is in humans. Second, the brain lysates, unlike the LUHMES cell culture, are not exclusively constituted by dopaminergic neurons. Third, LUHMES cells are incapable of removing MPP⁺, while an entire organism can detoxify. Fourth, rodents are generally less susceptible to toxins. Fifth, SIRT1 degradation is slower. All these are good arguments to further investigate the *in vivo* model, but the final and verified read out of SIRT1 function, the deacetylation of H3K14, confirms that SIRT1 activity is also thwarted by MPP⁺ and protected by PHT *in vivo*.

5.3 MPP⁺ disrupts the SIRT homoeostasis

While SIRT1 is predominantly nuclear and only a smaller fraction of the protein is located to the cytosol, SIRT2 is the exact opposite. Both SIRTs overlap in deacetylation H4K16 (Vaquero et al., 2004; Vaquero et al., 2006), thus observed increase in SIRT2 transcription (Fig. 4.20) might be a compensatory process for SIRT1 loss. SIRT1 deacetylates and deactivates the transcription factors TP53 (Vaziri et al., 2001), EP300 (Bouras et al., 2005) and V-rel avian reticuloendotheliosis viral oncogene homolog A (RELA) (Yeung et al., 2004). These transcription factors may also be negatively regulated by SIRT2 (Jin et al., 2008; Black et al., 2008; Rothgiesser et al., 2010). SIRT1, however, may also affect energy homoeostasis by interacting with AMPK (Hou et al., 2008), the major energy sensor, that evaluates the cellular AMP/ATP ratio (Moore et al., 1991) and activates

glycolytic (Marsin et al., 2000) or beta oxidation related proteins (Hardie et al., 2002), if said ratio is too high. SIRT2 cannot affect AMPK, but rather regulates the acetylation status of the cytoskeleton and thus has an important role for vesicle trafficking (Budayeva et al., 2016). Possibly, a regulatory axis between SIRT1 and SIRT2 exists that enhances one if the other is not present in sufficient number. Since SIRT1 and SIRT2 have a high overlap in many but not all functions, this may allow for a regulation of these specific tasks, while keeping the general tasks running. In PD models, SIRT2 over-expression is a common phenomenon (Liu et al., 2014), that could be caused by reduced SIRT1 activity.

In mitochondria, SIRT3 regulates respiratory activity (Ahn et al., 2008), mtDNA transcription (Liu et al., 2014) and the TCA cycle (Ozden et al., 2014) among others. In the nucleus, SIRT3 regulates stress response genes (Iwahara et al., 2012). Depending on its whereabouts, SIRT3 appears at different sizes. The full-length protein is only encountered in the nucleus (Scher et al., 2007), while the smaller form is exclusively mitochondrial since it is a result of cleavage by the MPP (Schwer et al., 2002). This allows to discern the localization by size of the protein. Like SIRT1, SIRT3 has also been linked to ageing (Brown et al., 2013). A mutation inside an enhancer sequence of SIRT3 has often been observed in long-lived individuals (Bellizzi et al., 2005) and SIRT3 knock-out mice have demonstrated neuronal degeneration in their SN *pars compacta* (Shi et al., 2017). Interestingly, regarding histones, SIRT3 has been shown to deacetylate H3K9 and H4K16 (Scher et al., 2007), a locus also deacetylated by SIRT1 and SIRT2 (Vaquero et al., 2004; Vaquero et al., 2006). Meanwhile, in MPP⁺ stressed cells, the nuclear form of SIRT3 is heavily induced and persists in cells treated with PHT/MPP⁺ (Fig. 4.6). This is likely a result of redistribution, since total SIRT3 protein levels remain unchanged.

Since exclusive PHT treatment showed no effect on SIRT3 in any way, the SIRT3 re-localization is not a response to the increased ROS, but rather to the respiratory breakdown. This would also partly exclude a compensatory effect of SIRT3, although SIRT1 and SIRT3 share two target histone lysines. Like the protein levels of the mitochondrial form, decreased SIRT3 transcription, however, is averted by PHT and thus ROS dependant (Fig. 4.20). This transcriptional rescue may account for the observed increase in total SIRT3 protein observed in only the PHT/MPP⁺ treated cells. Intriguingly, the decrease of mitochondrial SIRT3 in MPP⁺ treated cells is accompanied by a higher turnover that is also averted by PHT, while nuclear SIRT3 does not accumulate in autophagosomes under any treatment. This may be a hint towards a higher turnover of mitochondria altogether. The *in vivo* data complement this to some degree (Fig. 4.9). Here presumably only the nuclear form of SIRT3 was observable, yet murine SIRT3 seems to lack the recognition site for MPP cleavage. Thus, SIRT3 is most likely regulated differently than in human cells. The observed decrease may likely be caused by a general decrease in mitochondria like the human mitochondrial SIRT3.

Unlike SIRT3's, SIRT4's target spectrum is much smaller. It is exclusively mitochondrial and for example inhibits the pyruvate dehydrogenase complex (Mathias, et al. 2014) that catalyses the reaction of pyruvate to acetyl-CoA (Coxon et al., 1949). SIRT4 transcription is unaffected by MPP⁺ treatment, yet PHT causes its transcription to increase (Fig. 4.20). Interestingly, SIRT4 transcription is negatively coupled to mammalian target of rapamycin complex 1 (mTORC1) activity (Csibi et al., 2013), which in turn is inhibited by AMPK (Inoki et al., 2003), which is activated by ATP depletion (Moore et al., 1991). Thus, energy depletion drives SIRT4 transcription and is likely responsible for the observed transcriptional increase in PHT/MPP⁺ treated cells. In general, SIRT4 inhibits mitochondrial acetyl-CoA production outside of beta-oxidation. Interestingly, an artificial depletion of acetyl-CoA would also indirectly inhibit HATs. *In vivo* results suggest a decline in SIRT4 protein levels in MPTP treated animals (Fig. 4.9). This may be related to an overall decrease of mitochondria similar to SIRT3.

SIRT5 activates carbamoyl phosphate synthase 1 (CPS1) (Tan et al., 2014) of the urea cycle, which metabolises ammonium to urea (Krebs et al., 1932). This process initially consumes ATP and feeds the TCA cycle through fumarate to form NADH+H⁺ (Shambaugh, 1977), which could be used to generate more ATP than previously expended through the respiratory chain. Since the latter does not work properly in MPP⁺ treated cells, the urea cycle would turn into an ATP and NAD⁺ sink. Thus, SIRT5 transcription is repressed in cells treated with MPP⁺ or PHT/MPP⁺ (Fig. 4.20).

SIRT6 is nuclear and exhibits deacetylase activity towards H3K9 (Michishita et al., 2008) and H3K56 (Michishita et al., 2009) and mediates DNA double strand break repair (Mao et al., 2011). SIRT6 transcription is not regulated in any treatment group (Fig. 4.20). This may point towards no increase in nuclear DNA damage.

SIRT7 is nucleolar and has so far only been shown to deacetylate H3K18 (Barber et al., 2002) in context of rRNA transcription through stimulation of RNA polymerase I dependant transcription (Ford et al., 2006). Increased rRNA transcription through SIRT7 up-regulation could point towards a higher requirement of ribosomes due to higher protein biosynthesis demand (Fig. 4.20).

5.4 MPP⁺ disrupts the HDAC/HAT homoeostasis

The impact of most SIRTs extends far beyond just transcriptional regulation. This is not necessarily true for the other HDACs. HDAC1 and HDAC2, for example, mainly govern histone acetylation levels. They may also deacetylate some transcription factors but have not been shown to immediately interfere with cellular metabolism. In previous studies, HDAC1 and HDAC2 have been implicated as the main source of accumulation of lysine acetylations in PD models, because of their accumulation inside of autophagosomes resulting in a decrease of protein level (Park et al.,

2016). However, it has to be considered, that HDAC1 and HDAC2 require functional SIRT1. Once they have deacetylated a lysine, the acetyl group sticks to the HDAC (Qiu et al., 2006) and needs to be removed by SIRT1 (Dobbin et al., 2013). If SIRT1 is not present, every HDAC1 and HDAC2 enzyme could catalyse exactly one reaction and would then need to be replaced. An increased degradation and the in this work observed increased transcription of HDAC1 and HDAC2 would lead to an increased turnover caused by SIRT1 deficiency (Fig. 4.21). This would also explain the protective properties of PHT.

HDAC3 also affects only proteins directly affecting transcription. It has been, however, shown to be a co-activator of the nuclear factor, erythroid 2 like 2 (NFE2L2) transcription factor to promote cell survival in oxidative conditions (Martin et al., 2014). These circumstances reflect the regulations observed in this work. ROS cause increased transcription levels, which are abolished by PHT (Fig. 4.21).

The regulatory properties of HDAC4 are mostly similar to those of the others. However, one of its targets appears oddly specific. It may deacetylate the chaperones heat-shock 70 kDa protein 1A (HSPA1A) and HSPA1B. Depending on their acetylation status, these chaperones either target misfolded proteins for refolding if acetylated or proteasomal degradation if not acetylated (Seo et al., 2016). The observed down-regulation of HDAC4 under MPP⁺ and PHT/MPP⁺ would thus cause the proteins to be rather targeted for refolding (Fig. 4.21).

HDAC5 is another major regulator of histone acetylation. So far, its targets have only been related to transcription factors and histones. It has, however, been implicated in memory consolidation (Agis-Balboa et al., 2013) and addiction (Taniguchi et al., 2017). The observed up-regulations could thus be related to neuronal reformation or protection (Fig. 4.21).

Unlike the other so far described HDACs, HDAC6 has a major task outside of the nucleus away from the histones and transcription factor it may also affect. If the proteasomal degradation system and the chaperone system overburdened by an amount of misfolded or damaged proteins, HDAC6 mediates their storage in aggresomes by linking them to a dynein motor protein. The aggresomes are subsequently targeted for autophagic degradation (Kawaguchi et al., 2003). Increased ROS lead to an increase in misfolded proteins that need to be degraded (Haynes et al., 2004). The observed regulations of HDAC6 are likely related to this rather specific task of HDAC6 (Fig. 4.21).

The HDACs HDAC7, HDAC8 and HDAC9 are more or less not regulated in any treatment group (Fig. 4.21). So far, they also have not been implicated in anything bar histone or transcription factor deacetylation. The absence of regulations can thus not be interpreted in any way.

HDAC10, on the other hand, has been implicated in lysosomal exocytosis in neuroblastoma cells (Ridinger et al., 2018). It is thus relevant for the clearance of damaged proteins out of the cellular body. In light of this, the observed up-regulations of HDAC10 can be explained with an increased

amount of damaged proteins (Fig. 4.21).

Finally, HDAC11, of course, also regulates histone and transcription factor acetylation. A unique regulation of HDAC11 has been shown in knock out mice that showed a lesser tendency to become obese while under a high fat diet (Sun et al., 2018). This might implicate an involvement of HDAC11 in energy homeostasis either direct or indirect. This may explain the elevated transcription levels observed in cells treated with MPP⁺ and PHT/MPP⁺ (Fig. 4.21).

On the other side of lysine acetylation, some HATs are also regulated when treated with MPP⁺ or PHT/MPP⁺. To be precise, 9 out of 14 HATs are significantly down-regulated by MPP⁺ (Fig. 4.22). This is likely a regulation to compensate the so far described loss of HDAC activity. Interestingly, 6 (KAT6A (Qiu et al., 2012), KAT6B (Klein et al., 2017), EP300 (Ogryzko et al., 1996), CREBBP (Ogryzko et al., 1996), NCOA1 (Spencer et al., 1997) and KAT2B (Vicent et al., 2009) of the 9 down-regulated enzymes exhibit acetyltransferase activity towards H3, while two (NCOA2, NCOA3) of the other three show no transferase activity towards histones. This is likely a cellular response to the high H3 acetylation levels since SIRT2 and SIRT3 exhibit almost no deacetylase activity towards H3 and thus cannot compensate loss of SIRT1 function.

5.5 ROS dependant loss of DNMT3B causes DNA hypomethylation

The mechanisms governing DNA methylation and demethylation rely on two protein families. DNMTs transfer a methyl-group from S-adenosyl methionine (SAM) to the 5' position of the DNA base cytosine (Pradhan et al., 1999). This usually causes the chromatin to condense because DNMTs often work in concert with other enzymes like HDACs (Fuks et al., 2000). TETs hydrolyse the methyl group, which ultimately results in replacement of the base with an unmodified cytosine by means of base excision repair (BER) (Weber et al., 2016). Together these enzymes work dynamically in concert. Disturbances in this tandem may cause severe alterations to the DNA methylome due to the mechanics behind DNMT dynamics.

The DNMT protein family merely consists of three proteins. The so-called maintenance DNMT, DNMT1 (Pradhan et al., 1999), and the *de novo* DNMTs, DNMT3A and DNMT3B (Okano et al., 1999). During a cells development or adaptive processes, DNMT3A and DNMT3B place fresh methylations that are conserved by DNMT1 or removed by a TET. To place the right methylation at the right time, DNMT3A and DNMT3B rely on other factors to guide them. However, some of these factors may no longer be present in differentiated cells and a loss of associated methylations cannot be restored. On the other hand, TET1 and TET3 feature a CXXC domain that allows them to bind DNA (Iyer et al., 2009), while TET2 relies on cofactors since it lacks said domain.

First and foremost in regard to DNA methylation previous studies were able to confidentially reveal

that PD models as well as affected humans show decreased levels of DNA methylation (Desplats et al., 2011). In this work, these findings were confirmed (Fig. 4.10). MPP⁺ treated LUHMES cells showed reduced levels of 5-methylcytosine. Since co-treatment with PHT blocked the MPP⁺ mediated reduction, the depletion of 5-methylcytosine is likely related to ROS. The underlying mechanism is most probably related to DNMTs, since SIRT1 has been shown to be a common interactor of those (Kashiwagi et al., 2011).

DNMT1 was mainly localized to the nucleus, where most of the cellular DNA is located. Upon MPP⁺ treatment this changed. Most of the protein moved to the cytosol, leaving the nucleus almost empty (Fig. 4.11). Since the antioxidant PHT was unable to avert this, the re-localization of DNMT1 cannot be held responsible for the observed DNA hypomethylation. It is nonetheless an interesting development. Considering the decrease in transcription of DNMT1 which also is ROS independent (Fig. 4.23), the cells appear to actively lock the protein out of the nucleus. Interestingly, DNMT1 has been shown to localize to mitochondria to methylate mitochondrial DNA (Shock et al., 2011). Since MPP⁺ is first and foremost a mitochondrial poison, DNMT1 may be needed to protect mtDNA. This could be supported by the behaviour of DNMT1 in 6-thioguanine treated cells. This guanine analogue is implemented in newly synthesized DNA (Lepage, 1963), which is in post mitotic cells only occurring in mitochondria, and interferes with the replication and methylation process (Hogarth et al., 2008). Thus, DNMT1 would be required to maintain DNA methylation in newly synthesized mtDNA.

DNMT3A was localized to the nucleus and the cytosol with a conspicuous perinuclear focus per cell (Fig. 4.12). Since DNMT3A has also been implicated in mtDNA methylation, the cytosolic fraction is likely associated to mitochondria (Chestnut et al., 2011). MPP⁺ treatment did not affect transcription levels of DNMT3A, but protein levels were decreased, which PHT could also not prevent (Fig. 4.12 and 4.23). Interestingly, 6-thioguanine, again, mimicked the MPP⁺ effect. This could mean that rather the observed stress on DNA methylation could cause the regulations regarding DNMT1 and DNMT3A than the increased oxidative stress.

DNMT3B is the only DNMT that was not described in mitochondria and was only located to the nucleus (Fig. 4.13). In case of this protein, the MPP⁺ associated decline in protein level was blocked by PHT (Fig. 4.13 and 4.14). Thus, DNMT3B must be responsible for the observed DNA hypomethylation, since it is the only DNMT responsive to PHT treatment. Indeed, the protein levels are even increased compared to the control. This likely means that DNMT3B compensates the translocated DNMT1 and adopts its nuclear tasks, while DNMT1 takes care of mtDNA methylation. Western blots of DNMT3B, however, revealed a different picture. Human DNMT3B actually has different isoforms, a lot of which are between 95-100 kDa and one at 70 kDa. Since the larger isoforms are this similar in size, they rather appear as a smear on the blot than a precise band (Fig.

4.14). This allows to compare the protein levels of some isoforms separately. These Western blots revealed both isoforms to be regulated in the same way. DNMT3B protein levels, however, were also elevated in cells treated only with PHT. Thus, the elevated DNMT3B levels in the MPP⁺/PHT treated group could also be considered a side effect of PHT. Unfortunately, the results from cells treated with MPP⁺/MPHT were inconclusive due to high variances, but at least in two out of three samples DNMT3B levels were elevated. This would support the hypothesis that DNMT3B is affected by PHT independent of its antioxidative properties. Interestingly, the DNMT3B transcription is down-regulated in samples treated with MPP⁺ and PHT/MPP⁺ (Fig. 4.23), somewhat contradicting the elevated protein levels observed after PHT treatment.

Taken together the *in vitro* results regarding DNMT3B paint a very diverse picture, which gives rise to different questions that need to be addressed. It is definitely responsible for the MPP⁺ mediated DNA hypomethylation. Although PHTs seem to have a side effect on DNMT3B levels, the underlying mechanism, however, is also likely to be related to ROS. The protein is constituted by many cysteines and methionines, the most ROS vulnerable amino acids. The reduced amount of DNMT3B protein is likely a result of increased degradation and decreased gene transcription. The transcriptional effect observed in PHT/MPP⁺ treated cells may also be independent from the MPP⁺ regulation and rather be caused by a negative feedback loop resulting in the same regulation.

Due to difficulties of the experimental procedures, the *in vivo* samples could not be investigated in regard to DNA methylation, but the lysates allowed to investigate the responsible protein DNMT3B. Of the different isoforms only one at ~100 kDa gave a reliable signal and thus evaluation was restricted to this isoform (Fig. 4.14). The midbrain lysates confirmed the *in vitro* data concerning protein levels, emphasizing that these are not cell culture artefacts but relevant to the dopaminergic cell loss.

Intriguingly, mutations in the DNMT3B gene have been implicated in a rare form of familial PD (Chen et al., 2017). Furthermore, DNMT3B is an interactor of SIRT1 that work in tandem to establish and maintain heterochromatin. A complex dependant on DNMT3B, SIRT1 and H1 has even been described to be of major importance catalysing epigenetic rearrangements (Kashiwagi et al., 2011). Thus, an impairment of this specific complex is very likely. Interestingly, H1 is recruited by SIRT1 (Vaquero et al., 2004) and then H1 recruits DNMT3B (Yang et al., 2013) (Fig. 5.1). Whether the DNMT3B is indeed damaged by the ROS, or whether it can no longer access the DNA due to H1 displacement, becomes idle and is thus degraded, cannot be assessed at this point. Future DNMT3B over-expression studies might deliver much needed answers.

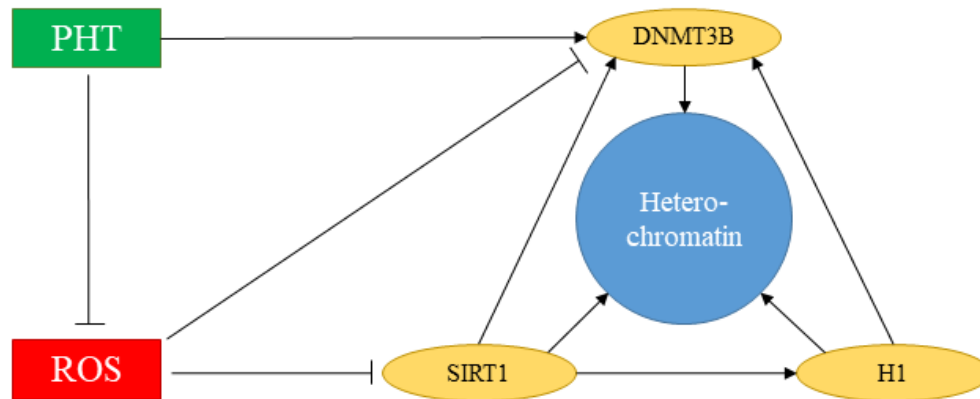


Figure 5.1: ROS dependant loss of heterochromatin. SIRT1, H1 and DNMT3B work in tandem to generate heterochromatin. Since SIRT1 is damaged by ROS, it can no longer recruit neither H1 nor DNMT3B to the chromatin, resulting in a loss of heterochromatin. If PHT is present, heterochromatin can be assembled since ROS mediated SIRT1 damage is quenched.

Robust knowledge of TET function is primarily gathered in embryonic studies due to their exceedingly high activity during developmental processes (Cimmino et al., 2011). They have, however, also been described in highly active levels in neuronal cells of the hippocampus (Chen et al., 2012). Knock-out studies have revealed, that TET2 and TET3 govern different time points and aspects of differentiation processes (Li et al., 2015), while TET3 expression levels were also increased after neuronal injury (Weng et al., 2017). MPP⁺ treated cells exhibit higher levels of TET1 transcription, but lower levels of TET3 transcription and no effect on TET2 transcription (Fig. 4.23), while PHT swaps the effects of TET2 and TET3. Unfortunately, since the underlying dynamics of TETs is not well understood and target genes seem to depend also on interacting transcription factors, the implications of these regulations cannot be fully grasped at this stage. It can only be stated, that a shift in TET transcription likely causes different sets of genes to become activated and may play a role in the observed DNA hypomethylation under MPP⁺.

5.6 Increased supply of energy generators in the MPP⁺ model of PD

As mentioned, MPP⁺ complex I inhibition takes away the cell's main energy source, the oxidative phosphorylation through the respiratory chain (Nicklas et al., 1985). Without a functional complex I, the membrane potential of the inner mitochondrial membrane weakens (Ghelli et al., 1997). If the cellular energy system collapses, it appears logical, that the cell would try to produce more tools to generate energy. Indeed, transcription of complex V related nuclear genes is up-regulated in MPP⁺ treated cells, with the exception of ATP synthase subunit S (ATP5S) which is down-regulated (Fig.

4.15). This could theoretically be compensated through ATP5SL. Although this protein has so far only been described in one study as a complex I assembly factor (Stroud et al., 2016), it could also surrogate ATP5S due to its structural similarities. To solidify this claim, further studies have to be considered.

Overall complexes IV, III and I also show strong up-regulations in MPP⁺ treated cells, while complex II also trends towards an overall up-regulation. Interestingly the regulations regarding complex II are the weakest, although it is the only alternative to complex I to generate ATP through the respiratory chain. Unlike complex V, the complexes III and IV have no component that is down-regulated.

Complex I, on the other hand, has a few more genes down-regulated, but remains generally up-regulated nonetheless. Together these data points suggest a higher requirement for generation of mitochondrial complexes under MPP⁺ stress conditions. Interestingly, most of these up-regulations disappear in PHT/MPP⁺ treated cells. This could be interpreted in two ways. First, due to the presence of PHT, the mitochondria are more healthy and thus the stimulus to generate more complexes is weakened. Second, the cells try to compensate the energetic loss through anaerobic means. If the cells overall abdicate respiration they do not require high levels of nuclear encoded complex subunits. Future studies need to address these points by looking at the mitochondrial respiration rate and the LDH activity to compare aerobic vs. anaerobic respiration. Looking at the transcription rate of other players of the energy metabolism may also yield first insights into the possible implications.

Transcription of glycolytic enzymes is heavily up-regulated in MPP⁺ treated cells and remains that way in PHT/MPP⁺ treated cells, although transcription of most is reduced through PHT (Fig. 4.19). Out of those not significantly genes regulated through PHT, three stick out. Hexokinases 1 and 2 (HK1, HK2) phosphorylate glucose to glucose-6-phosphate (Lowry et al., 1964, Tsai et al., 1996) and thus catalyse the first step of glycolysis. Unlike glucose, glucose-6-phosphate can no longer leave the cell (Berg et al., 2002) and the final commitment to glycolysis is catalysed by the rate limiting enzyme phosphofructokinase (PFK), which turns fructose-6-phosphate into fructose-1,6-bisphosphate (Yi et al., 2012). LUHMES cells express all three types of PFKs PKF platelet (PFKP), PFK muscle (PFKM) and PFK liver (PFKL) (Fig. 4.19). The regulatory effects are strongest on PFKP and it remains up-regulated under PHT, while PFKM up-regulation is averted by PHT. The observed up-regulations must thus rather be caused by the energetic dysbalance than ROS, since PHT does not down-regulate these adaptations in a significant manner, especially not the rate-limiting enzymes' transcription. Furthermore, this also likely leads to increased glycolytic activity, which would require increased amount of cellular glucose to successfully uphold the energy supply. Neurons transport glucose using GLUT3 (Maher et al., 1991). Cells treated with MPP⁺ and

PHT/MPP⁺, but not with PHT, feature higher levels of GLUT3, supporting the cell with enough glucose to compensate for respiratory decline (Fig. 4.20).

The TCA cycle requires acetyl-CoA as a substrate to generate citrate from oxalacetate. The citrate is then subsequently degraded to oxalacetate. During one step of the cycle, succinyl-CoA is transformed to succinate by succinate-CoA ligase (SUCL) that also generates one molecule of GTP which can be transformed to ATP by nucleoside-diphosphate kinases (NDPKs) (Krebs et al., 1937). The SUCL is constituted by two subunits succinyl-CoA synthetase subunit alpha (SUCLG1) and GTP-specific succinyl-CoA synthetase subunit beta (SUCLG2) (Nishimura, 1968). However, SUCLG2 can also be replaced by ATP-specific succinyl-CoA synthetase subunit beta (SUCLA2), that has been shown to rather generate ATP than GTP (Johnson et al., 1998). Interestingly, this ATP specific subunit's MPP⁺ dependant up-regulation is not averted by PHT, unlike SUCLG1 and SUCLG2 (Fig. 4.19). As the glycolysis, the TCA cycle components are significantly up-regulated in MPP⁺ treated cells in a way that is unresponsive to PHT. This also concludes, that cells try to use the TCA cycle is used to generate more ATP.

The mitochondrial complex I is not only responsible for successful respiration, it also regenerates NAD⁺, a co-factor of many enzymes like SIRT1 (Vaziri et al., 2001), for example. The complex I disruption by MPP⁺ must thus also lead to a ROS independent decline in NAD⁺ levels. On top of that, high glycolytic activity and acceleration of the TCA cycle to compensate for the ATP depletion will also require high amounts of NAD⁺. These can also theoretically be supplied by turning pyruvate into lactate through lactate dehydrogenases (LDHs). Indeed, transcription of two LDHs, LDHA and LDHB, is up-regulated in cells treated with MPP⁺ (Fig. 4.19). Pyruvate is the final product of glycolysis and may also be turned into acetyl-CoA by the pyruvate dehydrogenase complex to fuel the TCA cycle (Coxon et al., 1949). Most of this complexes components (dihydrolipoamide dehydrogenase (DLSD), dihydrolipoamide S-acetyltransferase (DLAT), pyruvate dehydrogenase complex component X (PDHX) and pyruvate dehydrogenase E1 beta subunit (PDHB) however, are down-regulated in MPP⁺ treated cells and remain so in PHT/MPP⁺ treated cells. Only the pyruvate dehydrogenase E1 alpha 1 subunit (PDHA1) is up-regulated. Without the other components, however, activity is very unlikely. The high expression of SIRT4 in PHT/MPP⁺ treated cells may inhibit this complex through DLAT hydrolysis (Mathias et al., 2014) even further to favour the formation of lactate through LDH.

Furthermore, pyruvate may be supplied by the decarboxylation of malate through malic enzymes (MEs) (Chang et al., 2003). Both expressed MEs, ME1 and ME2, are up-regulated in cells treated with MPP⁺. The cytosolic ME1, remains up-regulated in PHT/MPP⁺ treated cells, while the mitochondrial, ME2, does not. This would further decrease the pyruvate availability for the pyruvate dehydrogenase complex. Together, these developments point towards a compensatory

NAD⁺ production via LDHs. These observations regarding the expression of LDHs and glycolytic enzymes may solidify the idea of a switch between aerobic and anaerobic metabolism. However, this still needs to be addressed and verified in future studies, to give chapter and verse for this hypothesis.

Finally, the cell may uphold its energy supply through the beta-oxidation of fatty acids (Knoop, 1904). This process occurs not in the cytosol, but in mitochondria (Lehninger, 1945). Genes related to mitochondrial beta oxidation are up-regulated in cells treated with MPP⁺ and remain that way in cells treated with PHT/MPP⁺ (Fig. 4.19). The beta-oxidation may yield FADH₂, which is fed into the complex II to uphold membrane potential. Its high activity may thus help to compensate for the loss of complex I. It becomes even more important, since the NAD⁺ production compensation through LDHs and the reduction of the pyruvate dehydrogenase complex blocks the main source of acetyl-CoA for the TCA cycle, which is required to uphold the energy balance.

Taken together, these regulations paint a complex picture of the way the cell tries to restore its energetic deficit, when the complex I is inactive (Fig. 5.2). Further studies are required to solidify this, although these adaptations appear logical. Energy production through the TCA cycle or beta-oxidation, however, is also part of the respiratory chain through complex II, yet overall, these data may also suggest a switch to anaerobic respiration.

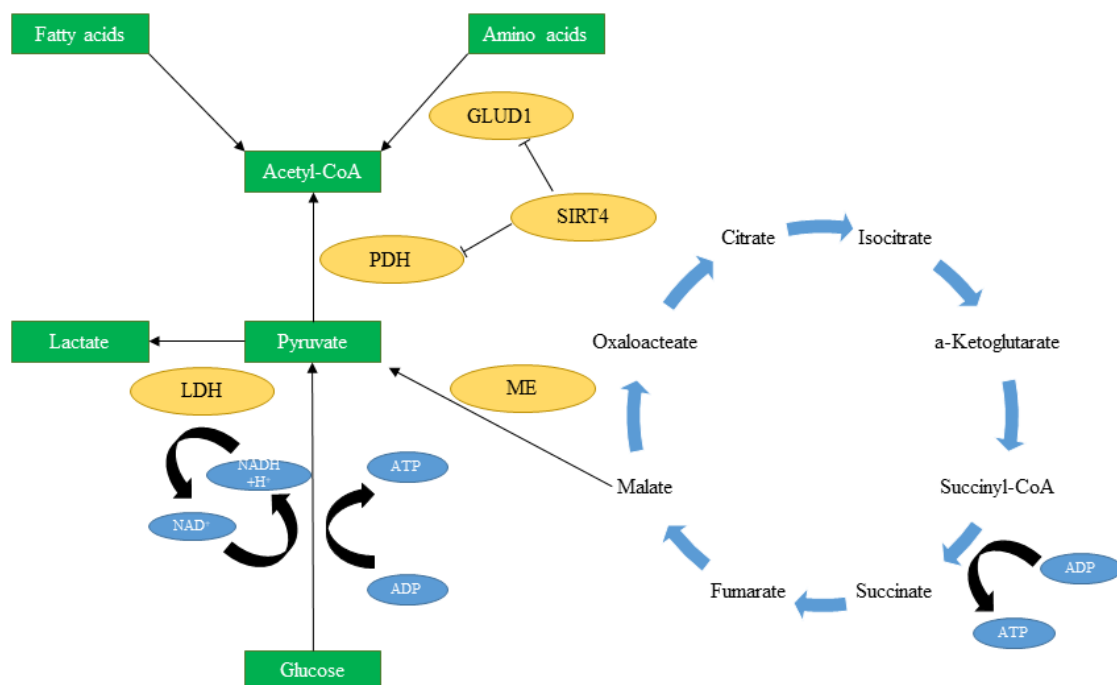


Figure 5.2: Restoration of energy dysbalance. Glucose is degraded through glycolysis to pyruvate, which in turn is transformed into lactate by LHD to regenerate lost NAD⁺. SIRT4 inhibits PDH and glutamate dehydrogenase 1 (GLUD1), thus causing acetyl-CoA to be limited and pyruvate to be rather pushed towards LDH. Fatty acid degradation through beta-oxidation still yields acetyl-CoA, which is utilized in the TCA cycle to gain energy and form malate, which is transformed into pyruvate by ME.

5.7 Mitochondria in MPP⁺ treated cells favour replication over transcription

Genes encoding proteins for the respiratory chain are not exclusively nuclear. Central proteins of the complexes I, III, IV and V, but not complex II, are encoded on the mtDNA. In contrast to the nuclear encoded genes, the mitochondrial encoded complex subunits are severely down-regulated in MPP⁺ treated cells (Fig. 4.16). Since all subunits are required for successful complex assembly, reduced levels of mitochondrial transcripts would leave the complex proteins dormant and unassembled inside the matrix. These effects persisted through PHT co-treatment. The implications of this are not so easily grasped.

It is important to note that replication and transcription of mtDNA are highly exclusive. If the DNA replicates, transcription cannot occur and vice versa. This is regulated by an enzymatic switch catalysed through TEFM (Agaronyan et al., 2015). It is thus not surprising that TEFM transcription as well as protein levels are decreased in MPP⁺ and PHT/MPP⁺ treated cells (Fig. 4.17).

The canonical set-up for mitochondrial replication consists of TOP1MT, TWNK, SSBP1, POLRMT, POLG and POLG2. Interestingly, an up-regulation in MPP⁺ treated cells was restricted only to TOP1MT and POLG2 (Fig. 4.17). The other replication components were either not regulated, POLRMT and POLG, or down-regulated, TWNK and SSBP1. These observations would not immediately point towards higher replicative activity in those cells. Co-treatment with PHT, however, had a positive effect on POLRMT and POLG transcription. It also showed a protective effect on TWNK transcription levels, although the transcription remained down-regulated still, while the same was true for TOP1MT transcription in a mirrored matter. This left four of six components up-regulated, while TWNK and SSBP1 remained down-regulated.

Interestingly, SSBP1 is not the only SSBP1 observed in mitochondria. SSBP2 has also been found in mitochondria *in vivo* (Kato et al., 2009) and turned out to be up-regulated in both treatment groups (Fig. 4.17). On the other hand, TWNK is not the only helicase described in mitochondria. DNA2 (Zheng et al., 2008), PIF1 (Futami et al., 2007) and SUPV3L1 (Minczuk et al., 2002) have also been detected in mitochondria. Of those three DNA2 was the only helicase up-regulated in PHT/MPP⁺ treated cells, while the other two were down-regulated. Overall, the required proteins are up-regulated in their transcription in at least in PHT/MPP⁺ treated cells. Together with the observed TEFM effect, this gives a strong argument for increased replicative activity.

The fact that DNA2 is up-regulated, while all other mitochondrial helicases are down-regulated, sticks out. Interestingly, DNA2 is reportedly quite competent at resolving G4-quadruplexes (Lin et al., 2013), secondary DNA structures that result from a palindromic convergence of four guanines (Gellert et al., 1962). These quadruplexes may also lead to decreased transcription (Rhodes et al., 2015). They are stabilized by a cation in the midst of the four guanines bound through hydrogen

bonds (Fig. 5.3) and they have been shown to be extremely stable when the cation is replaced by a cobalt bound porphyrin (Sabater et al., 2015). Especially the ability of cobalt porphyrin to trap superoxide (Collman et al., 2002) could point towards a ROS protection system that wraps up the mitochondrial DNA in G4-quadruplexes. This becomes even more likely when considering the fact that the DNA base with the highest mutation rate is cytosine (Duncan et al., 1980). Yet through the G4 structures, the DNA repair system would be able to identify correct guanines and successfully repair damaged cytosines.

All these data regarding mitochondrial DNA replication could point to the same adaptation process already mentioned earlier. Since only a fraction of mitochondria in PHT/MPP⁺ treated cells respire, only that specific fraction requires transcription of mtDNA encoded genes. The cells treated with only MPP⁺, however, showed only a partial increase of the mitochondrial replication system, while the transcription is down-regulated in the same manner as the other treatment group. The defence system of the mitochondria may already take action here, but the signal cannot be transferred correctly to the nucleus to adapt in the optimal way because the ROS interfere with the signal or cause a stronger response.

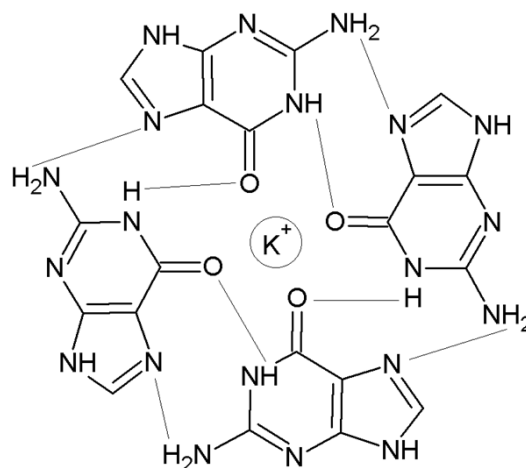


Figure 5.3: G4-quadruplex. Structural overview of a G4-quadruplex with its hydrogen bonds and a cation in form of potassium.

5.8 PHT the future PD drug?

Since the mechanism behind PHTs protection regarding ROS sensitive epigenetic systems in the MPP⁺/MPTP became clearer during the course of this work, future studies have to move the investigations slowly towards human studies and clinical trials, but a few other things have to be considered:

First, the actual mechanism behind the protection. *In vivo* the dopaminergic cells of the SN survived the MPTP mediated stress and were healthy if the mice were also treated with PHT (Fig. 4.7). This was accompanied by improved motoric behaviour. However, this model relies on acute toxicity of

MPP⁺, which is flushed out of the organism over time (Nishi et al., 1989). Thus, the cells only experience a strong wave of stress that declines again, while in PD the stress does not disappear in the same manner. This would create a necessity for a longterm PHT treatment regimen for patients. But this is where the *in vitro* model trumps the *in vivo* model. The LUHMES cells are unable to get rid of the MPP⁺ because they lack the appropriate proteins cytochrome P450 2D6 and 3A (Mann et al., 2010), which forces them to adapt to a chronic situation. However, these cells, despite being able to survive (Fig. 4.1), seem to be unable to fully adapt. When compared to the cells treated with PHT/MPP⁺, it appears as if they are caught between two states and only PHT can push them over the edge to adjust to their new environment.

This is even further solidified by the observed epigenetic changes. The MPP⁺ treated cells start to remodel their chromatin, they open the chromatin around new genes to enhance their transcription, but they are unable to close the chromatin around others, due to the absence of SIRT1, H1 and DNMT3B. This leads to genomic instability and can over long times become very dangerous for the cell or the organism since open chromatin is much more prone for induction of mutations. The same epigenetic changes can also be observed *in vivo*. It can thus be stated, that SIRT1 and DNMT3B are of utmost importance for the final epigenetic adaptation that is required for solving the energy problem posed by a degenerated complex I. These two proteins would thus also be suitable targets for future more direct treatment options.

Second, PHT is merely an antioxidant, albeit a very potent one (Fig. 4.2). Not every case of PD is the same. In some cases increased ROS may cause the disease, but not in all. It is thus to be expected, that PHT would only show benefits in those cases. Positive effects in familial forms of PD, for example, are likely much smaller, if present at all. Nevertheless, considering the momentary regular treatment options, PHT treatment may be very beneficial. Administration of L-DOPA or MAO-B inhibitors cause dopamine to be present in higher levels, which leads to a regeneration of dopaminergic activity in the SN. Dopamine itself, however, is prone to become a radical propagator. Thus, high dopamine levels may increase free cellular radicals that can be removed by PHT.

Third, the physiological availability of nutrients is not represented by *in vitro* cell culture media. The metabolic adaptation of PHT/MPP⁺ treated cells requires high levels of glucose, pyruvate and lipids to survive. Physiological concentrations of these nutrients may be too low to support these cells. Thus, a dietary change for the patients seems to be appropriate as well. PHT may help the cells to survive the ROS and adapt, but it cannot provide the energy for survival directly.

After careful consideration of these major points, PHT may very well become a possible treatment option for PD patients in the future. However, for successful treatments it is also necessary to find earlier biomarkers of the disease since PHT can only protect the remaining cells, not regenerate the already dead.

6 Literature

Agaronyan K, Morozov YI, Anikin M, Temiakov D. "Mitochondrial biology. Replication-transcription switch in human mitochondria". *Science*. 2015 Jan 30;347(6221):548-51.

Agis-Balboa RC, Pavelka Z, Kerimoglu C, Fischer A. "Loss of HDAC5 impairs memory function: implications for Alzheimer's disease". *J Alzheimers Dis*. 2013;33(1):35-44.

Ahn BH, Kim HS, Song S, Lee IH, Liu J, Vassilopoulos A, Deng CX, Finkel T. "A role for the mitochondrial deacetylase Sirt3 in regulating energy homeostasis". *Proc Natl Acad Sci U S A*. 2008 Sep 23;105(38):14447-52.

Ahuja N, Schwer B, Carobbio S, Waltregny D, North BJ, Castronovo V, Maechler P, Verdin E. "Regulation of insulin secretion by SIRT4, a mitochondrial ADP-ribosyltransferase". *J Biol Chem*. 2007 Nov 16;282(46):33583-92.

Aitken RJ, Buckingham D, Harkiss D. "Use of a xanthine oxidase free radical generating system to investigate the cytotoxic effects of reactive oxygen species on human spermatozoa". *J Reprod Fertil*. 1993 Mar;97(2):441-50.

Allfrey VG, Faulkner R, Mirksy AE. "Acetylation and methylation of histones and their possible role in the regulation of RNA synthesis". *Proc Natl Acad Sci U S A*. 1964 May;51:786-94.

Andrew R, Watson DG, Best SA, Midgley JM, Wenlong H, Petty RKH. "The determination of hydroxydopamines and other trace amines in the urine of parkinsonian patients and normal controls". *Neurochem. Res*. 1993 18 1175–1177.

Ano Y, Sakudo A, Kimata T, Uraki R, Sugiura K, Onodera T. "Oxidative damage to neurons caused by the induction of microglial NADPH oxidase in encephalomyocarditis virus infection". *Neurosci Lett*. 2010 Jan 18;469(1):39-43.

Astiz M, de Alaniz MJ, Marra CA. "The oxidative damage and inflammation caused by pesticides are reverted by lipoic acid in rat brain". *Neurochem Int*. 2012 Dec;61(7):1231-41.

- Atherton JF, Bevan MD. "Ionic mechanisms underlying autonomous action potential generation in the somata and dendrites of GABAergic substantia nigra pars reticulata neurons in vitro". *J Neurosci*. 2005 Sep 7;25(36):8272-81.
- Augusto O, Linares E, Giorgio S. "Possible roles of nitric oxide and peroxynitrite in murine leishmaniasis". *Braz J Med Biol Res*. 1996 Jul;29(7):853-62
- Axelrod J. "O-methylation of epinephrine and other catechols in vitro and in vivo". *Science*. 1957 Aug 30;126(3270):400-1.
- Ayala A, Muñoz MF, Argüelles S. "Lipid peroxidation: production, metabolism, and signaling mechanisms of malondialdehyde and 4-hydroxy-2-nonenal". *Oxid Med Cell Longev*. 2014;2014:360438.
- Bailey DC, Todt CE, Burchfield SL, Pressley AS, Denney RD, Snapp IB, Negga R, Traynor WL, Fitsanakis VA. "Chronic exposure to a glyphosate-containing pesticide leads to mitochondrial dysfunction and increased reactive oxygen species production in *Caenorhabditis elegans*". *Environ Toxicol Pharmacol*. 2018 Jan;57:46-52.
- Bandyopadhyay D, Medrano EE. "The emerging role of epigenetics in cellular and organismal aging". *Exp Gerontol*. 2003 Nov-Dec;38(11-12):1299-307.
- Bannister AJ, Zegerman P, Partridge JF, Miska EA, Thomas JO, Allshire RC, Kouzarides T. "Selective recognition of methylated lysine 9 on histone H3 by the HP1 chromo domain". *Nature*. 2001 Mar 1;410(6824):120-4.
- Barber MF, Michishita-Kioi E, Xi Y, Tasselli L, Kioi M, Moqtaderi Z, Tennen RI, Paredes S, Young NL, Chen K, Struhl K, Garcia BA, Gozani O, Li W, Chua KF. "SIRT7 links H3K18 deacetylation to maintenance of oncogenic transformation". *Nature*. 2012 Jul 5;487(7405):114-8.
- Baumberger JP, Jürgensen JJ, Bardwell K. "The coupled redox potential of the lactate-enzyme-pyruvate system". *J Gen Physiol*. 1933 Jul 20;16(6):961-76.

- Beal MF, Matthews RT, Tieleman A, Shults CW. "Coenzyme Q10 attenuates the 1-methyl-4-phenyl-1,2,3,4-tetrahydropyridine (MPTP) induced loss of striatal dopamine and dopaminergic axons in aged mice". *Brain Res.* 1998 Feb 2;783(1):109-14.
- Bednar J, Garcia-Saez I, Boopathi R, Cutter AR, Papai G, Reymer A, Syed SH, Lone IN, Tonchev O, Crucifix C, Menoni H, Papin C, Skoufias DA, Kurumizaka H, Lavery R, Hamiche A, Hayes JJ, Schultz P, Angelov D, Petosa C, Dimitrov S. "Structure and Dynamics of a 197 bp Nucleosome in Complex with Linker Histone H1". *Mol Cell.* 2017 May 4;66(3):384-397.e8.
- Bélanger M, Magistretti PJ. "The role of astroglia in neuroprotection". *Dialogues Clin Neurosci.* 2009;11(3):281-95.
- Bellizzi D, Rose G, Cavalcante P, Covello G, Dato S, De Rango F, Greco V, Maggiolini M, Feraco E, Mari V, Franceschi C, Passarino G, De Benedictis G. "A novel VNTR enhancer within the SIRT3 gene, a human homologue of SIR2, is associated with survival at oldest ages". *Genomics.* 2005 Feb;85(2):258-63.
- Benzie IF. "Lipid peroxidation: a review of causes, consequences, measurement and dietary influences". *Int J Food Sci Nutr.* 1996 May;47(3):233-61.
- Berg JM, Tymoczko JL, Stryer L. "Biochemistry. 5th edition". New York: W H Freeman; 2002. Section 16.1, Glycolysis Is an Energy-Conversion Pathway in Many Organisms.
- Betarbet R, Sherer TB, MacKenzie G, Garcia-Osuna M, Panov AV, Greenamyre JT. "Chronic systemic pesticide exposure reproduces features of Parkinson's disease". *Nat Neurosci.* 2000 Dec;3(12):1301-6.
- Berry C, La Vecchia C, Nicotera P. "Paraquat and Parkinson's disease". *Cell Death Differ.* 2010 Jul;17(7):1115-25.
- Bieri JG. "An effect of selenium and cystine on lipide peroxidation in tissues deficient in vitamin E". *Nature.* 1959 Oct 10;184(Suppl 15):1148-9.
- Bird A. "Perceptions of epigenetics". *Nature.* 2007 May 24;447(7143):396-8.

- Birkmayer W, Hornykiewicz O. "The L-dihydroxyphenylalanine (L-DOPA) effect in Parkinson's syndrome in man: On the pathogenesis and treatment of Parkinson akinesia". *Arch Psychiatr Nervenkr Z Gesamte Neurol Psychiatr*. 1962;203:560-74.
- Black JC, Mosley A, Kitada T, Washburn M, Carey M. "The SIRT2 deacetylase regulates autoacetylation of p300". *Mol Cell*. 2008 Nov 7;32(3):449-55.
- Blanch M, Mosquera JL, Ansoleaga B, Ferrer I, Barrachina M. "Altered Mitochondrial DNA Methylation Pattern in Alzheimer Disease-Related Pathology and in Parkinson Disease". *Am J Pathol*. 2016 Feb;186(2):385-97.
- Blandini F, Armentero MT, Martignoni E. "The 6-hydroxydopamine model: news from the past". *Parkinsonism Relat Disord*. 2008;14 Suppl 2:S124-9.
- Blascko H. "The specific action of L-dopa decarboxylase". *J Physiol (Lond)* 1939;96(50):50-51.
- Bochtler M, Ditzel L, Groll M, Hartmann C, Huber R. "The proteasome". *Annu Rev Biophys Biomol Struct*. 1999;28:295-317.
- Bondy SC, Naderi S. "Contribution of hepatic cytochrome P450 systems to the generation of reactive oxygen species". *Biochem Pharmacol*. 1994 Jul 5;48(1):155-9.
- Borgstahl GE, Parge HE, Hickey MJ, Beyer WF Jr, Hallewell RA, Tainer JA. "The structure of human mitochondrial manganese superoxide dismutase reveals a novel tetrameric interface of two 4-helix bundles". *Cell*. 1992 Oct 2;71(1):107-18.
- Bouras T, Fu M, Sauve AA, Wang F, Quong AA, Perkins ND, Hay RT, Gu W, Pestell RG. "SIRT1 deacetylation and repression of p300 involves lysine residues 1020/1024 within the cell cycle regulatory domain 1". *J Biol Chem*. 2005 Mar 18;280(11):10264-76.
- Bowers MB Jr, Van Woert M, Davis L. "Sexual behavior during L-dopa treatment for Parkinsonism". *Am J Psychiatry*. 1971 Jun;127(12):1691-3.

- Braak H, Bohl JR, Müller CM, Rüb U, de Vos RA, Del Tredici K. "The staging procedure for the inclusion body pathology associated with sporadic Parkinson's disease reconsidered". *Mov Disord.* 2006 Dec;21(12):2042-51.
- Breckenridge CG, Hoff HE. "Pontine and medullary regulation of respiration in the cat". *Am J Physiol.* 1950 Feb;160(2):385-94.
- Brewer JM. "Artifact produced in disc electrophoresis by ammonium persulfate". *Science.* 1967 Apr 14;156(3772):256-7.
- Brooks AI, Chadwick CA, Gelbard HA, Cory-Slechta DA, Federoff HJ. "Paraquat elicited neurobehavioral syndrome caused by dopaminergic neuron loss". *Brain Res.* 1999 Mar 27;823(1-2):1-10.
- Brown K, Xie S, Qiu X, Mohrin M, Shin J, Liu Y, Zhang D, Scadden DT, Chen D. "SIRT3 reverses aging-associated degeneration". *Cell Rep.* 2013 Feb 21;3(2):319-27.
- Brumlik J, Boshes B. "The mechanism of bradykinesia in parkinsonism". *Neurology.* 1966 Apr;16(4):337-44.
- Budayeva HG, Cristea IM. "Human Sirtuin 2 Localization, Transient Interactions, and Impact on the Proteome Point to Its Role in Intracellular Trafficking". *Mol Cell Proteomics.* 2016 Oct;15(10):3107-3125.
- Buhmann C, Arlt S, Kontush A, Möller-Bertram T, Sperber S, Oechsner M, Stuerenburg HJ, Beisiegel U. "Plasma and CSF markers of oxidative stress are increased in Parkinson's disease and influenced by antiparkinsonian medication". *Neurobiol Dis.* 2004 Feb;15(1):160-70.
- Bunyan J, Green J, Murrell EA, Diplock AT, Cawthorne MA. "On the postulated peroxidation of unsaturated lipids in the tissues of vitamin E-deficient rats". *Br J Nutr.* 1968 Feb;22(1):97-110.
- Burmester T, Weich B, Reinhardt S, Hankeln T. "A vertebrate globin expressed in the brain". *Nature.* 2000 Sep 28;407(6803):520-3.

- Burmester T, Hankeln T. "What is the function of neuroglobin?". *J Exp Biol.* 2009 May;212(Pt 10):1423-8.
- Burré J, Sharma M, Tsetsenis T, Buchman V, Etherton MR, Südhof TC. "Alpha-synuclein promotes SNARE-complex assembly in vivo and in vitro". *Science.* 2010 Sep 24;329(5999):1663-7.
- Burton JL, Cartlidge M, Cartlidge NE, Shuster S. "Sebum excretion in Parkinsonism". *Br J Dermatol.* 1973 Mar;88(3):263-6.
- Bus JS, Gibson JE. "Paraquat: model for oxidant-initiated toxicity". *Environ Health Perspect.* 1984 Apr;55:37-46.
- Byun SK, An TH, Son MJ, Lee DS, Kang HS¹, Lee EW, Han BS, Kim WK, Bae KH, Oh KJ, Lee SC. "HDAC11 Inhibits Myoblast Differentiation through Repression of MyoD-Dependent Transcription". *Mol Cells.* 2017 Sep 30;40(9):667-676.
- Caboni P, Sherer TB, Zhang N, Taylor G, Na HM, Greenamyre JT, Casida JE. "Rotenone, deguelin, their metabolites, and the rat model of Parkinson's disease". *Chem Res Toxicol.* 2004 Nov;17(11):1540-8.
- Calderón-Garcidueñas L, Azzarelli B, Acuna H, Garcia R, Gambling TM, Osnaya N, Monroy S, DEL Tizapantzi MR, Carson JL, Villarreal-Calderon A, Rewcastle B. "Air pollution and brain damage". *Toxicol Pathol.* 2002 May-Jun;30(3):373-89.
- Calderón-Garcidueñas L, Solt AC, Henríquez-Roldán C, Torres-Jardón R, Nuse B, Herritt L, Villarreal-Calderón R, Osnaya N, Stone I, García R, Brooks DM, González-Maciel A, Reynoso-Robles R, Delgado-Chávez R, Reed W. "Long-term air pollution exposure is associated with neuroinflammation, an altered innate immune response, disruption of the blood-brain barrier, ultrafine particulate deposition, and accumulation of amyloid beta-42 and alpha-synuclein in children and young adults". *Toxicol Pathol.* 2008 Feb;36(2):289-310.
- Chandler SP, Guschin D, Landsberger N, Wolffe AP. "The methyl-CpG binding transcriptional repressor MeCP2 stably associates with nucleosomal DNA". *Biochemistry.* 1999 Jun 1;38(22):7008-18.

- Chang GG, Tong L. "Structure and function of malic enzymes, a new class of oxidative decarboxylases". *Biochemistry*. 2003 Nov 11;42(44):12721-33.
- Charcot JM, Freud S. "Neue Vorlesungen über die Krankheiten des Nervensystems". Toeplitz & Deuticke. 1886.
- Chattopadhyay S, Datta SK, Mahato SB. "Production of L-DOPA from cell suspension culture of *Mucuna pruriens* f. *pruriens*". *Plant Cell Rep*. 1994 Jun;13(9):519-22.
- Chawla S, Vanhoutte P, Arnold FJ, Huang CL, Bading H. "Neuronal activity-dependent nucleocytoplasmic shuttling of HDAC4 and HDAC5". *J Neurochem*. 2003 Apr;85(1):151-9.
- Chen D, Ma H, Hong H, Koh SS, Huang SM, Schurter BT, Aswad DW, Stallcup MR. "Regulation of transcription by a protein methyltransferase". *Science*. 1999 Jun 25;284(5423):2174-7.
- Chen H, Dzitoyeva S, Manev H. "Effect of aging on 5-hydroxymethylcytosine in the mouse hippocampus". *Restor Neurol Neurosci*. 2012;30(3):237-45.
- Chen T, Ueda Y, Dodge JE, Wang Z, Li E. "Establishment and maintenance of genomic methylation patterns in mouse embryonic stem cells by Dnmt3a and Dnmt3b". *Mol Cell Biol*. 2003 Aug;23(16):5594-605.
- Chen X, Xiao Y, Wei L, Wu Y, Lu J, Guo W, Huang S, Zhou M, Mo M, Li Z, Cen L, Li S, Yang C, Wu Z, Hu S, Pei Z, Yang X, Qu S, Xu P. "Association of DNMT3b gene variants with sporadic Parkinson's disease in a Chinese Han population". *J Gene Med*. 2017 Nov;19(11):360-365.
- Chestnut BA, Chang Q, Price A, Lesuisse C, Wong M, Martin LJ. "Epigenetic regulation of motor neuron cell death through DNA methylation". *J Neurosci*. 2011 Nov 16;31(46):16619-36.
- Christophorou MA, Castelo-Branco G, Halley-Stott RP, Oliveira CS, Loos R, Radzisheuskaya A, Mowen KA, Bertone P, Silva JC, Zernicka-Goetz M, Nielsen ML, Gurdon JB, Kouzarides T. "Citrullination regulates pluripotency and histone H1 binding to chromatin". *Nature*. 2014 Mar 6;507(7490):104-8.

- Chu NS, Bloom FE. "Activity patterns of catecholamine-containing pontine neurons in the dorso-lateral tegmentum of unrestrained cats". *J Neurobiol.* 1974;5(6):527-44.
- Cimmino L, Abdel-Wahab O, Levine RL, Aifantis I. "TET family proteins and their role in stem cell differentiation and transformation". *Cell Stem Cell.* 2011 Sep 2;9(3):193-204.
- Cohet Y. "Epigenetic influences on the lifespan of the *Drosophila*: existence of an optimal growth temperature for adult longevity". *Exp Gerontol.* 1975 Aug;10(3-4):181-4.
- Collman JP, Berg KE, Sunderland CJ, Aukauloo A, Vance MA, Solomon EI. "Distal metal effects in cobalt porphyrins related to CcO". *Inorg Chem.* 2002 Dec 16;41(25):6583-96.
- Cotzias GC. "L-Dopa for Parkinsonism". *N Engl J Med.* 1968 Mar 14;278(11):630.
- Courtiol E, Wilson DA. "The Olfactory Mosaic: Bringing an Olfactory Network Together for Odor Perception" . *Perception.* 2017 Mar-Apr;46(3-4):320-332.
- Court of first instance of the european union. "The court of first instance annuls the directive authorizing paraquat as an active plant protection substance". 2007 Press releases No° 45/07.
- Covey MV, Murphy MP, Hobbs CE, Smith RA, Oorschot DE. "Effect of the mitochondrial antioxidant, Mito Vitamin E, on hypoxic-ischemic striatal injury in neonatal rats: a dose-response and stereological study". *Exp Neurol.* 2006 Jun;199(2):513-9.
- Cox D, Ecroyd H. "The small heat shock proteins α B-crystallin (HSPB5) and Hsp27 (HSPB1) inhibit the intracellular aggregation of α -synuclein". *Cell Stress Chaperones* 2017 Jul;22(4): 589–600.
- Coxon RV, Liebecq C, Peters RA. "The pyruvate-oxidase system in brain and the tricarboxylic acid cycle". *Biochem J.* 1949;45(3):320-5.
- Cragg BG. "Responses of the hippocampus to stimulation of the olfactory bulb and of various afferent nerves in five mammals". *Exp Neurol.* 1960 Oct;2:547-72.

- Csibi A, Fendt SM, Li C, Poulogiannis G, Choo AY, Chapski DJ, Jeong SM, Dempsey JM, Parkhitko A, Morrison T, Henske EP, Haigis MC, Cantley LC, Stephanopoulos G, Yu J, Blenis J. “The mTORC1 pathway stimulates glutamine metabolism and cell proliferation by repressing SIRT4”. *Cell*. 2013 May 9;153(4):840-54.
- Curtius HC, Wolhensberger M, Steinmann B, Redweik S. “Mass fragmentography of dopamine and 6-OH-dopamine. Application to the determination of dopamine in human brain biopsies from the caudate nucleus”. *J Chromatogr*. 1974 99 529–540.
- Cutler RG, Rodriguez H. “Critical Reviews of Oxidative Stress and Aging: Advances in Basic Science, Diagnostics and Intervention”. Volume 2 Hackensack, NJ: World Scientific Publishing, 2003
- da Fonseca AC, Matias D, Garcia C, Amaral R, Geraldo LH, Freitas C, Lima FR. “The impact of microglial activation on blood-brain barrier in brain diseases”. *Front Cell Neurosci*. 2014 Nov 3;8:362.
- Davey WP. “On the decomposition of H₂O₂”. *Science*. 1925 Apr 10;61(1580):388-9.
- Davis GC, Williams AC, Markey SP, Ebert MH, Caine ED, Reichert CM, Kopin IJ. “Chronic Parkinsonism secondary to intravenous injection of meperidine analogues”. *Psychiatry Res*. 1979 Dec;1(3):249-54.
- Deas E, Cremades N, Angelova PR, Ludtmann MH, Yao Z, Chen S, Horrocks MH, Banushi B, Little D, Devine MJ, Gissen P, Klenerman D, Dobson CM, Wood NW, Gandhi S, Abramov AY. “Alpha-Synuclein Oligomers Interact with Metal Ions to Induce Oxidative Stress and Neuronal Death in Parkinson's Disease”. *Antioxid Redox Signal*. 2016 Mar 1;24(7):376-91.
- De Marinis M, Stocchi F, Testa SR, De Pandis F, Agnoli A. “Alterations of thermoregulation in Parkinson's disease”. *Funct Neurol*. 1991 Jul-Sep;6(3):279-83.
- Deng H, Wang P, Jankovic J. “The genetics of Parkinson disease”. *Ageing Res Rev*. 2018 Mar;42:72-85.

- Desplats P, Spencer B, Coffee E, Patel P, Michael S, Patrick C, Adame A, Rockenstein E, Masliah E. "Alpha-synuclein sequesters Dnmt1 from the nucleus: a novel mechanism for epigenetic alterations in Lewy body diseases". *J Biol Chem*. 2011 Mar 18;286(11):9031-7.
- Dhalluin C, Carlson JE, Zeng L, He C, Aggarwal AK, Zhou MM. "Structure and ligand of a histone acetyltransferase bromodomain". *Nature*. 1999 Jun 3;399(6735):491-6.
- Dick FD, De Palma G, Ahmadi A, Scott NW, Prescott GJ, Bennett J, Semple S, Dick S, Counsell C, Mozzoni P, Haites N, Wettinger SB, Mutti A, Otelea M, Seaton A, Söderkvist P, Felice A; Geoparkinson study group. "Environmental risk factors for Parkinson's disease and parkinsonism: the Geoparkinson study". *Occup Environ Med*. 2007 Oct;64(10):666-72.
- Dobbin MM, Madabhushi R, Pan L, Chen Y, Kim D, Gao J, Ahanonu B, Pao PC, Qiu Y, Zhao Y, Tsai LH. "SIRT1 collaborates with ATM and HDAC1 to maintain genomic stability in neurons". *Nat Neurosci*. 2013 Aug;16(8):1008-15.
- Dobretsov GE, Borschevskaya TA, Petrov VA, Vladimirov YA. "The increase of phospholipid bilayer rigidity after lipid peroxidation". *FEBS Lett*. 1977 Dec 1;84(1):125-8.
- Doi M, Hirayama J, Sassone-Corsi P. "Circadian regulator CLOCK is a histone acetyltransferase". *Cell*. 2006 May 5;125(3):497-508.
- Doughan AK, Dikalov SI. "Mitochondrial redox cycling of mitoquinone leads to superoxide production and cellular apoptosis". *Antioxid Redox Signal*. 2007 Nov;9(11):1825-36.
- Downs JA, Lowndes NF, Jackson SP. "A role for *Saccharomyces cerevisiae* histone H2A in DNA repair". *Nature*. 2000 Dec 21-28;408(6815):1001-4.
- Duce JA, Smith DP, Blake RE, Crouch PJ, Li QX, Masters CL, Trounce IA. "Linker histone H1 binds to disease associated amyloid-like fibrils". *J Mol Biol*. 2006 Aug 18;361(3):493-505.
- Duncan BK, Miller JH. "Mutagenic deamination of cytosine residues in DNA". *Nature*. 1980 Oct 9;287(5782):560-1.

- Ebeling W. "DDT and rotenone used in oil to control the California red scale". *J Econ Entomol.* 1945 Oct;38:556-63.
- Edwards LL, Quigley EM, Pfeiffer RF. "Gastrointestinal dysfunction in Parkinson's disease: frequency and pathophysiology". *Neurology.* 1992 Apr;42(4):726-32.
- Ehrlich M, Gama-Sosa MA, Huang LH, Midgett RM, Kuo KC, McCune RA, Gehrke C. "Amount and distribution of 5-methylcytosine in human DNA from different types of tissues of cells". *Nucleic Acids Res.* 1982 Apr 24;10(8):2709-21.
- Engelender S. "Ubiquitination of alpha-synuclein and autophagy in Parkinson's disease". *Autophagy.* 2008 Apr;4(3):372-4.
- Eskandarian HA, Impens F, Nahori MA, Soubigou G, Coppée JY, Cossart P, Hamon MA. "A role for SIRT2-dependent histone H3K18 deacetylation in bacterial infection". *Science.* 2013 Aug 2;341(6145):1238858.
- Etminan M, Gill SS, Samii A. "Intake of vitamin E, vitamin C, and carotenoids and the risk of Parkinson's disease: a meta-analysis". *Lancet Neurol.* 2005 Jun;4(6):362-5.
- Fahn S. "A pilot trial of high-dose alpha-tocopherol and ascorbate in early Parkinson's disease". *Ann Neurol.* 1992;32 Suppl:S128-32.
- Fearnley JM, Lees AJ. "Ageing and Parkinson's disease: substantia nigra regional selectivity". *Brain.* 1991;114:2283-2301.
- Fenton HJH. "Oxidation of tartaric acid in presence of iron". *J. Chem. Soc.* 1894, Trans. 65 (65): 899-911.
- Fedorow H, Tribl F, Halliday G, Gerlach M, Riederer P, Double KL. "Neuromelanin in human dopamine neurons: comparison with peripheral melanins and relevance to Parkinson's disease". *Prog Neurobiol.* 2005 Feb;75(2):109-24.
- Fernández-Santiago R, Carballo-Carbajal I, Castellano G, Torrent R, Richaud Y, Sánchez-Danés A, Vilarrasa-Blasi R, Sánchez-Pla A, Mosquera JL, Soriano J, López-Barneo J, Canals JM,

- Alberch J, Raya Á, Vila M, Consiglio A, Martín-Subero J, Ezquerra M, Tolosa E. “Aberrant epigenome in iPSC-derived dopaminergic neurons from Parkinson's disease patients“. *EMBO Mol Med.* 2015 Dec;7(12):1529-46.
- Fischle W, Dequiedt F, Fillion M, Hendzel MJ, Voelter W, Verdin E. “Human HDAC7 histone deacetylase activity is associated with HDAC3 in vivo“. *J Biol Chem.* 2001 Sep 21;276(38):35826-35.
- Ford E, Voit R, Liszt G, Magin C, Grummt I, Guarente L. “Mammalian Sir2 homolog SIRT7 is an activator of RNA polymerase I transcription“. *Genes Dev.* 2006 May 1;20(9):1075-80.
- Franco R, Schoneveld O, Georgakilas AG, Panayiotidis MI. “Oxidative stress, DNA methylation and carcinogenesis“. *Cancer Lett.* 2008 Jul 18;266(1):6-11.
- Francois C, Nguyen-Legros J, Percheron G. “Topographical and cytological localization of iron in rat and monkey brains“, *Brain Res.* 1981 Jun 29;215(1-2):317-22.
- Frei B, Kim MC, Ames BN. “Ubiquinol-10 is an effective lipid-soluble antioxidant at physiological concentrations“. *Proc Natl Acad Sci U S A.* 1990 Jun;87(12):4879-83.
- Fu R, Shen Q, Xu P, Luo JJ, Tang Y; “Phagocytosis of microglia in the central nervous system diseases“. *Mol Neurobiol.* 2014 Jun;49(3):1422-34.
- Fuchs J. “Oxidative injury in Dermatopathology“. Springer Verlag Berlin Heidelberg, 1992.
- Fujita H, Oikawa I, Ihara H, Takagi SF. “Centrifugal regulation of olfactory bulb activity as studied by stimulation of the amygdala and the anterior limb of the anterior commissure. *Jpn J Physiol.* 1964 Dec 15;14:615-29.
- Fuks F, Burgers WA, Brehm A, Hughes-Davies L, Kouzarides T. “DNA methyltransferase Dnmt1 associates with histone deacetylase activity“. *Nat Genet.* 2000 Jan;24(1):88-91.
- Futami K, Shimamoto A, Furuichi Y. “Mitochondrial and nuclear localization of human Pif1 helicase“. *Biol Pharm Bull.* 2007 Sep;30(9):1685-92.

- Gao L, Cueto MA, Asselbergs F, Atadja P. "Cloning and functional characterization of HDAC11, a novel member of the human histone deacetylase family". *J Biol Chem*. 2002 Jul 12;277(28):25748-55.
- Galenus A, Durling RJ. "Galenus Latinus". Stuttgart: Steiner 1976.
- García Ruiz PJ. "Prehistory of Parkinson's disease". *Neurologia*. 2004 Dec;19(10):735-7.
- Gayatri S, Bedford MT. "Readers of histone methylarginine marks". *Biochim Biophys Acta*. 2014 Aug;1839(8):702-10.
- Gellert M, Lipsett MN, Davies DR. "Helix formation by guanylic acid". *Proc Natl Acad Sci U S A*. 1962 Dec 15;48:2013-8.
- Geraghty AA, Lindsay KL, Alberdi G, McAuliffe FM, Gibney ER. "Nutrition During Pregnancy Impacts Offspring's Epigenetic Status-Evidence from Human and Animal Studies". *Nutr Metab Insights*. 2016 Feb 16;8(Suppl 1):41-7.
- Gerashchenko D, Blanco-Centurion CA, Miller JD, Shiromani PJ. "Insomnia following hypocretin2-saporin lesions of the substantia nigra". *Neuroscience*. 2006;137(1):29-36.
- Gerstenbrand F, Prosenz P. "[On the treatment of Parkinson's syndrome with monoamine oxidase inhibitors alone and in combination with L-dopa]". *Praxis*. 1965 Nov 18;54(46):1373-7.
- Ghelli A, Benelli B, Esposti MD. "Measurement of the membrane potential generated by complex I in submitochondrial particles". *J Biochem*. 1997 Apr;121(4):746-55.
- Ghosh A, Chandran K, Kalivendi SV, Joseph J, Antholine WE, Hillard CJ, Kanthasamy A, Kanthasamy A, Kalyanaraman B. "Neuroprotection by a mitochondria-targeted drug in a Parkinson's disease model". *Free Radic Biol Med*. 2010 Dec 1;49(11):1674-84.
- Gilbert N, Boyle S, Sutherland H, de Las Heras J, Allan J, Jenuwein T, Bickmore WA. "Formation of facultative heterochromatin in the absence of HP1". *EMBO J*. 2003 Oct 15;22(20):5540-50.

- Giordano S, Lee J, Darley-USmar VM, Zhang J. "Distinct effects of rotenone, 1-methyl-4-phenylpyridinium and 6-hydroxydopamine on cellular bioenergetics and cell death". *PLoS One*. 2012;7(9):e44610.
- Goldman JE, Yen SH, Chiu FC, Peress NS. "Lewy bodies of Parkinson's disease contain neurofilament antigens". *Science*. 1983 Sep 9;221(4615):1082-4.
- Graham DG. "Oxidative pathways for catecholamines in the genesis of neuromelanin and cytotoxic quinones". *Mol Pharmacol*. 1978 Jul;14(4):633-43.
- Grant PA, Eberharter A, John S, Cook RG, Turner BM, Workman JL. "Expanded lysine acetylation specificity of Gcn5 in native complexes". *J Biol Chem*. 1999 Feb 26;274(9):5895-900.
- Greenwalt JW, Schnaitman C. "An appraisal of the use of monoamine oxidase as an enzyme marker for the outer mitochondrial membrane". *J. Cell. Biol.*, 46 (1970) 173-179.
- Gu H, Liang Y, Mandel G, Roizman B. "Components of the REST/CoREST/histone deacetylase repressor complex are disrupted, modified, and translocated in HSV-1-infected cells". *Proc Natl Acad Sci U S A*. 2005 May 24;102(21):7571-6.
- Guaiquil VH, Vera JC, Golde DW. "Mechanism of vitamin C inhibition of cell death induced by oxidative stress in glutathione-depleted HL-60 cells". *J Biol Chem*. 2001 Nov 2;276(44):40955-61.
- Gundersen V. "Protein aggregation in Parkinson's disease". *Acta Neurol Scand Suppl*. 2010; (190):82-7.
- Gurgueira SA, Lawrence J, Coull B, Murthy GG, González-Flecha B. "Rapid increases in the steady-state concentration of reactive oxygen species in the lungs and heart after particulate air pollution inhalation". *Environ Health Perspect*. 2002 Aug;110(8):749-55.
- Gutman J, Leibowitz U, Bergmann F. "Effect of brain stem transections on blood pressure responses to medullary stimulation". *Arch Int Physiol Biochim*. 1962 Dec;70:671-81.

- Gutteridge JM. "Antioxidant properties of caeruloplasmin towards iron- and copper-dependent oxygen radical formation". FEBS Lett. 1983 Jun 27;157(1):37-40.
- Gutteridge JM. "Lipid peroxidation initiated by superoxide-dependent hydroxyl radicals using complexed iron and hydrogen peroxide". FEBS Lett. 1984 Jul 9;172(2):245-9.
- Haavik J, Toska K. "Tyrosine hydroxylase and Parkinson's disease". Mol Neurobiol. 1998 Jun;16(3):285-309.
- Haber S. "Perspective on basal ganglia connections as described by Nauta and Mehler in 1966: Where we were and how this paper effected where we are now". Brain Res. 2016 Aug 15;1645:4-7.
- Hachiya N, Mihara K, Suda K, Horst M, Schatz G, Lithgow T. "Reconstitution of the initial steps of mitochondrial protein import". Nature. 1995 Aug 24;376(6542):705-9.
- Hagiwara T, Nakashima K, Hirano H, Senshu T, Yamada M. "Deimination of arginine residues in nucleophosmin/B23 and histones in HL-60 granulocytes". Biochem Biophys Res Commun. 2002 Jan 25;290(3):979-83.
- Haigis MC, Mostoslavsky R, Haigis KM, Fahie K, Christodoulou DC, Murphy AJ, Valenzuela DM, Yancopoulos GD, Karow M, Blander G, Wolberger C, Prolla TA, Weindruch R, Alt FW, Guarente L. "SIRT4 inhibits glutamate dehydrogenase and opposes the effects of calorie restriction in pancreatic beta cells". Cell. 2006 Sep 8;126(5):941-54.
- Hajieva P, Mocko JB, Moosmann B, Behl C. "Novel imine antioxidants at low nanomolar concentrations protect dopaminergic cells from oxidative neurotoxicity". J Neurochem. 2009 Jul;110(1):118-32.
- Halliwell B, Foyer CH. "Ascorbic acid, metal ions and the superoxide radical". Biochem J. 1976 Jun 1;155(3):697-700.
- Halliwell B, Gutteridge JMC. "Free Radicals in Biology and Medicine". Oxford University Press, Oxford, 1999.

- Hanson LR, Frey WH 2nd. “Intranasal delivery bypasses the blood-brain barrier to target therapeutic agents to the central nervous system and treat neurodegenerative disease”. *BMC Neurosci.* 2008 Dec 10;9 Suppl 3:S5.
- Hardie DG, Pan DA. “Regulation of fatty acid synthesis and oxidation by the AMP-activated protein kinase”. *Biochem Soc Trans.* 2002 Nov;30(Pt 6):1064-70.
- Harman D. “Origin and evolution of the free radical theory of aging: a brief personal history, 1954–2009”. *Biogerontology.* 2009 Dec;10(6):773-81.
- Harrison JE, Schultz J. “Studies on the chlorinating activity of myeloperoxidase”. *J Biol Chem.* 1976 Mar 10;251(5):1371-4.
- Harrison RM, Jones M. “The chemical-composition of airborne particles in the uk atmosphere”. *Sci Total Environ* 1995;168:195-214. *FEBS Lett.* 1983 Jun 27;157(1):37-40.
- Hata K, Okano M, Lei H, Li E. “Dnmt3L cooperates with the Dnmt3 family of de novo DNA methyltransferases to establish maternal imprints in mice“. *Development.* 2002 Apr;129(8):1983-93.
- Haynes CM, Titus EA, Cooper AA. “Degradation of misfolded proteins prevents ER-derived oxidative stress and cell death”. *Mol Cell.* 2004 Sep 10;15(5):767-76.
- He YF, Li BZ, Li Z, Liu P, Wang Y, Tang Q, Ding J, Jia Y, Chen Z, Li L, Sun Y, Li X, Dai Q, Song CX, Zhang K, He C, Xu GL. “Tet-mediated formation of 5-carboxylcytosine and its excision by TDG in mammalian DNA“. *Science.* 2011 Sep 2;333(6047):1303-7.
- Heikkila RE, Manzino L. “Ascorbic acid, redox cycling, lipid peroxidation, and the binding of dopamine receptor antagonists”. *Ann N Y Acad Sci.* 1987;498:63-76.
- Henchcliffe C, Beal MF. “Mitochondrial biology and oxidative stress in Parkinson disease pathogenesis”. *Nat Clin Pract Neurol.* 2008 Nov;4(11):600-9.
- Herrero MT, Hirsch EC, Kastner A, Luquin MR, Javoy-Agid F, Gonzalo LM, Obeso JA, Agid Y. “Neuromelanin accumulation with age in catecholaminergic neurons from Macaca

- fascicularis brainstem". *Dev Neurosci.* 1993;15(1):37-48.
- Hunot S, Hirsch EC. "Neuroinflammatory processes in Parkinson's disease." *Ann Neurol.* 2003;53 Suppl 3:S49-58; discussion S58-60.
- Hoffman PN, Lasek RJ. "The slow component of axonal transport. Identification of major structural polypeptides of the axon and their generality among mammalian neurons". *J Cell Biol.* 1975 Aug;66(2):351-66.
- Hogarth LA, Redfern CP, Teodoridis JM, Hall AG, Anderson H, Case MC, Coulthard SA. "The effect of thiopurine drugs on DNA methylation in relation to TPMT expression". *Biochem Pharmacol.* 2008 Oct 15;76(8):1024-35.
- Horgan DJ, Singer TP. "Reaction sites of rotenone in the respiratory chain and in soluble DPNH-coenzyme Q reductase". *Biochem Biophys Res Commun.* 1967 May 5;27(3):356-60.
- Hornykiewicz O, Kish SJ. "Biochemical pathophysiology of Parkinson's disease", *Adv Neurol.* 1987;45:19-34.
- Horvath TL, Diano S, Leranath C, Garcia-Segura LM, Cowley MA, Shanabrough M, Elsworth JD, Sotonyi P, Roth RH, Dietrich EH, Matthews RT, Barnstable CJ, Redmond DE Jr. "Coenzyme Q induces nigral mitochondrial uncoupling and prevents dopamine cell loss in a primate model of Parkinson's disease". *Endocrinology.* 2003 Jul;144(7):2757-60.
- Hotchkiss RD. "The quantitative separation of purines, pyrimidines, and nucleosides by paper chromatography". *J Biol Chem.* 1948 Aug;175(1):315-32.
- Hou X, Xu S, Maitland-Toolan KA, Sato K, Jiang B, Ido Y, Lan F, Walsh K, Wierzbicki M, Verbeuren TJ, Cohen RA, Zang M. "SIRT1 regulates hepatocyte lipid metabolism through activating AMP-activated protein kinase". *J Biol Chem.* 2008 Jul 18;283(29):20015-26.
- Howitz KT, Bitterman KJ, Cohen HY, Lamming DW, Lavu S, Wood JG, Zipkin RE, Chung P, Kisielewski A, Zhang LL, Scherer B, Sinclair DA. "Small molecule activators of sirtuins extend *Saccharomyces cerevisiae* lifespan". *Nature.* 2003 Sep 11;425(6954):191-6.

- Hsu TC. "Differential rate in RNA synthesis between euchromatin and heterochromatin". *Exp Cell Res.* 1962 Aug;27:332-4.
- Huang R, Xu Y, Wan W, Shou X, Qian J, You Z, Liu B, Chang C, Zhou T, Lippincott-Schwartz J, Liu W. "Deacetylation of nuclear LC3 drives autophagy initiation under starvation". *Mol Cell.* 2015 Feb 5;57(3):456-66.
- Imai S, Armstrong CM, Kaeberlein M, Guarente L. "Transcriptional silencing and longevity protein Sir2 is an NAD-dependent histone deacetylase". *Nature.* 2000 Feb 17;403(6771):795-800.
- Inoki K, Zhu T, Guan KL. "TSC2 mediates cellular energy response to control cell growth and survival". *Cell.* 2003 Nov 26;115(5):577-90.
- Ishizawa T, Mattila P, Davies P, Wang D, Dickson DW. "Colocalization of tau and alpha-synuclein epitopes in Lewy bodies". *J Neuropathol Exp Neurol.* 2003 Apr;62(4):389-97.
- Ito S, Shen L, Dai Q, Wu SC, Collins LB, Swenberg JA, He C, Zhang Y. "Tet proteins can convert 5-methylcytosine to 5-formylcytosine and 5-carboxylcytosine". *Science.* 2011 Sep 2;333(6047):1300-3.
- Ivannikov MV, Sugimori M, Llinás RR. "Calcium clearance and its energy requirements in cerebellar neurons", *Cell Calcium.* 2010 Jun;47(6):507-13.
- Iwahara T, Bonasio R, Narendra V, Reinberg D. "SIRT3 functions in the nucleus in the control of stress-related gene expression". *Mol Cell Biol.* 2012 Dec;32(24):5022-34.
- Iyer LM, Tahiliani M, Rao A, Aravind L. "Prediction of novel families of enzymes involved in oxidative and other complex modifications of bases in nucleic acids". *Cell Cycle.* 2009 Jun 1;8(11):1698-710.
- Jackson M, Krassowska A, Gilbert N, Chevassut T, Forrester L, Ansell J, Ramsahoye B. "Severe global DNA hypomethylation blocks differentiation and induces histone hyperacetylation in embryonic stem cells". *Mol Cell Biol.* 2004 Oct;24(20):8862-71.

- Jacquet K, Fradet-Turcotte A, Avvakumov N, Lambert JP, Roques C, Pandita RK, Paquet E, Herst P, Gingras AC, Pandita TK, Legube G, Doyon Y, Durocher D, Côté J. “The TIP60 Complex Regulates Bivalent Chromatin Recognition by 53BP1 through Direct H4K20me Binding and H2AK15 Acetylation”. *Mol Cell*. 2016 May 5;62(3):409-421.
- Jahanshahi M, Jones CR, Dirnberger G, Frith CD. “The substantia nigra pars compacta and temporal processing”. *J Neurosci*. 2006 Nov 22;26(47):12266-73.
- James AM, Cochemé HM, Smith RA, Murphy MP. “Interactions of mitochondria-targeted and untargeted ubiquinones with the mitochondrial respiratory chain and reactive oxygen species. Implications for the use of exogenous ubiquinones as therapies and experimental tools”. *J Biol Chem*. 2005 Jun 3;280(22):21295-312.
- Jellinger KA. “Neuropathology of sporadic Parkinson's disease: evaluation and changes of concepts”. *Mov Disord*. 2012 Jan;27(1):8-30.
- Jenner P, Olanow CW. “Oxidative stress and the pathogenesis of Parkinson's disease”. *Neurology*. 1996 Dec;47(6 Suppl 3):S161-70.
- Jeziorska DM, Murray RJS, De Gobbi M, Gaentzsch R, Garrick D, Ayyub H, Chen T, Li E, Telenius J, Lynch M, Graham B, Smith AJH, Lund JN, Hughes JR, Higgs DR, Tufarelli C. “DNA methylation of intragenic CpG islands depends on their transcriptional activity during differentiation and disease”. *Proc Natl Acad Sci U S A*. 2017 Sep 5;114(36):E7526-E7535.
- Jin YH, Kim YJ, Kim DW, Baek KH, Kang BY, Yeo CY, Lee KY. “Sirt2 interacts with 14-3-3 beta/gamma and down-regulates the activity of p53”. *Biochem Biophys Res Commun*. 2008 Apr 11;368(3):690-5.
- Johnson CA, White DA, Lavender JS, O'Neill LP, Turner BM. “Human class I histone deacetylase complexes show enhanced catalytic activity in the presence of ATP and co-immunoprecipitate with the ATP-dependent chaperone protein Hsp70”. *J Biol Chem*. 2002 Mar 15;277(11):9590-7.

- Johnson JD, Muhonen WW, Lambeth DO. "Characterization of the ATP- and GTP-specific succinyl-CoA synthetases in pigeon. The enzymes incorporate the same alpha-subunit". *J Biol Chem*. 1998 Oct 16;273(42):27573-9.
- Jowaed A, Schmitt I, Kaut O, Wüllner U. "Methylation regulates alpha-synuclein expression and is decreased in Parkinson's disease patients' brains". *J Neurosci*. 2010 May 5;30(18):6355-9.
- Kaeberlein M, McVey M, Guarente L. "The SIR2/3/4 complex and SIR2 alone promote longevity in *Saccharomyces cerevisiae* by two different mechanisms". *Genes Dev*. 1999 Oct 1;13(19):2570-80.
- Kageyama T, Nakamura M, Matsuo A, Yamasaki Y, Takakura Y, Hashida M, Kanai Y, Naito M, Tsuruo T, Minato N, Shimohama S. "The 4F2hc/LAT1 complex transports L-DOPA across the blood-brain barrier". *Brain Res*. 2000 Oct 6;879(1-2):115-21.
- Kaneta H, Fujimoto D. "A histone deacetylase capable of deacetylating chromatin-bound histone". *J Biochem*. 1974 Oct;76(4):905-7.
- Kao HY, Lee CH, Komarov A, Han CC, Evans RM. "Isolation and characterization of mammalian HDAC10, a novel histone deacetylase". *J Biol Chem*. 2002 Jan 4;277(1):187-93.
- Karmodiya K, Krebs AR, Oulad-Abdelghani M, Kimura H, Tora L. "H3K9 and H3K14 acetylation co-occur at many gene regulatory elements, while H3K14ac marks a subset of inactive inducible promoters in mouse embryonic stem cells". *BMC Genomics*. 2012 Aug 24;13:424.
- Kashiwagi K, Nimura K, Ura K, Kaneda Y. "DNA methyltransferase 3b preferentially associates with condensed chromatin". *Nucleic Acids Res*. 2011 Feb;39(3):874-88.
- Kašuba V, Milić M, Rozgaj R, Kopjar N, Mladinić M, Žunec S, Vrdoljak AL, Pavičić I, Čermak AMM, Pizent A, Lovaković BT, Želježić D. "Effects of low doses of glyphosate on DNA damage, cell proliferation and oxidative stress in the HepG2 cell line". *Environ Sci Pollut Res Int*. 2017 Aug;24(23):19267-19281.
- Kato Y, Kato T, Ono T, Susa T, Kitahara K, Matsumoto K. "Intracellular localization of porcine single-strand binding protein 2". *J Cell Biochem*. 2009 Apr 1;106(5):912-9.

- Kaut O, Schmitt I, Wüllner U. "Genome-scale methylation analysis of Parkinson's disease patients' brains reveals DNA hypomethylation and increased mRNA expression of cytochrome P450 2E1". *Neurogenetics*. 2012 Feb;13(1):87-91.
- Kawaguchi Y, Kovacs JJ, McLaurin A, Vance JM, Ito A, Yao TP. "The deacetylase HDAC6 regulates aggresome formation and cell viability in response to misfolded protein stress". *Cell*. 2003 Dec 12;115(6):727-38.
- Kawasaki H, Schiltz L, Chiu R, Itakura K, Taira K, Nakatani Y, Yokoyama KK. "ATF-2 has intrinsic histone acetyltransferase activity which is modulated by phosphorylation". *Nature*. 2000 May 11;405(6783):195-200.
- Kearney TR. "Parkinson's disease presenting as depressive illness". *J Ir Med Assoc*. 1964 Apr;54:117-9.
- Kelly RDW, Chandru A, Watson PJ, Song Y, Blades M, Robertson NS, Jamieson AG, Schwabe JWR, Cowley SM. "Histone deacetylase (HDAC) 1 and 2 complexes regulate both histone acetylation and crotonylation in vivo". *Sci Rep*. 2018 Oct 2;8(1):14690.
- Kelso GF, Porteous CM, Coulter CV, Hughes G, Porteous WK, Ledgerwood EC, Smith RA, Murphy MP. "Selective targeting of a redox-active ubiquinone to mitochondria within cells: antioxidant and antiapoptotic properties". *J Biol Chem*. 2001 Feb 16;276(7):4588-96.
- Kimura S, Noda T, Yoshimori T. "Dissection of the autophagosome maturation process by a novel reporter protein, tandem fluorescent-tagged LC3". *Autophagy*. 2007 Sep-Oct;3(5):452-60.
- Kiran S, Chatterjee N, Singh S, Kaul SC, Wadhwa R, Ramakrishna G. "Intracellular distribution of human SIRT7 and mapping of the nuclear/nucleolar localization signal. *FEBS J*. 2013 Jul;280(14):3451-66.
- Kitayama S, Wang JB, Uhl GR. "Dopamine transporter mutants selectively enhance MPP+ transport". *Synapse*. 1993 Sep;15(1):58-62.

- Klein BJ, Simithy J, Wang X, Ahn J, Andrews FH, Zhang Y, Côté J, Shi X, Garcia BA, Kutateladze TG. "Recognition of Histone H3K14 Acylation by MORF". *Structure*. 2017 Apr 4;25(4):650-654.e2.
- Klein C, Westenberger A. "Genetics of Parkinson's Disease". *Cold Spring Harb Perspect Med*. 2012 Jan; 2(1): a008888.
- Knoop F. "Der Abbau aromatischer Fettsäuren im Tierkörper". *Beitr Chem Physiol Pathol*. 1904;6:150–162.
- Koller W, O'Hara R, Weiner W, Lang A, Nutt J, Agid Y, Bonnet AM, Jankovic J. "Relationship of aging to Parkinson's disease". *Adv Neurol*. 1987;45:317-21.
- Kornberg RD. "Chromatin structure: a repeating unit of histones and DNA". *Science*. 1974 May 24;184(4139):868-71.
- Koutnikova H, Campuzano V, Koenig M. "Maturation of wild-type and mutated frataxin by the mitochondrial processing peptidase". *Hum Mol Genet*. 1998 Sep;7(9):1485-9.
- Kowall NW, Hantraye P, Brouillet E, Beal MF, McKee AC, Ferrante RJ. "MPTP induces alpha-synuclein aggregation in the substantia nigra of baboons". *Neuroreport*. 2000 Jan 17;11(1):211-3.
- Krebs HA, Henseleit K. "Untersuchungen über die Harnstoffbildung in Tierkörpern". *Z. Physiol. Chem.*, 210: 33, 1932
- Krebs HA, Johnson WA. "Metabolism of ketonic acids in animal tissues". *Biochem J*. 1937 Apr;31(4):645-60.
- Kueh AJ, Dixon MP, Voss AK, Thomas T. "HBO1 is required for H3K14 acetylation and normal transcriptional activity during embryonic development". *Mol Cell Biol*. 2011 Feb;31(4):845-60.

- Kundu S, Stone EA. "Composition and sources of fine particulate matter across urban and rural sites in the Midwestern United States. "Environ Sci Process Impacts. 2014 May;16(6):1360-70.
- Lan F, Cacicedo JM, Ruderman N, Ido Y. "SIRT1 modulation of the acetylation status, cytosolic localization, and activity of LKB1. Possible role in AMP-activated protein kinase activation". J Biol Chem. 2008 Oct 10;283(41):27628-35.
- Lander ES, Linton LM, Birren B, Nusbaum C, Zody MC, Baldwin J, Devon K, Dewar K, Doyle M, FitzHugh W, Funke R, Gage D, Harris K, Heaford A, Howland J, Kann L, Lehoczky J, LeVine R, McEwan P, McKernan K, Meldrim J, Mesirov JP, Miranda C, Morris W, Naylor J, Raymond C, Rosetti M, Santos R, Sheridan A, Sougnez C, Stange-Thomann Y, Stojanovic N et al., "Initial sequencing and analysis of the human genome". Nature. 2001 Feb 15;409(6822):860-921.
- Langston JW, Ballard P, Tetrad JW, Irwin I. "Chronic Parkinsonism in humans due to a product of meperidine-analog synthesis". Science. 1983 Feb 25;219(4587):979-80.
- Langston JW, Langston EB, Irwin I. "MPTP-induced parkinsonism in human and non-human primates--clinical and experimental aspects". Acta Neurol Scand Suppl. 1984;100:49-54.
- Langston JW, Palfreman J. "The Case of the Frozen Addicts: How the Solution of a Medical Mystery Revolutionized the Understanding of Parkinson's Disease". IOS Press 2014.
- Larsen NB, Rasmussen M, Rasmussen LJ. "Nuclear and mitochondrial DNA repair: similar pathways?". Mitochondrion. 2005 Apr;5(2):89-108.
- Lau PN, Cheung P. "Histone code pathway involving H3 S28 phosphorylation and K27 acetylation activates transcription and antagonizes polycomb silencing". Proc Natl Acad Sci U S A. 2011 Feb 15;108(7):2801-6.
- Le Guerroué F, Eck F, Jung J, Starzetz T, Mittelbronn M, Kaulich M, Behrends C. "Autophagosomal Content Profiling Reveals an LC3C-Dependent Piecemeal Mitophagy Pathway". Mol Cell. 2017 Nov 16;68(4):786-796.e6.

- Lehninger AL. "Fatty acid oxidation and the Krebs trocarboxylic acid cycle". *J Biol Chem.* 1945;161:413.
- Leonhardt H, Page AW, Weier HU, Bestor TH. "A targeting sequence directs DNA methyltransferase to sites of DNA replication in mammalian nuclei". *Cell.* 1992 Nov 27;71(5):865-73.
- Lepage GA. "Basic biochemical effects and mechanism of action of 6-thioguanine". *Cancer Res.* 1963 Sep;23:1202-6.
- Lewy FH, Forster E. "Handbuch der Neurologie: Paralysis agitans". Springer Verlag 1912, 920-933.
- Li C, Lan Y, Schwartz-Orbach L, Korol E, Tahiliani M, Evans T, Goll MG. "Overlapping Requirements for Tet2 and Tet3 in Normal Development and Hematopoietic Stem Cell Emergence". *Cell Rep.* 2015 Aug 18;12(7):1133-43.
- Li N, Ragheb K, Lawler G, Sturgis J, Rajwa B, Melendez JA, Robinson JP; "Mitochondrial complex I inhibitor rotenone induces apoptosis through enhancing mitochondrial reactive oxygen species production". *J Biol Chem.* 2003 Mar 7;278(10):8516-25.
- Liang CL, Wang TT, Luby-Phelps K, German DC. "Mitochondria mass is low in mouse substantia nigra dopamine neurons: implications for Parkinson's disease", *Exp Neurol.* 2007 Feb;203(2):370-80.
- Lieberman EA, Topaly VP, Tsofina LM, Jasaitis AA, Skulachev VP. "Mechanism of coupling of oxidative phosphorylation and the membrane potential of mitochondria". *Nature.* 1969 Jun 14;222(5198):1076-8.
- Lin W, Sampathi S, Dai H, Liu C, Zhou M, Hu J, Huang Q, Campbell J, Shin-Ya K, Zheng L, Chai W, Shen B. "Mammalian DNA2 helicase/nuclease cleaves G-quadruplex DNA and is required for telomere integrity". *EMBO J.* 2013 May 15;32(10):1425-39.
- Lister R, Mukamel EA, Nery JR, Urich M, Puddifoot CA, Johnson ND, Lucero J, Huang Y, Dwork AJ, Schultz MD, Yu M, Tonti-Filippini J, Heyn H, Hu S, Wu JC, Rao A, Esteller M, He C, Haghghi FG, Sejnowski TJ, Behrens MM, Ecker JR. "Global epigenomic reconfiguration

- during mammalian brain development“. *Science*. 2013 Aug 9;341(6146):1237905..
- Liszt G, Ford E, Kurtev M, Guarente L. “Mouse Sir2 homolog SIRT6 is a nuclear ADP-ribosyltransferase”. *J Biol Chem*. 2005 Jun 3;280(22):21313-20.
- Liu L, Arun A, Ellis L, Peritore C, Donmez G. “SIRT2 enhances 1-methyl-4-phenyl-1,2,3,6-tetrahydropyridine (MPTP)-induced nigrostriatal damage via apoptotic pathway”. *Front Aging Neurosci*. 2014 Aug 11;6:184.
- Liu L, Nam M, Fan W, Akie TE, Hoaglin DC, Gao G, Keaney JF Jr, Cooper MP. “Nutrient sensing by the mitochondrial transcription machinery dictates oxidative phosphorylation”. *J Clin Invest*. 2014 Feb;124(2):768-84.
- Liu Z, Lenardo MJ. “Reactive oxygen species regulate autophagy through redox-sensitive proteases”. *Dev Cell*. 2007 Apr;12(4):484-5.
- Ljungman M, Hanawalt PC. “Efficient protection against oxidative DNA damage in chromatin“. *Mol Carcinog*. 1992;5(4):264-9.
- Lo WS, Trievel RC, Rojas JR, Duggan L, Hsu JY, Allis CD, Marmorstein R, Berger SL. “Phosphorylation of serine 10 in histone H3 is functionally linked in vitro and in vivo to Gcn5-mediated acetylation at lysine 14“. *Mol Cell*. 2000 Jun;5(6):917-26.
- Loew O. “A new enzyme of general occurrence in organisms”. *Science*. 1900 May 4;11(279):701-2.
- Longo VD, Kennedy BK. “Sirtuins in aging and age-related disease”. *Cell*. 2006 Jul 28;126(2):257-68.
- Lowry OH, Passonneau JV. “The relationships between substrates and enzymes of glycolysis in brain”. *J Biol Chem*. 1964 Jan;239:31-42.
- Lu LY, Wu J, Ye L, Gavrilina GB, Saunders TL, Yu X. “RNF8-dependent histone modifications regulate nucleosome removal during spermatogenesis”. *Dev Cell*. 2010 Mar 16;18(3):371-84.

- Lyon MF. "Gene action in the X-chromosome of the mouse (*Mus musculus* L.)". *Nature*. 1961 Apr 22;190:372-3.
- Maher F, Davies-Hill TM, Lysko PG, Henneberry RC, Simpson IA. "Expression of two glucose transporters, GLUT1 and GLUT3, in cultured cerebellar neurons: Evidence for neuron-specific expression of GLUT3". *Mol Cell Neurosci*. 1991 Aug;2(4):351-60.
- Mailly P, Charpier S, Menetrey A, Deniau JM. "Three-dimensional organization of the recurrent axon collateral network of the substantia nigra pars reticulata neurons in the rat". *J Neurosci*. 2003 Jun 15;23(12):5247-57.
- Maiti A, Drohat AC. "Thymine DNA glycosylase can rapidly excise 5-formylcytosine and 5-carboxylcytosine: potential implications for active demethylation of CpG sites". *J Biol Chem*. 2011 Oct 14;286(41):35334-8.
- Mann A, Tyndale RF. "Cytochrome P450 2D6 enzyme neuroprotects against 1-methyl-4-phenylpyridinium toxicity in SH-SY5Y neuronal cells". *Eur J Neurosci*. 2010 Apr;31(7):1185-93.
- Manning-Bog AB, McCormack AL, Li J, Uversky VN, Fink AL, Di Monte DA. "The herbicide paraquat causes up-regulation and aggregation of alpha-synuclein in mice: paraquat and alpha-synuclein". *J Biol Chem*. 2002 Jan 18;277(3):1641-4.
- Mao Z, Hine C, Tian X, Van Meter M, Au M, Vaidya A, Seluanov A, Gorbunova V. "SIRT6 promotes DNA repair under stress by activating PARP1". *Science*. 2011 Jun 17;332(6036):1443-6.
- Marsden CD, Barry PE, Parkes JD, Zilkha KJ. "Treatment of Parkinson's disease with levodopa combined with L-alpha-methyldopahydrazine, an inhibitor of extracerebral DOPA decarboxylase". *J Neurol Neurosurg Psychiatry*. 1973 Feb;36(1):10-4.
- Marsin AS, Bertrand L, Rider MH, Deprez J, Beauvoys C, Vincent MF, Van den Berghe G, Carling D, Hue L. "Phosphorylation and activation of heart PFK-2 by AMPK has a role in the stimulation of glycolysis during ischaemia". *Curr Biol*. 2000 Oct 19;10(20):1247-55.

- Martin D, Li Y, Yang J, Wang G, Margariti A, Jiang Z, Yu H, Zampetaki A, Hu Y, Xu Q, Zeng L. “Unspliced X-box-binding protein 1 (XBP1) protects endothelial cells from oxidative stress through interaction with histone deacetylase 3”. *J Biol Chem*. 2014 Oct 31;289(44):30625-34.
- Marushige K. “Activation of chromatin by acetylation of histone side chains“. *Proc Natl Acad Sci U S A*. 1976 Nov;73(11):3937-41.
- Masliah E, Dumaop W, Galasko D, Desplats P. “Distinctive patterns of DNA methylation associated with Parkinson disease: identification of concordant epigenetic changes in brain and peripheral blood leukocytes“. *Epigenetics*. 2013 Oct;8(10):1030-8.
- Mateus VL, Gonçalves Monteiro IL, Chávez Rocha RC, Dillenburg Saint'Pierre T, Gioda A; “Study of the chemical composition of particulate matter from the Rio de Janeiro metropolitan region, Brazil, by inductively coupled plasma-mass spectrometry and optical emission spectrometry”. *Spectrochimica Acta Part B: Atomic Spectroscopy* Volume 86, 1 August 2013, Pages 131-136.
- Mathias RA, Greco TM, Oberstein A, Budayeva HG, Chakrabarti R, Rowland EA, Kang Y, Shenk T, Cristea IM. “Sirtuin 4 is a lipoamidase regulating pyruvate dehydrogenase complex activity”. *Cell*. 2014 Dec 18;159(7):1615-25.
- Matsumoto L, Takuma H, Tamaoka A, Kurisaki H, Date H, Tsuji S, Iwata A. “CpG demethylation enhances alpha-synuclein expression and affects the pathogenesis of Parkinson's disease“. *PLoS One*. 2010 Nov 24;5(11):e15522.
- McCord JM, Fridovich I. “Superoxide dismutase. An enzymic function for erythrocyte hemocuprein (hemocuprein)”. *J Biol Chem*. 1969 Nov 25;244(22):6049-55.
- McLeod JG. “Pathophysiology of Parkinson's disease”. *Aust N Z J Med*. 1971 May;1.
- Meyerhof O, Oesper P. “The Mechanism of the Oxidative Reaction in Fermentation.” *J. Biol. Chem.* (1947) 170, 1-22.

- Michishita E, McCord RA, Berber E, Kioi M, Padilla-Nash H, Damian M, Cheung P, Kusumoto R, Kawahara TL, Barrett JC, Chang HY, Bohr VA, Ried T, Gozani O, Chua KF. "SIRT6 is a histone H3 lysine 9 deacetylase that modulates telomeric chromatin". *Nature*. 2008 Mar 27;452(7186):492-6.
- Michishita E, McCord RA, Boxer LD, Barber MF, Hong T, Gozani O, Chua KF. "Cell cycle-dependent deacetylation of telomeric histone H3 lysine K56 by human SIRT6". *Cell Cycle*. 2009 Aug 15;8(16):2664-6.
- Miesel R, Sanocka D, Kurpisz M, Kröger H. "Antiinflammatory effects of NADPH oxidase inhibitors". *Inflammation*. 1995 Jun;19(3):347-62.
- Minczuk M, Piwowarski J, Papworth MA, Awiszus K, Schalinski S, Dziembowski A, Dmochowska A, Bartnik E, Tokatlidis K, Stepień PP, Borowski P. "Localisation of the human hSuv3p helicase in the mitochondrial matrix and its preferential unwinding of dsDNA". *Nucleic Acids Res*. 2002 Dec 1;30(23):5074-86.
- Miska EA, Langley E, Wolf D, Karlsson C, Pines J, Kouzarides T. "Differential localization of HDAC4 orchestrates muscle differentiation". *Nucleic Acids Res*. 2001 Aug 15;29(16):3439-47.
- Mizushima N, Komatsu M. "Autophagy: renovation of cells and tissues". *Cell*. 2011 Nov 11;147(4):728-41.
- Mocko JB, Kern A, Moosmann B, Behl C, Hajjeva P. "Phenothiazines interfere with dopaminergic neurodegeneration in *Caenorhabditis elegans* models of Parkinson's disease". *Neurobiol Dis*. 2010 Oct;40(1):120-9.
- Monk M. "Genomic imprinting. Memories of mother and father". *Nature*. 1987 Jul 1 22;328(6127):203-4.
- Moon Y, Lee KH, Park JH, Geum D, Kim K. "Mitochondrial membrane depolarization and the selective death of dopaminergic neurons by rotenone: protective effect of coenzyme Q10". *J Neurochem*. 2005 Jun;93(5):1199-208.

- Moore F, Weekes J, Hardie DG. "Evidence that AMP triggers phosphorylation as well as direct allosteric activation of rat liver AMP-activated protein kinase. A sensitive mechanism to protect the cell against ATP depletion". *Eur J Biochem.* 1991 Aug 1;199(3):691-7.
- Moosmann B, Skutella T, Beyer K, Behl C. "Protective activity of aromatic amines and imines against oxidative nerve cell death.". *Biol Chem.* 2001 Nov;382(11):1601-12.
- Mosharov EV, Gong LW, Khanna B, Sulzer D, Lindau M. "Intracellular patch electrochemistry: regulation of cytosolic catecholamines in chromaffin cells". *J Neurosci.* 2003 Jul 2;23(13):5835-45.
- Mütze S, Hebling U, Stremmel W, Wang J, Arnhold J, Pantopoulos K, Mueller S. "Myeloperoxidase-derived hypochlorous acid antagonizes the oxidative stress-mediated activation of iron regulatory protein 1". *J Biol Chem.* 2003 Oct 17;278(42):40542-9.
- Murnaghan GF. "Neurogenic disorders of the bladder in Parkinsonism". *Br J Urol.* 1961 Dec;33:403-9.
- Murofushi T, Mizuno M, Osanai R, Hayashida T. "Olfactory dysfunction in Parkinson's disease". *ORL J Otorhinolaryngol Relat Spec.* 1991;53(3):143-6.
- Nagatsu T, Levitt M, Udenfriend S. "Tyrosine hydroxylase. The initial step in norepinephrine biosynthesis". *J Biol Chem.* 1964 Sep;239:2910-7.
- Nakagawa T, Lomb DJ, Haigis MC, Guarente L. "SIRT5 Deacetylates carbamoyl phosphate synthetase 1 and regulates the urea cycle". *Cell.* 2009 May 1;137(3):560-70.
- Napper AD, Hixon J, McDonagh T, Keavey K, Pons JF, Barker J, Yau WT, Amouzegh P, Flegg A, Hamelin E, Thomas RJ, Kates M, Jones S, Navia MA, Saunders JO, DiStefano PS, Curtis R. "Discovery of indoles as potent and selective inhibitors of the deacetylase SIRT1". *J Med Chem.* 2005 Dec 15;48(25):8045-54.
- Neal JW, Pearson RC, Cole G, Powell TP. "Neuronal hypertrophy in the pars reticulata of the substantia nigra in Parkinson's disease". *Neuropathol Appl Neurobiol.* 1991 Jun;17(3):203-6.

- Nesterova TB, Popova BC, Cobb BS, Norton S, Senner CE, Tang YA, Spruce T, Rodriguez TA, Sado T, Merkenschlager M, Brockdorff N. "Dicer regulates Xist promoter methylation in ES cells indirectly through transcriptional control of Dnmt3a". *Epigenetics Chromatin*. 2008 Oct 27;1(1):2.
- Nicklas WJ, Vyas I, Heikkila RE. "Inhibition of NADH-linked oxidation in brain mitochondria by 1-methyl-4-phenyl-pyridine, a metabolite of the neurotoxin, 1-methyl-4-phenyl-1,2,5,6-tetrahydropyridine". *Life Sci*. 1985 Jul 1;36(26):2503-8.
- Nielsen AL, Oulad-Abdelghani M, Ortiz JA, Remboutsika E, Chambon P, Losson R. "Heterochromatin formation in mammalian cells: interaction between histones and HP1 proteins". *Mol Cell*. 2001 Apr;7(4):729-39.
- Nieto N, Friedman SL, Cederbaum AI. "Cytochrome P450 2E1-derived reactive oxygen species mediate paracrine stimulation of collagen I protein synthesis by hepatic stellate cells". *J Biol Chem*. 2002 Mar 22;277(12):9853-64.
- NINDS NET-PD Investigators. "A randomized clinical trial of coenzyme Q10 and GPI-1485 in early Parkinson disease". *Neurology*. 2007 Jan 2;68(1):20-8.
- Nishi K, Kondo T, Narabayashi H. "Difference in recovery patterns of striatal dopamine content, tyrosine hydroxylase activity and total bipterin content after 1-methyl-4-phenyl-1,2,3,6-tetrahydropyridine (MPTP) administration: a comparison of young and older mice". *Brain Res*. 1989 Jun 5;489(1):157-62.
- Nishimura JS. "Succinyl-CoA synthetase structure-function relationships and other considerations". *Adv Enzymol Relat Areas Mol Biol*. 1986;58:141-72.
- North BJ, Marshall BL, Borra MT, Denu JM, Verdin E. "The human Sir2 ortholog, SIRT2, is an NAD⁺-dependent tubulin deacetylase". *Mol Cell*. 2003 Feb;11(2):437-44.
- Oberg KE. "The site of the action of rotenone in the respiratory chain". *Exp Cell Res*. 1961 Jun;24:163-4.

- Ogryzko VV, Schiltz RL, Russanova V, Howard BH, Nakatani Y. "The transcriptional coactivators p300 and CBP are histone acetyltransferases". *Cell*. 1996 Nov 29;87(5):953-9.
- Ohlow MJ, Moosmann B. "Phenothiazine: the seven lives of pharmacology's first lead structure". *Drug Discov Today*. 2011 Feb;16(3-4):119-31.
- Ohno S, Kaplan WD, Kinoshita R. "Formation of the sex chromatin by a single X-chromosome in liver cells of *Rattus norvegicus*". *Exp Cell Res*. 1959 Oct;18:415-8.
- Okano M, Bell DW, Haber DA, Li E. "DNA methyltransferases Dnmt3a and Dnmt3b are essential for de novo methylation and mammalian development". *Cell*. 1999 Oct 29;99(3):247-57.
- Onyango P, Celic I, McCaffery JM, Boeke JD, Feinberg AP. "SIRT3, a human SIR2 homologue, is an NAD-dependent deacetylase localized to mitochondria". *Proc Natl Acad Sci U S A*. 2002 Oct 15;99(21):13653-8.
- Ozden O, Park SH, Wagner BA, Song HY, Zhu Y, Vassilopoulos A, Jung B, Buettner GR, Gius D. "SIRT3 deacetylates and increases pyruvate dehydrogenase activity in cancer cells". *Free Radic Biol Med*. 2014 Nov;76:163-172.
- Öztürk MA, Cojocaru V, Wade RC. "Dependence of Chromatin Structure on Linker Histone Sequence and Posttranslational Modification". *Biophys J*. 2018 May 22;114(10):2363-2375.
- Pacher P, Beckman JS, Liaudet L. "Nitric oxide and peroxynitrite in health and disease". *Physiol Rev*. 2007 Jan;87(1):315-424.
- Park G, Tan J, Garcia G, Kang Y, Salvesen G, Zhang Z. "Regulation of Histone Acetylation by Autophagy in Parkinson Disease". *J Biol Chem*. 2016 Feb 12;291(7):3531-40.
- Parkinson J. "An essay on the shaking palsy". *J Neuropsychiatry Clin Neurosci*. 2002 Spring;14(2):223-36 (reprint)
- Parkinson Study Group. "Effects of tocopherol and deprenyl on the progression of disability in early Parkinson's disease". *N Engl J Med*. 1993 Jan 21;328(3):176-83.

- Pendleton RG, Gessner G, Jenkins B. "The long term effects of an inhibitor of phenylethanolamine N-methyltransferase upon adrenal epinephrine biosynthesis". *Naunyn Schmiedebergs Arch Pharmacol.* 1976 Nov;295(2):127-33.
- Peng L, Yuan Z, Ling H, Fukasawa K, Robertson K, Olashaw N, Koomen J, Chen J, Lane WS, Seto E. "SIRT1 deacetylates the DNA methyltransferase 1 (DNMT1) protein and alters its activities". *Mol Cell Biol.* 2011 Dec;31(23):4720-34.
- Pereira WE, Hoyano Y, Summons RE, Bacon VA, Duffield AM. "Chlorination studies. II. The reaction of aqueous hypochlorous acid with alpha-amino acids and dipeptides". *Biochim Biophys Acta.* 1973 Jun 20;313(1):170-80.
- Perrino C, Marcovecchio F, Tofful L, Canepari S. "Particulate matter concentration and chemical composition in the metro system of Rome, Italy". *Environ Sci Pollut Res Int.* 2015 Jun;22(12):9204-14.
- Peters J. "The role of genomic imprinting in biology and disease: an expanding view". *Nat Rev Genet.* 2014 Aug;15(8):517-30.
- Pikaart MJ, Recillas-Targa F, Felsenfeld G. "Loss of transcriptional activity of a transgene is accompanied by DNA methylation and histone deacetylation and is prevented by insulators". *Genes Dev.* 1998 Sep 15;12(18):2852-62.
- Pillus L, Rine J. "Epigenetic inheritance of transcriptional states in *S. cerevisiae*". *Cell.* 1989 Nov 17;59(4):637-47.
- Popović-Bijelić A, Mojović M, Stamenković S, Jovanović M, Selaković V, Andjus P, Bačić G. "Iron-sulfur cluster damage by the superoxide radical in neural tissues of the SOD1(G93A) ALS rat model". *Free Radic Biol Med.* 2016 Jul;96:313-22.
- Pradhan S, Bacolla A, Wells RD, Roberts RJ. "Recombinant human DNA (cytosine-5) methyltransferase. I. Expression, purification, and comparison of de novo and maintenance methylation". *J Biol Chem.* 1999 Nov 12;274(46):33002-10.

- Pruitt K, Zinn RL, Ohm JE, McGarvey KM, Kang SH, Watkins DN, Herman JG, Baylin SB. "Inhibition of SIRT1 reactivates silenced cancer genes without loss of promoter DNA hypermethylation". *PLoS Genet.* 2006 Mar;2(3):e40.
- Przedborski S, Levivier M, Jiang H, Ferreira M, Jackson-Lewis V, Donaldson D, Togasaki DM. "Dose-dependent lesions of the dopaminergic nigrostriatal pathway induced by intrastriatal injection of 6-hydroxydopamine". *Neuroscience.* 1995 Aug;67(3):631-47.
- Qian MX, Pang Y, Liu CH, Haratake K, Du BY, Ji DY, Wang GF, Zhu QQ, Song W, Yu Y, Zhang XX, Huang HT, Miao S, Chen LB, Zhang ZH, Liang YN, Liu S, Cha H, Yang D, Zhai Y, Komatsu T, Tsuruta F, Li H, Cao C, Li W, Li GH, Cheng Y, Chiba T, Wang L, Goldberg AL, Shen Y, Qiu XB. "Acetylation-mediated proteasomal degradation of core histones during DNA repair and spermatogenesis". *Cell.* 2013 May 23;153(5):1012-24.
- Qing H, Wong W, McGeer EG, McGeer PL. "Lrrk2 phosphorylates alpha synuclein at serine 129: Parkinson disease implications". *Biochem Biophys Res Commun.* 2009 Sep 11;387(1):149-52
- Qiu Y, Liu L, Zhao C, Han C, Li F, Zhang J, Wang Y, Li G, Mei Y, Wu M, Wu J, Shi Y. "Combinatorial readout of unmodified H3R2 and acetylated H3K14 by the tandem PHD finger of MOZ reveals a regulatory mechanism for HOXA9 transcription". *Genes Dev.* 2012 Jun 15;26(12):1376-91.
- Qiu Y, Zhao Y, Becker M, John S, Parekh BS, Huang S, Hendarwanto A, Martinez ED, Chen Y, Lu H, Adkins NL, Stavreva DA, Wiench M, Georgel PT, Schiltz RL, Hager GL. "HDAC1 acetylation is linked to progressive modulation of steroid receptor-induced gene transcription". *Mol Cell.* 2006 Jun 9;22(5):669-79.
- Rabey JM, Hefti F. "Neuromelanin synthesis in rat and human substantia nigra". *J Neural Transm Park Dis Dement Sect.* 1990;2(1):1-14.
- Racey LA, Byvoet P. "Histone acetyltransferase in chromatin. Evidence for in vitro enzymatic transfer of acetate from acetyl-coenzyme A to histones". *Exp Cell Res.* 1971 Feb;64(2):366-70.

- Radogna F, Cerella C, Gaigneaux A, Christov C, Dicato M, Diederich M. "Cell type-dependent ROS and mitophagy response leads to apoptosis or necroptosis in neuroblastoma". *Oncogene*. 2016 Jul 21;35(29):3839-53.
- Ramirez A, Heimbach A, Gründemann J, Stiller B, Hampshire D, Cid LP, Goebel I, Mubaidin AF, Wriekat AL, Roeper J, Al-Din A, Hillmer AM, Karsak M, Liss B, Woods CG, Behrens MI, Kubisch C. "Hereditary parkinsonism with dementia is caused by mutations in ATP13A2, encoding a lysosomal type 5 P-type ATPase". *Nat Genet*. 2006 Oct;38(10):1184-91.
- Ransom BR, Kunis DM, Irwin I, Langston JW. "Astrocytes convert the parkinsonism inducing neurotoxin, MPTP, to its active metabolite, MPP⁺". *Neurosci Lett*. 1987 Apr 10;75(3):323-8.
- Rappold PM, Cui M, Chesser AS, Tibbett J, Grima JC, Duan L, Sen N, Javitch JA, Tieu K. "Paraquat neurotoxicity is mediated by the dopamine transporter and organic cation transporter-3". *Proc Natl Acad Sci U S A*. 2011 Dec 20;108(51):20766-71.
- Ratnam S, Mertineit C, Ding F, Howell CY, Clarke HJ, Bestor TH, Chaillet JR, Trasler JM. "Dynamics of Dnmt1 methyltransferase expression and intracellular localization during oogenesis and preimplantation development". *Dev Biol*. 2002 May 15;245(2):304-14.
- Reches A, Fahn S. "Catechol-O-methyltransferase and Parkinson's disease". *Adv Neurol*. 1984;40:171-9.
- Rekas A, Adda CG, Andrew Aquilina J, Barnham KJ, Sunde M, Galatis D, Williamson NA, Masters CL, Anders RF, Robinson CV, Cappai R, Carver JA. "Interaction of the molecular chaperone alphaB-crystallin with alpha-synuclein: effects on amyloid fibril formation and chaperone activity". *J Mol Biol*. 2004 Jul 23;340(5):1167-83.
- Reth M. "Hydrogen peroxide as second messenger in lymphocyte activation". *Nat Immunol*. 2002 Dec;3(12):1129-34.
- Rhee I, Jair KW, Yen RW, Lengauer C, Herman JG, Kinzler KW, Vogelstein B, Baylin SB, Schuebel KE. "CpG methylation is maintained in human cancer cells lacking DNMT1". *Nature*. 2000 Apr 27;404(6781):1003-7.

- Rhee SG. "Cell signaling. H₂O₂, a necessary evil for cell signaling". *Science*. 2006 Jun 30;312(5782):1882-3".
- Rhodes D, Lipps HJ. "G-quadruplexes and their regulatory roles in biology". *Nucleic Acids Res*. 2015 Oct 15;43(18):8627-37.
- Riachi NJ, LaManna JC, Harik SI. "Entry of 1-methyl-4-phenyl-1,2,3,6-tetrahydropyridine into the rat brain". *J Pharmacol Exp Ther*. 1989 Jun;249(3):744-8.
- Rice JC, Briggs SD, Ueberheide B, Barber CM, Shabanowitz J, Hunt DF, Shinkai Y, Allis CD. "Histone methyltransferases direct different degrees of methylation to define distinct chromatin domains". *Mol Cell*. 2003 Dec;12(6):1591-8.
- Ridinger J, Koeneke E, Kolbinger FR, Koerholz K, Mahboobi S, Hellweg L, Gunkel N, Miller AK, Peterziel H, Schmezer P, Hamacher-Brady A, Witt O, Oehme I. "Dual role of HDAC10 in lysosomal exocytosis and DNA repair promotes neuroblastoma chemoresistance". *Sci Rep*. 2018 Jul 3;8(1):10039.
- Rine J, Herskowitz I. "Four genes responsible for a position effect on expression from HML and HMR in *Saccharomyces cerevisiae*". *Genetics*. 1987 May;116(1):9-22.
- Rodgers JT, Lerin C, Haas W, Gygi SP, Spiegelman BM, Puigserver P. "Nutrient control of glucose homeostasis through a complex of PGC-1alpha and SIRT1". *Nature*. 2005 Mar 3;434(7029):113-8.
- Rösl F, Arab A, Klevenz B, zur Hausen H. "The effect of DNA methylation on gene regulation of human papillomaviruses". *J Gen Virol*. 1993 May;74 (Pt 5):791-801.
- Rogers D. "Bradyphrenia in Parkinson's disease". *Br J Hosp Med*. 1988 Feb;39(2):128, 130.
- Roghani M, Behzadi G. "Neuroprotective effect of vitamin E on the early model of Parkinson's disease in rat: behavioral and histochemical evidence". *Brain Res*. 2001 Feb 16;892(1):211-7.

- Roos RA, Vredevoogd CB. "Pain in muscles and joints as the initial symptom of Parkinson disease". *Ned Tijdschr Geneeskd*. 1989 May 13;133(19):961-2.
- Rosen A. "Augmentation of cardiac contractile force and heart rate by medulla oblongata stimulation in the cat". *Acta Physiol Scand*. 1961 Nov-Dec;53:255-69.
- Rosengren E. "On the role of monoamine oxidase for the inactivation of dopamine in brain". *Acta Physiol Scand*. 1960 Aug 25;49:370-5.
- Ross MF, Kelso GF, Blaikie FH, James AM, Cochemé HM, Filipovska A, Da Ros T, Hurd TR, Smith RA, Murphy MP. "Lipophilic triphenylphosphonium cations as tools in mitochondrial bioenergetics and free radical biology". *Biochemistry (Mosc)*. 2005 Feb;70(2):222-30.
- Rothgiesser KM, Erener S, Waibel S, Lüscher B, Hottiger MO. "SIRT2 regulates NF- κ B dependent gene expression through deacetylation of p65 Lys310". *J Cell Sci*. 2010 Dec 15;123(Pt 24):4251-8.
- Rothman N, Smith MT, Hayes RB, Traver RD, Hoener B, Campleman S, Li GL, Dosemeci M, Linet M, Zhang L, Xi L, Wacholder S, Lu W, Meyer KB, Titenko-Holland N, Stewart JT, Yin S, Ross D. "Benzene poisoning, a risk factor for hematological malignancy, is associated with the NQO1 609C-->T mutation and rapid fractional excretion of chlorzoxazone". *Cancer Res*. 1997 Jul 15;57(14):2839-42.
- Rozas G, Labandeira García JL. "Drug-free evaluation of rat models of parkinsonism and nigral grafts using a new automated rotarod test". *Brain Res*. 1997 Feb 28;749(2):188-99.
- Rudow G, O'Brien R, Savonenko AV, Resnick SM, Zonderman AB, Pletnikova O, Marsh L, Dawson TM, Crain BJ, West MJ, Troncoso JC. "Morphometry of the human substantia nigra in ageing and Parkinson's disease". *Acta Neuropathol*. 2008 Apr;115(4):461-70.
- Ruggieri S, Stocchi F, Denaro A, Baronti F, Agnoli A. "The role of MAO-b inhibitors in the treatment of Parkinson's disease". *J Neural Transm Suppl*. 1986;22:227-33.

- Sabater L, Fang PJ, Chang CF, De Rache A, Prado E, Dejeu J, Garofalo A, Lin JH, Mergny JL, Defrancq E, Pratviel G. "Cobalt(III)porphyrin to target G-quadruplex DNA". *Dalton Trans.* 2015 Feb 28;44(8):3701-7.
- Saha A, Goldstein S, Cabelli D, Czapski G. "Determination of optimal conditions for synthesis of peroxyxynitrite by mixing acidified hydrogen peroxide with nitrite". *Free Radic Biol Med.* 1998 Mar 1;24(4):653-9.
- Saksouk N, Simboeck E, Déjardin J. "Constitutive heterochromatin formation and transcription in mammals". *Epigenetics Chromatin.* 2015 Jan 15;8:3.
- Sanghera MK, Trulson ME, German DC. "Electrophysiological properties of mouse dopamine neurons: in vivo and in vitro studies", *Neuroscience.* 1984 Jul;12(3):793-801.
- Sato M, Hikosaka O. "Role of primate substantia nigra pars reticulata in reward-oriented saccadic eye movement". *J Neurosci.* 2002 Mar 15;22(6):2363-73.
- Satoh T, Eguchi K, Watabe K. "Functional relationship between cat brainstem neurons during sleep and wakefulness". *Physiol Behav.* 1979 Apr;22(4):741-5.
- Saxonov S, Berg P, Brutlag DL. "A genome-wide analysis of CpG dinucleotides in the human genome distinguishes two distinct classes of promoters". *Proc Natl Acad Sci U S A.* 2006 Jan 31;103(5):1412-7.
- Schapira AH, Cooper JM, Dexter D, Clark JB, Jenner P, Marsden CD. "Mitochondrial complex I deficiency in Parkinson's disease". *J Neurochem.* 1990 Mar;54(3):823-7.
- Scher MB, Vaquero A, Reinberg D. "SirT3 is a nuclear NAD⁺-dependent histone deacetylase that translocates to the mitochondria upon cellular stress". *Genes Dev.* 2007 Apr 15;21(8):920-8.
- Schmitt I, Kaut O, Khazneh H, deBoni L, Ahmad A, Berg D, Klein C, Fröhlich H, Wüllner U. "L-dopa increases α -synuclein DNA methylation in Parkinson's disease patients in vivo and in vitro". *Mov Disord.* 2015 Nov;30(13):1794-801.

- Schwer B, North BJ, Frye RA, Ott M, Verdin E. “The human silent information regulator (Sir)2 homologue hSIRT3 is a mitochondrial nicotinamide adenine dinucleotide-dependent deacetylase”. *J Cell Biol.* 2002 Aug 19;158(4):647-57.
- Seaver LC, Imlay JA. “Are respiratory enzymes the primary sources of intracellular hydrogen peroxide?”. *J Biol Chem.* 2004 Nov 19;279(47):48742-50.
- Semchuk KM, Love EJ, Lee RG. “Parkinson's disease and exposure to agricultural work and pesticide chemicals” . *Neurology.* 1992 Jul;42(7):1328-35.
- Sen S, Sanyal S, Srivastava DK, Dasgupta D, Roy S, Das C. “Transcription factor 19 interacts with histone 3 lysine 4 trimethylation and controls gluconeogenesis via the nucleosome-remodeling-deacetylase complex”. *J Biol Chem.* 2017 Dec 15;292(50):20362-20378.
- Seo JH, Park JH, Lee EJ, Vo TT, Choi H, Kim JY, Jang JK, Wee HJ, Lee HS, Jang SH, Park ZY, Jeong J, Lee KJ, Seok SH, Park JY, Lee BJ, Lee MN, Oh GT, Kim KW. “ARD1-mediated Hsp70 acetylation balances stress-induced protein refolding and degradation”. *Nat Commun.* 2016 Oct 6;7:12882.
- Shambaugh GE 3rd. “Urea biosynthesis I. The urea cycle and relationships to the citric acid cycle”. *Am J Clin Nutr.* 1977 Dec;30(12):2083-7.
- Shao D, Fry JL, Han J, Hou X, Pimentel DR, Matsui R, Cohen RA, Bachschmid MM. “A redox-resistant sirtuin-1 mutant protects against hepatic metabolic and oxidant stress”. *J Biol Chem.* 2014 Mar 14;289(11):7293-306.
- Sharov VS, Schöneich C. “Diastereoselective protein methionine oxidation by reactive oxygen species and diastereoselective repair by methionine sulfoxide reductase”. *Free Radic Biol Med.* 2000 Nov 15;29(10):986-94.
- Sherer TB, Kim JH, Betarbet R, Greenamyre JT. “Subcutaneous rotenone exposure causes highly selective dopaminergic degeneration and alpha-synuclein aggregation“. *Exp Neurol.* 2003 Jan;179(1):9-16.

- Shi H, Deng HX, Gius D, Schumacker PT, Surmeier DJ, Ma YC. "Sirt3 protects dopaminergic neurons from mitochondrial oxidative stress". *Hum Mol Genet.* 2017 May 15;26(10):1915-1926.
- Shi Y, Lan F, Matson C, Mulligan P, Whetstine JR, Cole PA, Casero RA, Shi Y. "Histone demethylation mediated by the nuclear amine oxidase homolog LSD1". *Cell.* 2004 Dec 29;119(7):941-53.
- Shock LS, Thakkar PV, Peterson EJ, Moran RG, Taylor SM. "DNA methyltransferase 1, cytosine methylation, and cytosine hydroxymethylation in mammalian mitochondria". *Proc. Natl. Acad. Sci. U. S. A.*, 108 (2011), pp. 3630–3635.
- Simons M, Nave KA. "Oligodendrocytes: Myelination and Axonal Support". *Cold Spring Harb Perspect Biol.* 2015 Jun 22;8(1):a020479.
- Singer TP, Ramsay RR, McKeown K, Trevor A, Castagnoli NE Jr. "Mechanism of the neurotoxicity of 1-methyl-4-phenylpyridinium (MPP+), the toxic bioactivation product of 1-methyl-4-phenyl-1,2,3,6-tetrahydropyridine (MPTP)". *Toxicology.* 1988 Apr;49(1):17-23.
- Singh P, Hanson PS, Morris CM. "SIRT1 ameliorates oxidative stress induced neural cell death and is down-regulated in Parkinson's disease". *BMC Neurosci.* 2017 Jun 2;18(1):46.
- Singh S, Shi T, Duffin R, Albrecht C, van Berlo D, Höhr D, Fubini B, Martra G, Fenoglio I, Borm PJ, Schins RP. "Endocytosis, oxidative stress and IL-8 expression in human lung epithelial cells upon treatment with fine and ultrafine TiO₂: role of the specific surface area and of surface methylation of the particles". *Toxicol Appl Pharmacol.* 2007 Jul 15;222(2):141-51.
- Sinsheimer RL. "The action of pancreatic deoxyribonuclease. II. Isomeric dinucleotides". *J Biol Chem.* 1955 Aug;215(2):579-83.
- Smirnova L, Harris G, Delp J, Valadares M, Pamies D, Hogberg HT, Waldmann T, Leist M, Hartung T. "A LUHMES 3D dopaminergic neuronal model for neurotoxicity testing allowing long-term exposure and cellular resilience analysis". *Arch Toxicol.* 2016 Nov;90(11):2725-2743.

- Smith PK, Krohn RI, Hermanson GT, Mallia AK, Gartner FH, Provenzano MD, Fujimoto EK, Goeke NM, Olson BJ, Klenk DC. "Measurement of protein using bicinchoninic acid". *Anal Biochem.* 1985 Oct;150(1):76-85.
- Smith RA, Porteous CM, Coulter CV, Murphy MP. "Selective targeting of an antioxidant to mitochondria". *Eur J Biochem.* 1999 Aug;263(3):709-16.
- Smith RA, Porteous CM, Gane AM, Murphy MP. "Delivery of bioactive molecules to mitochondria in vivo". *Proc Natl Acad Sci U S A.* 2003 Apr 29;100(9):5407-12. Epub 2003 Apr 15.
- Smolen JE, Shohet SB. "Permeability changes induced by peroxidation in liposomes prepared from human erythrocyte lipids". *J Lipid Res.* 1974 May;15(3):273-80.
- Snow BJ, Rolfe FL, Lockhart MM, Frampton CM, O'Sullivan JD, Fung V, Smith RA, Murphy MP, Taylor KM; Protect Study Group. "A double-blind, placebo-controlled study to assess the mitochondria-targeted antioxidant MitoQ as a disease-modifying therapy in Parkinson's disease". *Mov Disord.* 2010 Aug 15;25(11):1670-4.
- Song C, Kanthasamy A, Anantharam V, Sun F, Kanthasamy AG. "Environmental neurotoxic pesticide increases histone acetylation to promote apoptosis in dopaminergic neuronal cells: relevance to epigenetic mechanisms of neurodegeneration". *Mol Pharmacol.* 2010;77:621-632.
- Soto-Otero R, Méndez-Alvarez E, Hermida-Ameijeiras A, Muñoz-Patiño AM, Labandeira-Garcia JL. "Autoxidation and neurotoxicity of 6-hydroxydopamine in the presence of some antioxidants: potential implication in relation to the pathogenesis of Parkinson's disease". *J Neurochem.* 2000 Apr;74(4):1605-12.
- Sousa JS, D'Imprima E, Vonck J. "Mitochondrial Respiratory Chain Complexes". *Subcell Biochem.* 2018;87:167-227.
- Spencer TE, Jenster G, Burcin MM, Allis CD, Zhou J, Mizzen CA, McKenna NJ, Onate SA, Tsai SY, Tsai MJ, O'Malley BW. "Steroid receptor coactivator-1 is a histone acetyltransferase". *Nature.* 1997 Sep 11;389(6647):194-8.

- Stroud DA, Surgenor EE, Formosa LE, Reljic B, Frazier AE, Dibley MG, Osellame LD, Stait T, Beilharz TH, Thorburn DR, Salim A, Ryan MT. "Accessory subunits are integral for assembly and function of human mitochondrial complex I". *Nature*. 2016 Oct 6;538(7623):123-126.
- Sugo N, Oshiro H, Takemura M, Kobayashi T, Kohno Y, Uesaka N, Song WJ, Yamamoto N. "Nucleocytoplasmic translocation of HDAC9 regulates gene expression and dendritic growth in developing cortical neurons". *Eur J Neurosci*. 2010 May;31(9):1521-32.
- Sun L, Fang J. "Macromolecular crowding effect is critical for maintaining SIRT1's nuclear localization in cancer cells". *Cell Cycle*. 2016 Oct;15(19):2647-2655.
- Sun L, Marin de Evsikova C, Bian K, Achille A, Telles E, Pei H, Seto E. "Programming and Regulation of Metabolic Homeostasis by HDAC11". *EBioMedicine*. 2018 Jul;33:157-168.
- Sundaresan NR, Gupta M, Kim G, Rajamohan SB, Isbatan A, Gupta MP. "Sirt3 blocks the cardiac hypertrophic response by augmenting Foxo3a-dependent antioxidant defense mechanisms in mice". *J Clin Invest*. 2009 Sep;119(9):2758-71.
- Sweeney MD, Sagare AP, Zlokovic BV. "Blood-brain barrier breakdown in Alzheimer disease and other neurodegenerative disorders". *Nat Rev Neurol*. 2018 Mar;14(3):133-150.
- Szwagierczak A, Bultmann S, Schmidt CS, Spada F, Leonhardt H. "Sensitive enzymatic quantification of 5-hydroxymethylcytosine in genomic DNA". *Nucleic Acids Res*. 2010 Oct;38(19):e181.
- Tahiliani M, Koh KP, Shen Y, Pastor WA, Bandukwala H, Brudno Y, Agarwal S, Iyer LM, Liu DR, Aravind L, Rao A. "Conversion of 5-methylcytosine to 5-hydroxymethylcytosine in mammalian DNA by MLL partner TET1". *Science*. 2009 May 15;324(5929):930-5.
- Tainer JA, Getzoff ED, Richardson JS, Richardson DC. "Structure and mechanism of copper, zinc superoxide dismutase". *Nature*. 1983 Nov 17-23;306(5940):284-7.
- Tan M, Peng C, Anderson KA, Chhoy P, Xie Z, Dai L, Park J, Chen Y, Huang H, Zhang Y, Ro J, Wagner GR, Green MF, Madsen AS, Schmiesing J, Peterson BS, Xu G, Ilkayeva OR,

- Muehlbauer MJ, Braulke T, Mühlhausen C, Backos DS, Olsen CA, McGuire PJ, Pletcher SD, Lombard DB, Hirschey MD, Zhao Y. “Lysine glutarylation is a protein posttranslational modification regulated by SIRT5”. *Cell Metab.* 2014 Apr 1;19(4):605-17.
- Tanaka M, Kovalenko SA, Gong JS, Borgeld HJ, Katsumata K, Hayakawa M, Yoneda M, Ozawa T. “Accumulation of deletions and point mutations in mitochondrial genome in degenerative diseases”. *Ann N Y Acad Sci.* 1996 Jun 15;786:102-11.
- Taniguchi M, Carreira MB, Cooper YA, Bobadilla AC, Heinsbroek JA, Koike N, Larson EB, Balmuth EA, Hughes BW, Penrod RD, Kumar J, Smith LN, Guzman D, Takahashi JS, Kim TK, Kalivas PW, Self DW, Lin Y, Cowan CW. “HDAC5 and Its Target Gene, Npas4, Function in the Nucleus Accumbens to Regulate Cocaine-Conditioned Behaviors”. *Neuron.* 2017 Sep 27;96(1):130-144.e6.
- Tanner CM, Kamel F, Ross GW, Hoppin JA, Goldman SM, Korell M, Marras C, Bhudhikanok GS, Kasten M, Chade AR, Comyns K, Richards MB, Meng C, Priestley B, Fernandez HH, Cambi F, Umbach DM, Blair A, Sandler DP, Langston JW. “Rotenone, paraquat, and Parkinson's disease” . *Environ Health Perspect.* 2011 Jun;119(6):866-72.
- Thomas EL. “Myeloperoxidase-hydrogen peroxide-chloride antimicrobial system: effect of exogenous amines on antibacterial action against *Escherichia coli*”. *Infect Immun.* 1979 Jul;25(1):110-6.
- Tippin DB, Sundaralingam M. “Nine polymorphic crystal structures of d(CCGGGCCCGG), d(CCGGGCCm5CGG), d(Cm5CGGGCCm5CGG) and d(CCGGGCC(Br)5CGG) in three different conformations: effects of spermine binding and methylation on the bending and condensation of A-DNA”. *J Mol Biol.* 1997 Apr 18;267(5):1171-85.
- Traber MG, Atkinson J. “Vitamin E, antioxidant and nothing more“. *Free Radic Biol Med.* 2007 Jul 1;43(1):4-15.
- Traub MM, Rothwell JC, Marsden CD. “Anticipatory postural reflexes in Parkinson's disease and other akinetic-rigid syndromes and in cerebellar ataxia”. *Brain.* 1980 Jun;103(2):393-412.

- Trojer P, Li G, Sims RJ 3rd, Vaquero A, Kalakonda N, Boccuni P, Lee D, Erdjument-Bromage H, Tempst P, Nimer SD, Wang YH, Reinberg D. "L3MBTL1, a histone-methylation-dependent chromatin lock". *Cell*. 2007 Jun 1;129(5):915-28.
- Tsai HJ, Wilson JE. "Functional organization of mammalian hexokinases: both N- and C-terminal halves of the rat type II isozyme possess catalytic sites". *Arch Biochem Biophys*. 1996 May 1;329(1):17-23.
- Tsukada Y, Fang J, Erdjument-Bromage H, Warren ME, Borchers CH, Tempst P, Zhang Y. "Histone demethylation by a family of JmjC domain-containing proteins". *Nature*. 2006 Feb 16;439(7078):811-6.
- Tubbs RS, Loukas M, Shoja MM, Mortazavi MM, Cohen-Gadol AA. "Félix Vicq d'Azyr (1746-1794): early founder of neuroanatomy and royal French physician". *Childs Nerv Syst*. 2011 Jul;27(7):1031-4.
- Turrens JF, Boveris A. "Generation of superoxide anion by the NADH dehydrogenase of bovine heart mitochondria". *Biochem J*. 1980 Nov 1; 191(2): 421–427.
- Turrens JF, Alexandre A, Lehninger AL; "Ubisemiquinone is the electron donor for superoxide formation by complex III of heart mitochondria". *Arch Biochem Biophys*. 1985 Mar;237(2):408-14.
- Ungerstedt U. "6-Hydroxy-dopamine induced degeneration of central monoamine neurons". *Eur J Pharmacol*. 1968 Dec;5(1):107-10.
- Van den Wyngaert I, de Vries W, Kremer A, Neefs J, Verhasselt P, Luyten WH, Kass SU. "Cloning and characterization of human histone deacetylase 8". *FEBS Lett*. 2000 Jul 28;478(1-2):77-83.
- Vanderhaeghen JJ, Périer O, Sternon JE. "Pathological findings in idiopathic orthostatic hypotension. Its relationship with Parkinson's disease". *Arch Neurol*. 1970 Mar;22(3):207-14.

- Van der Schoot JB, Creveling CR. "Substrates and inhibitors of dopamine-beta-hydroxylase (DBH)". *Adv Drug Res.* 1965;2:47-88.
- Van Wieringen A. "Bensarazid with L-dopa in the treatment of parkinson's disease". *S Afr Med J.* 1974 Feb 9;48(6):206-9.
- Vaquero A, Scher M, Lee D, Erdjument-Bromage H, Tempst P, Reinberg D. "Human SirT1 interacts with histone H1 and promotes formation of facultative heterochromatin". *Mol Cell.* 2004 Oct 8;16(1):93-105.
- Vaquero A, Scher MB, Lee DH, Sutton A, Cheng HL, Alt FW, Serrano L, Sternglanz R, Reinberg D. "SirT2 is a histone deacetylase with preference for histone H4 Lys 16 during mitosis". *Genes Dev.* 2006 May 15;20(10):1256-61.
- Vaquero A, Sternglanz R, Reinberg D. "NAD⁺-dependent deacetylation of H4 lysine 16 by class III HDACs". *Oncogene.* 2007 Aug 13;26(37):5505-20.
- Vaziri H, Dessain SK, Ng Eaton E, Imai SI, Frye RA, Pandita TK, Guarente L, Weinberg RA. "hSIR2(SIRT1) functions as an NAD-dependent p53 deacetylase". *Cell.* 2001 Oct 19;107(2):149-59.
- Verdel A, Curtet S, Brocard MP, Rousseaux S, Lemerrier C, Yoshida M, Khochbin S. "Active maintenance of mHDA2/mHDAC6 histone-deacetylase in the cytoplasm". *Curr Biol.* 2000 Jun 15;10(12):747-9.
- Veredas FJ, Cantón FR, Aledo JC. "Methionine residues around phosphorylation sites are preferentially oxidized in vivo under stress conditions". *Sci Rep.* 2017 Jan 12;7:40403.
- Vermeulen M, Carrozza MJ, Lasonder E, Workman JL, Logie C, Stunnenberg HG. "In vitro targeting reveals intrinsic histone tail specificity of the Sin3/histone deacetylase and N-CoR/SMRT corepressor complexes". *Mol Cell Biol.* 2004 Mar;24(6):2364-72.
- Vermunt MW, Reinink P, Korving J, de Bruijn E, Creyghton PM, Basak O, Geeven G, Toonen PW, Lansu N, Meunier C, van Heesch S; Netherlands Brain Bank, Clevers H, de Laat W, Cuppen E, Creyghton MP. "Large-scale identification of coregulated enhancer networks in the adult

- human brain". *Cell Rep.* 2014 Oct 23;9(2):767-79.
- Verreault A, Kaufman PD, Kobayashi R, Stillman B. "Nucleosomal DNA regulates the core-histone-binding subunit of the human Hat1 acetyltransferase". *Curr Biol.* 1998 Jan 15;8(2):96-108.
- Viatour P, Legrand-Poels S, van Lint C, Warnier M, Merville MP, Gielen J, Piette J, Bours V, Chariot A. "Cytoplasmic I κ B increases NF- κ B-independent transcription through binding to histone deacetylase (HDAC) 1 and HDAC3". *J Biol Chem.* 2003 Nov 21;278(47):46541-8.
- Vicent GP, Zaurin R, Nacht AS, Li A, Font-Mateu J, Le Dily F, Vermeulen M, Mann M, Beato M. "Two chromatin remodeling activities cooperate during activation of hormone responsive promoters". *PLoS Genet.* 2009 Jul;5(7):e1000567.
- Vila M, Jackson-Lewis V, Guégan C, Wu DC, Teismann P, Choi DK, Tieu K, Przedborski S; "The role of glial cells in Parkinson's disease". *Curr Opin Neurol.* 2001 Aug;14(4):483-9.
- Vinken PJ, Bruyn GW. "Intoxications of the Nervous System". Elsevier Health Sciences. 1994 p. 369.
- Voss AK, Collin C, Dixon MP, Thomas T. "Moz and retinoic acid coordinately regulate H3K9 acetylation, Hox gene expression, and segment identity". *Dev Cell.* 2009 Nov;17(5):674-86.
- Wakeling LA, Ions LJ, Escolme SM, Cockell SJ, Su T, Dey M, Hampton EV, Jenkins G, Wainwright LJ, McKay JA, Ford D. "SIRT1 affects DNA methylation of polycomb group protein target genes, a hotspot of the epigenetic shift observed in ageing". *Hum Genomics.* 2015 Jun 24;9:14.
- Wang X, Quinn PJ. "Vitamin E and its function in membranes". *Prog Lipid Res.* 1999 Jul;38(4):309-36.
- Watson CJ, Collier P, Tea I, Neary R, Watson JA, Robinson C, Phelan D, Ledwidge MT, McDonald KM, McCann A, Sharaf O, Baugh JA. "Hypoxia-induced epigenetic modifications are associated with cardiac tissue fibrosis and the development of a myofibroblast-like

phenotype“. *Hum Mol Genet.* 2014 Apr 15;23(8):2176-88.

Weber AR, Krawczyk C, Robertson AB, Kuśnierczyk A, Vågbo CB, Schuermann D, Klungland A, Schär P. “Biochemical reconstitution of TET1-TDG-BER-dependent active DNA demethylation reveals a highly coordinated mechanism“. *Nat Commun.* 2016 Mar 2;7:10806.

Weng YL, An R, Cassin J, Joseph J, Mi R, Wang C, Zhong C, Jin SG, Pfeifer GP, Bellacosa A, Dong X, Hoke A, He Z, Song H, Ming GL. “An Intrinsic Epigenetic Barrier for Functional Axon Regeneration“. *Neuron.* 2017 Apr 19;94(2):337-346.e6.

Williams ZR, Goodman CB, Soliman KF. “Anaerobic glycolysis protection against 1-methyl-4-phenylpyridinium (MPP+) toxicity in C6 glioma cells“. *Neurochem Res.* 2007 Jun;32(6):1071-80.

Wilson DF, Harrison DK, Vinogradov SA. “Oxygen, pH, and mitochondrial oxidative phosphorylation“. *J Appl Physiol (1985).* 2012 Dec 15;113(12):1838-45.

Winkler GS, Kristjuhan A, Erdjument-Bromage H, Tempst P, Svejstrup JQ. “Elongator is a histone H3 and H4 acetyltransferase important for normal histone acetylation levels in vivo“. *Proc Natl Acad Sci U S A.* 2002 Mar 19;99(6):3517-22.

Winslow AR, Chen CW, Corrochano S, Acevedo-Arozena A, Gordon DE, Peden AA, Lichtenberg M, Menzies FM, Ravikumar B, Imarisio S, Brown S, O'Kane CJ, Rubinsztein DC. “ α -Synuclein impairs macroautophagy: implications for Parkinson's disease“. *J Cell Biol.* 2010 Sep 20;190(6):1023-37.

Wolfson N, Wilbur KM, Bernheim F. “Lipid peroxide formation in regenerating rat liver“. *Exp Cell Res.* 1956 Apr;10(2):556-8.

Yang SM, Kim BJ, Norwood Toro L, Skoultchi AI. “H1 linker histone promotes epigenetic silencing by regulating both DNA methylation and histone H3 methylation“. *Proc Natl Acad Sci U S A.* 2013 Jan 29;110(5):1708-13.

- Yeung F, Hoberg JE, Ramsey CS, Keller MD, Jones DR, Frye RA, Mayo MW. "Modulation of NF-kappaB-dependent transcription and cell survival by the SIRT1 deacetylase". *EMBO J.* 2004 Jun 16;23(12):2369-80.
- Yi W, Clark PM, Mason DE, Keenan MC, Hill C, Goddard WA 3rd, Peters EC, Driggers EM, Hsieh-Wilson LC. "Phosphofructokinase 1 glycosylation regulates cell growth and metabolism". *Science.* 2012 Aug 24;337(6097):975-80.
- Yoshida M, Kijima M, Akita M, Beppu T. "Potent and specific inhibition of mammalian histone deacetylase both in vivo and in vitro by trichostatin A". *J Biol Chem.* 1990 Oct 5;265(28):17174-9.
- Yoshimori T, Yamamoto A, Moriyama Y, Futai M, Tashiro Y. "Bafilomycin A1, a specific inhibitor of vacuolar-type H(+)-ATPase, inhibits acidification and protein degradation in lysosomes of cultured cells". *J Biol Chem.* 1991 Sep 15;266(26):17707-12.
- Zanchi AC, Venturini CD, Saiki M, Nascimento Saldiva PH, Tannhauser Barros HM, Rhoden CR. "Chronic nasal instillation of residual-oil fly ash (ROFA) induces brain lipid peroxidation and behavioral changes in rats". *Inhal Toxicol.* 2008 Jul;20(9):795-800.
- Zecca L, Tampellini D, Gerlach M, Riederer P, Fariello RG, Sulzer D. "Substantia nigra neuromelanin: structure, synthesis, and molecular behaviour". *Molecular Pathology.* 2001;54(6):414-418.
- Zhang SM, Hernán MA, Chen H, Spiegelman D, Willett WC, Ascherio A. "Intakes of vitamins E and C, carotenoids, vitamin supplements, and PD risk". *Neurology.* 2002 Oct 22;59(8):1161-9.
- Zhang ZN, Zhang JS, Xiang J, Yu ZH, Zhang W, Cai M, Li XT, Wu T, Li WW, Cai DF;. "Subcutaneous rotenone rat model of Parkinson's disease: Dose exploration study". *Brain Res.* 2017 Jan 15;1655:104-113.
- Zheng L, Zhou M, Guo Z, Lu H, Qian L, Dai H, Qiu J, Yakubovskaya E, Bogenhagen DF, Demple B, Shen B. "Human DNA2 is a mitochondrial nuclease/helicase for efficient processing of DNA replication and repair intermediates". *Mol Cell.* 2008 Nov 7;32(3):325-36.

- Zhou FM, Lee CR. "Intrinsic and integrative properties of substantia nigra pars reticulata neurons". *Neuroscience*. 2011 Dec 15;198:69-94.
- Zhou YB, Gerchman SE, Ramakrishnan V, Travers A, Muyldermans S. "Position and orientation of the globular domain of linker histone H5 on the nucleosome". *Nature*. 1998 Sep 24;395(6700):402-5.
- Zlokovic BV. "The blood-brain barrier in health and chronic neurodegenerative disorders". *Neuron*. 2008 Jan 24;57(2):178-201.
- Zolovick AJ, Stern WC, Jalowiec JE, Panksepp J, Morgane PJ. "Sleep-waking patterns and brain biogenic amine levels in cats after administration of 6-hydroxydopamine into the dorsolateral pontine tegmentum". *Pharmacol Biochem Behav*. 1973 Sep-Oct;1(5):557-67.
- Zucca FA, Segura-Aguilar J, Ferrari E, Muñoz P, Paris I, Sulzer D, Sarna T, Casella L, Zecca L;. "Interactions of iron, dopamine and neuromelanin pathways in brain aging and Parkinson's disease". *Prog Neurobiol*. 2017 Aug;155:96-119.

Lebenslauf

Persönliche Daten:

Name: Marius Wilhelm Baeken
Familienstand: Verheiratet
Adresse: Holunderweg 23, 55128 Mainz
Geburtsdatum: 04.12.1990
Geburtsort: Jülich
Staatsangehörigkeit: Deutsch

Wissenschaftlicher Werdegang

| | | |
|-------------|----------------------|---|
| 2015 – 2019 | Dr. rer. nat | Institut für Pathobiochemie, Universitäts- medizin der Johannes Gutenberg- Universität Mainz, Deutschland |
| 2013-2015 | M. Sc. Anthropologie | Johannes Gutenberg-Universität Mainz, Fachbereich Biologie, Deutschland |
| 2010-2013 | B. Sc. Biologie | Johannes Gutenberg-Universität Mainz, Fachbereich Biologie, Deutschland |

Publikationen

Hajieva P, **Baeken MW**, Moosmann B. “The role of Plasma Membrane Calcium ATPases (PMCA) in neurodegenerative disorders“. *Neurosci Lett.* 2018 Jan 10;663:29-38.

Weckmann K, Diefenthaler P, **Baeken MW**, Yusifli K, Turck CW, Asara JM, Behl C, Hajieva P. “Metabolomics profiling reveals differential adaptation of major energy metabolism pathways associated with autophagy upon oxygen and glucose reduction“. *Sci Rep.* 2018 Feb 5;8(1):2337.

Baeken MW, Weckmann K, Diefenthaler P, Schulte J, Moosmann B, Behl C, Hajieva P. “Novel insights into the cellular localization and regulation of the autophagosomal proteins LC3A, LC3B and LC3C“. *Cells* (In revision).

Baeken MW, Moosmann B, Richly H, Behl C, Hajieva P. “Coordinated epigenetic reorganization of neuronal metabolism in experimental Parkinson’s disease through a mitochondrial redox signal suppressing sirtuins and DNMTs“. (Under submission).

Yusifli K, **Baeken MW**, Weckmann K, Wolfrum U, Sehn E, Turck CW, Asara JM, Behl C, Hajieva P. “Linking neuronal and astrocytic glucose metabolism to autophagy: An adaptational response towards oxygen and glucose reduction“. (Under submission)